8224

Meridian

Exhibits

1, 2, 3

STATE OF NEW MEXICO

OIL CONSERVATION COMMISSION

IN THE MATTER OF THE HEARING CALLED BY THE OIL CONSERVATION COMMISSION ON ITS OWN MOTION TO DEFINE THE VERTICAL AND AREAL EXTENT OF AQUIFERS POTENTIALLY VULNERABLE TO CONTAMINATION BY THE SURFACE DISPOSITION OF WATER PRODUCED IN CONJUNCTION WITH THE PRODUCTION OF OIL AND GAS IN McKINLEY, RIO ARRIBA, SANDOVAL AND SAN JUAN COUNTIES, NEW MEXICO

CASE No. 8224

EXHIBIT I

INTERVENOR MERIDIAN OIL, INC.

MECHANISMS OF ATTENUATION

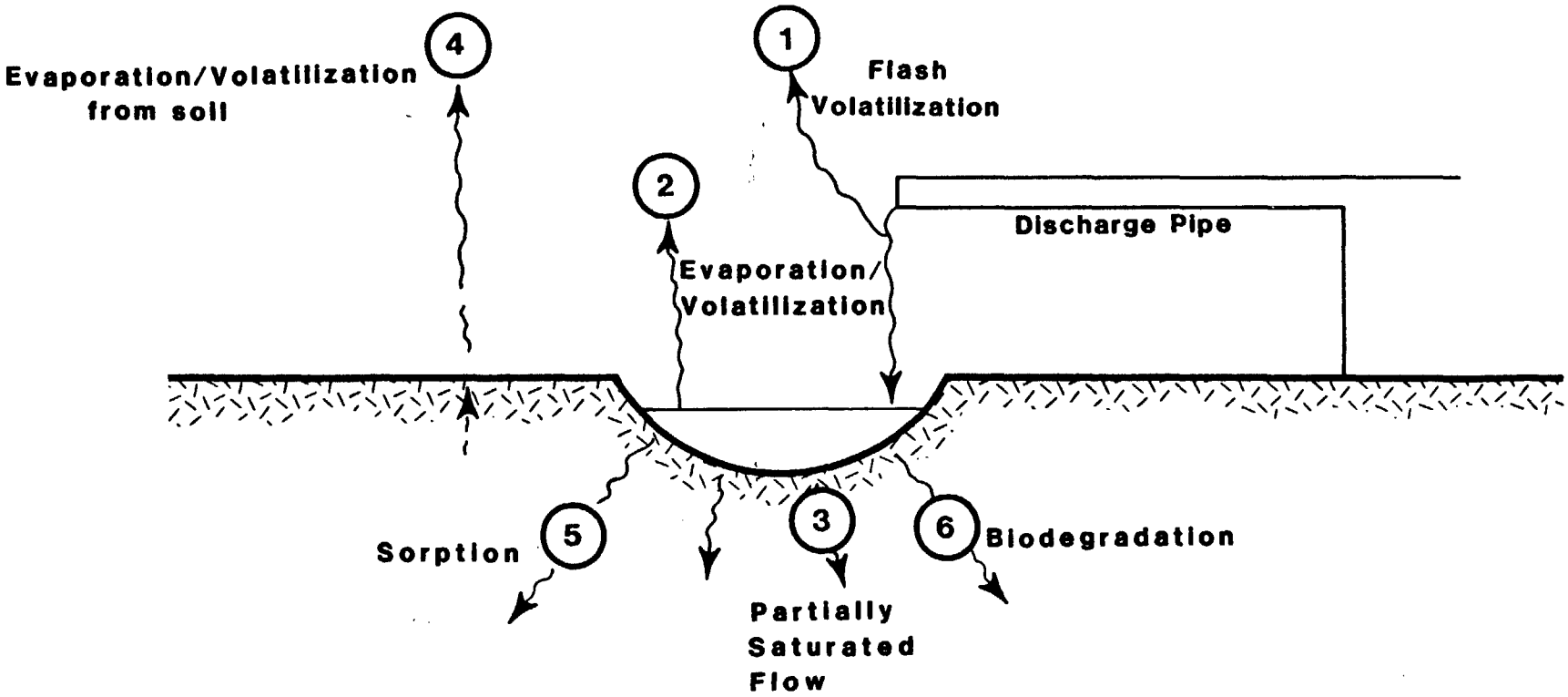

2

SUMMARY OF FARMINGTON, N.M. CLIMATOLOGICAL DATA

Month	[a] Pan Evap. IN.	[b] Wind Naut. MI/D	[c] Temp. °F	[d] Lake Evap. IN.	[b] PPT IN.
1 Jan	1.50	41.6	30.7	1.10	.52
2 Feb	2.24	48.9	36.2	1.98	.55
3 Mar	5.98	62.6	41.8	4.15	.61
4 Apr	8.23	62.3	44.9	5.31	.58
5 May	9.72	43.9	55.9	6.35	.46
6 Jan	11.22	33.3	66.3	8.79	.40
7 Jul	10.47	22.8	74.0	6.83	.91
8 Aug	8.23	19.7	75.2	5.25	1.01
9 Sep	7.48	19.7	67.7	4.84	.96
10 Oct	5.24	24.8	54.5	4.88	.99
11 Nov	2.99	36.0	40.5	1.54	.45
12 Dec	1.50	35.2	22.5	0.61	.63
Totals	74.80			51.63	8.07

a = National Oceanic and Atmospheric Administration, 1983; Distribution based on Table 26, Albuquerque, N.M. State Engineer Tech. Rpt. 32: Blaney & Hason, 1965.

b = New Mexico Climatological Data. Precipitation, Temperature, Evaporation, and Wind: Monthly and Annual Means: 1850-1975; W-K Summers and Associates, Socorro, N.M.; May, 1975; Farmington 4NE, 36°45', 108° 10', 5395 ft.

c = National Oceanic and Atmospheric Administration, 1983.

d = U.S.EPA - 625/1-83-015; Design Manual - Municipal Wastewater Stabilization Ponds, October, 1983. Office of Water Program Operations, Washington D.C. 20460.

2

Source: New Mexico Energy Research and Development Institute Draft Report "Alternative Disposal Methods for Oil and Gas Production Wastewater in the San Juan Basin."

United States
Environmental Protection
Agency

Office of Water
Planning and Standards (WH-553)
Washington DC 20460

November 1979
EPA-440/4-79-029b

Water

EPA

Water-Related Environmental Fate of 129 Priority Pollutants

Part II. Halogenated Ethers, Monocyclic Aromatics, Phthalate Esters, Polycyclic Aromatic Hydrocarbons, Nitrosamines, Miscellaneous Compounds and Halogenated Aliphatic Hydrocarbons

71. BENZENE

71.1 Statement of Probable Fate

Based on the information found, it appears that the predominant process for removal of benzene from the water column is volatilization to the atmosphere. That portion of the benzene which volatilizes to the atmosphere is probably depleted at a fairly rapid rate due to attack by hydroxyl radicals. It must be noted, however, that the solubility of benzene in water is relatively high; consequently, persistence of some benzene in the water column would be expected. Although the role of benzene sorption onto sediments and suspended solids cannot be established based on the reviewed literature, there is evidence of gradual biodegradation of benzene at low concentrations by aquatic microorganisms. The rate of benzene biodegradation is enhanced when other hydrocarbons are present.

71.2 Identification

Benzene has been detected in finished drinking water (U.S. Environmental Protection Agency 1975), in water and sediment samples from the lower Tennessee River in ppb concentrations (Goodley and Gordon 1976) and in the atmosphere (Howard and Durkin 1974). The chemical structure of benzene is shown below.

Benzene

CAS NO. 71-43-2
TSL NO. CY 14000

Alternate Names

Benzol
Cyclohexatriene

71.3 Physical Properties

The general physical properties of benzene are as follows.

Molecular weight (Weast 1977)	78.12
Melting point (Weast 1977)	5.5°C

inferred that direct oxidation of benzene in environmental waters is unlikely.

Inasmuch as the main transport process that would account for removal of benzene from water appears to be volatilization, the atmospheric destruction of benzene probably is much more likely than any other fate process. These complex photochemical reactions have been studied in simulated smog chambers (Altshuller et al. 1962; Laity et al. 1973) that measured the rate of disappearance of the volatilized organic material. The half-conversion time of m-xylene and 1,3,5-trimethylbenzene have been reported to be somewhat less than four hours (Altshuller et al. 1962). From this value and the table of relative reactivities given by Laity et al. (1973), it can be inferred that the corresponding range for the half-conversion time for benzene would be approximately 20 to 50 hours. This value for the estimated half-conversion time of benzene is in reasonable agreement with the estimated half-life of benzene proposed by Darnall et al. (1976) of 2.4 to 24 hours. This half-life value is based on the assumptions that benzene depletion is due solely to attack by hydroxyl radical (OH·), and that even high concentrations of ozone present in ambient atmospheres will not contribute significantly to the photooxidation of alkanes and aromatics, in general. A second-order rate of reaction of benzene with hydroxyl radicals of 0.85×10^{-9} $l.mol^{-1}sec^{-1}$ has been obtained by Darnall et al. (1976) by averaging rates from smog chamber data by Hansen et al. (1975) and Davis et al. (1975). The temporal stability of benzene under actual atmospheric conditions is, as yet, unknown. Experiments performed in laboratory irradiation chambers are usually conducted for relatively short periods and cannot account for all of the meterological variables within a natural airshed.

71.4.3 Hydrolysis

No specific information pertaining to the hydrolysis of benzene under ambient conditions was found. The hydrolysis of benzene is an unlikely process under environmental conditions since nucleophilic attack of the aromatic ring by water or hydroxide ion will be impeded by its negative charge-density (Morrison and Boyd 1973).

71.4.4 Volatilization

The half-life with respect to volatilization from a water column one meter thick has been estimated by Mackay and Leinonen (1975) to be 4.81 hours for benzene at 25°C; at 10°C the half-life with respect to volatilization from the same depth of water has been estimated to be 5.03 hours. Mackay and Leinonen (1975) point out that for benzene the rates and half-lives of volatilization are insensitive to temperature and that temperature only affects the rate of volatilization significantly if the system

when present in combination with dodecane, or with dodecane and naphthalene. This utilization was suggested by Walker and Colwell (1975) to most likely occur as a result of co-oxidation or because of a lower concentration of benzene present than when petroleum-degrading bacteria were treated with benzene alone. Since measurable utilization of benzene at a 0.1% concentration occurred for more than 30% (68 of 200) of the pure cultures of hydrocarbon-utililizing bacteria, Walker and Colwell (1975) feel that the latter explanation cannot be excluded.

Gibson (1976) and Gibson et al. (1968) conducted experiments to determine the metabolic pathway involved in the microbial, oxidative degradation of benzene. Although the microorganism used in these experiments, Pseudomonas putida, could utilize benzene as the sole source of carbon and energy for growth, toluene served as a better substrate, and cells grown with toluene were used to investigate benzene metabolism. Gibson (1976) found that the initial reactions in the bacterial oxidation of aromatic hydrocarbons involved the formation of cis-dihydrodiols which undergo further oxidation to yield catechols. Gibson (1976) found that mammals, on the other hand, oxidize benzene to arene oxides which are hydrated to form trans-dihydrodiols prior to oxidation to yield catechols.

For several reasons, the view that only a few genera of bacteria such as Pseudomonas (Gibson 1976), and Achromobacter (Claus and Walker 1964) can utilize benzene as a sole carbon source may not be valid. The usual enrichment procedures for isolating such bacteria tend to select only those that grow rapidly. Vigorous growth in pure culture is a great advantage in biochemical studies but may not encompass all of the more important features of a natural habitat. A specific compound may in fact be readily metabolized in soil despite the failure to isolate single microbial species capable of using that compound as a sole carbon source (National Research Council 1977). On the other hand, the isolation of single species cabable of using a test compound as a sole carbon source must also be viewed with caution. An organism capable of using a test substrate as a sole carbon source in pure culture may not be able to assimilate the compound under natural conditions. Generally, the concentration of substrate used in pure culture studies is considerably higher than normally encountered in nature. As a result, the enzymes essential for biodegradation may not be induced under natural conditions. Further, pure culture studies rarely lead to useful degradation rate information (Howard and Durkin 1974).

Helfgott et al. (1977) report the refractory index (often referred to as the biorefractory index by other authors) of benzene to be 0.23

Table 71-1

Summary of Aquatic Fate of Benzene

Environmental Process	Summary Statement	Rate	Half-Life ($t_{1/2}$)	Confidence of Data
Photolysis	Since the ozone layer in the upper atmosphere effectively filters out wavelengths of light less than 290 nm, direct excitation of benzene in the aquatic or atmospheric environment is unlikely unless a substantial wavelength shift is caused by the media.	-	-	Low
Oxidation[a]	Direct oxidation of benzene in environmental waters is unlikely. Smog chamber data, however, indicate that benzene is photooxidized at a rapid rate in the atmosphere.	0.85×10^{-9} l.mol^{-1}sec^{-1} [d]	20 to 50 hours[b] 2.4 to 24 hours[c]	Medium
Hydrolysis	Probably not a significant fate process.	-	-	Medium
Volatilization	Probably the primary transport process.	-	4.81 hours[e]	Medium
Sorption	No specific information. The log P value for benzene indicates that sorption may occur.	-	-	Low
Bioaccumulation	The log P value of benzene indicates a low bioaccumulation potential for benzene.	-	-	Low
Biotransformation and Biodegradation	Benzene can be utilized as the sole source of carbon by several microorganisms and is probably biodegradable at a slow rate.	-	-	Medium

a. The predominant environmental process which is thought to determine the fate of the compound.

b. This half-life is calculated from the half-conversion time for benzene based on smog chamber data by Altshuller et al. (1962) and the table of relative reactivities given by Laity et al. (1973).

c. This half-life is the estimated half-life value proposed by Darnall et al. (1976) and is based on the assumption that benzene depletion is due solely to attack by hydroxyl radical.

d. This second-order rate of reaction of benzene with hydroxyl radicals has been obtained by Darnall et al. (1976) by averaging rates from smog chamber data by Hansen et al. (1975) and Davis et al. (1975).

e. This is the half-life estimated by Mackay and Leinonen (1975) for volatilization of benzene from a water column one meter thick at 25°C. This rate of volatilization varies with the environmental situation encountered.

Laity, J.L., I.G. Burstain, and B.R. Appel. 1973. Photochemical smog and the atmospheric reactions of solvents. Chap. 7, pp. 95-112. Solvents Theory and Practice. R.W. Tess (ed.) Advances in Chemistry Series 124. Am. Chem. Soc., Washington, D.C.

Leo, A., C. Hansch, and D. Elkins. 1971. Partition coefficients and their uses. Chem. Rev. 71:525-616.

Mackay, D. and A.W. Wolkoff. 1973. Rate of evaporation of low-solubility contaminants from water bodies to atmosphere. Environ. Sci. Technol. 7(7):611-614.

Mackay, D. and P.J. Leinonen. 1975. Rate of evaporation of low-solubility contaminants from water bodies to atmosphere. Environ. Sci. Technol. 9(13):1178-1180.

Morrison, R.T. and R.N. Boyd. 1973. Organic chemistry. 3rd Edition. Allyn and Bacon, Inc., Boston. 1258p.

National Research Council. 1977. Fates of pollutants. Research and development needs. National Academy of Sciences, Washington, D.C. 144p.

Neely, W.B., D.R. Branson, and G.E. Blau. 1974. Partition coefficient to measure bioconcentration potential of organic chemicals in fish. Environ. Sci. Technol. 8:1113-1115.

Silverstein, R.M. and G.C. Bassler. 1968. Spectrometric identification of organic compounds. 2nd Edition. John Wiley and Sons, New York. 256 p.

Thom, N.S. and A.R. Agg. 1975. The breakdown of synthetic organic compounds in biological processes. Proc. Roy. Soc. Lond. B 189:347-357.

U.S. Environmental Protection Agency. 1975. Preliminary assessment of suspected carcinogens in drinking water. U.S. Environmental Protection Agency, (Office of Toxic Substances), Washington, D.C. 33p. EPA 560/4-75-003.

Walker, J.D. and R.R. Colwell. 1975. Degradation of hydrocarbons and mixed hydrocarbon substrate by microorganisms from Chesapeake Bay. Prog. Water Technol. 7(3-4):783-791.

80. TOLUENE

80.1 Statement of Probable Fate

From the available data it appears that the principal mechanism for removal of toluene from the aquatic environment is volatilization. The atmospheric photodestruction of toluene probably subordinates all other fates. Adsorption on sediments and suspended solids probably plays a role in the fate of toluene, but it cannot be established quantitatively at this time. The data do not allow the estimation of the relative importance of biodegradation in the determination of the fate of toluene in the aquatic environment.

80.2 Identification

Toluene has been detected at several geographical locations in finished drinking water, industrial effluents, and ambient surface waters (Shackelford and Keith 1976). The structure of toluene is shown below.

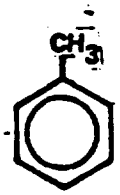

Toluene

CAS NO. 108-88-3
TSL NO. XS 52500

Alternate Names

Toluol
Phenylmethane
Methylbenzene
Methylbenzol
Methacide

80.3 Physical Properties

The general physical properties of toluene are as follows.

Molecular weight (Weast 1977)	92.13
Melting point (Weast 1977)	-95°C
Boiling point (Weast 1977)	110.6°C

80.4.2 Oxidation

Toluene is readily oxidized in the liquid phase by molecular oxygen, but this oxidation is effectively inhibited by the presence of water (Stephens and Roduta 1935). Reaction of toluene in water with hydroxyl radicals from the irradiation of hydrogen peroxide produces benzaldehyde, benzyl alcohol, and an isomeric mixture of cresols (Jefcoate et al. 1969). No data were found from which a relevant rate of oxidation of toluene in environmental waters could be determined.

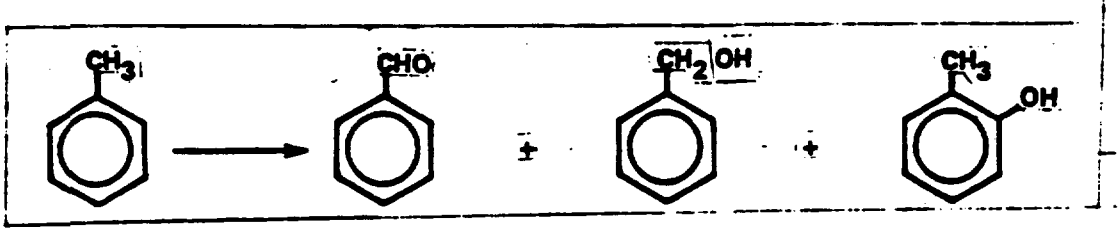

80.4.3 Hydrolysis

No data have been found that would support any role for hydrolysis at ambient environmental conditions.

80.4.4 Volatilization

The half-life with respect to volatilization from a water column one meter thick has been estimated by Mackay and Leinonen (1975) to be 5.18 hr for toluene. Some assumptions made in this estimation were: 1) the contaminant concentration is in solution, rather than in suspended, colloidal, ionic, complexed, or adsorbed form; 2) the vapor is in equilibrium with the liquid at the interface; 3) water diffusion or mixing is sufficiently rapid so that the concentration at the interface approaches that of the bulk of the water; and 4) the rate of evaporation of water is negligibly affected by the presence of the contaminants.

80.4.5 Sorption

Although no specific environmental sorption studies were found in the reviewed literature, the log octanol/water partition coefficient (log P= 2.69; Tute 1971) indicates that sorption processes may be significant for toluene. Presumably, toluene will be adsorbed by sedimentary organic material, but the extent to which this absorption will interfere with volatilization has not been considered.

Table 80-1

Summary of Aquatic Fate of Toluene

Environmental Process	Summary Statement	Rate	Half-Life ($t_{1/2}$)	Confidence of Data
Photolysis	Direct photolytic cleavage is energetically improbable in the troposphere.	-	-	Medium
Oxidation	Probably not important as an aquatic fate; however, atmospheric photooxidation subordinates all other fate processes.	-	~12 hr.	Medium
Hydrolysis	Not aquatically significant	-	-	High
Volatilization	Significant transport process responsible for removal of toluene from water.	.193 hr^{-1}	5.18 hrs.	Medium
Adsorption	Relative importance cannot be determined.	-	-	Low
Bioaccumulation	Probably not important.	-	-	Low
Biodegradation	Relative importance cannot be determined.	-	-	Low

Tute, M.S. 1971. Principles and practice of Hansch analysis: a guide to structure-activity correlation for the medicinal chemist. Adv. Drug Res. 5:1-77.

Weast, R.C. (ed.) 1977. CRC handbook of chemisty and physics. CRC Press, Inc., Cleveland, Ohio. 2398p.

Wei, K.S. and A.H. Adelman. 1969. The photooxidation of toluene. The role of an excited charge-transfer complex. Tetrahedron Lett. (38):3297-3300.

VOLATILIZATION HALF LIVES IN WATER FOR
BENZENE AND TOLUENE

Number of Half Lives	Benzene (hrs)	Toluene (hrs)	Percent Remaining
0	-	-	100
1	4.8	5.2	50
2	9.6	10.4	25
3	14.4	15.6	12.5
4	19.2	20.8	6.25
5 1 day	24	26	3.125
6	28.8	31.2	1.56
7	33.6	36.4	.78
8	38.4	41.6	.39
9	43.2	46.8	.195
10 2 days	48	52	.0975
11	52.8	57.2	.04875
12	57.6	62.4	.024375
13	62.4	67.6	.01218
14	67.2	72.8	.00609
15 3 days	72	78	.00305

VOLATILIZATION

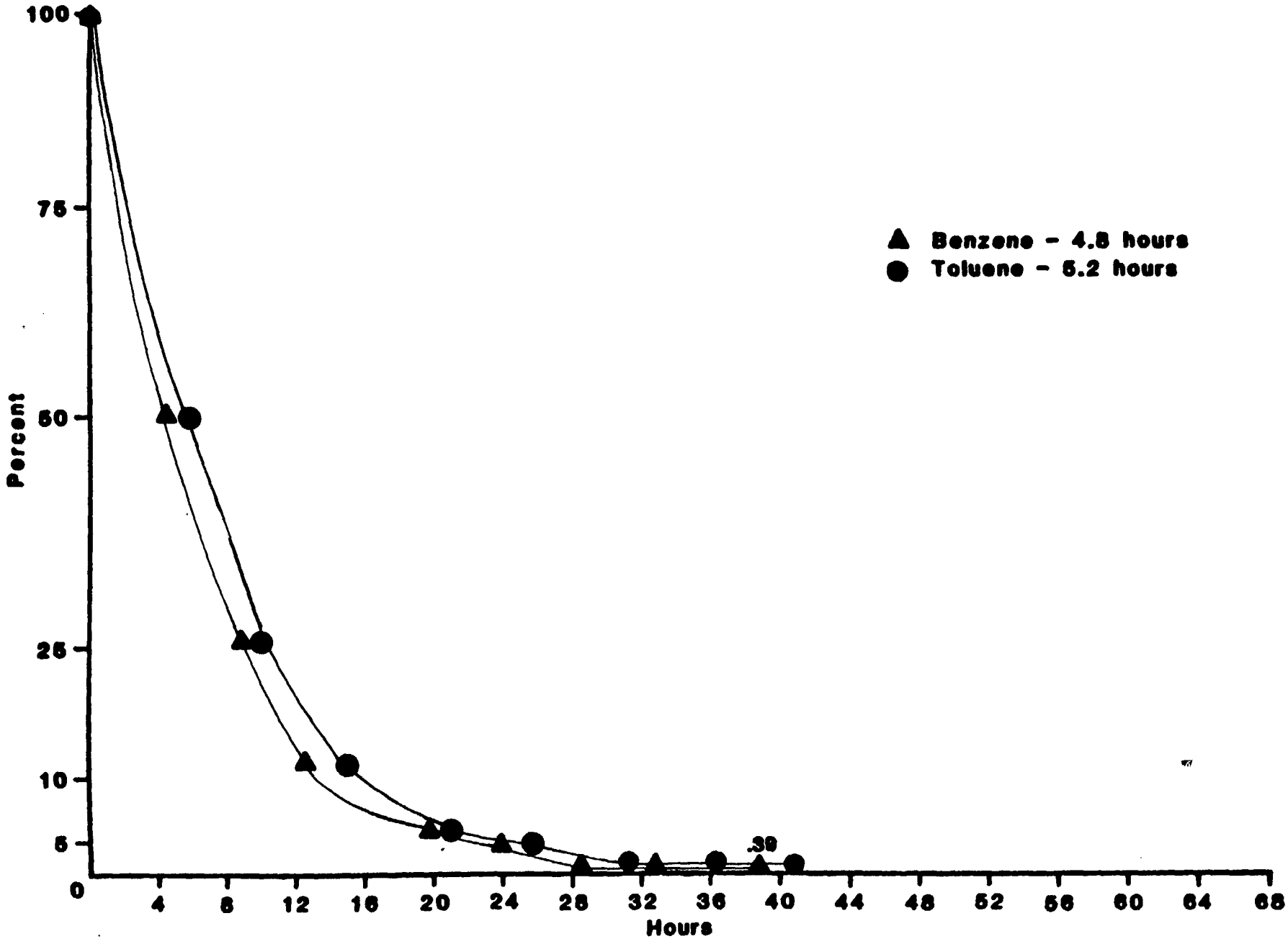

ONE DIMENSIONAL SATURATED FLOW

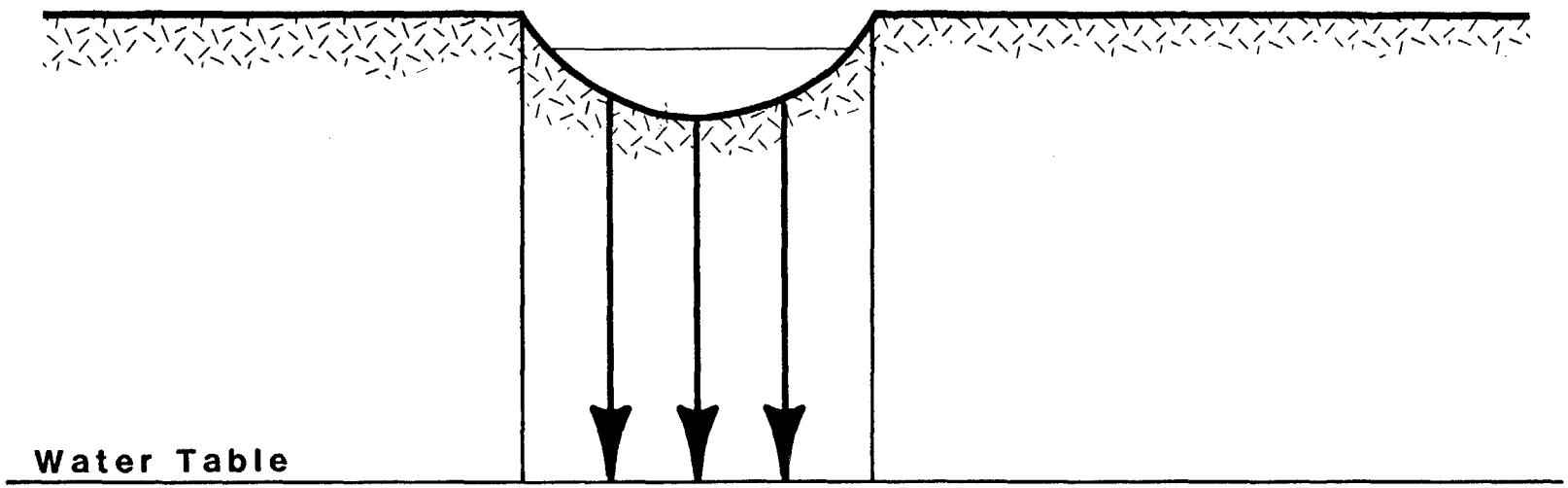

TWO DIMENSIONAL PARTIALLY SATURATED FLOW

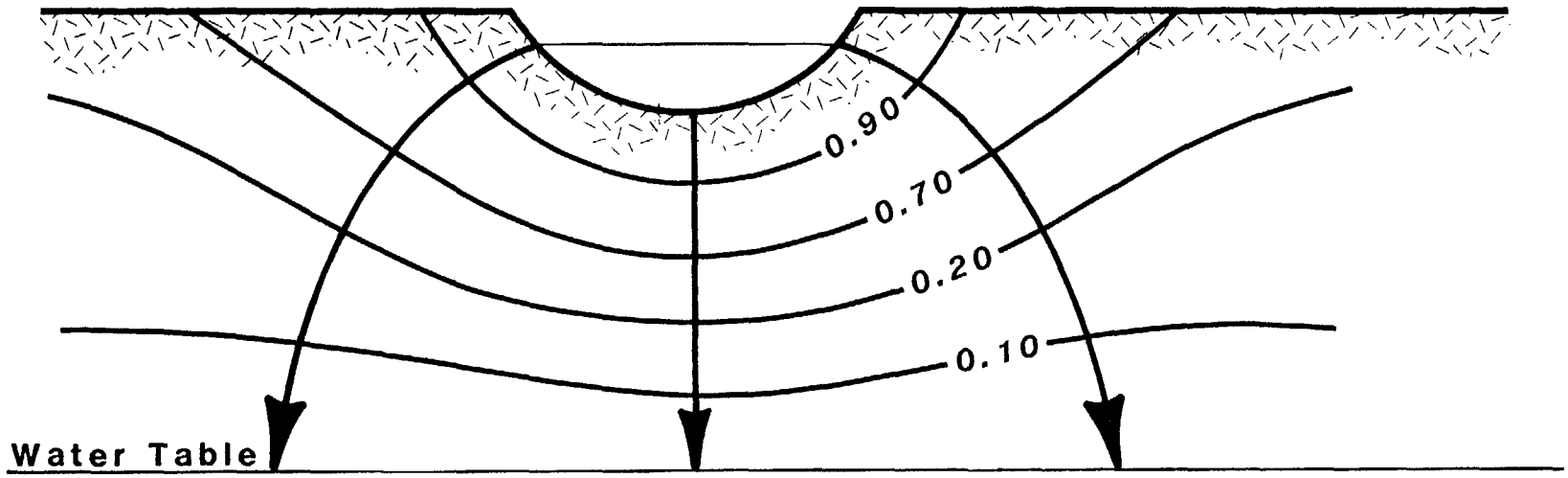

...AL OF GEOPHYSICAL RESEARCH VOL. 68, NO. 20 OCTOBER 15, 1963

Methods for Solving Problems of Multidimensional, Partially Saturated Steady Flow in Soils

A. E. REISENAUER

Geochemical and Geophysical Research
Hanford Laboratories, Richland, Washington

Abstract. A computer program for solving steady-state Darcian transport of fluid in heterogeneous, partially saturated, porous mediums is described. The program is capable of handling one-, two-, and three-dimensional and axisymmetrical problems with up to 8000 grid points. Instability of the equations and its control are discussed. Solutions of typical problems that are important in industrial waste disposal, irrigation, and drainage are presented.

INTRODUCTION

...drologic research conducted by the General Electric Company at Hanford Laboratories ...ludes studies of saturated and partially saturated flow in porous mediums. These studies are ...rected primarily toward obtaining a better ...derstanding of the rates of movement of ...dioactive liquid waste and distribution pat...rns in the vadose and saturated zones. Although this research is related principally to ...e atomic energy field, a knowledge of the pat...rn and rate of waste and groundwater move...ent has application to hydrologic problems in ...ide variety of other practical situations. ...ese include the disposal of industrial effluents, ...moval of excess water through drainage, and ...e utilization and replenishment of deep aquifers for water supply and irrigation. In investigations of radioactive waste disposal the demand for precision in knowing where, at what ..., and in what quantities movement occurs ...y be more critical than in other applications. ...redicting flow rates and patterns can often ...e accomplished through the solution of a ...undary value problem describing the flow system. The diversity of practical problems requires flexibility in the methods of solution. Accordingly, a variety of mathematical methods ...e judiciously selected and combined to form ...e basis for the Hanford-developed computer ...ogram, 'Steady Darcian Flow in Soils,' to be ...scribed here. Solutions of several typical ...eady-flow problems are presented to illustrate ...e effect of soil types and soil heterogeneities. ...e computer program was written to handle ...turated flow, partially saturated flow, or both in combination, since the distinction is rather arbitrary. That is, saturation is a special case of partial saturation where every pore is filled with a single fluid. For the purpose of this paper, cases involving partially saturated flow will be discussed.

DISCUSSION

Basic equations. The basic equations and assumptions are derived and discussed in detail elsewhere by *Scheidegger* [1960], *Richards* [1931], *Nelson* [1962], and others. It will be sufficient here to state that the generalized Darcy expression was used with the proper equations of state and conservation of mass to give the following equation in cartesian coordinates:

$$K\left[\frac{\partial^2\phi}{\partial x^2}+\frac{\partial^2\phi}{\partial y^2}+\frac{\partial^2\phi}{\partial z^2}\right] + \frac{\partial K}{\partial x}\frac{\partial\phi}{\partial x}+\frac{\partial K}{\partial y}\frac{\partial\phi}{\partial y}+\frac{\partial K}{\partial z}\frac{\partial\phi}{\partial z}=0 \qquad (1)$$

In addition to (1), three other relationships are used for partially saturated flow systems. They are

$$\theta = F(P_c) \qquad (2)$$

$$K = f(P_c) \qquad (3)$$

$$P_c = -P/\rho g = z-\phi \qquad (4)$$

where

$F(P_c)$ is the functional relationship of moisture content to capillary pressure head.

$f(P_c)$ is the functional relationship of moisture conductance to capillary pressure head.

K is the capillary conductivity of the soil. (K is a function of capillary pressure head during partial saturation, becoming the hydraulic conductivity or permeability at saturation. Since the soil is assumed to be nonhomogeneous, K is also a function of space, i.e., of x, y, and z.)

$\phi = P/\rho g + z$ is the piezometric head, hydraulic potential, or potential function.

P is the hydraulic pressure.

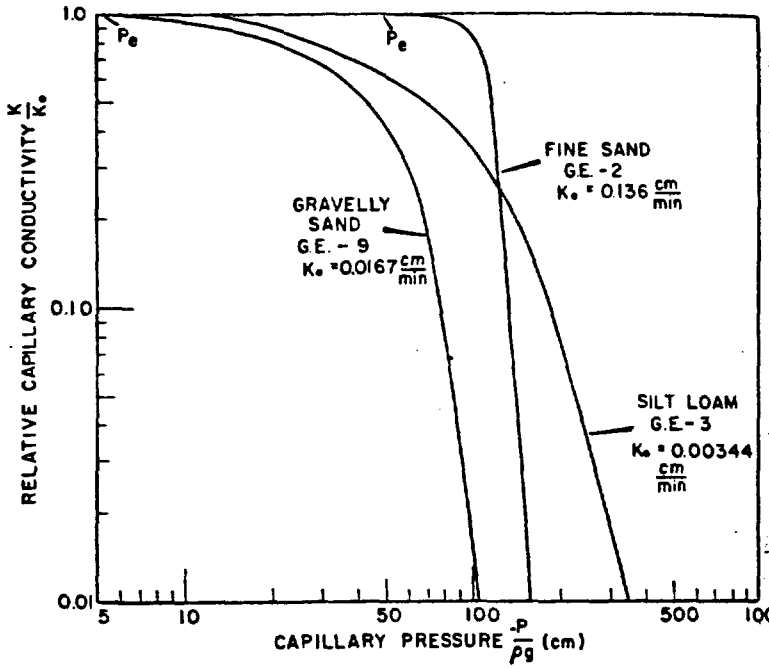

Fig. 1. Capillary conductivity—capillary pressure relationships for typical Hanford soils.

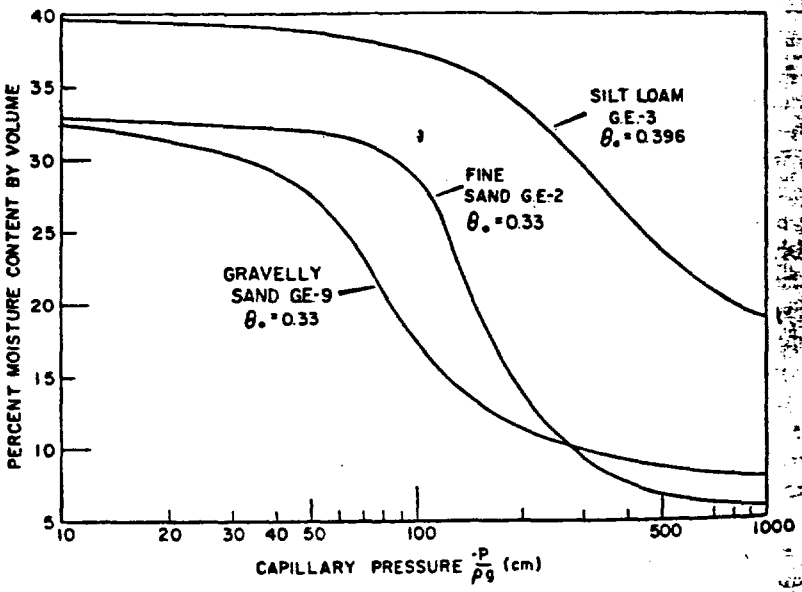

Fig. 2. Moisture content—capillary pressure relationships for typical Hanford soils.

P_e is the capillary pressu
for negative P.
z is the displacement
the capillary pressure
first soil pore begins to
z is the position head or
to location in the gravit

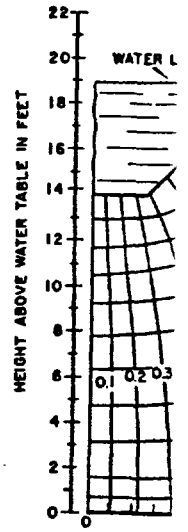

Fig. 3. Two-dimensi

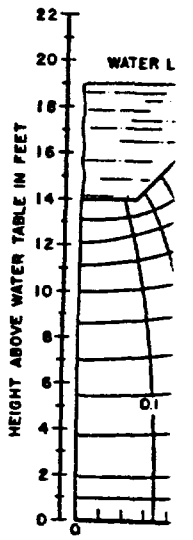

Fig. 4. Axisymmetri

P_c is the capillary pressure head, defined only for negative P.

P_d is the displacement pressure of the soil, the capillary pressure head at which the first soil pore begins to drain.

z is the position head or potential energy due to location in the gravitational field.

θ is the moisture content on a volume basis.

ρ is the fluid density.

g is the gravitational field strength.

x, y, z are the coordinate directions, z being oriented parallel to the earth's gravitational vector.

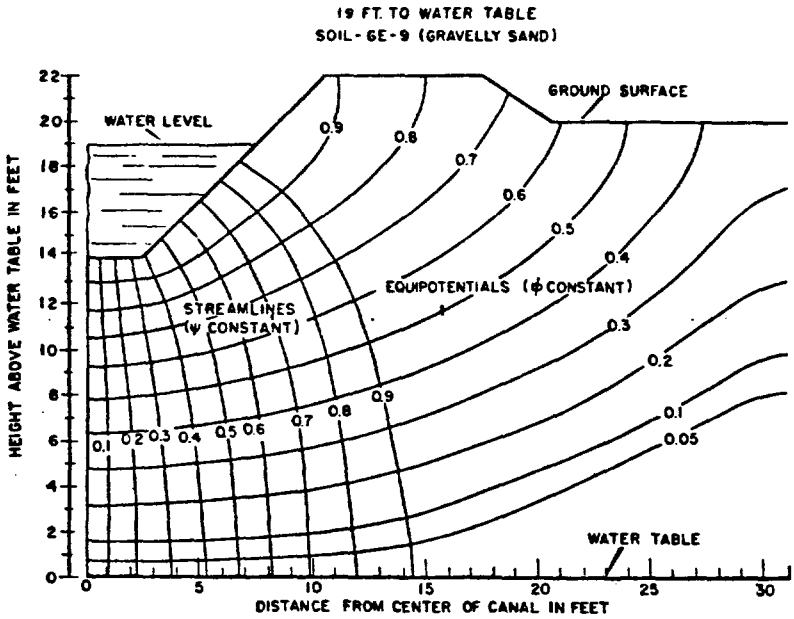

Fig. 3. Two-dimensional flow pattern below a 15-foot canal with homogeneous soil.

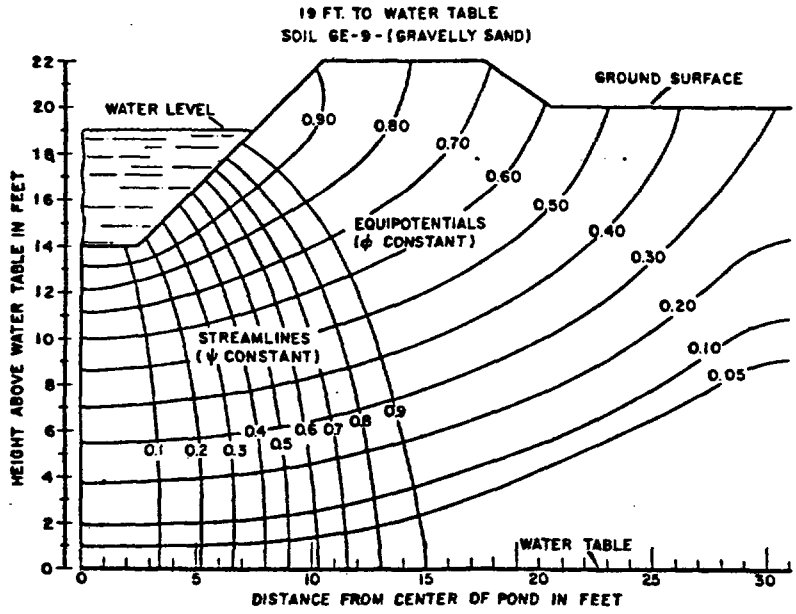

Fig. 4. Axisymmetrical flow pattern below a 15-foot pond with homogeneous soil.

ILLEGIBLE

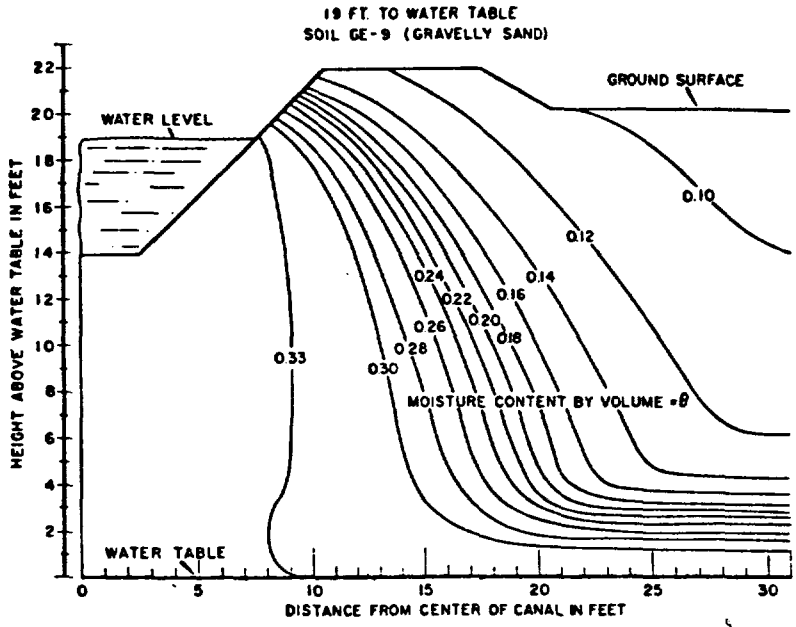

Fig. 5. Two-dimensional moisture pattern below a 15-foot canal in homogeneous soil.

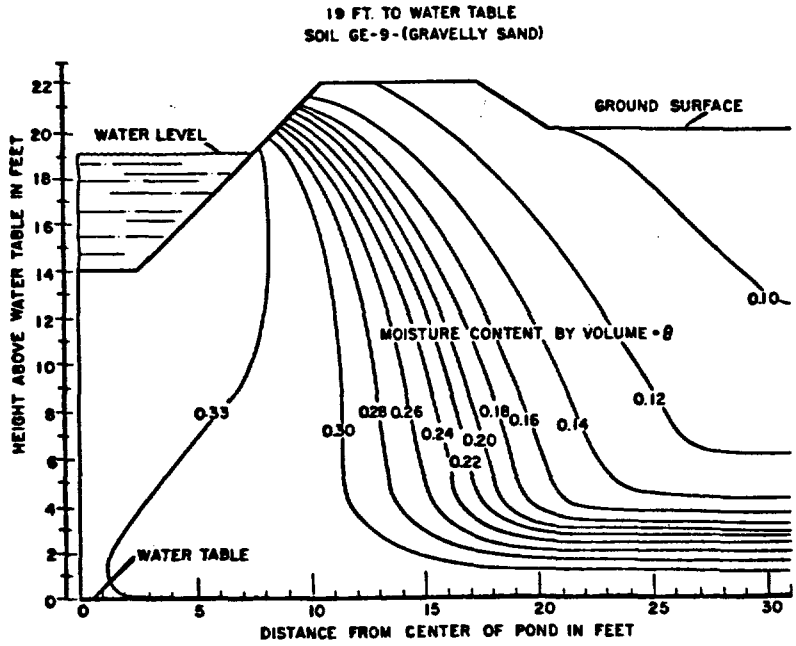

Fig. 6. Axisymmetric moisture content pattern below a 15-foot pond in homogeneous soil.

Finite difference expressions. Finite difference techniques were used to reduce the partial differential equations to a system of simultaneous equations for computer solution. A modified Gauss-Sidel iterative method [*Forsythe*, 1956] was selected because of the nonlinearity of the equations.

Central differences were used throughout as estimates of the first derivatives, and the usual combined forward and backward differences were used to represent the second partial derivatives. Substitution of these approximations into (1) yields the following finite difference form of the equation:

SOLVI

$$\left[\frac{\varphi_{i+1,j,k}+\varphi_{i-1,j}}{\lambda^2}\right.$$

$$+\frac{\varphi_{i,j+1,k}+\varphi_{i,j-}}{\lambda^2}$$

$$+\frac{\varphi_{i,j,k+1}+\varphi_{i,j,}}{\lambda^2}$$

$$+\left[\frac{K_{i+1,j,k}-K}{2\lambda}\right.$$

$$\frac{\varphi_{i+1,j,k}-\varphi_{i-1,}}{2\lambda}$$

$$+\left[\frac{K_{i,j+1,k}-K}{2\lambda}\right.$$

$$\frac{\varphi_{i,j+1,k}-\varphi_{i,j-}}{2\lambda}$$

$$+\left[\frac{K_{i,j,k+1}-K}{2\lambda}\right.$$

$$\frac{\varphi_{i,j,k+1}-\varphi_{i,j,}}{2\lambda}$$

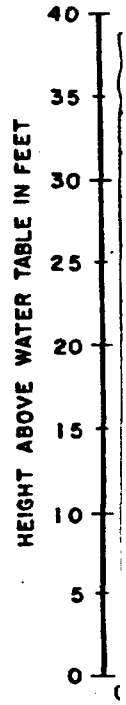

Fig. 7. Two-d

$$\left[\frac{\varphi_{i+1,j,k} + \varphi_{i-1,j,k} - 2\varphi_{i,j,k}}{\lambda^2} + \frac{\varphi_{i,j+1,k} + \varphi_{i,j-1,k} - 2\varphi_{i,j,k}}{\lambda^2} + \frac{\varphi_{i,j,k+1} + \varphi_{i,j,k-1} - 2\varphi_{i,j,k}}{\lambda^2}\right] + \left[\frac{K_{i+1,j,k} - K_{i-1,j,k}}{2\lambda}\right]\left[\frac{\varphi_{i+1,j,k} - \varphi_{i-1,j,k}}{2\lambda}\right] + \left[\frac{K_{i,j+1,k} - K_{i,j-1,k}}{2\lambda}\right]\left[\frac{\varphi_{i,j+1,k} - \varphi_{i,j-1,k}}{2\lambda}\right] + \left[\frac{K_{i,j,k+1} - K_{i,j,k-1}}{2\lambda}\right]\left[\frac{\varphi_{i,j,k+1} - \varphi_{i,j,k-1}}{2\lambda}\right] = 0 \quad (5)$$

where i, j, and k are the index integers of the grid points in the x, y, and z directions.

Solution method. In using this iterative method we (1) provide an initial estimate of the potential ϕ at every grid point, (2) substitute ϕ and the spatial location into equations that determine the capillary conductivity K from the soils data, (3) substitute the required K and ϕ into the appropriate finite difference improvement formula, depending on the dimensionality of the problem, to obtain an improved potential, and (4) return the improved ϕ to the equation that determines K. We continue cycling until the change in potential is insignificantly small.

The number of iterations, or successive improvements, depends on the goodness of the initial estimate of the potentials, on the size of the problem, and on the amount of increased convergence brought about by over-relaxation.

The computer program. The computer program, written for an IBM 7090, can handle one-, two-, and three-dimensional and axisymmetrical problems with up to 8000 grid points.

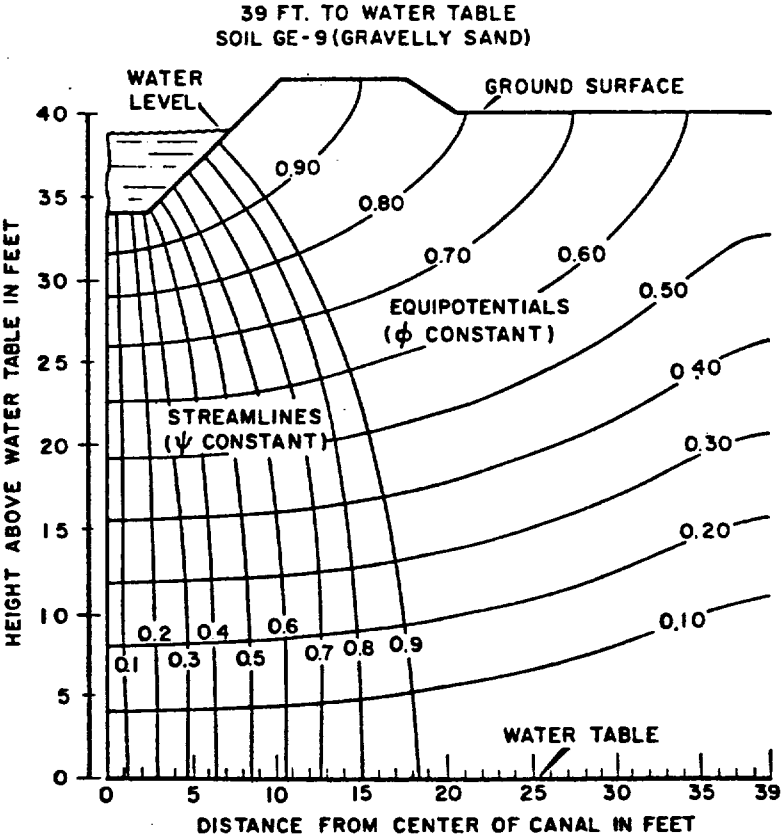

Fig. 7. Two-dimensional flow pattern below a 15-foot canal in homogeneous soil.

Four 8000-word matrices are stored in the computer memory for immediate access. This results in a very efficient computation with an average of about 400 grid calculations per second. Even at this rate very large problems may require 30 minutes or more of computer time; smaller problems require 5 to 10 minutes. The details of the program are presented by *Reisenauer et al.* [1963]; they are only summarized here.

A full range of boundary conditions is available because the system is sufficiently flexible so that every grid point can be individually controlled for the type of boundary. Soils may be heterogeneous or homogeneous because a soil identification matrix is stored in the computer memory. Also, soils may be repeated in the problem as many times as is necessary to describe the soil pattern.

A merging method allows both the type of calculation and the type of soil to be stored in a single computer word. This saves considerable storage and makes it possible to solve the 800 grid-point problems.

Descriptive data for up to fifteen different soils can be included in any one problem. These data, which are the functional relationship $f(P_s)$ expressed in (3), are the properties of the soil in question as measured with the fluid of interest, and they must be experimentally obtained. The conductivity–pressure relationships during wetting for three typical Hanford soils are shown in Figure 1. The information plotted on logarithmic coordinates is mathematically described by dividing the curve into parts in order to conserve computer storage. The parts consist of a constant value up to the displacement pressure P_s, a table of values to round the curve, and an exponential fit to describe the straight line.

The same program can be used to calculate the moisture content from the final potential by using the functional relationship $F(P_s)$ in

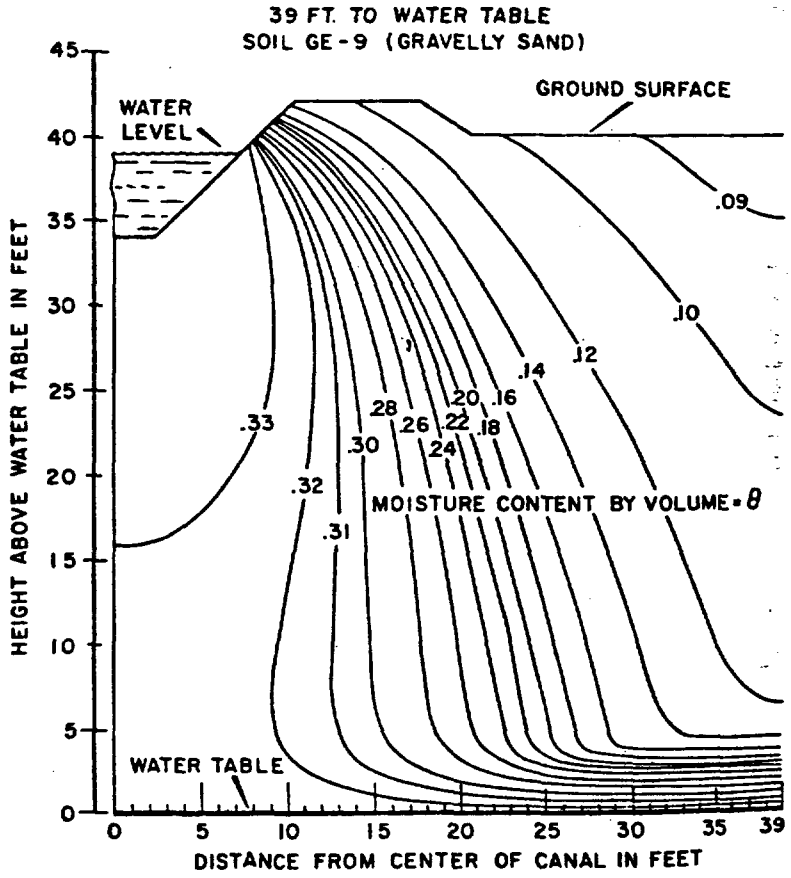

Fig. 8. Two-dimensional moisture content pattern below a 15-foot canal in homogeneous soil

SOLVIN

Figure 2 shows a mo
ssure relationship for
re 1.

Convergence and stab
nearity of the basic
ms of convergence and s
tion method for a g
itions. Several techni
e these problems. In t
conductivity values a
entials; thus when a
the conductivity is
For a better estimat
the minimal surrou
In our experience
verge unless this is do
To accelerate convergen
an optimum over-re
s internally computed
ed by *Young* [1954
ewer [1960], works ex

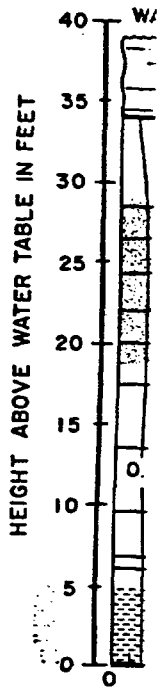

Fig. 9. Two-dim

...akes it possible to solve the ...
...roblems.
...data for up to fifteen diff...
...luded in any one problem. T...
...are the functional relation...
...ssed in (3), are the properties o...
...as measured with the flu...
...hey must be experimentally ...
...conductivity–pressure relation...
...for three typical Hanford ...
...igure 1. The information pl...
...mic coordinates is mathemati...
...dividing the curve into par...
...rve computer storage. The ...
...nstant value up to the disp...
...re P_c, a table of values to round ...
...exponential fit to describe ...
...program can be used to calc...
...re content from the final pote...
...functional relationship $F(P$, ...

...E
...AND)
...GI UND SURFACE

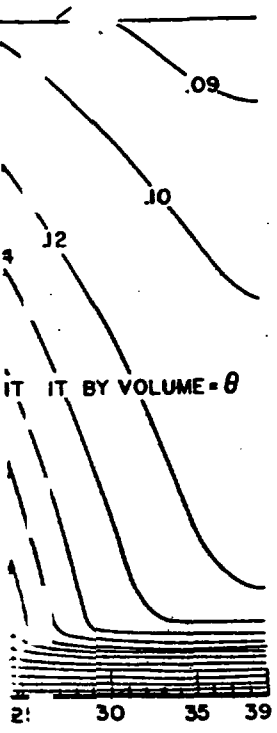

...15-foot canal in homogeneous ...

...2). Figure 2 shows a moisture content–capillary ...essure relationship for the same soils used in ...igure 1.

Convergence and stability. Inherent in the ...nonlinearity of the basic equation are the prob...s of convergence and stability of the iterative ...ution method for a given set of boundary ...conditions. Several techniques are used to over...e these problems. In the process of iteration ...e conductivity values are calculated from the ...entials; thus when a new potential is calcu...ed the conductivity is lagging by one itera... For a better estimate of this K, the values ...m the minimal surrounding nodes are aver...d. In our experience the iteration will not ...verge unless this is done.

To accelerate convergence and save computer ..., an optimum over-relaxation factor is used. ...s internally computed optimum factor,[4] de...bed by *Young* [1954] and *Forsythe and ...ow* [1960], works extremely well in prob...lems of saturated flow where the basic equations reduce to linear form. In partially saturated flow an upper limit of 1.2 is imposed to maintain stability. This is not always sufficient, however; a method for detecting instability is incorporated in the over-relaxation calculation. When instability occurs an empirical equation is used which returns to the program an over-relaxation factor less than 1. The result is a tendency toward averaging the potential values which effectively damps the oscillations.

Another method of reducing instability and speeding convergence is related to an optimum order in which the system of equations is solved. A real understanding of such convergent sequences must await the results of *Steward* [1962], *Newton* [1962], and others working in this area of applied mathematics. We have found, however, that instabilities can be controlled by using a movable initial point which in effect rearranges the order of iteration. When

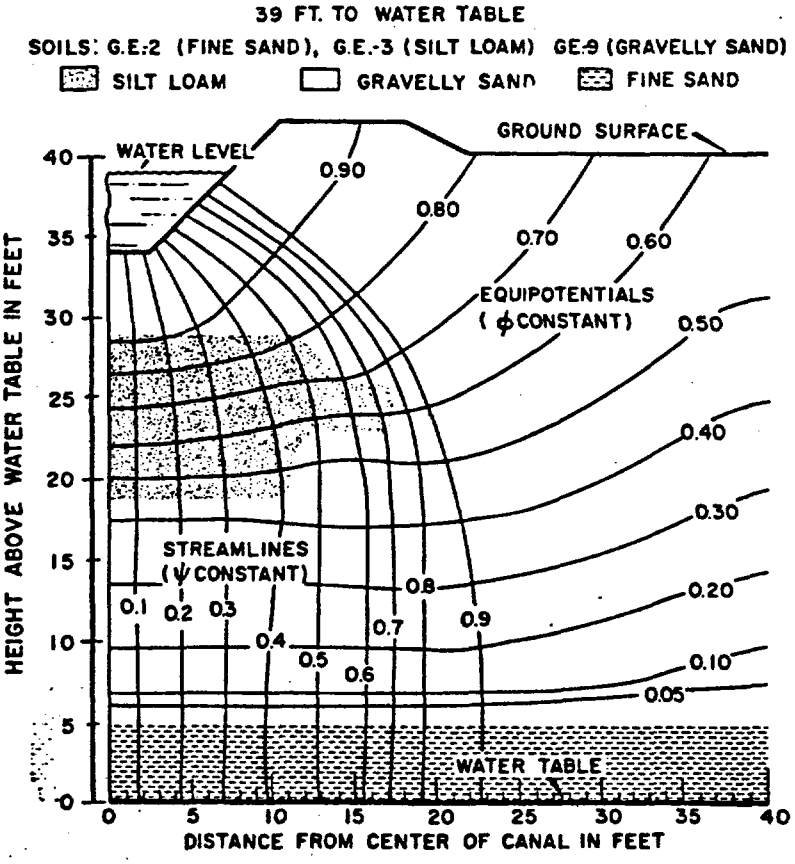

Fig. 9. Two-dimensional flow pattern below a 15-foot canal in heterogeneous soil.

the initial point is moved to the point of greatest disturbance, instabilities are attenuated and the iteration ordinarily converges. The judicious use of these various controls has enabled us to overcome instabilities encountered in previous programs.

Typical solutions. Several typical problems have been solved which will illustrate a few of the solutions that are possible with these techniques. The solutions permit comparisons to be made between different flow systems. The streamlines and equipotential lines for a two-dimensional, partially saturated flow system are shown in Figure 3. The source is an infinitely long trench or unlined canal. The soil, shown as gravelly sand [*U. S. Dept. Agr.*, 1951] in Figures 1 and 2, is homogeneous and isotropic. The flow system is 19 feet from the water surface to the *groundwater* table. The quantity of flow into the soil is 26.1 ft²/day per linear foot of trench. Figure 4 shows a similar flow problem rotated about the axis of symmetry on the left boundary. The canal has now become a pond 15 feet in diameter. Only minor differences are noticeable in the potential patterns: the streamlines are less uniformly spaced and more widely spread at the center because of the geometry of the flow system. The total quantity of flow from the pond is 437 ft³/day.

The moisture distribution beneath the canal is shown in Figure 5. A volume fraction moisture content of 0.33 is the saturation value for this soil. The zone lying directly beneath the canal and extending to the water table is saturated. In comparison, Figure 6 shows the moisture distribution for the axisymmetric case. The zone of saturation in this instance is much more 'turnip-shaped.' Another feature, most distinguishable at the right of Figure 6, is the gradual, rather than sudden, decrease in moisture which occurs above the water table.

Figure 7 shows streamlines and equipotentials

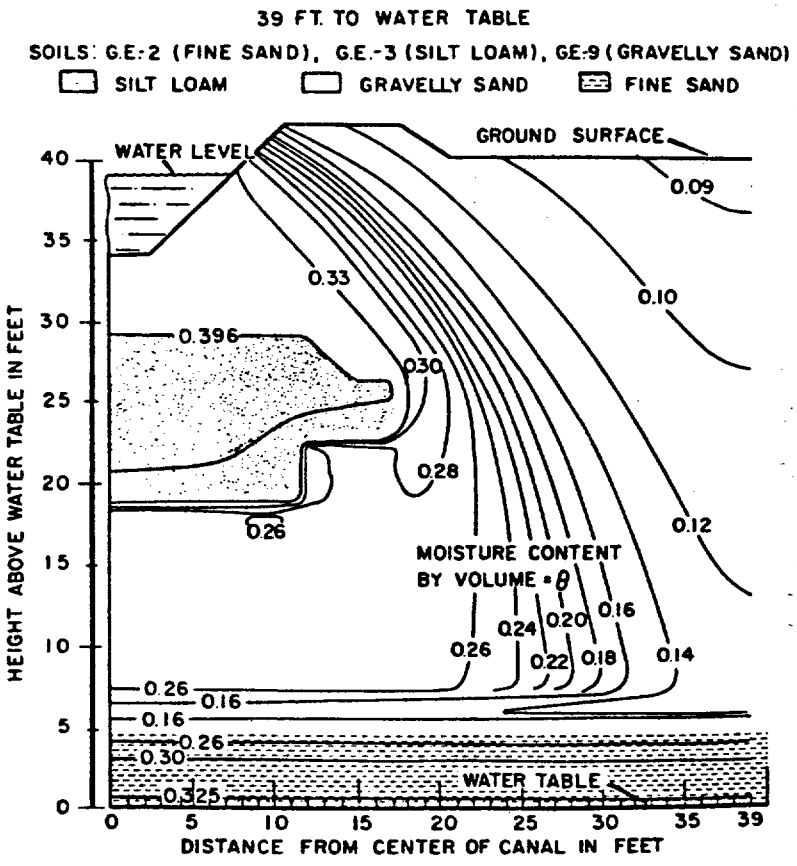

Fig. 10. Two-dimensional moisture content pattern below a 15-foot canal in heterogeneous soil.

ILLEGIBLE

faces as defined for a flow system similar to of the canal in which the depth to the water le was increased by 20 ft. The spreading of e equipotentials downward is evident. The r quantity for this system is 26.1 ft³/day per ear feet of canal. The moisture distribution ern in Figure 8 shows the saturated zone eath the canal to be separated from the er table. A pattern of equipotentials and eamlines for a flow system identical in most rds to that of Figure 7 but with heteroge- soil is shown in Figure 9. All three soils ted in Figures 1 and 2 were used in estab- the soil pattern. A thick lens of silt loam between the water table and the canal, and ver of fine sand extends 5 feet above the er table. Several distortions caused by the variations occur in the equipotentials and eamlines. The moisture distribution pattern igure 10 differs appreciably from that of the geneous-soil flow system (Figure 8). The of silt loam is saturated at a volume frac- moisture content of 0.396. The soil directly eath this lens is partially saturated at 0.28, the fine sand at the bottom has desaturated rt of the overlying coarser material. The ated flows show that heterogeneity has a icant influence on the water loss from the l. The ratio of the loss from the canal in geneous soil to the loss from the canal in geneous soil is 0.54.

Summary

he application of these methods, in combi- with reliable microgeological and soil- eter characterization studies, is expected to contribute much useful information on waste movement and distribution patterns in the vadose zone beneath disposal sites. Extension of this work to solve other hydrologic problems also appears promising.

References

Forsythe, G. E., What are relaxation methods?, in *Modern Mathematics for the Engineer*, edited by E. F. Beckenback, pp. 428–447, McGraw-Hill Book Company, New York, 1956.

Forsythe, G. E., and W. R. Wascow, *Finite-Difference Methods for Partial Differential Equations*, John Wiley & Sons, New York, 1960.

Nelson, R. W., Steady Darcian transport of fluids in heterogeneous partially saturated porous media, 1, mathematical and numerical formulation, *HW-72335, 1, AEC Res. Develop. Rept.*, June 1962.

Newton, T. A., Graph theory and systems of equations, *HW-74787*, Hanford document (in press), HAPO, Richland, Washington.

Reisenauer, A. E., R. W. Nelson, and C. N. Knudsen, Steady Darcian transport of fluids in heterogenous partially saturated porous media, 2, The computer program, *HW-72335, 2, AEC Res. Develop. Rept.* (in preparation), 1963.

Richards, L. A., Capillary conduction of liquids through porous mediums, *Physics, 1*, 318–333, 1931.

Scheidegger, A. E., *The Physics of Flow through Porous Media*, pp. 91–111, University of Toronto Press, 1960.

Steward, D. V., On an approach to techniques for analysis of the structure of large systems of equations, *Siam Rev., 4*, 321–342, 1962.

U. S. Dept. of Agriculture, *Soil Surv. Manual, Agr. Handbook, 18*, August 1951.

Young, D., Iterative methods for solving partial differential equations of elliptic type, *Trans. Am. Math. Soc., 76*, 92–111, 1954.

(Manuscript received March 28, 1963; revised June 25, 1963.)

EVAPORATION/VOLATILIZATION FROM SOIL

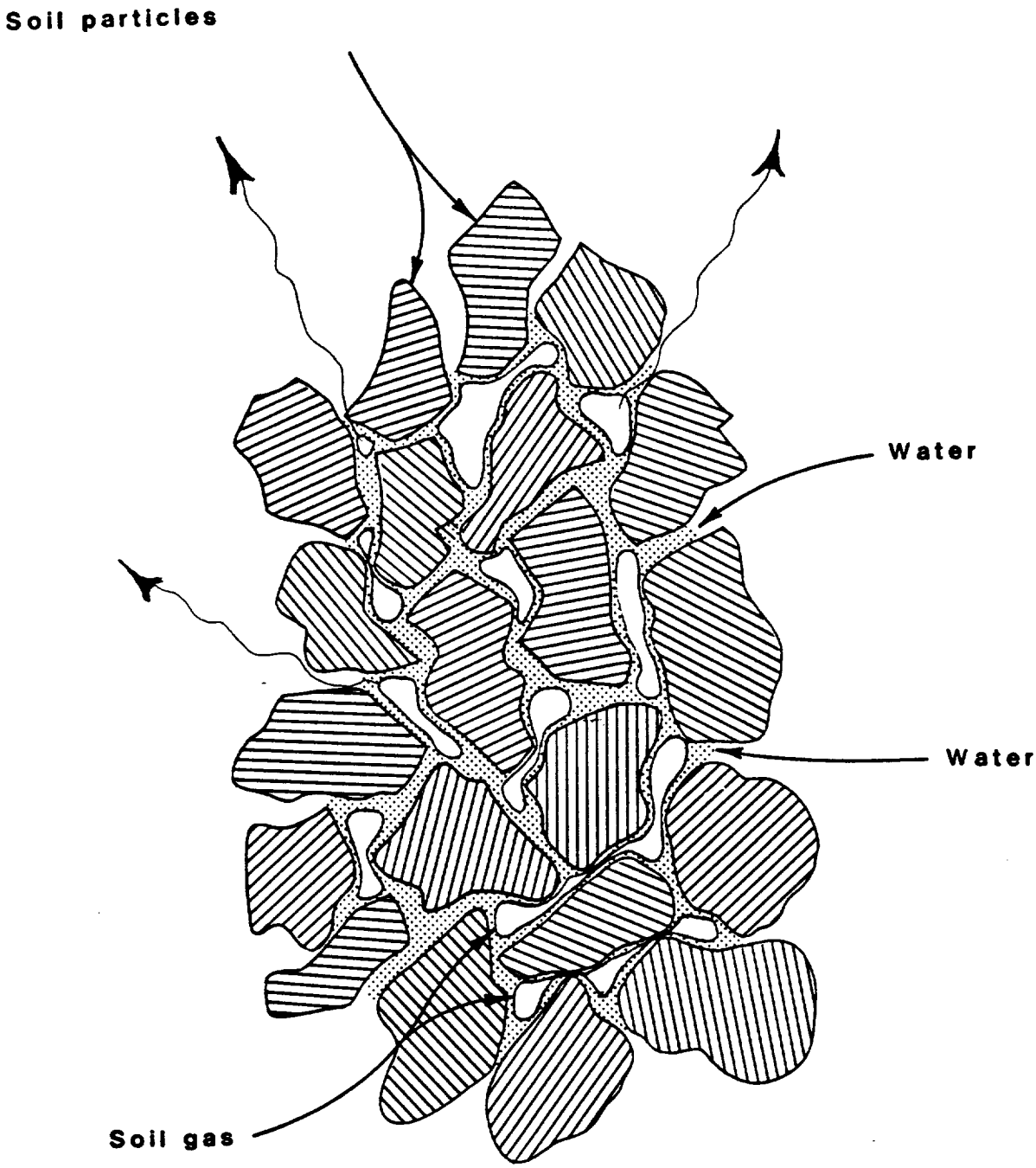

Moisture Movement in Porous Materials under Temperature Gradients

J. R. Philip and D. A. de Vries

Abstract—A theory of moisture movement in porous materials under temperature gradients is developed which explains apparently discordant experimental information, including (a) the large value of the apparent vapor transfer, (b) effect of moisture content on net moisture transfer, and (c) the transfer of latent heat by distillation.

The previous simple theory of water vapor diffusion in porous media under temperature gradients neglected the interaction of vapor, liquid and solid phases, and the difference between average temperature gradient in the air-filled pores and in the soil as a whole. With these factors taken into account, an (admittedly approximate) analysis is developed which predicts orders of magnitude and general behavior in satisfactory agreement with the experimental facts.

An important implication of the present approach is that experimental methods used to distinguish between liquid and vapor transfer have not done so, since what has been supposed to be vapor transfer has actually been series-parallel flow through liquid 'islands' located in a vapor continuum.

Equations describing moisture and heat transfer in porous materials under combined moisture and temperature gradients are developed. Four moisture-dependent diffusivities arising in this connection are discussed briefly.

Introduction

In recent years there has been much interest in the physics of moisture movement in porous media under temperature gradients. Apart from its significance to such problems as those of heat and moisture transfer in building materials, (thermal) insulating materials and clothing, this question is of great importance in microhydrological and micrometeorological studies. The physical theory of many microhydrological phenomena which may be safely taken to be isothermal is well advanced [*Philip*, 1957b]; but analysis of such problems as the heat and moisture balance during evaporation from soils requires an understanding of the influence of temperature gradients on soil water movement.

To the present time an adequate physical explanation of the growing body of experimental data on this topic has not been provided. A number of mechanisms have been invoked to account for the facts, but have not led to a plausible explanation. In this communication we show that the facts which have provoked these speculations can be explained in terms of the classical mechanisms of vapor diffusion and liquid movement by capillarity.

The Facts to be Reconciled

The facts to be explained or reconciled may be grouped under four heads:

(a) *The large value of the apparent vapor transfer* —This aspect has received the most attention. Many workers either explicitly state or give data which imply that observed water vapor transfer under temperature gradients greatly exceeds that predicted by the theory of vapor diffusion modified to take account both of the reduction of diffusion cross-section by the solid matrix and the liquid water and of the tortuosity of the diffusion path through the medium. Much of this work cannot be analyzed quantitatively, since either the boundary conditions are too complicated or else the data reported miss out one or more important determinants of the system. However, three groups have given quantitative comparisons between observed (presumed) vapor transfer and the predictions of the 'simple theory.' These comparisons are summarized in Table 1, to which are added the results of some further examinations of the data by the present authors.

(b) *Effect of moisture content on moisture transfer* —Many investigators [e.g. *Smith*, 1943; *Jones and Kohnke*, 1952; *Gurr* and others, 1952; *Hadley and Eisenstadt*, 1955] have observed that moisture transfer under temperature gradients is negligibly small both in very dry and in very wet media, but attains a fairly well-defined maximum at an intermediate moisture content which appears to depend both on the soil-water tension and on the air-filled porespace. Jones and Kohnke report this maximum as occurring at tensions ranging from 60 cm (sand) to 6000 cm (loam), corresponding to volumetric moisture contents (θ cm³ of liquid water/cm³) 0.03 to 0.105. Other data are in general agreement. Although the simple theory predicts a point of max-

TABLE 1 – *Experimental data on water-vapor transfer in soils under temperature gradients*

Authors	How movement identified as in vapor phase	Porosity $\theta + a$	Volumetric moisture content θ	Volumetric air content a	Ratio of observed transfer to value predicted by simple theory ν	Remarks[b]
Gurr and others [1952]	Liquid flow assumed proportional to Cl movement (NaCl used as tracer)	0.472[a]	0.074	0.398[a]	3.6	Uncertainty in this value about 10%
Taylor and *Cavazza* [1954]	Gaps in column presumed to restrict movement to vapor phase	0.555[a]	0.206[a]	0.349	18	Recomputed by us (from Fig. 5 after one day).
		0.657[a]	0.158[a]	0.499	9.8	Computed by us (from Fig. 4 after 2 days).
Rollins and others [1954]	Liquid return flow (cold to hot) via external capillary presumed to equal vapor flow (hot to cold) in column	0.690	0.179	0.511	4.6	Computed by us (from Fig. 6)
		0.541	0.202	0.339	4.6	" " " (trial no. 7)
		0.521	0.260	0.261	5.7	" " " (from Fig. 7)
		0.503	0.288	0.215	6.0	Computed by Rollins and others (trial no. 1)
		0.452	0.303	0.149	6.8	Computed by us (from Fig. 8)
		0.407	0.329	0.078	9.8	" " " (from Fig. 9)

[a] These values computed on assumption that S.G. of soil material = 2.65.
[b] Figure numbers in this column refer to figures appearing in the corresponding paper cited in column 1.

mum vapor transfer, this is generally at much too low a moisture content to agree with observation.

(c) *The transfer of latent heat by distillation*—Investigations [*Krischer* and *Rohnalter*, 1940; *de Vries*, 1952ab] have shown that the mechanism of vapor diffusion accounts quite adequately for the contribution of heat transfer by distillation to the apparent thermal conductivity of porous materials. These investigations did not depend on detailed use of the 'simple theory.'

(d) *Effect of air pressure on apparent vapor transfer* Molecular diffusion is proportional to the mean free path, which varies inversely with gas pressure. *Jennings* and others [1952] have confirmed this behavior qualitatively for moisture transfer under temperature gradients in soils, though their data are not amenable to quantitative analysis.

The situation is, then, that the experimental data of (a) and (b) do not conform to the simple vapor-diffusion theory, but that the aspects of the problem mentioned under (c) and (d) can be explained in terms of molecular diffusion. It is important to note that the application of molecular diffusion concepts to (c) and (d) does not involve the detailed application of the 'simple theory.'

THE SIMPLE THEORY OF VAPOR TRANSFER

We need to present this theory briefly before proceeding to our explanation of these matters. The equation of vapor diffusion, modified so as to apply in porous media [*Penman*, 1940; *Krischer* and *Rohnalter*, 1940; *van Bavel*, 1952; *Rollins* and *others*, 1954] may be written

$$q_{vap} = -D_{atm} \nu \alpha a \nabla \rho \qquad (1)$$

where q_{vap} is the vector vapor flux density, gm cm^{-2} sec^{-1}

D_{atm} is the molecular diffusivity of water vapor in air, cm^2 sec^{-1}

α is a tortuosity factor allowing for the extra path length

a is the volumetric air content of the medium (cm^3 of air/cm^3)

ρ is the density of water vapor, gm cm^{-3}

ν is the 'mass-flow factor' introduced to allow for the mass flow of vapor arising from the difference in boundary conditions governing the air and vapor components of the diffusion system.

Krischer and Rohnalter found that D_{atm} for diffusion due to a temperature gradient could be represented by the expression $4.42 \times 10^4 T^{2.3}/P$ in the range 20°–70°C, where T is the absolute temperature, °K, and P is the total gas pressure, mm Hg. Data for isothermal conditions [*Mache*, 1910; *Summerhays*, 1930; *Schirmer*, 1938] differ appreciably from this at temperatures above 40°C and there is scope for further investigation of water vapor diffusion under a temperature gradient. We use values of D_{atm} given by Krischer and Rohnal-

ter's relationship where numerical values are needed.

Stefan [see, for example, *Partington*, 1949, p. 912] showed that for steady diffusion in a closed system between an evaporating source and a condensing sink

$$\nu = P/(P - p) \tag{2}$$

where p is the partial pressure of water vapor, mm Hg. It is by no means obvious that ν will assume this value under non-stationary conditions. However the order of magnitude of the deviation of ν from unity follows from (2); ν is clearly quite close to 1 at normal soil temperatures.

Extended Treatment of Vapor Transfer

In this section we show how (1) may be extended to give (a) a separation of the 'isothermal' and 'thermal' components of vapor transfer, and (b) the effect of relative humidity (or soil water pressure) on the transfer. It will be noted that these developments depend only on the proportionality of the vapor flux to the vapor-density gradient. This is retained in the revised theory presented later in the paper, so that these results (modified in the case of thermal transfer) are also relevant there.

We introduce the thermodynamic relationship [see *Edlefsen* and *Anderson*, 1943, p. 260]

$$\rho = \rho_0 h = \rho_0 \exp(\Psi g/RT) \tag{3}$$

where ρ_0 is the density of saturated water vapor, gm cm^{-3}

h is the relative humidity

g is the acceleration due to gravity, cm sec^{-2}

R ($= 4.615 \times 10^6$) is the gas constant of water vapor, erg gm^{-1} °C^{-1}

Ψ is the water pressure in cm in thermodynamic equilibrium with the water in the medium, with atmospheric pressure as datum; thus Ψ is negative in unsaturated media. It will be noted that Ψ depends on θ and on T. In this communication we take as negligible the influence of soluble salts in the water on h and Ψ (as here defined).

Hence

$$\nabla\rho = h\nabla\rho_0 + \rho_0\nabla h \tag{4}$$

Before proceeding, we must discuss the influence of temperature on h for a constant value of θ. The roles of physical adsorption and capillary condensation in determining the adsorption isotherm (and hence the $\Psi(\theta)$ relation) of a liquid in a porous material have been reviewed by *Carman* [1953]. At low values of h physical adsorption is dominant, while capillary condensation is the important process at high values of h. The data of *Carman* and *Raal* [1951] suggest that $h = 0.6$ is a suitable (though arbitrary) transition point. Here, then, we assume that $h(\theta)$ and $\Psi(\theta)$ are determined by physical adsorption for $h < 0.6$ and by capillarity for $h > 0.6$. Physical adsorption depends primarily on h, and for a fixed h, $-(1/\theta)(\partial\theta/\partial T)$ is somewhat less than the coefficient of thermal expansion of the free liquid [see, for example, *McBain*, 1932, p. 143]. From this it is easily checked that, for $h < 0.6$, $\partial h/\partial T = 0$ to a good approximation. On the other hand, capillarity depends on the surface tension, σ dyne cm^{-1}, so that in the region of capillary condensation Ψ is proportional to σ and $\partial\Psi/\partial T$ is equal to $(\Psi/\sigma)(d\sigma/dT)$. We use this value of $\partial\Psi/\partial T$ in the later developments. However, it will be found that, provided $h > 0.6$, the resulting temperature effect on h is so small that we may safely put $\partial h/\partial T = 0$. Therefore we may take $\partial h/\partial T = 0$ in the full range of h.

Reverting to (4), we see that ρ_0 is a function of T only and h is a function of θ only. Therefore (4) becomes

$$\nabla\rho = h\frac{d\rho_0}{dT}\nabla T + \rho_0\frac{dh}{d\theta}\nabla\theta \tag{5}$$

Using (3) to evaluate $dh/d\theta$, we obtain

$$\nabla\rho = h\frac{d\rho_0}{dT}\nabla T + \frac{g\rho}{RT}\frac{\partial\Psi}{\partial\theta}\nabla\theta \tag{6}$$

Putting (6) in (1), we get an equation of the form

$$q_{vap}p/\rho_w = -D_{T vap}\nabla T - D_{\theta vap}\nabla\theta \tag{7}$$

where ρ_w gm cm^{-3} is the density of (liquid) water. We have thus separated the flux into two components, that due to the temperature gradient and that due to the moisture gradient. The evaluation of the isothermal vapor diffusivity, $D_{\theta vap}$, has been given elsewhere [*Philip*, 1955] and need not detain us at this point. Our interest is in the thermal vapor diffusivity $D_{T vap}$ which, according to the preceding simple theory, is given by

$$D_{T vap} = D_{atm}\nu\alpha h\beta/\rho_w \tag{8}$$

Here we have written β for $d\rho_0/dT$. β is, of course, temperature dependent, but we may reasonably adopt the constant value 1.05×10^{-6} gm cm^{-3} °C^{-1} as representative of the temperature range 10°C to 30°C, which will be typical for applications discussed in this paper.

As an illustrative example we have calculated $D_{T\text{vap}}$ (and the diffusivities $D_{T\text{liq}}$ and D_T to be defined later) for Yolo light clay on the basis of the $\Psi(\theta)$ and $K(\theta)$ relationships for this soil given by *Moore* [1939]. Further we have adopted the following values for constants occurring in (8): $\frac{1}{2}$ for α [*Penman*, 1940; *de Vries*, 1950b], 0.274 cm² sec⁻¹ for D_{atm} at 20°C [*Krischer* and *Rohnalter*, 1940], 1.73×10^{-6} gm cm⁻³ for ρ_0 at 20°C, 1.00 for ρ_w and 1.024 for ν at 20°C. The results are shown in Figure 1.

The original formulation of (1) by Penman was for the diffusion of CS_2 and CH_3COCH_3, neither of which, presumably, interacted with either the liquid or solid phases of the medium. Applications of this equation to water vapor by *Penman* and *Schofield* [1939], *de Vries* [1950a], *Gurr* and others, [1952], *Philip* [1953], *Taylor* and *Cavazza* [1954], *Rollins* and others [1954] have disregarded the interaction of the water vapor with the liquid and solid phases. We therefore remark at this stage that the failure of this theory of moisture transfer should occasion no surprise, and leave the question of how the theory is to be modified to a later point in this paper.

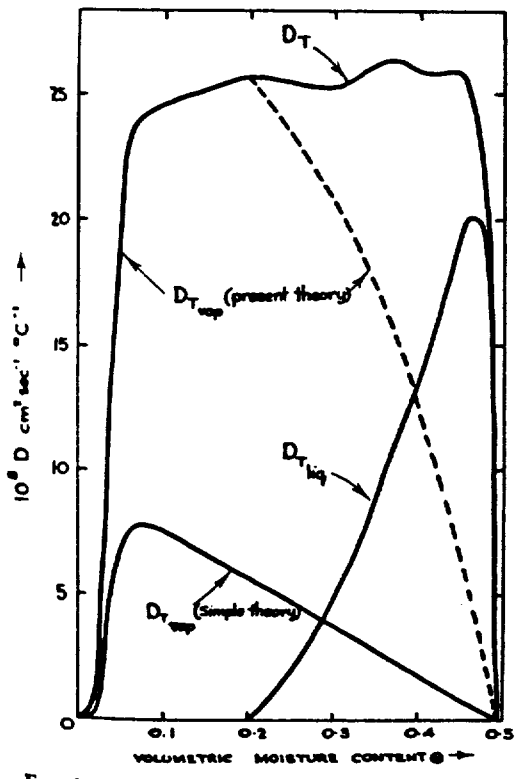

FIG. 1 – Thermal vapor diffusivity $D_{T\text{vap}}$, both according to the simple theory and according to the present theory; thermal liquid diffusivity $D_{T\text{liq}}$; thermal moisture diffusivity, D_T; all as functions of moisture content for Yolo light clay at 20°C

LIQUID TRANSFER

Liquid flow also enters into the general picture of soil-water phenomena involving temperature gradients. In this section we provide a general theory of liquid movement in porous media under temperature and moisture gradients. In the final section of the paper this is integrated with the approach to vapor transfer to provide a general theory of liquid and vapor transfer under temperature and moisture gradients.

Darcy's law for liquid transfer in unsaturated media [*Childs* and *Collis-George*, 1950] may be written

$$q_{\text{liq}}/\rho_w = -K\nabla\Phi \tag{9}$$

where q_{liq} is the vector liquid-flux density, gm cm⁻² sec⁻¹

K is the (unsaturated) hydraulic conductivity, cm sec⁻¹

Φ is the total potential, cm

If we regard Φ as comprising pressure and gravitational components

$$\Phi = \Psi + z \tag{10}$$

where z is the vertical ordinate, positive upwards.

It will be clear from the previous discussion that in the θ range where liquid transfer occurs ($K > 0$) Ψ is determined by capillarity, hence

$$\frac{\partial\Psi}{\partial T} = \frac{\Psi}{\sigma}\frac{d\sigma}{dT} = \gamma\Psi \tag{11}$$

Using (10) and (11) in (9), we obtain

$$q_{\text{liq}}/\rho_w = -K\gamma\Psi\nabla T - K(\partial\Psi/\partial\theta)\nabla\theta - Ki \tag{12}$$

where i is the unit vector in the positive z direction. Clearly (12) is of the form

$$q_{\text{liq}}/\rho_w = -D_{T\text{liq}}\nabla T - D_{\theta\text{liq}}\nabla\theta - Ki \tag{13}$$

We have thus separated the liquid flux into three components, that due to the temperature gradient, that due to the moisture gradient and that due to gravity. The latter two have received rather detailed treatment elsewhere [*Klute*, 1952; *Philip*, 1955, 1957a]; our special interest here is with the thermal liquid diffusivity, $D_{T\text{liq}} = K\gamma\Psi$. γ is temperature dependent, but we may reasonably adopt the constant value -2.09×10^{-2}°C⁻¹ as representative of the temperature range 10°C to 30°C. Using this value, and the K and Ψ data of Moore for Yolo light clay, we then obtain the

relationship for $D_{T\text{liq}}$ as a function of θ which is shown in Figure 1.

Here we tentatively accept the validity of this theory of the liquid transfer under temperature gradients. The results of *Richards* and others [1938] and *Gardner* [1955] suggest that the temperature coefficient of Ψ may exceed the temperature coefficient of σ. However the experiments of both papers include extraneous factors which make this interpretation of their data uncertain.

Interaction of Vapor and Liquid Phases

The disposition of liquid water in fairly dry media.—Let us examine the disposition of water in a fairly dry medium, so dry, we shall suppose, that liquid continuity does not exist or is, at any rate, so poor that K (and hence $D_{T\text{liq}}$) assume very small values; that is, $\theta < \theta_K$ where θ_K is the moisture content at which K falls to some small arbitrary fraction of its saturated value. (We use the term 'liquid' here to denote water capable of viscous flow. Of course, even when liquid continuity does not exist, the water molecules adsorbed on the surface of the matrix of the medium form bridges between the isolated pores or wedges of liquid water. According to *Quirk* [1955], a complete monolayer is adsorbed on soil at $h \simeq 0.20$; that is, at $\Psi \simeq -2.2 \times 10^6$ cm at 20°C.) The system will still contain liquid water, but this will occur (either wholly or almost wholly) in isolated pockets, filling small pores or forming wedges about the points of contact between the grains of the medium. Such an 'island' (as we shall call these pockets) is shown in Figure 2.

Movement of water through liquid islands during vapor transfer—The solid curves of Figure 2 show the two menisci of the island when it is in thermodynamic equilibrium with its surroundings. Note that the curvatures are equal. We now suppose that a vapor pressure gradient due to a temperature field produces a vapor flux in the direction indicated by the arrow of the figure. The resulting condensation at A and evaporation at B tends to decrease the curvature of A and increase the curvature at B. This continues until the capillary flow through the island produced by the growing difference of curvatures A and B equals the rate of condensation at A and the rate of evaporation at B. The broken curves represent the new menisci at A and B. It is easily checked that for all likely orders of magnitude of the island dimensions, the necessary change in curvature will be so small that it is simply and rapidly attained.

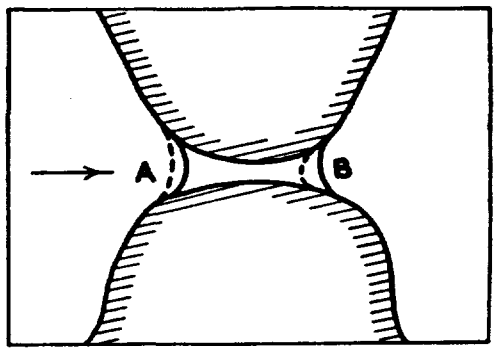

Fig. 2 – Moisture transfer through a liquid island. Arrow indicates direction of transfer

Moisture transfer in fairly dry media—We therefore regard moisture transfer under temperature gradients in fairly dry media as a series-parallel process of flow through regions of vapor and liquid. The vapor flux is determined by the vapor-pressure gradient across the air-filled pores; the flux through the liquid islands adjusts itself to equal this vapor flux.

A detailed analysis based on these ideas would involve investigation of the fine structure of the temperature and vapor fields in the air-filled pores. This would be very complicated and is not attempted here. Instead we evaluate q_{vap} on the basis of certain simplifying assumptions. We emphasize that this treatment must be regarded as no more than a first approximation; nevertheless it incorporates the essential ideas outlined above and will be seen to give results in fair agreement with the available experimental data.

The vapor flux density due to the temperature gradient in a single air-filled pore may be written as

$$-D_{atm}\rho_v h\beta(\nabla T)_a \qquad (14)$$

where $(\nabla T)_a$ denotes the temperature gradient in the pore. This expression follows immediately from equations (7) and (8) by substituting one for αa; its use presupposes similarity of temperature and vapor fields in the pore. This expression holds also for the mean flux density in all air-filled pores if, hereafter, we *reinterpret* $(\nabla T)_a$ as the average temperature gradient in these pores.

According to the ideas developed above, the total cross section available for transfer is equal to that occupied by air and liquid. We now assume that the mean flux density in the connecting liquid islands is equal to that in the air-filled pores, a concept which receives support from the above-mentioned property of the islands of accommodating the vapor flux.

The total vapor flux density due to the temperature gradient is thus

$$-(a+\theta)D_{atm}p\beta(\nabla T)_a = -D_{T\,vap}\nabla T \quad (15)$$

where $D_{T\,vap}$ now denotes the value of the thermal vapor diffusivity predicted by the revised theory. We introduce no tortuosity factor here since this is already taken into account in the average $(\nabla T)_a$.

The ratio η of the vapor transfer given by the present theory to that given by the simple theory follows from (7), (8), and (15)

$$\eta = \frac{a+\theta}{\alpha a} \cdot \frac{(\nabla T)_a}{\nabla T} \quad (16)$$

The first factor making up η, $(a+\theta)/\alpha a$, is simply evaluated. We denote the second, $(\nabla T)_a/\nabla T$, (that is, the ratio of the average temperature gradient in the air-filled pores to the overall temperature gradient) by the symbol ζ and proceed to indicate how it may be evaluated.

De Vries [1952ab] gives a method of calculating the thermal conductivity of soils by treating the soil as a continuous medium (water or air) in which 'particles' of soil and air or water are randomly dispersed. On the basis of certain plausible assumptions about the shape of these particles, values of the ratios between the average temperature gradients in the particles and in the medium can be computed from their respective thermal conductivities. The value of ζ follows immediately from these ratios and the volume fractions of the different components

$$\zeta = \frac{(\nabla T)_a}{a(\nabla T)_a + \theta(\nabla T)_w + (1-a-\theta)(\nabla T)_s} \quad (17)$$

where $(\nabla T)_a$, $(\nabla T)_w$ and $(\nabla T)_s$ are the temperature gradients averaged over the volumes occupied respectively by air, water, and solid.

Values of ζ at 20°C calculated in this way are shown in Table 2. Two values have been adopted for the thermal conductivity of the soil particles, namely, 7×10^{-3} cal cm^{-1} sec^{-1} °C^{-1}, which holds for most soil minerals [*de Vries*, 1952ab; *Smith*, 1942] and 20×10^{-3} cal cm^{-1} sec^{-1} °C^{-1}, which holds for quartz. The values computed for quartz are shown in brackets in the table. Values of the thermal conductivities of air and water at 20°C, 0.0615×10^{-3} and 1.42×10^{-3} cal cm^{-1} sec^{-1} °C^{-1}, were used. The additional apparent conductivity of the air due to the vapor transfer λ_{vap} was taken into account by the means indicated in the next section. Use of this table should give ζ accurately enough for approximate application of the theory in the temperature range 10°C to 30°C. Since λ_{vap} increases rapidly with increasing temperature it cannot be used for a wider range of temperatures.

Note on adsorbed phase—To this point we have neglected the possibility of transfer in the adsorbed phase. Examination of this aspect is complicated by the fact that surface migration is governed by the gradient of h rather than that of ρ. Part of the vapor that evaporates from or condenses on these surfaces may recirculate in a single air-filled pore through the process of surface migration. However, it seems unlikely to us that the total transfer can be much affected by diffusion in the adsorbed phase.

Note on terminology—A question of terminology arises. What we should call 'vapor' and what 'liquid' flux in this complicated series-parallel system. For some purposes there is little need to distinguish between the phases, but the distinction becomes important, for example, when the transfer of soluble salts under thermal gradients is studied.

We shall use the term 'liquid transfer' to describe the transfer which occurs exclusively in the liquid phase; all transfer in excess of the liquid transfer we shall term 'vapor transfer.' Thus in the absence of liquid continuity all transfer is vapor transfer. It is in this sense which we use $D_{T\,vap}$ in equation (15).

Moisture transfer with liquid continuity—When $\theta > \theta_K$ the preceding model fails. At moderate moisture contents continuity of both liquid and vapor phases may exist, together with islands of both phases. As θ increases still further vapor continuity fails and the system comprises vapor islands in a liquid continuum.

With increasing moisture content and increasing degree of liquid continuity, the liquid phase transfer due to temperature-induced capillary potential gradients becomes dominant. The decrease in vapor-induced transfer through the liquid islands may be attributed not only to a reduction in the number of islands and in the opportunity for vapor transfer, but also to a growth of the size of the

TABLE 2 – *Values of ζ at 20°C for different porosities and moisture contents*[a]

θ	Values of ζ for $a+\theta$ =		
	0.7	0.5	0.3
0.0	1.4 (1.4)	1.9 (2.0)	3.0 (3.2)
0.1	1.3 (1.4)	1.7 (1.9)	2.0 (2.7)
0.3	1.5 (1.6)	1.7 (2.0)	2.1 (2.9)
0.5	1.5 (1.6)	1.8 (2.2)	
0.7	1.6 (1.8)		

[a] Note that for $a = 0$, ζ means $\lim_{a \to 0} \zeta(a)$.

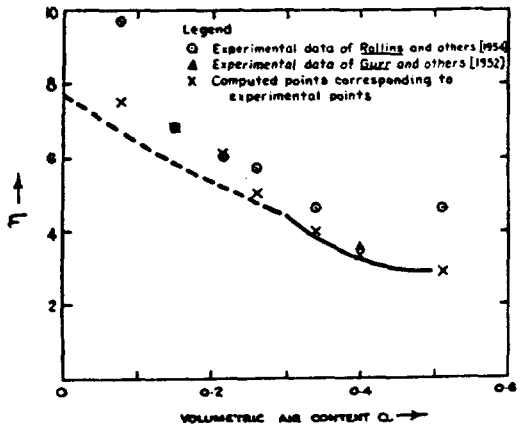

FIG. 3 – Ratio of 'vapor' transfer (either as predicted by present theory or observed) to prediction of simple theory, η, as a function of volumetric air content a; curve shows theoretical relationship for Yolo light clay.

islands which remain and an increase in the radii of curvature of the menisci to the point where automatic adjustment to the vapor flux is no longer possible.

This system will be even more complicated to analyze than the one without liquid continuity. It is reasonable to suppose, however, that, as θ increases above the value θ_K, the effective cross-section for combined liquid-vapor transfer will decrease steadily. This may be expressed by replacing $a + \theta$ in (15) by a factor $a + f(a)\theta$, where $f(a) = 1$ for $a \geq a_K$; a_K denotes the value of a at $\theta = \theta_K$. As a first approximation we tentatively propose $f = a/a_K$; thus $f \to 0$ as $a \to 0$.

In Figure 1 we show for comparative purposes $D_{T\text{vap}}$ for Yolo light clay computed by means of the present theory. In the calculations we assumed that the sand fraction of the soil (23.8 per cent) consisted of quartz; we also used the value $\theta_K = 0.2$, in accordance with Moore's data. The corresponding $\eta(a)$ relationships for Yolo light clay is shown by the curve of Figure 3. We recognize the uncertainty of the basis for computing η for $a < a_K$ by using a broken curve in this region.

We are now in a position to explain and reconcile the experimental data introduced at the beginning of this paper.

A Reconciliation of the Facts

(a) *The large value of the apparent vapor transfer* —None of the methods employed by the experimenters listed in Table 1 distinguishes between pure vapor transfer and series-parallel transfer through a vapor continuum and liquid islands. (To the tabulated list we may add the technique of *Hadley* and *Eisenstadt* [1955], who attempted to distinguish the phases by using a radioactive tracer salt.) In other words, rather than distinguishing phases, these methods indicate as liquid phase movement only that which occurs exclusively in the liquid continuum; that is, the definitions of liquid transfer and vapor transfer we adopt agree with the suppositions of the experimenters.

The data of *Rollins* and others [1954] are the most suitable for a comparison of theory and experiment, since no appreciable liquid flow from cold to warm occurred in their columns, the cold and the warm side being connected by a capillary tube with a resistance to liquid flow small in comparison with the resistance of the column itself. As a consequence moisture was fairly evenly distributed in the columns throughout the experiments and in most experiments no moisture gradient existed in the center part of the column.

'Experimental' values of η deduced directly from their data are given in Table 1 and shown by open circles on Figure 3. The corresponding values of $\eta(a)$ predicted by the present theory (that is, computed from the data of *Rollins* and others [1954] on porosity, etc.) are shown by crosses. For computing points at small a, it was necessary to assume a value of $a_K(0.2)$, since no Ψ or K data were given for the silt loam of these experiments, and to adopt the values of f suggested in the previous section. The agreement between the experimental points and the theoretical values is quite satisfactory in view of the approximate character of the analysis and the possible experimental errors, which we estimate to be of the order of five to ten per cent. No explanation can be offered for the comparatively large discrepancy at $a = 0.51$; the experimental value for this case appears to be rather high in comparison with the other experimental data. For $a = 0.078$ the differences between observed and calculated values may be caused by the fact that the contribution of liquid flow ($= -D_{T\text{liq}}\nabla T$) has not been taken into account. This cannot be checked, however, as no data on $D_{T\text{liq}}$ are available for this soil.

The single experimental value of η given by *Gurr* and others [1952] is also in good agreement with the value computed from our theory. These are shown by the triangle and the corresponding cross on Figure 3. This may be partly fortuitous since the experimental value is an average over five days with changing moisture distribution. However, the vapor transfer was calculated by *Gurr* and others [1952] for "the plane at which the initial water content remained unchanged."

The large values of η deduced from the experi-

ments of Taylor and Cavazza have not been included in Figure 3 since the analysis of these experiments is greatly complicated by the presence of air gaps in the soil columns. From an estimate of the thermal conductivities of the soil slices we calculate the temperature gradient in these gaps to be about four times as large as the mean temperature gradient. This leads to a calculated vapor flux across the gaps adjoining the central slice approximately ten per cent higher than the observed flux. This could mean that the central slices act as 'islands' with moderately low resistance to moisture flow. In fact the observed moisture gradients in the slices would cause a flow from warm to cold. We stress, however, that these experiments cannot really be analysed quantitatively on the basis of the available data.

We revert to the experiments of *Rollins* and others [1954] to remark on the influence of temperature on the observed vapor transfer. These authors measured vapor transfer in the same columns (that is, at the same values of a and θ) over different temperature ranges; namely 40°C − 2°C, 30°C − 2°C, 20°C − 1°C, and 10° − 0°C. The temperature coefficient of the observed vapor transfer was only slightly smaller than that given by the simple theory, but agreed even better with that predicted by the present theory, this being due to a small negative temperature coefficient of ζ.

(b) *Effect of moisture content on net moisture transfer*—Before explaining the data of *Smith* [1943], *Jones* and *Kohnke* [1952], *Gurr* and others [1952] on the variation of thermal moisture transfer with mean initial moisture content, we recall that these experiments were on closed systems, so that their observations were not of total moisture transfer, but of the net transfer. When the mean moisture content was so low that no liquid continuity existed in the column (and this was so for the drier columns of these experiments), the net transfer observed was in fact equal to the total transfer. At this moisture level transfer will be exclusively vapor transfer (using the terminology we propose), so that the transfer increases rapidly with moisture content rather like $D_{T\text{vap}}$. Since in each column there will exist a range of θ, which increases with the net transfer, the experimental results will tend to represent a smoothed $D_{T\text{vap}}$ curve.

This situation changes radically once θ exceeds θ_g. Then a liquid phase return flow produced by the moisture gradient will tend to balance the thermal vapor transfer and reduce the net transfer. This will begin to operate when part of the column attains a moisture content greater than θ_g, and we should expect net transfer to decrease rapidly as θ increases, until it becomes effectively zero when the mean θ is a little in excess of θ_g. It follows that the maximum net transfer will occur at a mean θ somewhat less than θ_g; exactly how much less than θ_g will depend, among other things, on the length of the column and the duration of the experiment.

We recall the data of Jones and Kohnke and other investigators on the effect of texture on the point of maximum observed net transfer; namely, that this point occurs at small tensions but rather low moisture contents in coarse-textured soils, while in fine-textured soils it occurs at greater tensions but at relatively high moisture contents. The effect of texture on θ_g is entirely parallel to this [*Moore*, 1939]. This parallelism may seem fortuitous; however, the preceding discussion of the relationship between θ_g and the point of maximum transfer suggests the existence of a real physical relationship.

It is thus seen that the present theory accounts both for the rapid increase with mean moisture content up to the point of maximum net transfer and for the steep decrease as θ increases further. It also explains the way in which the effect of mean moisture content on net transfer varies with soil texture.

(c) *The transfer of latent heat by distillation*—According to the simple theory the heat flux by distillation would be $-LD_{\text{atm}}\nu a a h \beta \nabla T$ where L is the latent heat of vaporization of water. A similar expression was given by *de Vries* [1950a] in a first attempt to assess the influence of vapor diffusion on heat transfer in soils.

In subsequent papers *de Vries* [1952ab] developed a method of calculating the thermal conductivity of soils from their composition. Here a more rational method of taking the distillation effect into account, first suggested by *Krischer* and *Rohnalter* [1940], was adopted. In this method the contribution of vapor distillation to the heat transfer is first calculated for the air-filled pores separately. It follows immediately from (14) that this produces an apparent increase of the thermal conductivity in these pores by an amount λ_{vap} given by

$$\lambda_{\text{vap}} = LD_{\text{atm}}\nu h \beta \qquad (18)$$

(De Vries used an expression for λ_{vap} equivalent to (18) but with $h = 1$ and applied the results at moisture contents above 'wilting percentage.' For smaller moisture contents he assumed linear decrease of λ_{vap} with θ. Eq. (18) is more general,

applying to the full range of h and θ. Note that λ_l, $\lambda_l^{(v)}$ in *de Vries* [1952ab] correspond to our λ_a, λ_{vap}.) Then in calculating λ, the overall thermal conductivity of the soil, the value $\lambda_a + \lambda_{vap}$ is inserted for the conductivity of the air-filled pores, λ_a being the normal thermal conductivity of air.

This theory predicts thermal conductivities for a wide variety of soils and for the temperature range 0 to 75°C in good agreement with experimental data. (A difficulty arises in computing λ in a narrow range of low moisture contents for reasons unrelated to the present discussion. We refer to the original papers for treatment of this point.)

This second theory of the distillation effect is seen to be entirely consistent with the present theory of thermal moisture transfer. In principle one should also take into account sensible heat transfer by liquid flow through the islands. This can easily be shown to be negligible.

(d) *Effect of air pressure on apparent vapor transfer*—The explanation of the data of *Jennings* and others [1952] involved the concept of vapor diffusion as the governing mechanism and depended only on this aspect of the simple theory. The present theory retains this concept and therefore agrees just as well with the observation that transfer decreases as gas pressure increases.

The situation, then, is that the present theory retains the concept of vapor diffusion as the governing mechanism of transfer (at least in dry soils), which had received support from the observations of (c) and (d), and at the same time provides a quite comprehensive (and reasonably quantitative) explanation of the apparently conflicting evidence presented under (a) and (b).

Relation of the present theory to that of Smith [1943]—There are certain points of similarity between the present theory and that of *Smith* [1943]. The distinction is, essentially, that Smith envisaged the process of vapor distillation as triggering off the transfer in a series of discrete steps, while it appears to us that the process will very rapidly become continuous. By treating it as such we have been able to make this first attempt at analyzing the phenomenon quantitatively. In addition, we have, of course, attempted to take into account the fine structure of the temperature field in the medium.

The Equations of Moisture and Heat Transfer

We conclude this paper by presenting the system of equations which describe moisture and heat transfer under combined moisture and temperature gradients in porous materials. We begin by reverting to (7) for the vapor transfer, which we previously derived from the simple vapor theory; we now require to reinterpret the diffusivities of (7) in terms of the present theory.

The simple theory gives for the isothermal vapor diffusivity

$$D_{\theta vap} = \frac{D_{atm} v \alpha a g \rho}{\rho_w RT} \frac{\partial \Psi}{\partial \theta} \qquad (19)$$

The mechanism of transfer operating in the thermal case fails here, since the vapor pressure gradient is now due solely to the moisture gradient, and in general, very small changes in the curvature of a meniscus will be sufficient to reverse the direction of vapor movement. Accordingly, the simple theory may be expected to hold reasonably well for isothermal vapor transfer, that is, the values of $D_{\theta vap}$ given by *Philip* [1955] and (19) should be reasonably correct. (The D_{vap} of *Philip* [1955] corresponds to $D_{\theta vap}$ here. He omitted the factor v (which, as we remark above, is close to unity for most applications to nature) and also the factor $1/\rho_w$, so that although numerically correct, his D_{vap}, as it stands, is in the units gm cm^{-1} sec^{-1}. This view is supported by the data of *Staple* and *Lehane* [1954].

We also use here (12) and (13), describing liquid phase movement. Combining (13) with (7) we obtain

$$q/\rho_w = -D_T \nabla T - D_\theta \nabla \theta - Ki \qquad (20)$$

where q gm cm^{-2} sec^{-1} is the total flux density of water, and

$$D_T = D_{Tliq} + D_{Tvap} \qquad (21)$$

$$D_\theta = D_{\theta liq} + D_{\theta vap} \qquad (22)$$

D_T, the thermal moisture diffusivity, has been computed for our illustrative Yolo clay and is shown in Figure 1. The relative constancy of D_T over a large part of the θ-range must be regarded as a coincidence due to the fact that in this case the maximum values of D_{Tliq} and D_{Tvap} are of about the same order of magnitude. We expect that in coarser-textured soils than the Yolo light clay the maximum value of D_{Tliq} will exceed the maximum of D_{Tvap} and tend to dominate the shape of D_T. Conversely, our expectation is that D_{Tvap} would be more important in finer-textured soils and would largely determine the shape of D_T. D_θ, the isothermal moisture diffusivity, has been discussed elsewhere [*Philip*, 1955].

Differentiating (20) and applying the continuity

requirement, we obtain the general differential equation describing moisture movement in porous materials under combined temperature and moisture gradients

$$\frac{\partial \theta}{\partial t} = \nabla \cdot (D_T \nabla T) + \nabla \cdot (D_\theta \nabla \theta) + \frac{\partial K}{\partial z} \quad (23)$$

Eq. (23) depends, among other things, on the uniqueness of the $\Psi(\theta)$ relation. The existence of hysteresis in $\Psi(\theta)$ [*Haines*, 1930], which may occur if some parts of the medium are gaining moisture and other parts are losing it, may invalidate the use of (20).

It is seen that the significant characteristics of the soil are the diffusivities, D_T and D_θ, and the hydraulic conductivity K. When more detail is required D_T and D_θ must be split into their components $D_{T\text{liq}}$, $D_{T\text{vap}}$; $D_{\theta\text{liq}}$, $D_{\theta\text{vap}}$. The two liquid diffusivities tend to be the most important ones at high moisture contents, whilst the two vapor diffusivities are dominant at low moisture contents.

Finally, we may write the heat conduction equation for the soil

$$C\frac{\partial T}{\partial t} = \nabla \cdot (\lambda \nabla T) - L\nabla \cdot (D_{\theta\text{vap}} \nabla \theta) \quad (24)$$

where C cal cm^{-3} °C^{-1} is the volumetric heat capacity of the soil and λ cal sec^{-1} cm^{-1} °C^{-1} is the thermal conductivity (including the thermal distillation effect). Eq (24) is more general than the customary equation, the second term on the right-hand side representing distillation effects induced by the moisture gradient. It will be noted that (23) and (24), both equations of the diffusion type involving θ- and T-dependent diffusivities and conductivities as well as gradients of both θ and T, together govern the simultaneous moisture and heat fields in the soil.

References

CARMAN, P. C., Properties of capillary-held liquids, *J. Phys. Chem.*, **57**, 56–64, 1953.

CARMAN, P. C., AND F. A. RAAL, Physical adsorption of gases on porous solids, I, *Proc. R. Soc.*, London, **209A**, 59–69, 1951.

CHILDS, E. C., AND N. COLLIS-GEORGE, The permeability of porous materials, *Proc. R. Soc.*, London, **201A**, 392–405, 1950.

DE VRIES, D. A., Some remarks on heat transfer by vapour movement in soils. *Trans. 4th Intern. Cong. Soil Sci.*, **2**, 38–41, 1950a.

DE VRIES, D. A., Some remarks on gaseous diffusion in soils. *Trans. 4th Intern. Cong. Soil Sci.*, **2**, 41–43, 1950b.

DE VRIES, D. A. Het warmtegeleidingsvermogen van grond, *Med. Landbouwhogeschool*, Wageningen, **52**, 1-73, 1952a.

DE VRIES, D. A., The thermal conductivity of granular materials, *Annexe 1952-1 Bul. Inst. Intern. du Froid*, 115–131, 1952b.

EDLEFSEN, N. E., AND A. B. C. ANDERSON, The thermodynamics of soil moisture, *Hilgardia*, **16**, 31–299, 1943.

GARDNER, R., Relation of temperature to moisture tension of soil, *Soil Sci.*, **79**, 257–265, 1955.

GURR, C. G., T. J. MARSHALL, AND J. T. HUTTON, Movement of water in soil due to a temperature gradient, *Soil Sci.*, **74**, 335–345, 1952.

HADLEY, W. A., AND R. EISENSTADT, Thermally actuated moisture migration in granular media, *Trans. Amer. Geophys. Union*, **36**, 615–623, 1955.

HAINES, W. B., Studies in the physical properties of soils, V, *J. Agr. Sci.*, **20**, 97–116, 1930.

JENNINGS, J. E., P. R. B. HEYMANN, AND L. WOLPERT, Some laboratory studies of the migration of moisture in soils under temperature gradients, *S. Afr. Nat. Build. Res. Inst. Bul.*, *9*, pp. 29–46, 1952.

JONES, H. E., AND H. KOHNKE, The influence of soil moisture tension on vapor movement of soil water, *Soil Sci. Soc. Amer. Proc.*, **16**, 245–248, 1952.

KLUTE, A., A numerical method for solving the flow equation for water in unsaturated materials, *Soil Sci.*, **73**, 105–116, 1952.

KRISCHER, O., AND H. ROHNALTER, Wärmeleitung und Dampfdiffusion in feuchten Gutern, *Verein Deut. Ing.-Forschungsheft 402*, 1940.

MACHE, H., Über die Verdunstungsgeschwindigkeit des Wassers in Wasserstoff und Luft, *Math. Naturwiss. Sitz.Ber.*, Wien, **119**, 1399, 1910.

MCBAIN, J. W., *The sorption of gases and vapours by solids*, Routledge, London, 577 pp., 1932.

MOORE, R. E., Water conduction from shallow water tables, *Hilgardia*, **12**, 383–466, 1939.

PARTINGTON, J. R., *Advanced treatise on physical chemistry*, vol. 1, Longmans, Green and Co., London, 943 pp., 1949.

PENMAN, H. L., Gas and vapour movement in soil, I, *J. Agr. Sci.*, **30**, 437–462, 1940.

PENMAN, H. L., AND R. K. SCHOFIELD, Note submitted to 7th General Assembly of International Union of Geodesy and Geophysics, 1939.

PHILIP, J. R., Vapour movement in a soil mass with periodic surface temperature, *Aust. Conf. in Soil Sci. Proc. 2*, 4.4.1-7, 1953.

PHILIP, J. R., The concept of diffusion applied to soil water, *Proc. Nat. Acad. Sci. India*, **24** A, 93–104, 1955.

PHILIP, J. R., The theory of infiltration, part 1, *Soil Sci.*, **83** (in press), 1957a.

PHILIP, J. R., The physical principles of soil water movement during the irrigation cycle, *Proc. 3rd Int. Cong. Irrig. Drainage* (in press), 1957b.

QUIRK, J. P., Significance of surface areas calculated from water vapour sorption isotherms by use of the B.E.T. equation, *Soil Sci.*, **80**, 423–430, 1955.

RICHARDS, L. A., M. B. RUSSELL, AND O. R. NEAL, Further development on apparatus for field moisture studies, *Soil Sci. Soc. Amer. Proc.* (1937), **2**, 55–63, 1938.

ROLLINS, R. L., M. G. SPANGLER, AND D. KIRKHAM, Movement of soil moisture under a thermal gradient, *Highway Res. Board Proc.* **33**, 492–508, 1954.

SCHIRMER, R., Die Diffusionszahl von Wasserdampf-Luftgemischen und die Verdampfungsgeschwindig-

keit, *Zs. Ver. Deut. Ing., Beihefte Verfahrenstecknik 6*, 1938.

SMITH, W. O., The thermal conductivity of dry soil, *Soil Sci.*, **53**, 439–459, 1942.

SMITH, W. O., Thermal transfer of moisture in soils, *Trans. Amer. Geophys. Union*, **24**, 511–523, 1943.

STAPLE, W. J., AND J. J. LEHANE, Movement of moisture in unsaturated soils, *Canad. J. Agric. Sci.*, **34**, 329–342, 1954.

SUMMERHAYS, W. E., A determination of the coefficient of diffusion of water vapour, *Proc. Phys. Soc.*, **42**, 218–225, 1930.

TAYLOR, S. A., AND CAVAZZA, L., The movement of soil moisture in response to temperature gradients, *Soil Sci. Soc. Amer. Proc.*, **18**, 351–358, 1954.

VAN BAVEL, C. H. M., Gaseous diffusion and porosity in porous media, *Soil Sci.*, **73**, 91–104, 1952.

C.S.I.R.O., Division of Plant Industry, Deniliquin, N. S. W., Australia.

(Communicated manuscript received July 2, 1956, and, as revised, December 3, 1956; open for formal discussion until September 1, 1957.)

SORPTION

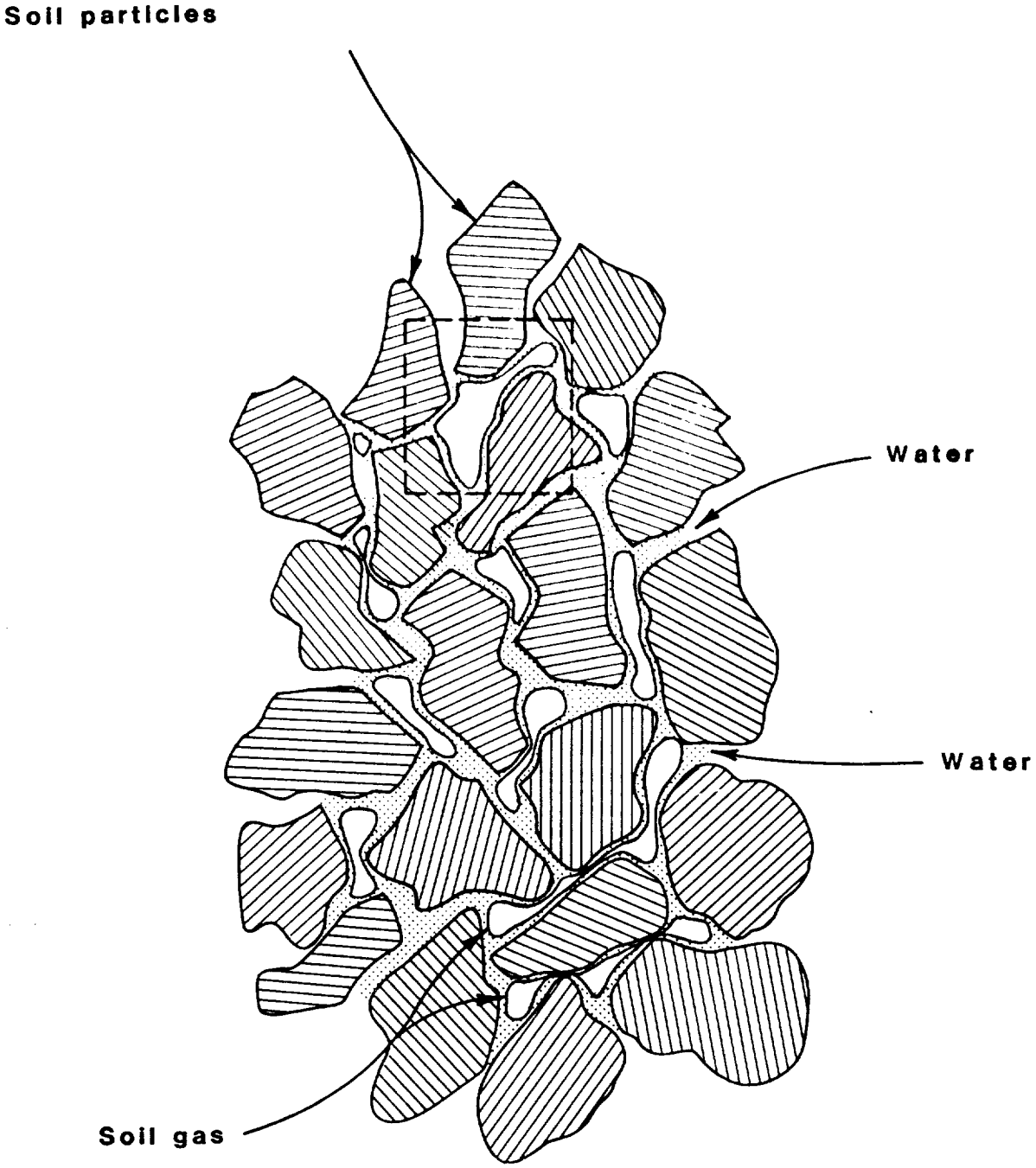

SOLUTE VELOCITY RETARDED BY SORPTION

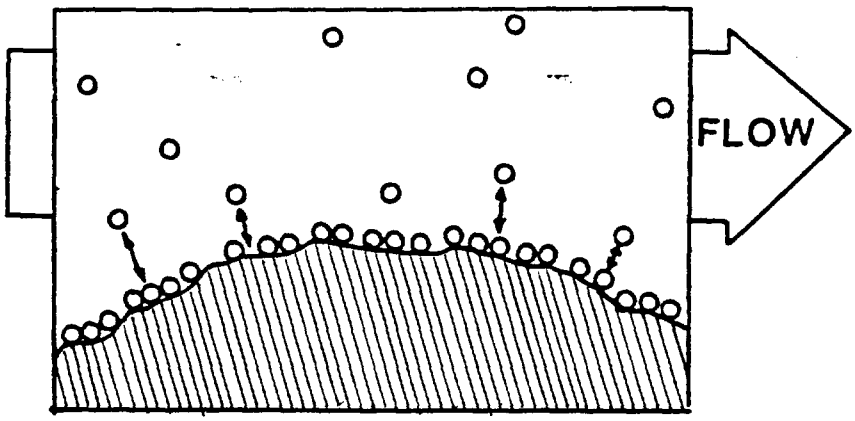

$$\frac{V_{water}}{V_{solute}} = \text{Retardation}$$

RETARDATION FACTORS

Compound	PERCENT ORGANIC CARBON		
	0.1%	1%	2%
Benzene	1.5 - 1.6	6 - 7	11 - 13
Toluene	1.6 - 3.8	7 - 29	13 - 57

Typical of Volatile organics

for PAHs 91-2500

Water Research Vol. 13, pp. 241 to 248
© Pergamon Press Ltd 1979. Printed in Great Britain.
0043-1354/79/0301-0241$02.00/0

SORPTION OF HYDROPHOBIC POLLUTANTS ON NATURAL SEDIMENTS

SAMUEL W. KARICKHOFF, DAVID S. BROWN and TRUDY A. SCOTT

Environmental Research Laboratory, U.S. Environmental Protection Agency, College Station Road, Athens, GA 30605, U.S.A.

(*Received* 4 *September* 1978)

Abstract—The sorption of hydrophobic compounds (aromatic hydrocarbons and chlorinated hydrocarbons) spanning a concentration range in water solubility from 500 parts per trillion (ppt) to 1800 parts per million (ppm) on local (North Georgia) pond and river sediments was investigated. The sorption isotherms were linear over a broad range of aqueous phase pollutant concentrations. The linear partition coefficients (K_p) were relatively independent of sediment concentrations and ionic strength in the suspensions. The K_p's were directly related to organic carbon content for given particle size isolates in the different sediments. On an organic carbon basis ($K_{oc} = K_p$/fraction organic carbon), the sand fraction (> 50 μm particle size) was a considerably less effective sorbent (50–90% reduction in K_{oc}) than the fines fraction (< 50 μm particles). Differences in sorption within the silt and clay fractions were largely related to differences in organic carbon content. Reasonable estimates of K_{oc}'s can be made from octanol/water distribution coefficients, which are widely catalogued or easily measured in the laboratory.

INTRODUCTION

The fate of hydrophobic organic pollutants (compounds having a water solubility of less than a few parts per million) in a natural water system is highly dependent upon their sorptive behavior. In addition to affecting the physical movement of pollutants, sorption can be involved directly in pollutant degradation via surface-associated chemical processes. Moreover, natural sediments can indirectly mediate solution-phase processes by altering the pollutant concentration in solution or by providing a buffered solution-phase ion suite that may affect the dielectric properties and acidity of the solution phase. A realistic key to predicting the environmental fate of hydrophobic compounds then, lies in an understanding of sediment-related processes.

Existing data point to a large number of different sorbent properties as keys to sorption in given situations (Hamaker, 1975; Pionke & Chesters, 1973; Bailey & White, 1970). The high degree of variability and complexity in sediment composition and potential sorptive interactions seems to preclude the possibility of developing a simple, systematic procedure for predicting sorption parameters. A general predictor, on the other hand, that would take into account detailed sorbent structure and associated physical properties would be useless for most applications because of its complexity. Acceptability of a predictor depends upon the use to be made of the resulting number(s), the span of environmental conditions over which the predictor is to be applied, and the degree of accuracy or precision required in its usage. The primary goal is to define a limited set of sorbent properties that can generate a sorption predictor (generally within a factor of 2) over a broad range of environmental conditions in sediment–water systems.

Significant contributions to the systematization and estimation of sorption in natural systems are the works of Lambert (1966, 1978, 1968) and co-workers (Lambert *et al.*, 1965). Lambert has demonstrated that for a given soil type, the sorption of neutral organic pesticides can be well correlated with the organic matter content of the soil. His approach corrects for sorptive differences in different soil types by defining an 'effective organic matter', which is derived for a given soil by normalizing soil sorption of a known compound to a reference or standard soil system. Lambert and others (Briggs, 1969; Hance, 1969) have utilized an extrathermodynamically based framework, similar to that used by Bark & Graham (1966) for chromatographic sorbents, to compute sorption constants. Lambert further suggested that the role of soil organic matter was similar to that of an organic solvent in solvent extraction and that the partitioning of a neutral organic compound between soil organic matter and water should correlate well with its partitioning between water and an immiscible organic solvent. Briggs (1973) developed a regression equation relating the soil sorption of phenyl urea herbicides to their octanol–water partitioning.

The work of Lambert and Briggs was done in pesticide-soil systems as was the overwhelming majority of sorption work in systems of environmental interest. The interrelationship of the sorption behavior of soils and sediment is largely unknown. Poinke & Chesters

Mention of trade names or commercial products does not constitute endorsement or recommendation for use by the U.S. Environmental Protection Agency.

Table 1. Materials used in study

Material	Description
Sediments	
Doe Run	Small pond sediment—grass watershed Sand (50%)*, silt (50%), clay (1%)
Hickory Hill	Small pond sediment—wooded watershed sand (50%), silt (50%), clay (1%)
Oconee River	Small river—sand (90%), silt (5%), clay (5%)
Class 1 hydrophobic compounds	
Pyrene	K & K Labs; recrystallized from ethanol
Methoxychlor	EPA, Research Triangle Park, NC; Standard—used as received
Tetracene	Analabs, Inc.; used as received
Anthracene	Analabs, Inc.; used as received
9-Methylanthracene	K & K Labs.; recrystallized from ethanol
Phenanthrene	K & K Labs.; recrystallized from ethanol
2,4,6,2',4',6'-Hexachlorobiphenyl	RFR Corp.; used as received
Class 2 hydrophobic compounds	
Naphthalene	Baker; extracted with, and recrystallized in, hot water
2-Methylnaphthalene	Eastman; extracted with, and recrystallized in, hot water
Benzene	Fisher; spectrograde, used as received

* Approximate particle size distribution in parentheses.

(1973) have reviewed interactions of pesticides with sediment–water systems and have outlined compositional distinctions between soils and sediments that can affect sorption. A key distinction between the two systems is particle size composition and its potential impact upon environmental behavior. Sediments are largely eroded soils that have been subjected to continuous redispersion and particle-size fractionation commencing with runoff and continuing with subsequent water-system processes. These processes are highly dependent upon the dynamics of the specific stream, river, pond, or lake and upon the dispersion properties of the parent soil. One result is that sediment within a given water compartment may contain a very narrow range of particle sizes. For example, a suspended sediment within a river system may be largely clay, a bottom sediment from the middle of the river largely sand, and a bottom sediment from the edge largely silt. Functional dependence on particle size could vary the degree of sorption in different river compartments or produce a nonuniform distribution of sorbed pollutant within the sediment. Richardson & Epstein (1971) showed that two hydrophobic compounds, DDT and methoxychlor, tend to concentrate in finer particle sizes (clay), whereas the more soluble endosulfan preferred coarser material.

The work reported investigated the sorption of polycyclic aromatics and chlorinated hydrocarbons, two hydrophobic organic families, on river and pond sediments. Special emphasis was placed on the sorption role of sediment particle size and organic matter content and upon the correlation of sorption with sorbate aqueous solubility and octanol/water distribution coefficients.

MATERIALS AND METHODS

Sediment preparation

The three bottom sediments (Table 1) collected for study provide a range of water sources and associated compositional differences; no effort was made to collect samples that would characterize a given source or geographical region. Particle size fractionation procedures were similar to those of Jackson (1956) except that no dispersants or other additives were used. The sand and silt fractions were separated by sedimentation and the clay retained in the suspended form. The sand and silt fractions were washed 5 times with the first two washes being retained for further separation. The particle size separates were: sand (>50 m), coarse silt (50–20 μm), medium silt (20–5 μm), fine silt (5–2 μm), and clay (>2 μm). Galbraith Laboratories, Inc., Knoxville, TN, performed the organic carbon analyses. Organic carbon was determined as total carbon (Leco dry combustion) minus inorganic carbonates (gas purge of acidified suspensions).

Sorption isotherms

Adsorption isotherms for a series of hydrophobic compounds (Table 1) were run by a variety of methods dependent upon the water solubility and volatility from sediment suspensions of the materials.

All isotherm determinations involved the equilibration at 25°C (±1°C) of variable concentrations of compound with constant concentrations of sediment. The sorbent concentrations (air-dry mass basis) generally used were 400 mg ml^{-1} of suspension for sand, 20 mg ml^{-1} for coarse and medium silt, 10 mg ml^{-1} for fine silt and 1 mg ml^{-1} for clay. These concentrations varied somewhat depending upon the amount of sediment fraction available.

The amounts of a given compound added to the sediment samples were chosen to give, on the high and low concentration ends of the isotherm, solution concentrations approximately 50 and 10%, respectively, of the compound water solubility. Each isotherm involved at least 12 interim points, and all isotherms were replicated at least once. Compounds were handled so as to minimize

exposure to laboratory lighting except in cases where light stability was checked. The mixing of the compounds and sediments proceeded in one of two ways:

1. Class 1 compounds (low volatility materials having water solubility of < 500 ppb). These low-water-solubility compounds are difficult to store and transfer in aqueous solutions. Also, the major portion of these compounds tended to sorb when an aqueous solution of the compound was mixed with sediment, which prevented the achievement of the desired isotherm span. To circumvent these problems, the compounds were 'plated' out of hexane or isooctane solutions onto Erlenmeyer flasks. Sediment suspensions were added, and the containers swirled on an oscillating shaker until equilibrium was achieved. Equilibration, as judged by sequential sampling, was generally achieved within 24 h. Unless the compound started to show losses (e.g. 3-ring polycyclics), however, the suspensions were allowed to mix for 48 h.

2. Class 2 compounds (volatile materials having a water solubility of ≥ 500 ppb). Aliquots of aqueous stock solutions of the hydrophobic compounds were mixed with sediment suspensions in stainless steel centrifuge tubes fitted with a sealable cap. Compound attenuation prohibited the attainment of a stable equilibrium such as was achieved for the previous group of compounds; 4–8 h of shaking was generally sufficient to produce a fairly constant (variation < 10%) partition response, yet not result in compound attenuation in excess of 10% of the total present.

Subsequent to compound–sediment equilibration, the suspensions were centrifuged at 20,000 rev min^{-1} (Sorvall RC2-B with SS-34 rotor) for 60 min. Analyses were run on water phase aliquots taken from the upper portion of the centrifuge tube; sorbed compound concentrations were computed by difference based on the total compound added. Mass balance was checked on about half of the samples by soxhlet extraction of the sediment phase with hexane. Recoveries were in excess of 90% for all compounds.

Analyses for polycyclic hydrocarbons were conducted by u.v. light absorption on a Perkin–Elmer 356 spectrophotometer; chlorinated hydrocarbon analyses were performed on a Tracor 222 gas chromatograph equipped with a Ni^{63} electron capture detector and a 3% SE-30 Gas Chrom Q Column.

Partitioning as measured via sediment–water phase separation effected by filtering the suspensions through Zitex membranes (75-F, 2–5 μm pore size, Chemplast, Inc., Wayne, NJ) was compared with centrifugation results for both pyrene and methoxychlor for Doe Run medium and coarse silt. Consecutive aliquots of the filtrate were analyzed until a constant response was obtained indicative that the test compound was not being further removed by the filter material.

Desorption isotherms for pyrene and methoxychlor were run on the Doe Run coarse silt. Sediment that had been equilibrated with the compounds was removed by sedimentation and centrifugation (to remove any unsettled particles). The compound-spiked sediment was resuspended and allowed to equilibrate under swirling for 24 h and partitioning was determined as in previous adsorption runs.

The dependence of adsorption isotherms on sediment concentration and salt content was determined for pyrene on the Doe Run medium silt. Silt concentrations were varied from 2 to 20 mg ml^{-1} in 2 mg ml^{-1} increments while keeping the pyrene concentration relative to dry mass sediment constant. In the salt-spiked isotherms, a series of isotherms were run wherein the NaCl additions to the suspensions were varied from 0 to 20 mg ml^{-1} of suspension in increments of 2 mg ml^{-1}.

Octanol water partitioning

Reagent grade octanol was extracted once with 0.1 N NaOH, twice with distilled water, and was subsequently distilled twice. The compounds were prepared in octanol at or near saturation concentrations for the solids or approximately 0.1% for liquids. A small volume of this octanol solution (1–5 ml) was equilibrated with variable volumes of water (determined by the amount of compound required for analysis and thus the analytical sensitivity and water solubility of the compound). After equilibration, the phases were separated and each phase analyzed for the designated compound. For many compounds (especially Class 1 compounds), a crystalline third phase appeared upon mixing the spiked octanol with water; in the presence of the crystalline phase, the aqueous phase concentrations were generally within experimental error of the distilled water solubilities. Phase separation for nonvolatile (class 1) compounds involved standing plus centrifugation to further resolve the phases. The volatile compounds (class 2) were equilibrated in sealed centrifuge tubes, centrifuged, and the liquid phases sampled out of the tubes. In all cases, the octanol-phase samples were diluted with hexane or isooctane for analysis; the water phase samples were extracted with hexane.

Additional distribution ratios were determined at reduced concentrations (i.e. water concentrations ≤ half the water solubility) by dilution of the stock octanol solutions prior to mixing with water. The presence of interfering, more-water-soluble-impurities was checked by sequentially equilibrating the spiked octanol with aliquots of water, and establishing the constancy of the partitioning ratio. All determinations were in quadruplicate, with at least eight total determinations per compound.

RESULTS AND DISCUSSION

Sorption isotherms on particle size isolates

In-depth studies of the dependence of sorption on sediment particle size and organic matter content were carried out on pyrene and methoxychlor. Representative adsorption isotherms on the particle size isolates are shown in Figs. 1 and 2. General features concerning the isotherms include:

1. The adsorption data for all systems fitted well to linear isotherms over a broad range of water phase concentrations. That is,

$$X = K_p C \quad (1)$$

where X denotes the concentration of sorbate on the sediment, relative to dry weight (for these compounds, conveniently expressed as ppb); C is the equilibrium solution sorbate concentration (ppb) and K_p is the partition coefficient. Deviations from linearity (least-squares fitted) approximated deviations in replicate determinations for individual isotherm points. As the sorbate water concentration approached 60–70% of the sorbate aqueous solubility, the isotherms typically bent upward, indicative of increased sorption. Because no distinction was made between sorbed and crystalline sorbate, however, these deviations from isotherm linearity may reflect the presence of a crystalline phase rather than increased sorption. Our study focused on the linear portion of the isotherms, which has more widespread environmental significance.

2. The sorption appeared reversible in all systems. Linear-least-squares fitting of the 'linear' portions of the isotherms gave ordinate intercepts that were small

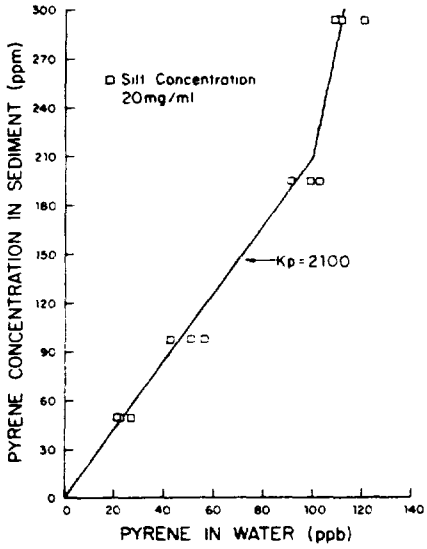

Fig. 1. Adsorption isotherm for pyrene on the Doe Run coarse silt.

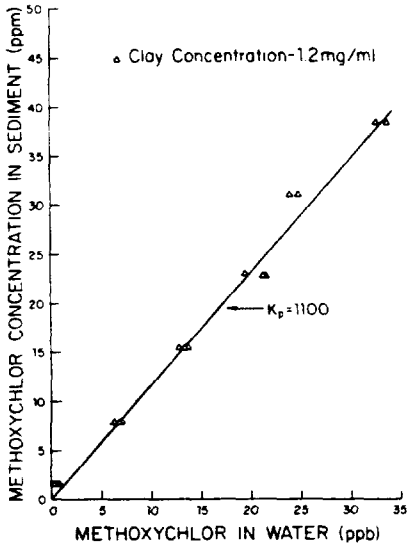

Fig. 2. Adsorption isotherm for methoxychlor on Hickory Hill clay.

(e.g. intercept was less than 20% of the lowest measured sorbed concentrations). In general there were as many negative-valued intercepts as positive. The average intercept value was near zero over all systems.

Desorption isotherms for both the pyrene and methoxychlor runs on the Doe Run coarse silt were within experimental error of the respective adsorption isotherms; no hysteretic effects were observed.

3. Filtering and centrifugation gave comparable isotherms. Isotherms determined on the Doe Run medium and coarse silts (pyrene and methoxychlor) by filtering the suspensions through halocarbon membranes were within experimental error of those determined by centrifugation.

4. The linear portion of the isotherms was independent of sediment concentration in dilute suspensions. Varying the Doe Run medium silt concentration from 2 to 20 mg ml^{-1} (2 mg ml^{-1} increments), while keeping the total pyrene concentration relative to dry silt mass constant at 30 ppm, produced no real (i.e. beyond experimental error) change in the aqueous phase concentration of pyrene (10 ± 2 ppb). When the total pyrene relative to sediment was increased to 150 ppm (near the limit of linear isotherm behavior), however, the same increase in sediment concentration produced a gradual decrease in aqueous-phase pyrene concentration from 50 ± 2 to 40 ± 5 ppb.

5. The isotherms showed only a slight dependence on ionic strength. The incremental addition of NaCl (0–20 mg ml^{-1} in 2 mg ml^{-1} increments) to a Doe Run medium silt—pyrene suspension resulted in an approximately linear increase in K_p. A salt content equal in mass to the sediment content (20 mg ml^{-1}) produced approximately a 15% increase in K_p over the 'no salt' system.

6. Sorbates in a mixture sorbed independently. The sorption isotherms of pyrene and phenanthrene were determined in combination and individually on both the Doe Run and Hickory Hill coarse silts. Only the linear portion of each isotherm was followed, but the combined isotherms showed no discernible sorptive interaction between these two sorbates.

Sorption dependence on sorbent properties

Table 2 shows the partition coefficients for pyrene and methoxychlor on the various particle size isolates. Organic matter content and sediment particle size were the two sorbent properties investigated. Pyrene and methoxychlor showed very similar sorptive dependencies on these sorbent properties. Figures 3 and 4 show the individual K_p's plotted as a function of organic carbon content. Two features of sorptive behavior are apparent in these figures. First, the K_p's of both pyrene and methoxychlor show, in general, a linear increase with organic carbon content. Least squares correlation coefficients (γ_{xy})* are indicated in the figures. Second, the functional behavior of the sand fraction can be distinguished from that of the finer (<50 μm) sediments. When sorption is 'keyed' solely to organic carbon, it is convenient to define

$$K_{oc} = K_p/oc, \qquad (2)$$

where oc is the fractional mass of organic carbon in the sediment. Table 3 gives the mean K_{oc}'s for pyrene and methoxychlor and variations over the sediments studied. A bell-shaped dependence of K_{oc} on particle size is apparent, starting with a low K_{oc} value for

* It should be emphasized that this empirical relationship does not determine that hydrophobic organic compounds are sorbed to organic components of the sediment, although this may in fact be the case. Instead, both sorption and organic carbon content may be directly related to another sediment property (or properties).

Table 2. Pyrene and methoxychlor sorption coefficients for linear portion of isotherms

Sediment size fraction	organic carbon	Pyrene K_p (r^2)		Pyrene K_{oc} ($\times 10^{-5}$)	Methoxychlor K_p (r^2)		Methoxychlor K_{oc} ($\times 10^{-5}$)
Hickory Hill							
Sand	0.13	42	(0.85)	0.32	53	(0.85)	0.41
Coarse silt	3.27	3000	(0.95)	0.92	2600	(0.97)	0.80
Medium silt	1.98	2500	(0.95)	1.3	1800	(0.91)	0.91
Fine silt	1.34	1500	(0.90)	1.1	1400	(0.97)	1.0
Clay	1.20	1400	(0.75)	1.2	1100	(0.99)	0.92
Doe Run							
Sand	0.086	9.4	(0.97)	0.11	8.3	(0.98)	0.097
Coarse silt	2.78	2100	(0.92)	0.76	2200	(0.93)	0.80
Medium silt	2.34	3000	(0.80)	1.3	1700	(0.94)	0.73
Fine silt	2.89	3600	(0.88)	1.2	2300	(0.95)	0.80
Clay	3.29	3800	(0.90)	1.2	2400	(0.98)	0.73
Oconee River							
Sand	0.57	68	(0.38)	0.12	95	(0.93)	0.17
Coarse silt	2.92	3200	(0.99)	1.1	2500	(0.97)	0.86
Medium silt	1.99	2300	(0.96)	1.2	2000	(0.93)	1.0
Fine silt	2.26	2500	(0.99)	1.1	2100	(0.96)	0.93
Clay*							

* The clay portion of this sediment was allowed to age in suspension and degraded substantially. Therefore, no sorption was done on this fraction.

the sand, increasing to a maximum in the medium or fine silt, then decreasing somewhat for clay-sized particles. For a whole sediment, the observed K_p is given by

$$K_p = \Sigma_i K_p^i f_i. \quad (3)$$

where i denotes the (i)th size fraction, and f_i is the fraction of the total mass represented by component i. By using organic carbon as the sole sorbent property required to determine K_p^i.

$$K_p = \Sigma_i K_{oc}^i f_i (oc)_i. \quad (4)$$

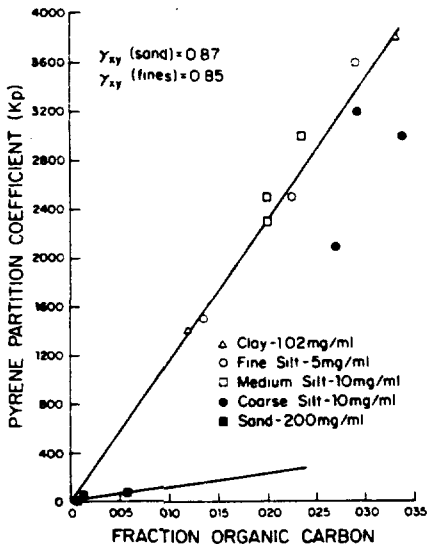

Fig. 3. Pyrene K_p as a function of sediment organic carbon.

Therefore, given the set of 'sediment-independent' K_{oc}^i, organic contents, and fractional masses of the size fraction, one can compute the composite K_p for any given sediment†. The K_{oc}^i could be determined by sorption measurements on particle-size isolates of any given sediment, but a simpler and more easily performed procedure was desirable.

For purposes of K_p estimation, the fines are not subdivided; the range in the variation of K_{oc} within the fines is acceptable, and most likely within the limits of accuracy available for definition of particle size distribution and/or organic carbon contents. For both methoxychlor and pyrene, the K_p's for sand were 0.5–4% of those for the next finer fraction. This was largely caused by the low organic carbon contents

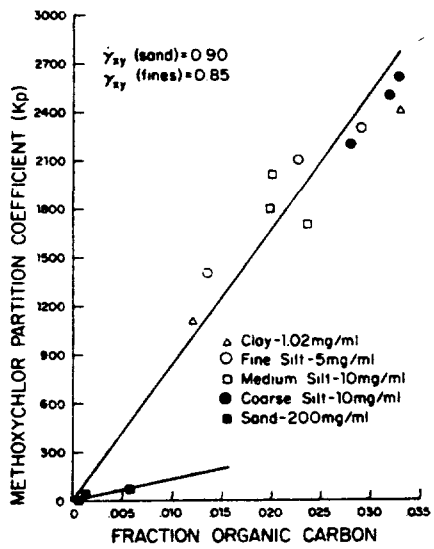

Fig. 4. Methoxychlor K_p as a function of sediment organic carbon.

† To date, only local sediments have been investigated; sediment collection is underway to extend this study to a national sediment basis.

Table 3. Average K_{oc} values on all sediments

Sediment	Pyrene	Methoxychlor
Sand	19,000 (0.65*)	23,000 (0.73)
Coarse silt	93,000 (0.18)	82,000 (0.04)
Medium silt	130,000 (0.05)	88,000 (0.16)
Fine silt	110,000 (0.05)	93,000 (0.11)
Clay	120,000 (0.00)	83,000 (0.16)

* Coefficient of variation = $\frac{\text{standard deviation taken over all sediments}}{\text{mean value}}$.

of the sand. Also, the K_{oc}'s for sand were generally less than half those for finer fractions. This reduces the sorptive contribution of the sand in a composite sediment to that of a diluent of the fines for most applications. In addition, replicate determinations of K_p on a given sand fraction frequently differed by a factor of 2. Therefore, to estimate the K_{oc} of sand as 20% of the K_{oc} for the fines should not introduce any substantial error into the estimation of a composite K_p for most sediments. The required set of K_{oc}^i is now reduced to a determination of K_{oc} for sediment fines ($< 50\,\mu$m).

Sorption dependence on sorbate properties

Table 4 shows water solubilities taken from the literature, octanol/water distribution coefficients (K_{ow}), and K_{oc}'s for a series of polycyclic aromatics and chlorinated hydrocarbons. The compounds were chosen to span the range in water solubility from approximately 1 ppb to 1000 ppm. The K_{oc}'s reported are averages for isotherms run on the coarse silt fractions of the Doe Run and Hickory Hill sediments. Figure 5 shows K_{oc}'s plotted against both water solubilities and octanol/water distribution coefficients. The correlation coefficient (γ_{xy}) between K_{oc}'s and K_{ow}'s was 0.98 and between K_{oc}'s and water solubilities was -0.20. The K_{oc} correlation with K_{ow} is excellent; there is a rather poor linear correlation in K_{oc} relating to compound solubility.

Linear least-squares fitting of the K_{ow} and K_{oc} data gave the equation:

$$K_{oc} = 0.63\,K_{ow}\ (r^2 = 0.96). \quad (5)$$

Fitting to an equation that established a non-zero ordinate intercept gave comparable fits (based on r^2) for a broad range of intercept values, because of the lack of data in the 'low' K_{oc}–K_{ow} region. Therefore, the intercept was dropped in favor of the simpler equation (5).

Least squares fitting the log–log plots in Fig. 5 gave

$$\log K_{oc} = 1.00 \log K_{ow} - 0.21\ (R^2 = 1.00) \quad (6)$$

and

$$\log K_{oc} = -0.54 \log S + 0.44\ (R^2 = 0.94), \quad (7)$$

where S is the water solubility expressed as mole fraction, and R^2 is the linear regression coefficient of determination. Equation (6) reduces to equation (5), indicative of the linear covariation of K_{oc} and K_{ow}. K_{oc} varies nonlinearly with S as described by equation (7).

These relationships associating sorption to octanol/water partitioning and solubility allow the K_{oc} for the 'fines' fraction of a sediment to be estimated from more easily determined and widely cataloged molecular parameters (Leo *et al.*, 1971). This K_{oc} estimate can be used in equation (4) to calculate a partition coefficient for a composite sediment.

Octanol/water partitioning provides a much better estimator for sediment–water partitioning than does solubility, which gives at best an order of magnitude estimate of K_{oc}. This derives from a combination of factors:

1. In a molecular sense, the partitioning of a compound between water and either sediment or octanol involves monomer distribution between two phases. On the other hand, saturated aqueous solutions involve the equilibration of primarily dissolved monomers with *crystalline* compounds. Thus, crystal energy contributions enter into water solubilities but do not affect the monomer-associated properties of K_{ow} and K_{oc}.

Table 4. Sorption dependence on sorbate properties

Compound	Water solubility Mole fraction $\times 10^9$	ppb	$K_{oc} \times 10^{-3}$	$K_{ow} \times 10^{-3}$	$\frac{K_{oc}}{K_{ow}}$
Pyrene	12*	135	84	150	0.56
Methoxychlor	6.3†	120	80	120	0.67
Naphthalene	4460	31,700	1.3	2.3	0.57
2-Methylnaphthalene	3220	25,400	8.5	13	0.65
Anthracene	7.57	73	26	35	0.74
9-Methylanthracene	24.4	261	65	117	0.56
Phenanthrene	130	1290	23	37	0.62
Tetracene	0.037	0.5	650	800	0.81
Hexachlorobiphenyl	0.048‡	0.95	1200	2200	0.55
Benzene	410,000§	1,780,000	0.083	0.13	0.64

* The polycyclic hydrocarbon solubilities were taken from Mackay & Shiu (1977).
† From Zepp *et al.* (1976).
‡ Measured by Chiou *et al.* (1977) for 2,4,5,2',4',5'hexachlorobiphenyl.
§ From McAuliffe (1966).

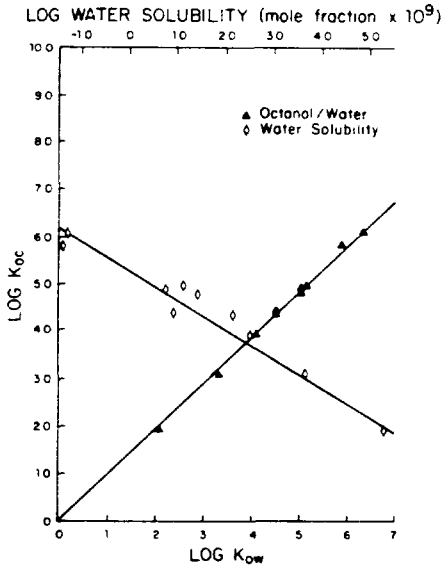

Fig. 5. Sorption K_{oc} as a function of compound water solubility and octanol/water distribution coefficients.

2. Both K_{ow}'s and K_{oc}'s listed in Table 4 are for systems wherein the aqueous solution concentrations of compound are considerably below the water solubility for the compound. As the water solubility is approached, K_{ow} shows a slight dependence on compound concentration, and the K_p (and thus K_{oc}) shows a very significant change with concentration. The reduced K_{oc} correlation with solubility could reflect the differences in 'water loading' in the respective systems.

3. The water solubilities are values from the literature, not run on the same compound samples as were the other data. Errors introduced in the absolute values of K_{ow} and K_{oc} as a result of impurities in the compounds will tend to cancel when the quantities are interrelated. Also, the solubilities were measured at various temperatures (22–25°C).

Octanol water partitioning

Literature K_{ow}'s for a given compound frequently vary over several orders of magnitude. This is especially true when the K_{ow}'s are 10^4 or greater. This variation is largely experimental in origin and stems primarily from the following sources:

1. Presence of impurities that are not analytically distinguished from the parent compound. Traces of more-water-soluble contaminants can substantially reduce the measured K_{ow}.

2. Compound loss from the water phase during phase separation and analysis. Hydrophobic organics tend to sorb or volatilize out of aqueous solutions during handling.

3. Contamination of water-phase sample with excess (beyond equilibrium value) octanol during the sampling process. Because of the magnitude of the K_{ow}, mass balance determination will often not reflect these errors in the water phase measurements.

In addition to these potentially large variations of experimental origin, smaller changes in K_{ow} were observed as a function of compound concentration. Not-all compounds were investigated in this respect, but the K_{ow}'s for the polycyclics in class 1 tended to increase (as much as 20%) as the aqueous concentration increased from half-saturation to saturation. The K_{ow}'s reported in Table 4 were measured at water concentrations of half-saturation or less (where no concentration dependence of K_{ow} was observed). The coefficient of variation for replicate determinations was generally less than 0.1 except in the case of hexachlorobiphenyl and tetracene, for which replicates varied as much as a factor of 2.

SUMMARY AND CONCLUSIONS

Sorption isotherms for all the hydrophobic compounds studied (water solubility from 500 ppt to 1800 ppm) were similar. They were linear over a broad range of aqueous phase compound concentrations. The linear partition coefficients (K_p) were relatively independent of sediment concentration and salt content in the suspensions. Mixtures of hydrophobic compounds sorbed independently through the linear portions of their respective isotherms. The K_p's for a given compound were directly related to organic carbon content for a given particle size isolate in different sediments. On an organic carbon basis (K_{oc}), the sand fraction was a considerably less effective sorbent (50–90% reduction in K_{oc}) than the fines fraction (sediment particles $< 50\,\mu m$). Differences in sorption within the silt and clay fractions were largely the result of differences in organic carbon content. The K_{oc}'s of the different hydrophobic compounds could be estimated from octanol/water distribution coefficients.

In conclusion, reasonable estimation (within a factor of 2) of the sorption behavior of hydrophobic pollutants can be made from a knowledge of the particle size distribution and associated organic carbon contents of the sediment and the octanol/water distribution coefficients of the pollutant. All of these sorbate-sorbent properties are either known or can be easily measured in the laboratory.

Acknowledgements—The authors thank Mr. G. L. Baughman for helpful discussions and Mr. Edmond Deluca for technical assistance.

REFERENCES

Bailey G. W. & White J. L. (1970) Factors influencing the adsorption, desorption and movement of pesticides in soil. *Residue Rev.* **32**, 29–92.

Bark L. S. & Graham R. J. T. (1966) Studies in the relationship between molecular structure and chromatographic behavior. *J. Chromatography* **25**, 357–366.

Briggs G. G. (1973) A simple relationship between soil sorption of organic chemicals and their octanol/water partition coefficients. *Proc. 7th Bri. Insecticide Fungicide Conf.* **11**, 475–478.

Briggs G. G. (1969) Molecular structure of herbicides and their sorption by soils. *Nature* **223**, 1288.
Chiou C. T., Freed V. H., Schmedding D. W. & Kohnert R. L. (1977) Partition coefficient and bioaccumulation of selected organic chemicals. *Environ. Sci. Technol.* **11**(5), 475–477.
Hamaker J. W. (1975) The interpretation of soil leaching experiments. In *Environmental Dynamics of Pesticides*, pp. 115–133. Plenum Press, New York.
Hance R. J. (1969) An empirical relationship between chemical structure and the sorption of some herbicides by soil. *J. agric. Fd Chem.* **17**, 667–668.
Jackson M. L. (1956) *Soil Chemical Analysis—Advanced Course*. U. of Wisconsin Press, Madison.
Lambert S. M. (1968) Omega (Ω) a useful index of soil sorption equilibria. *J. agric. Fd Chem.* **16**(2), 340–343.
Lambert S. M. (1967) Functional relationship between sorption in soil and chemical structure. *J. agric. Fd Chem.* **15**(4), 572–576.
Lambert S. M. (1966) The influence of soil-moisture on herbicidal response. *Weeds* **14**, 273–275.
Lambert S. M., Porter P. E. & Schieferstein H. (1965) Movement and sorption of chemicals applied to the soil. *Weeds* 13, 185–190.
Leo A., Hansch C. & Elkins D. (1971) Partition coefficients and their uses. *Chem. Rev.* **71**(6), 525–616.
Mackay D. & Shiu W. U. (1977) Aqueous solubility of polynuclear aromatic hydrocarbons. *J. Chem. Eng. Data* **22**(4), 399–402.
McAuliffe C. (1966) Solubility in water of paraffin, cycloparaffin, olefin, acetylene, cycloolefin and aromatic hydrocarbons. *J. Phys. Chem.* **70**(4), 1267–1275.
Pionke H. B. & Chesters G. (1973) Pesticide–sediment–water interactions. *J. Envir. Quality* **2**(1), 29–45.
Richardson E. M. & Epstein E. (1971) Retention of three insecticides on different size soil particles suspended in water. *Soil. Sci. Soc. Am. Proc.* **35**, 884–887.
Zepp R. G., Wolfe N. L., Gordon J. A. & Fincher R. C. (1976) Light-induced transformations of methoxychlor in aquatic systems. *J. agric. Fd Chem.* **24**(4), 727–733.

MAIN POINTS ABOUT BIODEGRADATION OF ORGANICS IN THE SUBSURFACE

1) Benzene and toluene are readily biodegradable by microorganisms (Tabak et al).

2) Microorganisms exist in the subsurface and they are metabolically active (Wilson and McNabb).

3) Aerobic biodegradation of benzene, toluene and related organic chemicals occurs in the subsurface (Wilson and McNabb, Bouwer and McCarty).

4) The aerobic degradation pathways of benzene and toluene lead to complete mineralization to carbon dioxide and water with no metabolites formed that are of human health or environmental concern.

5) Oxygen occurs at significant levels under most conditions in the subsurface - even in deeper aquifers.

6) Recent studies indicate toluene and possibly benzene may degrade under anaerobic conditions if such conditions do occur.

BIODEGRADATION

by Gary D. Miller, Ph.D.
Assistant Professor
Civil Engineering and Environmental Science
University of Oklahoma

Until the recent development of sampling methods to obtain uncontaminated subsoil material, there was a misconception that the subsurface (including aquifers) is devoid of living organisms. Early studies showed that microbial numbers decreased with soil depth. A number of investigators have recently shown that the subsurface contains a rich assemblage of microorganisms.

Evidence for the occurrence of microorganisms in the subsurface is now direct and conclusive. Microscopic and biochemical investigations using aseptically obtained aquifer material (i.e., uncontaminated by surface microbes) have clearly shown the existence of a sizable microflora (1-3). In addition, the activities of subsurface microorganisms have been detected by numerous investigators (3-11) and diverse physiological types such as heterotrophs, sulfate-reducers, acetogens and methanogens have been found in well waters, cores and drilling muds (4, 5). These studies reinforce a recent book (12) which reiterates the basic conclusion of McNabb and Dunlap (13); that there is little to preclude microbial proliferation in subsurface habitats.

The first attached paper by Tabek et al. (14) demonstrates the biodegradability of benzene, toluene and their derivatives in Table 3 (p. 1509). In this study it was found that 100% of the benzene and toluene was degraded within seven days in a flask. The next article by Wilson and McNabb (15) indicates in Table 1 the numbers of organisms that have been found in subsurface materials. In materials collected from the partially saturated zone (subsoil), from just above the water table and just below the water table, the numbers of microorganisms that occur are remarkably uniform. The numbers do not decline greatly with depth, they do not change greatly with season, and the numbers of organisms per gram dry weight of material are consistent in replicate bore holes at the same site. This confirms that the subsurface contains living microorganisms and is an important microbial habitat.

The second table in this article summarizes the results of several experiments on the biodegradability of organics in groundwater. For benzene and toluene, when the concentrations are above 100 parts per billion, it is probable that they are aerobically degraded. In fact, degradation of these two organic chemicals has occurred every time they have been tested with subsurface material. In recent studies with previously uncon-

taminated alluvial aquifer material from Lula, Oklahoma, toluene was biodegraded at a rate of about 250% per week in material from above the water table and at about 30% per week in aquifer material. This is illustrated in Figure 1, of this report, for two different depths in the subsurface.

Additional papers that indicate the biodegradation of organic pollutants in the subsurface are attached. The paper by Bouwer and McCarty (16) shows that nonchlorinated aromatics (Table 1) were degraded by more than 99% under aerobic conditions. They also indicate in Figure 3 that benzenes are degraded under aerobic conditions.

The aerobic degradation pathways for both benzene and toluene are well documented. As shown in Figure 2 of this report, benzene is degraded by bacteria to catechol (an alcohol), then to either an acid or an aldehyde by fission of the ring structure, followed by mineralization. There are two aerobic routes of metabolism for toluene (Figure 3). Both involve the production of catechols followed by ring fission and mineralization to CO_2 and water. Neither degradation pathway results in the formation of chemicals of known environmental or health concern.

Under most circumstances there are measurable levels of dissolved oxygen in the subsurface including the deeper groundwater. These concentrations typically range from around 2 milligrams per liter up to about 8 milligrams per liter. Thus, aerobic conditions and microbial metabolism would be expected in the unsaturated zone and in most groundwaters. Only under high levels of pollution would anaerobic conditions be likely to occur (18).

Until recently, it was thought that benzene, toluene and similar nonhalogenated aromatics are not degraded under anaerobic conditions. This may be because most experiments were conducted in the laboratory using pure cultures of microorganisms and single substrates. The most recent laboratory and field studies conducted with a mixture of microorganisms that occur in subsurface materials and with a mixture of substrates indicate that toluene and related aromatics can be degraded under methanogenic (anaerobic) conditions. These chemicals disappear more rapidly under field conditions than would be expected due to physical and chemical processes alone. This is at least indirect evidence for anaerobic microbial transformations of these chemicals (19, 20).

In summary, metabolically active microorganisms do occur in the subsurface and have been found in surprisingly large numbers in a wide range of materials that have been examined. These microorganisms naturally occur and have the demonstrated ability of metabolize or degrade benzene, toluene and many other organic pollutants in groundwater. The rate of degradation appears to be quite rapid under aerobic conditions which serves to attenuate

pollutant migration and decrease the mass of organics. Finally, the aerobic biodegradation pathways of benzene and toluene are known to result in metabolites that are not of health concern with the ultimate production of carbon dioxide and water.

Bibliography

1) Ghiorse, W. C. and D. L. Balkwill. 1983. Dev. Ind. Microbiol. 24: 213-224.

2) White, D. C. et al. 1983. Dev. Ind. Microbiol. 24: 201-211.

3) Webster, J. J. et al. 1985. Groundwater. 23: 17-25.

4) Dockins, W. S. et al. 1980. Geomicrobiol. J. 2: 83-98.

5) Godsy, E. M. and G. G. Ehrlich. 1978. J. Res. U. S. Geol. Surv. 6: 829-836.

6) Wilson, J. T. et al. 1983. Dev. Ind. Microbiol. 24: 225-233.

7) Suflita, J. M. and G. D. Miller. 1985. Env. Toxicol. Chem.: In press.

8) Ladd, T. I. et al. 1982. Appl. Environ. Microbiol. 44: 321-329.

9) Ogawa, I. et al. 1981. Talanta. 28: 725-729.

10) Leenheer, et al. 1976. Environ. Sci. Technol. 10: 445-451.

11) Roberts et al. 1980. J. Water Pollut. Control Fed. 52: 161-172.

12) Bitton, G. and C. P. Gerba. 1984. In Groundwater Pollution Microbiology. (Bitton G. and Gerba, C. P., ed). John Wiley & Sons, N.Y. pp. 1-7

13) McNabb, J. F. and W. J. Dunlap. 1975. Groundwater. 13: 33-34.

14) Tabak, H. et al. 1981. J. Water Pollut. Control Fed. 53: 1503-1518.

15) Wilson, J. T. and J. F. McNabb. 1983. EOS. 64: 505-507.

16) Bouwer, E. J. and P. L. McCarty. 1984. Ground water. 22: 433-440.

17) Perry, J. J. 1984. Petroleum Microbiology. (Atlas, R. M. ed.) MacMillan Publishing Co., N.Y. 61-97.

18) Winograd, I. J. and Robertson, F. N. 1982. Science. 216, June 11: 1227-1230

19) Rees, J. F., B. H. Wilson and J. T. Wilson. 1985. American Society for Microbiology. 85th Annual Meeting, Las Vegas, NV.: 258.

20) Reinhard, M. and N. L. Goodman. 1984. Env. Sci. and Tech. 18: 953-961

G. Miller

Biodegradability studies with organic priority pollutant compounds

Henry H. Tabak, Stephen A. Quave, Charles I. Mashni, Edwin F. Barth

This report deals with studies undertaken to determine the biodegradability of 114 organic priority pollutants included in the U. S. Environmental Protection Agency (EPA) Consent Decree list[1] to ascertain the extent of microbial degradation and to determine the acclimation periods.

With the rapid advances in industrial technology, there is an ever-increasing introduction rate of organic chemicals from the pharmaceutical, petrochemical, oil, solvents, paper, and other industries into water environments. The environmental fate of these organics depends on whether they bio-oxidize rapidly or very slowly, or are biologically recalcitrant, persist in watercourses, become adsorbed to sediment and mud particles and/or bioaccumulate in the food chain process. At the same time, some are toxic to animals and humans, and are physiologically active as well as potentially carcinogenic, posing the possibility of severe health problems.

EPA is consequently very much concerned with ever-increasing introduction of the potentially dangerous pollutants into the watercourses, because of the direct toxic effects on animal and human life or through the reuse of the inadequately treated waste. The agency is charged with the responsibility for setting guidelines and concentration limit standards for the priority pollutants. An intensive effort of determining the biodegradability of these compounds under both laboratory and natural conditions, along with the gathering of the chemical-physical treatability data, is of high agency priority. The acquisition of data on biodegradability and chemical-physical treatability of the priority pollutants is important for the establishment of treatability profiles for the various groups of organic compounds which compose the Consent Decree list.

Data were collected on the degradability and rate of acclimation of 96 compounds.

These biodegradability data are based on studies in which the priority pollutants were subjected to a specific set of controlled experimental conditions and culture-enrichment techniques within the framework of a static culture flask biodegradability screening test.

EXPERIMENTAL PROCEDURE

For this comprehensive screening the priority pollutants were divided into the following classes of organic compounds: phenols, phthalate esters, naphthalenes, monocyclic aromatics, polycyclic aromatics, polychlorinated biphenyls, halogenated ethers, nitrogenous organics, halogenated aliphatics, and organochlorine insecticides.

The biodegradability test method used in the studies was the static-culture flask-screening procedure of Bunch and Chambers,[2] utilizing biochemical oxygen demand (BOD) dilution water containing 5 mg of yeast extract per litre, as the synthetic medium; 5- and 10-mg/l concentrations of the test compound, a 7-day static incubation of 25°C in the dark, followed by three weekly subcultures (totaling 28 days of incubation), and incorporating settled domestic wastewater as microbial inoculum.

The test was modified[3] to include the capability of studying the biodegradation of water insoluble and/or volatile compounds comprising the priority pollutant list and to facilitate the use of both the gas-chromatographic (GC) as well as the dissolved organic carbon (DOC) and total organic carbon (TOC) analytical procedures for determining the extent of biodegradation of the test compound. The procedure was extended to include the experimental initials in the experimental-system series for the original culture and three subcultures to determine the initial concentration of test compound at the beginning of each incubation period. It also incorporated both the medium-inoculum control series to serve as blank controls for determining base lines for both GC analysis and for DOC and TOC, as well as the medium-substrate control series for determination of possible autooxidation, photolysis, and volatilization. Figure 1 shows the incubation of a non-volatile series with cotton-stoppered flasks. Figure 2 shows

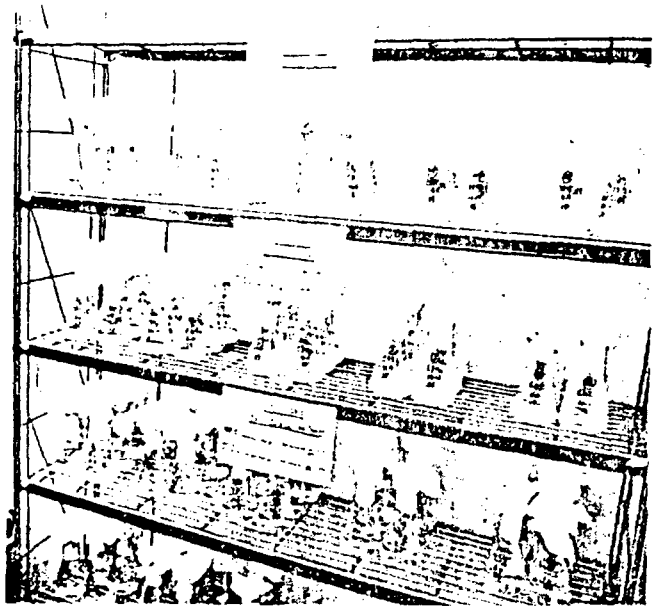

Figure 1—Incubation of non-volatile sample series.

the glass-stoppered vials used during incubation of volatile compounds.

A test protocol was developed to handle the weekly subcultures to fresh media, and to perform solvent extraction of the initial and incubated cultures, evaporate the solvent fractions by the Kuderna-Danish evaporation procedure; cleanup of concentrated solvent extracts for GC analysis and the processing of samples for both the TOC and COD.

Phenol was used as the biodegradable control compound in each biodegradability evaluation series to ensure viability of the wastewater inoculum.

Because each class of organic compounds had different chemical characteristics and solubilities, varied techniques were necessary to provide intimate organism-substrate contact during incubation and unmetabolized substrate recovery.

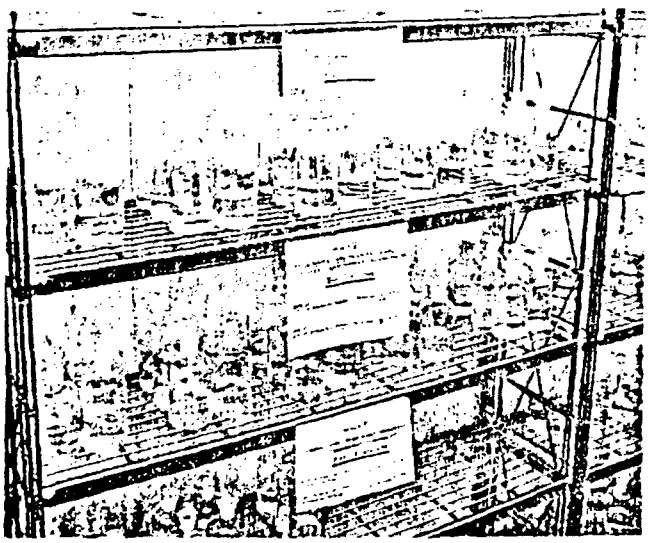

Figure 2—Incubation of volatile sample series.

Phenolic compounds. Stock solutions were prepared in distilled deionized water as 0.1% solutions by addition of sodium hydroxide to effect solution.

The flasks containing the medium, test compound, and inoculum, as well as the medium inoculum and medium test-compound-control flasks, were incubated in a constant-temperature room at 25°C in darkness. Duplicate samples at the beginning of each incubation period and triplicate samples at the end of 7-day incubation for each subculture were subjected to GC and DOC analysis. The culture samples were extracted three times with 20-ml portions of methylene chloride. The pooled-solvent extracts were evaporated by the Kuderna-Danish evaporation technique and the concentrated extracts were then processed for GC analysis. For DOC, the samples were membrane-filtered through a system using 0.22-μm-porosity filters.

The GC methodology was developed for the phenolic compounds present in aqueous culture media and in deionized water as single substrates. The extraction efficiency differed with each phenolic compound and recovery ranged from 87 to 95%. Results were fairly reproducible for several test runs with substrate dosed culture samples. Extractions were performed at pH 2.0.

Phthalate esters and naphthalene compounds. Stock solutions of the test compounds were prepared in absolute ethanol. Solutions of acenaphthene and acenaphthylene were made up as 2 and 4% ethanolic stock solutions respectively, while 10% ethanolic stock solutions were prepared with the remaining test compounds.

Homogenous suspensions of all the phthalate esters, except dimethyl phthalate and diethyl phthalate, and the naphthalene compounds in the synthetic medium were prepared by adding appropriate amounts of the test compound to prechilled synthetic medium in a heavy-duty blender and blending the medium for 2 minutes. Aqueous stock solutions (0.1%) of dimethyl and diethyl phthalates were used in dosing the synthetic medium without blending.

The blended substrate-containing media were then introduced into erlenmyer flasks and inoculated with prechilled yeast extract and settled domestic wastewater inoculum. The flasks containing the medium with the test compound and inoculum, as well as the medium-wastewater and medium-test compound control flasks, were incubated in a constant-temperature room at 25°C in darkness. Flasks were shaken on a daily basis during the incubation period.

The culture samples were extracted three times with 20-ml portions of methylene chloride at neutral pH, except for the control phenol culture samples which were acidified before extraction. The extraction, evap-

oration, and sparging procedure was that used for phenolic compounds.

The extraction efficiency differed with each of the phthalate esters and naphthalene compounds. Recovery ranged from 62 to 149% and was fairly reproducible for the several test runs with substrate-dosed culture samples.

Monocyclic aromatics. Stock solutions of benzene and nitrobenzene were prepared in deionized distilled water. Stock solutions of chlorobenzene, toluene, 2,4- and 2,6-dinitrotoluenes were prepared in absolute ethanol. Both the aqueous and ethanolic stock solutions were prepared as 10% solutions.

A triglyceride (Tributerin®) was used in making up stock solutions of the remaining test compounds, with the exception of hexachlorobenzene, in 10% concentrations. Tributerin® was shown to be a suitable emulsifying agent for the volatile benzenes (chlorinated benzenes and ethyl benzene) and a good vehicle for these extremely water-insoluble compounds.

Homogenous suspensions of ethyl benzene, 1,2-, 1,3-, and 1,4-dichlorobenzenes and 1,2,4-trichlorobenzene in the synthetic medium were prepared by adding appropriate amounts of tributerin® stock solutions of these test compounds to prechilled synthetic medium in a heavy-duty blender and blending the medium for 2 minutes. The same fine suspensions of chlorobenzene, 2,4- and 2,6-dinitrotoluene, and toluene in the synthetic medium were prepared by adding appropriate amounts of the ethanolic stock solutions of these compounds to prechilled synthetic medium. Aqueous stock solutions of benzene and nitrobenzene were used in dosing the synthetic medium without blending.

Hexachlorobenzene, as a 0.1% aqueous suspension, was subjected to ultrasonication for 4 hours. An appropriate volume of the sonicated hexachlorobenzene suspension was then added to prechilled synthetic medium and blended for 2 minutes to make up a fine homogenous suspension of this water-insoluble compound in culture media.

The substrate containing synthetic media were stored in 2-l glass-stoppered reagent bottles in a refrigerator before use.

Biodegradability studies with purgeable benzenes and toluene chlorobenzene, 1,2-, 1,3-, and 1,4-dichlorobenzene, trichlorobenzene, and ethyl benzene were carried out in 250-ml, glass-stoppered reagent bottles to minimize the volatilization of substrate, whereas the nonvolatile benzenes (nitrobenzene, 2,4-, and 2,6-dinitrotoluene, and hexachlorobenzene) were studied in cotton-stoppered Erlenmyer flasks. Both the unblended and blended substrate containing media in either reagent bottles or flasks were inoculated with prechilled yeast extract (5 mg/l) and settled domestic wastewater inoculum. The experimental as well as the medium-wastewater and medium-test compound volatility control bottles and flasks were incubated in a constant temperature room at 25°C in darkness.

Duplicate samples at the beginning of each incubation period and triplicate samples at the end of the 7-day incubation for the original and each subculture were subjected to GC, TOC, and DOC analysis, utilizing the extraction-evaporation methodology, as well as the membrane filtration technology (for DOC determinations) as employed for phenols, phthalates and naphthalenes.

The GC methodology was developed for each of the benzene and toluene compounds, with the emphasis on analyzing single-parent substrate in cultures uncontaminated with the other test compounds. Extraction efficiency differed with each compound and percentage of recovery ranged from 83 to 98% and was fairly reproducible for several test runs with each compound.

Polycyclic aromatic hydrocarbons, polychlorinated biphenyls, halogenated ethers, nitrosamines, phenylhydrazines and herbicides (Isophorone, Acrylonitrile and Acrolein). Stock solutions of polycyclic aromatic hydrocarbons (PAHs), polychlorinated biphenyls (PCBs), and diphenyl hydrazine were prepared in a polyoxyethylated vegetable oil that was shown to be a suitable emulsifying agent for some volatile chlorinated compounds and a good vehicle for these extremely water-insoluble compounds in aqueous media. Homogenous suspensions of anthracene 1,2-benzanthracene, and chrysene in the synthetic media were prepared by adding appropriate amounts of the solutions of those compounds to the prechilled media and blending it for 2 minutes. The fine suspensions of the other compounds in media were prepared by adding stock solutions to the media without subsequent blending.

Ethanolic stock solutions of haloethers, isophorone, and N-nitroso diphenylamine were used in making fine suspensions of these compounds in prechilled synthetic media without blending. Aqueous stock solutions of N-nitroso-di-n-propylamine, acrylonitrile, and acrolein were used to prepare the culture media.

The substrate containing synthetic media were stored in either 2-l erlenmyer flasks or glass-stoppered reagent bottles in a refrigerator before use.

Biodegradability studies with acrylonitrile, acrolein and three haloethers (4-chlorodiphenyl ether, 2-chloroethyl vinyl ether, and 4-bromodiphenyl ether) were carried out in 250-ml glass-stoppered reagent bottles to minimize volatilization, whereas all the other test compounds were studied in cotton-stoppered Erlenmyer flasks. Both the blended and unblended media in either reagent bottles or flasks were inoculated with prechilled yeast extract and settled domestic wastewater inoculum. The experimental, as well as the medium-wastewater and medium-test compound volatility control bottles and flasks, were incubated in a constant-temperature room at 25°C in darkness. The extraction, evaporation,

and sparging of samples as well as the TOC technology was the same as employed for phenols, phthalates, naphthalenes and benzenes.

The extraction efficiency differed with each of the test compounds and the recovery value ranged from 78 to 98% and were fairly reproducible for several test runs with each of the substrate-dosed cluture samples.

Halogenated aliphatics. Stock solutions of chlorinated ethanes, halomethanes, chloroethylenes, chloropropane and chloropropylene were prepared in absolute ethanol and used for dosing the prechilled synthetic media. Stock solutions were prepared in 10% concentrations. Stock solutions of hexachloro-1,3-butadiene and hexachlorocyclopentadiene were prepared in the polyoxyethylated vegetable oil. Fine suspensions of these two compounds in synthetic media were prepared by adding the appropriate volume of their non-ionic emulsifying agent stock solutions to media without subsequent blending.

The substrate containing synthetic media were stored in either 1- or 2-l glass-stoppered reagent bottles in a refrigerator before use.

Biodegradability studies with the halogenated aliphatics were carried out in 250-ml glass-stoppered reagent bottles to minimize possible volatilization of the test compounds. The substrate containing media in reagent bottles were inoculated with prechilled yeast extract and 10-ml of prechilled settled domestic wastewater inoculum. The experimental, as well as the medium-wastewater control bottles were incubated in a constant temperature room at 25°C in darkness.

Volatility controls, utilizing a nonbiological system (medium-test compound without inoculum) were held at both refrigerated and 25°C holding temperatures for 10 days and then analyzed by GC and for TOC to determine loss of substrate from volatilization.

The experimental cultures, as well as the media and volatility control, were analyzed by a direct injection method (without solvent extraction) chromatographically, with the use of a chromatograph, FID detector system, and a column of SP-1000 on Carbopac B. This procedure applied to chloroethane, halomethane, chloroethylene, chloropropane, and chloropropylene containing cultures.

Butadiene and pentadiene cultures samples were subjected to normal methylene chloride extraction, KD evaporation methodology, and GC analysis.

Organochlorine pesticides. Stock solutions of pesticides were prepared in a non-ionic emulsifying agent. The substrate containing media were stored in either 1- or 2-l glass-stoppered reagent bottles in a refrigerator before use. Appropriate volumes of the oil and stock solutions of pesticides were added to prechilled media and the substrate was thoroughly mixed with the use of a magnetic stirrer. The pesticides were studied in cotton-stoppered erlenmeyer flasks. The substrate containing synthetic media in Erlenmeyer flasks were inoculated with prechilled yeast extract and 10-ml of prechilled settled domestic wastewater inoculum.

The experimental, as well as the medium-wastewater and medium test compound volatility control flasks were incubated in a constant temperature at 25°C. Flasks were shaken for a few minutes on a daily basis during the original and subculture incubation periods.

The extraction of cultures was performed in separatory funnels using three 20-ml volumes of methylene chloride. The KD evaporation of solvent-pooled fractions and the sparging of solvent extracts in preparation for GC analysis was performed in the same manner as phenols, phthalates, benzenes, and naphthalenes.

The extraction efficiency differed with each of the pesticide compounds and recovery values ranged from 75 to 98% and were fairly reproducible for several test runs with each of the substrate-dosed culture samples.

The pesticides were analyzed on a chromatograph equipped with an FID detector system.

RESULTS

The results for each of the above classes are given in the form of a short narrative discussion and tabular presentation of the screening data with correlative data gleaned from the literature.

The indication of 100% biodegradation in the tabular data should not be interpreted as zero residual of the individual priority pollutant. The minimum sensitivity of the GC procedures used was about 0.1 mg/l. The GC analytical effort involved a massive number of analyses in order to verify recoveries, determine blanks, include controls, verify standard chemicals, and monitor replicate samples. In order to keep this effort at a manageable level, the GC methods for each class of compounds were not maximized for sensitivity.

Phenolic compounds. The biodegradability data from the static-culture-flask-biodegradation-screening test studies, based on GC analysis and TOC and DOC determinations, have demonstrated that phenol and the chlorinated, as well as the nitrated, phenols, with the exception of 4,4-dinitro-*o*-cresol, were significantly biodegraded, with either rapid or gradual adaptation periods necessary to achieve optimum biodegradation rates.

The biodegradability data are expressed in Table 1, which summarizes the average percentage of biodegradation for each compound and for each subculture.

Significant biodegradation with rapid acclimation was observed with phenol, 2-chlorophenol, 2,3-dichlorophenol, 2,4,6-trichlorophenol, 2,4-dimethylphenol, *p*-chloro-*m*-cresol, 2-nitrophenol, 4-nitrophenol, and 2,4-dinitrophenol with a range of average biodegradation between 60 to 100% achieved after the first week of incubation. Pentachlorophenol was shown to be signif-

Table 1—Biodegradability of phenolic compounds evaluated by the static-flask-screening method.

Test compound	Concentration of test compound (mg/ml)	Performance summary	Average of 3 test flasks (biodegradation of test compound in 7 days %)			
			Original culture	First subculture	Second subculture	Third subculture
Phenol	5	D	96	100	100	100
	10	D	97	100	100	100
2-Chloro phenol	5	D	86	100	100	100
	10	D	83	100	100	100
2,4-Dichloro phenol	5	D	100	99	98	100
	10	D	99	99	100	99
2,4,6-Trichloro phenol	5	D	100	100	100	100
	10	D	100	100	100	100
Pentachloro phenol	5	A	19	68	100	100
	10	A	16	0	0	99
2,4 Dimethyl phenol	5	D	100	100	100	100
	10	D	99	100	100	100
p-Chloro-*m*-cresol	5	D	78	100	100	100
	10	D	76	100	100	100
2-Nitro phenol	5	D	100	100	100	100
	10	D	100	100	100	100
4-Nitro phenol	5	D	100	100	100	100
	10	D	100	100	100	100
2,4-Dinitro phenol	5	D	60	100	100	100
	10	D	68	100	100	100
4,6-Dinitro-*o*-cresol	5	N	52	58	56	51
	10	N	0	5	11	14

D—Significant degradation, rapid adaptation.
A—Significant degradation, gradual adaptation.
N—Not significantly degraded under the conditions of test method.

icantly bio-oxidized but with a gradual adaptation process over a 2-week period to achieve 100% biodegradation in 5-mg/l substrate cultures and over a 4-week period to achieve 98 to 100% loss in 10-mg/l pentachlorophenol cultures.

The nitrocresol, 4,6-dinitro-*o*-cresol did not demonstrate significant bio-oxidation and necessary acclimation for optimum bio-oxidation activity within the 28-day incubation period under the enrichment-culture conditions of the test method.

In general, chlorophenols are more stable to biodegradation than phenol and the resistance to microbial catabolism is greatest among the more highly chlorinated phenols.[4]

Phthalate esters. Phthalate esters are reported to be metabolized in the aquatic environment by a variety of organisms and degraded by mixed microbial systems at rates which vary widely, depending on environmental conditions. These compounds undergo primary and ultimate biodegradation in naturally occurring microbial populations by mechanisms of enzymic hydrolysis. The rate of degradation depends on temperature, pH, the presence of oxygen and phthalate structure.[5]

The static-culture-flask biodegradability screening test data based on GC and TOC determinations have demonstrated that phthalate ester priority pollutants were significantly biodegraded with either rapid or gradual adaptation to achieve optimum biodegradation rates.

The biodegradability data are expressed in Table 2, which summarizes the average percentage of biodegradation for each test compound and subculture.

Significant biodegradation, with rapid acclimation was observed with the phthalate esters, dimethyl phthalate, diethyl phthalate, di-n-butyl phthalate, and butyl benzyl phthalate, with 100% losses achieved after the first week of incubation.

Bis-(2-ethylhexyl) phthalate (EHPE) and di-n-octyl phthalate (DOPE) were significantly bio-oxidized, but with a gradual adaptation process needed over a 3-week period to achieve 95 and 94% loss for EHPE and 94 and 93% loss for DOPE in 5- and 10-mg/l substrate containing cultures respectively at the end of the third subculture incubation. The phthalate esters, EHPE and DOPE, were thus proven the most persistent of the phthalates studies under the conditions of the static-flask screening test.

Naphthalenes. The degradation and metabolism of naphthalene and the identification of the metabolites is known from many studies with bacteria. Naphthalene is reported to be probably the most easily biodegraded polycyclic aromatic hydrocarbon. Biotransformation

Table 2—Biodegradability of phthalate esters and naphthalene compounds evaluated by static-flask-screening method.

Test compound	Concentration of test compound	Performance summary	Average of 3 test flasks (biodegradation of test compound in 7 days (%)) Original culture	First subculture	Second subculture	Third subculture
Dimethyl phthalate	5	D	100	100	100	100
	10	D	100	100	100	100
Diethyl phthalate	5	D	100	100	100	100
	10	D	100	100	100	100
Di-n-butyl phthalate	5	D	100	100	100	100
	10	D	100	100	100	100
Bis-(2-ethyl hexyl) phthalate	5	A	0	43	80	95
	10	A	0	47	89	93
Di-n-octyl phthalate	5	A	0	79	89	94
	10	A	0	42	93	92
Butyl benzyl phthalate	5	D	100	100	100	100
	10	D	100	100	100	100
Napthalene	5	D	100	100	100	100
	10	D	100	100	100	100
2-Chloro napthalene	5	D	100	100	100	100
	10	D	100	100	100	100
Acenapthene	5	D	95	100	100	100
	10		100	100	100	100
Acenaphthylene	5	D	100	97	96	98
	10	D	94	91	93	93

D—Significant degradation, rapid adaptation.
A—Significant degradation, gradual adaptation.

and biodegradation of naphthalene is rapid enough to make it a dominant fate process in an aquatic system.[6]

The biodegradability data for the priority-pollutant naphthalene compounds based on the static-culture-flask screening test have demonstrated that naphthalene, 2-chloronaphthalene, acenaphthene and acenaphthylene undergo significant biodissimilation in culture media dosed with 5- and 10-mg/l substrate concentration, with rapid acclimation periods for naphthalene oxidizing-enzyme induction to occur. The naphthalene and 2-chloronaphthalene compounds exhibit rapid biodegradation in culture media at the end of the first subculture, showing 100% loss of the substrate at the two concentrations. Acenaphthene was observed to show similarly high biodegradation activity, with 100% loss of substrate in 5- and 10-mg/l dosed cultures throughout the four incubation periods. Rapid dissimilation activity was also demonstrated for acenaphthylene, with ranges of 87 to 100% and 80 to 100% loss of substrate in cultures dosed with 5 and 10 mg/l, respectively, throughout the four 7-day incubation periods.

Table 2 summarizes the biodegradability data for the priority pollutant naphthalene compounds showing the average biodegradation for each test compound for each subculture.

Monocyclic aromatics. Based on the biodegradability data accumulated for the priority-pollutant benzenes, toluenes, and their chlorinated and nitrated derivatives, certain conclusions can be drawn about their relative susceptibility to microbial bio-oxidation, their persistence and stability in aqueous environments as well as about their toxicity to the wastewater microbiota.

The analytical data, based on GC and TOC determinations, have demonstrated significant biodegradation of some of the benzene and toluene compounds, with varying degrees of acclimation depending on the test compound and the dose concentration of substrate in the culture media. Polychlorinated benzenes and the dinitrotoluenes initially exhibited a significant bio-oxidative activity with gradual adaptation and induced enzyme formation, followed, however, by a deadaptive process from the loss of the metabolically efficient microbial population or the gradual build-up of toxicity of either the parent substrate or metabolic products to microbiota. Hexachlorobenzene was shown to be relatively resistant to dissimilation by the microorganisms under the conditions of the static-flask methodology.

Table 3 summarizes the average percentage of biodegradation for each test compound at the end of the original culture and each of the subculture incubation periods. Significant biodegradation with rapid acclimation was observed with benzene, toluene, and nitrobenzene. Toluene and nitrobenzene were shown to be

Table 3—Biodegradability of benzene, toluene and their derivatives evaluated by the static-screening-flask test method.

Test compound	Concentration of text compound (mg/l)	Performance summary	Average of 3 test flasks (biodegradation of test compound in 7 days (%))			
			Original culture	First subculture	Second subculture	Third subculture
Benzene	5	D	49	100	100	100
	10	D	37	95	100	95
Chlorobenzene	5	D	89	100	100	100
	10	A	30	77	100	100
1,2-Dichlorobenzene	5	T	45	66	48	29
	10	T	20	59	32	18
1,3-Dichlorobenzene	5	T	59	69	39	35
	10	T	58	67	31	33
1,4-Dichlorobenzene	5	T	55	61	34	16
	10	T	37	54	29	0
1,2,4-Trichlorobenzene	5	T	54	70	59	24
	10	T	43	54	14	0
Hexachlorobenzene	5	N	56	30	8	5
	10	N	21	3	0	0
Nitrobenzene	5	D	100	100	100	100
	10	D	87	97	100	100
Ethylbenzene	5	D	100	100	100	100
	10	A	69	78	87	100
Toluene	5	D	100	100	100	100
	10	D	100	100	100	100
2,4-Dinitrotoluene	5	T	77	61	50	27
	10	T	50	49	44	23
2,6-Dinitrotoleune	5	T	82	55	47	29
	10	T	57	49	35	13

D—Significant degradation with rapid adaptation.
A—Significant degradation with gradual adaptation.
T—Significant degradation with gradual adaptation followed by a deadaptive process in subsequent subcultures (toxicity).
N—Not significantly degraded under the conditions of the test method.

completely biodegradable after the first week of incubation at 5- and 10-mg/l levels. Benzene demonstrated complete dissimilation at these levels after the second week of incubation. Chlorobenzene and ethyl benzene exhibited complete losses after the second and third weeks of incubation, respectively, at the 5-mg/l level. At 10 mg/l of substrate, biodegradation was manifested by gradual adaptation of microbiota with 100% losses evidenced for chlorobenzene and ethyl benzene at the end of the second and third subculture periods, respectively.

A gradual acclimation process with significant bio-oxidation of the substrate was observed with 1,2-, 1,3-, and 1,4-dichlorobenzene, 1,3,4-trichlorobenzene, and with 2,4- and 2,6-dinitrotoluene. Subsequent subcultures demonstrated a reduction of the biodegradation rate with these test compounds and an accumulation of the parent compound in the culture media.

The gradual reduction of biodegradation activity with respect to the polychlorinated benzenes and dinitrated toluenes may be from the possible loss of synergistic activity on the substrate exhibited by the original heterogenous microbial population in the inoculum as a result of the subculture method, or from a retardation of the adaptive (induced) enzyme process because of possible accumulation of toxic by-products of metabolism.

Hexachlorobenzene did not demonstrate significant bio-oxidation and the necessary acclimation for bio-oxidative activity within the 28-day incubation period under the conditions of the static-flask-culture method.

The volatility control systems for the volatile benzene compounds provided data which demonstrated no significant losses of the substrate from culture media due to volatilization at 25°C holding temperature for 7-day periods.

Some species of soil bacteria and petroleum-degrading microorganisms have been reported to be capable of utilizing benzene, ethyl benzene, and toluene as a sole carbon source and the metabolic pathways involved in the microbial oxidative degradation of these compounds have been established. Nitrobenzene is reported to be potentially biodegradable in soil. The nitro substituent generally decreases the biodegradability of the

Table 4—Biodegradability of polycyclic aromatic hydrocarbons, halogenated ethers and polychlorinated biphenyls evaluated by the static screening flask test method.

Test compound	Concentration of test compound (mg/l)	Performance summary	Average of 3 test flasks (biodegradation of test compound in 7 days (%))			
			Original culture	First subculture	Second subculture	Third subculture
Polycyclic aromatic hydrocarbons						
Anthracene	5	A	43	70	84	92
	10	A	26	30	40	51
Phenanthrene	5	D	100	100	100	100
	10	D	100	100	100	100
Fluorene	5	A	82	53	67	77
	10	A	65	43	38	45
Fluoranthene	5	A	0	47	100	100
	10	N	0	0	0	0
1,2-Benzanthracene	5	N	16	41	35	0
	10	N	0	38	23	0
Pyrene	5	D	71	100	100	100
	10	N	11	2	0	0
Chrysene	5	A	6	65	53	59
	10	N	0	30	34	38
Halogenated ethers						
Bis-(2-chloroethyl) ether	5	D	100	100	100	100
	10	D	100	100	100	100
2-Chloroethyl vinyl ether	5	D	76	75	100	100
	10	D	52	68	100	100
4-Chlorodiphenyl ether	5	N	0	32	36	1
	10	N	0	28	5	0
4-Bromodiphenyl ether	5	N	0	19	36	0
	10	N	0	0	10	0
Bis-(2-chloroethoxy)methane	5	N	0	0	0	0
	10	N	0	0	0	0
Bis-(2-chloroisopropyl) ether	5	D	85	100	100	100
	10	D	63	100	100	100
Polychlorinated biphenyls						
PCB-1016	5	N	44	47	46	48
	10	N	22	46	20	13
PCB-1221	5	D	100	100	100	100
	10	D	99	100	100	100
PCB-1232	5	D	100	100	100	100
	10	D	100	100	100	100
PCB-1242	5	N	37	41	47	66
	10	N	34	33	15	0
PCB-1248	5	N	0	0	0	0
	10	N	0	0	0	0
PCB-1254	5	N	11	42	15	0
	10	N	10	26	0	0
PCB-1260	5	N	0	21	0	0
	10	N	0	6	0	0

D—Significant degradation with rapid adaptation
A—Significant degradation with gradual adaptation
N—Not significantly degraded under the conditions of the method

aromatic ring, and therefore, the polynitrobenzenes are decomposed very slowly. According to reported studies, the more highly halogenated the benzene molecule becomes, the more resistant it is to microbial degradation[7-9].

Polycyclic aromatic hydrocarbons, polychlorinated biphenyls and halogenated ethers.

Polycyclic Aromatic Hydrocarbons. The polycylic aromatic hydrocarbons (PAHS) demonstrated varied rates of biodegradation with different acclimation pe-

riods, depending on the test compound and the dose of substrate in culture media, as shown in Table 4. The tricyclic aromatic hydrocarbon, anthracene, showed significant bio-oxidation with gradual adaptation, with a loss of 92 and 51% of substrate at the end of the third subculture in cultures with initial levels of 5 and 10 mg/l, respectively. Significant biodegradation with gradual adaptation was also demonstrated in the case of fluorene, which exhibited 77 and 45% losses at the end of third subculture with the above initial concentrations.

Fluoranthene, pyrene and chrysene demonstrated significant degradation at 5-mg/l substrate levels, but low oxidative activity at 10 mg/l. The tetracyclic hydrocarbon, 1,2-benzanthracene, in contrast, did not demonstrate significant degradation and the necessary acclimation for oxidative activity during the four successive incubation periods.

The PAHs in general have been reported to be potentially biodegradable compounds, particularly by soil microorganisms and in soil systems which provide better conditions for biodegradation than aquatic systems.[10]

The biodegradability data have shown that the tricyclic aromatic hydrocarbons are more susceptible to biodegradative action than the tetracyclic and higher polycyclic hydrocarbons.

Polychlorinated biphenyls. The individual polychlorinated biphenyls (PCBs) vary widely in their susceptibility to biodegradation, as shown in Table 4. The mono-, di-, and trichlorinated species may be significantly biodegraded or biotransformed, as well as volatilized; whereas PCBs with five or more chlorine atoms per molecule have a tendency to adsorb to suspended materials and sediments, bioaccumulate because of very low solubility, photodissociate, and are quite resistant to biodegradation.[11-15] The priority pollutant PCBs are Aroclors or technical mixtures of individual PCBs made by the partial chlorination of biphenyl in the presence of suitable catalyst. The PCBs 1016, 1221, 1232, 1242, 1254, and 1260 are Arochlors which differ from one another in the average chlorine content on a weight basis and in types of the individual PCBs composing the mixture.

Biodegradability data with the priority pollutant PCB Aroclors, have demonstrated that PCB Aroclor 1221 (with an average chlorine content of 21% and limited to mono- and di-chloro isomers and PCB Aroclor 1232 (with an average chlorine content of 32% and limited to mono-, di-, tri-, and tetra-chloro isomers) were the only PCB Aroclors exhibiting significant biodegradation with rapid acclimation. PCB Aroclor 1016 (a new mixture limited to mono-, di-, tri-, and tetrachloro isomers) and PCB Aroclor 1242 (with an average chlorine content of 42% and limited to di-, tri-, and tetra-chloro isomers) showed little bio-oxidation at 5 mg/l, and no oxidative activity at 10 mg/l. PCB Aroclor 1248 (with an average chlorine content of 48% and limited to tri-, tetra-, and penta-chloro isomers), PCB Aroclor 1260 (with an average chlorine content of 60% and limited to penta-, hexa-, and hepta-chloro isomers) demonstrated recalcitrance to microbial metabolism at 5 and 10 mg/l. The biodegradability of PCBs is a function of the number of C-H bonds available for hydroxylation. The fewer the chlorine atoms, the more common the adjacent unchlorinated carbons, and the higher the rate of bio-oxidative activity.

Halogenated ethers. The 7-day incubation periods for each subculture as shown in Table 4 demonstrated that bis-(2-chloroethyl) ether, 2-chloroethyl vinyl ether, and bis(2-chloroisopropyl) ether are significantly biodegradable with slightly varied acclimation periods for optimum oxidative activity, whereas 4-chlorodiphenyl ether, 4-bromodiphenyl ether, and bis-(2-chloroethyl) methane demonstrated insignificant biodegradability, with successive reduction of bio-oxidative rates and accumulation of the parent compound in the culture media from the possible toxicity of substrate to microbiota.

The findings on the susceptibility of the chloroalkylethers to degradation are corroborated by reported data based on studies with river waters supplemented with wastewater inocula.[16] The haloaryl ethers, as well as the chloroethoxy ethers, are shown to bio-oxidize very slowly under the conditions used. The experimental conditions may not have permitted a proper enzyme induction period or natural selection of microorganisms. It may also be possible that structural configuration of these ethers imparts recalcitrance to dissimilation of the molecule by microorganisms. The static-flask results for these three classes of priority pollutants are shown in Table 4.

Nitrogenous organic compounds. The diphenylnitrosamine, N-nitroso-N-phenylbenzamine (N-nitrosodiphenylamine) was shown to be easily biodegradable by microorganisms, with rapid acclimation to 5-mg/l substrate doses and gradual acclimation to 10 mg/l of the substrate in culture media, whereas the dialkylnitrosamine, di-n-propylnitrosamine (N-nitrosodi-n-propylamine), was observed not to exhibit significant degradation at either concentration.

Based on the relatively few reported data found in the literature, the diphenylnitrosamine is more easily degraded by microorganisms than are dialkylnitrosamines.[17] The carcinogenic nitrosamine, dimethylnitrosamine, which was not included in the biodegradability studies, is reported to exhibit resistance to microbial degradation in soil and in wastewater, and is not affected by the anaerobic organisms in bog sediment.[18]

The hydrazobenzene, 1,2-diphenylhydrazine, exhibited significant biodegradation with gradual adaptation, with the metabolic activity leveling off in the last two

subcultures dosed with 5 mg/l of the substrate. At the initial concentrations of 10 mg/l, the significant bio-oxidative activity exhibited initially with gradual adaptation process, was followed by a deadaptive process and toxification in subsequent subcultures.

The compound is in easily reversible redox equilibrium with azobenzene, and the relative concentrations of the two compounds that will be present at any time depends upon the oxidation potential of the water sample.[19] The azobenzene which predominates in well-aerated water was found in insignificant concentrations in the static-flask medium-substrate control set-ups.

Herbicides. The unsaturated ketone (cyclohexeneone) isophorone was shown to exhibit rapid degradative activity by microorganisms that adapt themselves readily to dissimilate the substrate. The microbial metabolism of isophorone probably involves the oxidation of the allylic methyl group of isophorone to a carboxylic acid group, which is followed by the rupture of the cyclohexane ring and decarboxylation.[20]

The herbicide compound, acrylonitrile (vinyl cyanide) demonstrated ease in degradation with rapid adaptation and induced enzyme formation under the conditions of the enrichment culture technique of the static-flask screening studies. These findings are in agreement with reported studies on acetonitrile biodegradation, which demonstrate that the substrate is readily dissimilated by microorganisms of activated sludge and is not toxic to the microorganisms.[21]

Acrolein (an unsaturated aldehyde) was also shown to be easily dissimilated with rapid acclimation of microbiota to the substrate. These findings are corroborated by reported studies on acrolein biotransformation in activated sludge.[22-24]

Table 5 summarizes the biodegradability data of the studies with the nitrogenous organic compounds.

Halogenated aliphatics. Table 6 summarizes the analytical data based on GC and TOC determinations, and correlates the percentage of losses of the halogenated aliphatic priority pollutants in 7 days for the four successive incubation periods with the average percentage of removals of the substrate from volatilization in 10 days at refrigeration and 25°C.

The volatilization of the halogenated aliphatics reported are based on volatility controls utilizing non-biological systems (synthetic media without inoculum). This approach was used to provide the conditions for the highest possible volatilization in the sealed-bottle systems of the biodegradation screening test to occur, since volatilization is reported to depreciate considerably in solutions containing organic solids and/or microbial cultures.[25]

Chloroethanes. The chloroethane aliphatics, 1,1- and 1,2-dichloroethane, 1,1,1-, and 1,1,2-trichloroethane were shown to be potentially biodegradable, whereas 1,1,2,2-tetrachloroethane was observed not to support any bio-oxidative activity by microbiota under the conditions of the biodegradability test-method used. Tetrachloroethane was shown to exhibit higher resistance to bio-oxidation than the two trichloroethanes (1,1,1-

Table 5—Biodegradability of nitrogenous organics evaluated by the static screening flask test method.

Test compound	Concentration of test compound (mg/l)	Performance summary	Average of 3 test flasks (biodegradation of test compound in 7 days (%))			
			Original culture	First subculture	Second subculture	Third subculture
Nitrosamines						
N-Nitroso-di-N-propylamine	5	N	27	37	47	50
	10	N	0	8	40	40
N-Nitrosodiphenylamine	5	D	87	100	92	100
	10	A	47	63	95	98
Substituted benzenes						
Isophorone	5	D	100	100	100	100
	10	D	100	100	100	100
1,2-Diphenylhydrazine	5	T	80	73	66	77
	10	T	72	55	40	40
Acrylonitrile	5	D	100	100	100	100
	10	D	100	100	100	100
Acrolein	5	D	100	100	100	100
	10	D	100	100	100	100

D—Significant degradation with rapid adaptation
A—Significant degradation with gradual adaptation
T—Significant degradation with gradual adaptation followed by a deadaptive process (toxicity).
N—Not significantly degraded under the conditions of the test method

and 1,1,2-isomers) which in turn are more refractive to degradation than the two dichloroethanes. Rate of bio-oxidation was also shown to vary depending on the position of the chlorine atom on the C_2 carbon structure. Hexachloroethane, in contrast, exhibits significant degradative activity with rapid adaptation of the microbiota.

These findings are based on considering the relationship of the total percentage of loss data, with the volatility data of the chloroethane aliphatics. Whereas refrigeration temperature did not show any loss of substrate from volatility, losses from volatilization were observed at 25°C for the 10-day holding period. However, considering that the volatility losses were established for non-biological volatility control systems, the volatility losses in experimental biological set-ups were such that the loss of the substrate from biodegradative activity could be inferred. Based on literature data, the chloroethane aliphatics, 1,1- and 1,2-dichloroethane, and 1,1,1-trichloroethane are considered to be potentially biodegradable and will probably be destroyed during the aerobic treatment after a considerable period of acclimation, whereas tetrachloroethanes will exhibit recalcitrance to microbial activity and might be bio-oxidized only after very extensive acclimation periods.[26-28] Because of their lipophylicity, the dichloroethanes should not be bioaccumulated to a large extent, whereas the tri- and tetrachloroethanes, being lipophylic in nature, might have a tendency for accumulation.

Halomethanes. The halomethane aliphatics demonstrate different biodegradation rates and acclimation periods, depending on the test compound and substrate concentration in the culture media. Methylene chloride, bromochloromethane, and carbon tetrachloride were shown to exhibit rapid degradation, whereas chloroform shows significant dissimilation with gradual adaptation. Dichlorobromomethane and bromoform demonstrate 59 and 51% losses and 48 and 35% losses at 5 and 10 mg/l, respectively, at the end of the third subculture period. Chlorodibromomethane and trichlorodifluoromethane exhibit recalcitrance for the four 7-day incubation periods.

As in the case of chloroethane aliphatics, the biodegradability findings for halomethanes are based on evaluation of the effect that volatilization of these compounds might have on the bio-oxidative activity in the microbiota. The total losses of these substrates from culture media, as shown on Table 6, compared to the volatility losses for methylene chloride, bromochloromethane, carbon tetrachloride, chloroform, dichlorobromethane, and bromoform allow biodegradation to be inferred. In contrast, with chlorodibromo- and trichorofluoromethane, any possible loss of the substrate caused by bio-oxidative action was shown to be precluded by the loss resulting from volatilization.

Chloroethylenes. Based on the analytical data for the four incubation periods of the experimental culture series and on the analysis of the volatility, certain assessments may be made about the biodegradability of the chloroethylene aliphatics. The 1,1-dichloroethylene compound showed relatively significant biodegradation with gradual adaptation at the end of the first subculture period, with leveling off for the next two subculture periods. The volatilization of the substrate in the non-biological volatility control systems at 25°C, although significant, was observed not to be the dominant process, because of the relatively high total precentage of losses of the compound at the end of each successive incubation period.

The 1,2-cis- and 1,2-trans-dichloroethylenes exhibit slow biodegradative activity concomitant with the relatively moderate rate of volatilization established in the non-biological volatility control systems. Based on the total percentage of loss of substrate in culture media and the loss from volatilization, the 1,2-trans-dichloroethylene isomers can be considered more refractive to bio-oxidation than the 1,1-dichloroethylene compound. In general, the dichloroethylene carbon structure seems to confer a significant stability of the molecule to microbial bio-oxidative action.

The chloroethylene aliphatics, trichloroethylene, and tetrachloroethylene, were shown to be significantly biodegradable with gradual adaptation observed. The relatively significant volatilization in the non-biological volatility control series did not preclude the biodegradative activity of microbiota in culture media from the relatively high total percentage of loss of substrate throughout the study in comparison to the volatility percentage losses.

There was no evidence of loss of the substrate from volatilization under refrigeration noticed with the chloroethylenes or the halomethanes.

Dichloropropanes and dichloropropyleses. Biodegradability data indicate that 1,2-dichloropropane and 1,3-dichloropropylene are essentially biodegradable compounds, exhibiting relatively high biodegradative rates, with gradual adaptation of microbiota.

Considering the relatively insignificant volatilization of the chloropropane and chloropropylene aliphatics, the above compounds achieved 89 and 81% losses and 85 and 84% losses at 5 and 10 mg/l, respectively, at the end of the third subculture period. The total percentage of losses at the end of the respective incubation periods in the culture media were essentially from the bio-oxidative activity of the microbiota.

Literature data on 1,2-dichloropropane and 1,3-dichloropropylene corroborate the findings from the static-culture-flask biodegradability screening studies. They are considered biodegradable compounds based on the studies with soil and wastewater microorganisms.[29-31]

Table 6—Biodegradability and volatility studies with halogenated aliphatics evaluated by the static-screening-flask test method.

Test compound	Conc. (mg/l)	Performance summary	Average total loss of test compound in 7 days incubation time (%)				Volatilization loss (%)	
			Original	First	Second	Third	5° C	25° C
Chloroethanes								
1,1-Dichloroethane	5	A	50	78	85	91	0	19
	10	A	29	74	79	83	0	4
1,2-Dichloroethane	5	B	26	41	54	63	0	27
	10	B	20	35	51	53	0	5
1,1,1-Trichloroethane	5	B	29	64	76	83	0	27
	10	B	23	53	68	75	0	7
1,1,2-Trichloroethane	5	C	6	30	38	44	0	15
	10	C	0	27	30	39	0	3
1,1,2,2-Tetrachloroethane	5	N	0	12	27	29	0	7
	10	N	0	11	20	23	0	6
Hexachloroethane	5	D	100	100	100	100	0	0
	10	D	100	100	100	100	0	0
Halomethanes								
Methylene chloride	5	D	100	100	100	100	0	25
	10	D	100	100	100	100	0	6
Bromochloromethane	5	D	100	100	100	100	0	11
	10	D	100	100	100	100	0	3
Carbon tetrachloride	5	D	87	100	100	100	0	23
	10	D	80	100	100	100	0	5
Chloroform	5	A	49	85	92	100	0	24
	10	A	46	70	80	100	0	6
Dichlorobromomethane	5	A	35	54	56	59	0	8
	10	A	34	44	46	51	0	1
Bromoform	5	A	11	22	40	48	0	0
	10	A	4	14	31	35	0	0
Chlorodibromomethane	5	N	25	28	35	39	0	16
	10	N	10	12	21	25	0	3
Trichlorofluoromethane	5	N	59	61	65	73	5	58
	10	N	38	40	43	45	2	37
Chloroethylenes								
1,1-Dichloroethylene	5	A	78	100	100	100	0	24
	10	A	45	100	100	100	0	15
1,2-Dichloroethylene-cis	5	B	54	76	79	86	0	34
	10	B	43	75	78	84	0	27
1,2-Dichloroethylene-trans	5	B	67	79	88	95	0	33
	10	B	40	76	81	93	0	26
Trichloroethylene	5	A	64	73	82	87	0	29
	10	A	38	56	76	84	0	22
Tetrachloroethylene	5	A	45	54	69	87	0	23
	10	A	30	41	67	84	0	16
Chloropropanes								
1,2-Dichloropropane	5	A	42	70	79	89	0	3
	10	A	36	61	69	81	0	0
Chloropropylenes								
1,3-Dichloropropylene	5	A	55	65	75	85	0	19
	10	A	54	64	69	84	0	7
Chlorobutadienes								
Hexachloro-1,3-butadiene	5	D	100	100	100	100	0	1
	10	D	100	100	100	100	0	0
Chloropentadienes								
Hexachlorocyclopentadiene	5	D	100	100	100	100	0	0
	10	D	100	100	100	100	0	0

D—Significant degradation with rapid adaptation
A—Significant degradation with gradual adaptation
B—Slow to moderate biodegradative activity, concomitant with significant rate of volatilization.
C—Very slow biodegradative activity, with long adaptation period needed.
N—Not significantly degraded under the conditions of test method and/or precluded by extensive rate of volatilization.

Table 7—Biodegradability of organochlorine pesticides evaluated by the static screening flask test method.

Test compound	Concentration of test compound (mg/l)	Performance summary	Average of 3 test flasks biodegradation of test compound in 7 days (%)			
			Original culture	First subculture	Second subculture	Third subculture
Aldrin	5	N	0	0	0	0
	10	N	0	0	0	0
Dieldrin	5	N	0	0	0	0
	10	N	0	0	0	0
Chlordane	5	N	0	0	0	0
	10	N	0	0	0	0
DDT p,p'	5	N	0	0	0	0
	10	N	0	0	0	0
DDE p,p'	5	N	0	0	0	0
	10	N	0	0	0	0
DDD p,p'	5	N	0	0	0	0
	10	N	0	0	0	0
Endosulfan-alpha	5	N	0	0	0	0
	10	N	0	0	0	0
Endosulfan-beta	5	N	0	0	0	0
	10	N	0	0	0	0
Endosulfan sulfate	5	N	0	0	0	0
	10	N	0	0	0	0
Endrin	5	N	0	0	0	0
	10	N	0	0	0	0
Heptachlor	5	N	0	0	0	0
	10	N	0	0	0	0
Heptachlor epoxide	5	N	0	0	0	0
	10	N	0	0	0	0
Hexachlorocyclohexane	5	N	0	0	0	0
BHC-alpha	10	N	0	0	0	0
Hexachlorocyclohexane	5	N	0	0	0	0
β-BHC-beta	10	N	0	0	0	0
Hexachlorocyclohexane	5	N	0	0	0	0
δ-BHC-delta	10	N	0	0	0	0
Hexachlorocyclohexane	5	N	0	0	0	0
λ-BHC-gamma (lindane)	10	N	0	0	0	0

N—Not significantly degraded or biotransformed under the conditions of the biodegradability test procedure used (phenol control 100 percent degraded)

Chlorobutadienes and chloropentadienes. The compounds, hexachloro-1,3-butadiene and hexachlorocyclopentadiene, demonstrated a 100% loss of substrate at 5 and 10 mg/l at the end of the original culture incubation period and this bio-oxidative activity continued over the next three 7-day incubation periods. The volatility control systems showed almost no loss from volatilization of the two compounds at both the refrigeration and 25°C holding temperatures.

These data are in agreement with reported studies on hexachlorocyclopentadiene, which was shown to be degradable by the microorganisms of wastewater sludge and of an aquatic ecosystem.[32,33]

Organochlorine insecticides. The priority pollutants consisting of aldrin, dieldrin, chlordane, DDT p,p', DDE p,p', DDD p,p', endosulfan-alpha, endosulfan-eta, endosulfan sulfate, heptachlor, heptachlor epoxide, endrin, hexachlorocyclohexane isomers (alpha, beta, and delta) and lindane compounds were shown to be recalcitrant to bio-oxidative activity of wastewater microbiota at 5 and 10 mg/l for the four successive 7-day incubation periods of the static-flask-culture method. Data based on chromatographic analysis of methylene chloride extracts indicate 0% losses of the above insecticide compounds. The chromatographic results indicate no reduction of the chromatographic peaks characterizing each parent pesticide and concomitant absence of new peaks with different retention times suggesting possible transformation metabolites, thus providing evidence of persistence of the parent substrate.

Table 7 summarizes the biodegradability data with organochlorine insecticides for the successive 7-day incubation and subculture periods. Evidence of absence of any biodegradative activity in the static culture flask studies is corroborated by the results from literature-reported studies, with regards to the organochlorine pesticides, dieldrin, chlordane, DDE, DDD, endosulfan sulfate, endrin, and heptachlor epoxide.

Possible transformation activities by microorganisms in the static-culture-flask studies, such as epoxidation of aldrin to dieldrin; cometabolic transformation of DDT to DDE; possible transformation of endosulfan isomers to endosulfan sulfate and heptachlor to heptachlor epoxide; and transformation reaction of alpha, beta, and delta BHC isomers, as well as of lindane to metabolites, if present, were not established by the analytical procedures used.

These results on the chlorinated insecticides are consistent with published work on this class of compounds, which show resistance to biodegradation.[34-36]

Priority pollutants not evaluated by the static-flask test. This current work with priority pollutants comprises a total of 96 organic compounds belonging to several well-defined chemical classes. The EPA Consent Decree list includes 114 organic compounds. The additional 18 compounds were not included in the static culture flask biodegradability screening studies for the following reasons:

Polycyclic Aromatic Hydrocarbons		
Benzo(a)-pyrene	Carcinogenic compound	Included in Illinois Institute of Technology (IIT) Research Institute Contract Studies, Chicago, Ill. (EPA Contract #68-03-2834)
3,4-Benzofluoranthene	Carcinogenic compound	
Benzo(k)fluoranthene	Carcinogenic compound	
Benzo(g,h)perylene	Carcinogenic compound	
Dibenzo(a,h)anthracene	Carcinogenic compound	
Indeno(1,2,3-cd)pyrene	Carcinogenic compound	
Pesticides		
Toxaphene	Toxic or carcinogenic compound	Included in ITT Research Institute Contract Studies, Chicago, Ill.
Dioxin	Toxic or carcinogenic compound	
Endrin aldehyde	Compound unavailable	
Arylamines (biphenylamines)		
Benzidine	Carcinogenic compound	Included in IIT Research Institute Contract Studies Chicago, Ill. Published Continuous Feed Reactor Studies[37]
3,3'-Dichlorobenzidine	Carcinogenic compound	
Haloethers		
Bis-(2-chloromethyl) ether	Toxic and/or carcinogenic compound	Included in IIT Research Institute Contract Studies, Chicago, Ill.
N-nitrosodimethylamine	Carcinogenic compound	Included in IIT Research Institute Contract Studies Chicago, Ill.
Chloroethanes and Halomethanes		
Vinyl chloride	Carcinogenic compound	Included in IIT Research Contract Studies Chicago, Ill.
Chloroethane	Gas at room temperature	
Methyl chloride	Gas at room temperature	
Methyl bromide	Gas at room temperature	
Dichlorodifluoromethane	Gas at room temperature	

DISCUSSION

The static-culture-flask biodegradation screening technology used in this study made it possible to determine the biodegradability of each of the priority pollutants at two concentrations (5 and 10 mg/l) by wastewater microbiota, utilizing culture-enrichment techniques. Under normal waste treatment conditions, such culture-enrichment processes are different and the feed and sludge retention times may not always be optimum for the establishment of an acclimated microbial population to efficiently treat the priority pollutant. Furthermore, the concentration levels of the organic pollutants in wastewater will be significantly smaller than those used in the biodegradation studies, and as such, may not elicit an induction enzyme formation response by the activated sludge microbiota.

The assessments of the biodegradability of the priority pollutants with the use of the static-culture-flask method can be helpful, however, in predicting the treatability of these compounds by the normal wastewater treatment process, provided methodology is modified to allow for adaptation to these compounds to occur. The static-culture-flask data can be utilized to predict the possible recalcitrance, stability, and persistence in the effluents and in natural bodies of water, following effluent discharge, as well as the potential toxicity of the parent compound or their metabolites to microbiota of activated sludge during the waste treatment.

The completed studies have established a biodegradability profile for the priority pollutants constituting several classes of organic compounds included in the Consent Decree list. The findings from the biodegradability studies could be utilized in the development of bio-oxidative predictability patterns for closely related compounds.

In some cases, it was possible to compare the results of the simple static screening tests with published work that utilized a variety of biodegradation procedures. In all such cases, good agreement was noted.

The priority pollutants that were observed not to exhibit significant degradation under the conditions of the static-culture-flask methodology, cannot be presumed to be completely recalcitrant to microbial action. More rigorous biodegradability methods, such as shaker-flask techniques, soil percolation studies, aerated batch fermentation set-ups, and the continuous-feed aerated reactor technology could be utilized to provide optimum conditions for acclimation of microorganisms to dissimilate the compounds, and thus definitely ascertain the biodegradability of the pollutant that did not pass the static-culture-flask screening test.

ACKNOWLEDGMENTS

Credits. The authors wish to express their appreciation to Patricia A. Hamler for her technical assistance in sample and media preparations and in the culture-enrichment aspects of the study, Mark Meckes and Harold P. Clark in the cultural and analytical phases of the investigation, William Chaney for his efforts in the extraction of culture samples, Harold L. Sparks for the TOC analytical determination on samples, and Burney N. Jackson for his thorough involvement in the chromatography analytical phases of the study. Barry A. Coddens, Instructor at the College of Mount St. Joseph, aided in the project during the summer of 1979.

Authors. Henry H. Tabak, Stephen A. Quave, Charles I. Mashni, and Edwin F. Barth are all research chemists with the Municipal Environmental Research Laboratory of EPA, Cincinnati, Ohio.

REFERENCES

1. Natural Resources Defense Council, Inc. v. Train, 8 ERC 2120, 2122-29 (D.D.C. 1976).
2. Bunch, R. L., and Chambers, C. W., "A Biodegradability Test for Organic Compounds." *Jour. Water Poll. Control Fed.*, 39, 181 (1967).
3. Tabak, H. H., and Hannah, S., "Static Procedure for Biodegradability Determination." Internal EPA Report, Mun. Environ. Res. Lab., Cincinnati, Ohio (1979).
4. Tabak, H. H., *et al.*, "Microbial Metabolism of aromatic Compounds. I. Decomposition of Phenolic Compounds and Aromatic Hydrocarbons by Phenol-adapted Bacteria." *Jour. Bacteriol.*, 87, 4, 910 (1964).
5. Saeger, V. W., and Tucker, E. S., "Biodegradation of Phthalic Acid Esters in River Water and Activated Sludge." *Appl. Environ. Microbiol.* 31, 1, 29 (1976).
6. Gibson, D. T., "Microbial Degradation of Polycyclic Aromatic Hydrocarbons." *Proc. 3rd Intl. Biodegradation Symp.*, Applied Sci. Pub. Ltd., J. M. Sharpley and A. M. Kaplan (Eds.), (1975).
7. Alexander, M., and Lustigan, B. K., "Effect of Chemical structure on Microbial Degradation of Substituted Benzenes." *Jour. Agr. Food Chem.*, 14, 4, 410, (1966).
8. Gibson, D. T., *et al.*, "Oxidative Degradation of aromatic Hydrocarbons by Microorganisms. I. Enzymatic Formation of Catechol from Benzene." *Biochem.* 7, 2653 (1968).
9. Gibson, D. T., *et al.*, "Oxidative Degradation of Aromatic Hydrocarbons by Microorganisms. II. Metabolism of Halogenated Aromatic Hydrocarbons." *Biochem.*, 7, 11, 3795 (1968).
10. Radding, S. B., *et al.*, "The Environmental fate of Selected Polynuclear Aromatic Hydrocarbons." U. S. Environmental Protection Agency, OTS, Washington, D. C., EPA 560/5-75-009 (1976).
11. Clark, R. R., *et al.*, "Degradation of Polychlorinated Biphenyls by Mixed Microbial Cultures." *Appl. and Environ. Microbiol.*, 37, 4, 680 (1979).
12. Wong, P. T. S., and Kaiser, K. L. E., "Bacterial Degradation of PCB's. II. Rate Studies." *Bull. Environ. Contam. and Toxicol.*, 13, 2, 249 (1976).
13. Tucker, E. S., *et al.*, "Activated Sludge Primary Biodegradation of Polychlorinated Biphenyls." *Bull. Environ. Contam. and Toxicol.*, 14, 705 (1975).
14. Baxter, R. A. *et al.*, "The Degradation of Polychlorinated

Biphenyls by Microorganisms." *Sci. Total Environ.*, **4**, 53 (1975).

15. Tulp, M. T. M., *et al.*, "The Bacterial Metabolism of 4,4'-Dichlorophenyl and Its Suppression by Alternative Carbon Sources." *Chemosphere*, 1, 103 (1978).
16. Ludzak, F. J., and Ettinger, M. B., "Biodegradability of Organic chemicals Isolated from Rivers." *Purdue Univ. Eng. Bull.*, Ext. Ser. **115**, 278 (1963).
17. Tate, R. L. III, and Alexander, M., "Stability of Nitrosamines in Samples of Lake Water, Soil and Sewage." *Jour. Natl. Cancer Inst.*, **54**, 2, 327 (1975).
18. Tate, R. L. III, and Alexander, M., "Resistance of Nitrosamines to Microbial Attack." *Jour. Environ. Qual.*, **5**, 2, 131 (1976).
19. Versar, Inc., "Water-Related Environmental Fate of 129 Priority Pollutants, Vol. II. Ethers, Phthalate Esters and Nitrosamines." U. S. Environmental Protection Agency, Washington, D. C. EPA-440/4-79-029-b (1979).
20. Truhaut, R., *et al.*, "Metabolic Study of an Industrial Solvent, Isophorone in the Rabbit." *C. R. Acad. Sci.*, Ser. D., **271**, 15, 1333 (1970).
21. Lank, J. C., and Wallace, A. T., "Effect of Acrylonitrile on Anaerobic Digestion of Domestic sludge." *Purdue Univ. Eng. Bull.*, Ext. Ser. **137**, 2, 518 (1970).
22. Wierzbicki, T., and Wojcik, O., "Preliminary Trials on the Decomposition of Acrolein, Allyl Alcohol and Glycerol by Activated Sludge." *Zesz. Nauk. Politech. Slaska, Inz. Sanit.* (Pol.), 8, 173 (1965); *CA*68:1589z (1968).
23. Larson, R. G., "Biological Treatment in Water Conservation." *Amer. Chem. Soc. Div., Petrol. Chem.*, Preprints **12**, 4, A63 (1967).
24. Bowmer, K. H., *et al.* "Loss of Acrolein from Water by Volatilization and Degradation." *Weed Res.*, **14**, 325 (1974).
25. Mackay, D., *et al.* "Determination of Air-Water Henry's Law Constants for Hydrophobic Pollutants." *Environ. Sci. & Technol.*, **13**, 3, 323 (1979).
26. Thom, N. S., and Agg, A. R., "The Biodegradation of Synthetic Organic Compounds in Biological Processes." *Proc. Roy. Soc.*, B. **159**, 347 (1975).
27. Pearson, C. R., and McConnell, G., "Chlorinated C_1 and C_2 Hydrocarbons in the Marine Environment." *Proc. Roy. Soc.*, B., **189**, 305 (1975).
28. McConnell, G., *et al.*, "Chlorinated Hydrocarbons and the Environment." *Endeavor* (G. B.), **34**, 13 (1975).
29. Altman, J., and Lawlor, S., "The Effects of Some Chlorinated Hydrocarbons on Certain Soil Bacteria." *Jour. Appl. Bacteriol.*, **29**, 2, 260 (1966).
30. Roberts, T. R., and Stoydin, G., "The Degradation of (Z) and (E)-1,3-Dichloropropenes and 1,2-Dichloropropane in Soil." *Pest. Sci.*, **7**, 325 (1976).
31. Castro, C. E., and Belser, N. O., "Hydrolysis of Cis- and Trans-1,3-Dichloro-propene in Wet Soil." *Jour. Agri. Food Chem.*, **14**, 1, 69 (1966).
32. Lu, P. Y., *et al.*, "Evaluation of Environmental Distribution and Fate of Hexachlorocyclopentadiene, Chlordane, Heptachlor and Heptachlor Epoxide in a Laboratory Model Ecosystem." *Jour. Agr. Food Chem.*, **23**, 5, 967 (1975).
33. Whitmore, F. C., *et al.*, "Region IV Support at Morris Forman Wastewater Plant, Louisville, Kentucky." Task I, Final Report, EPA Contract 58-01-2618 (1977).
34. Bollag, J. M., "Microbial Transformation of Pesticides." *Advan. Appl. Microbiol.*, **18**, 75 (1974).
35. Pfister, R. N., "Interactions of Halogenated Pesticides and Microorganisms. A Review." *CRC Critical Reviews in Microbiol.* **21**, 1, 1 (1972).
36. Trudgill, *et al.*, "Effects of Organochlorine Insecticides on Bacterial Growth, Respiration and Viability." *Jour. Gen. Microbiol.*, **69**, 1, 1 (1971).
37. Tabak, H. H., and Barth, E. F., "Biodegradability of Benzidine in Aerobic Suspended Growth Reactors." *Jour. Water Poll. Control Fed.*, **50**, 3, 552 (1978).

G. Mille

EOS

Paper by Wilson & McNabb

Transactions, American Geophysical Union
Vol. 64 No. 33 August 16, 1983

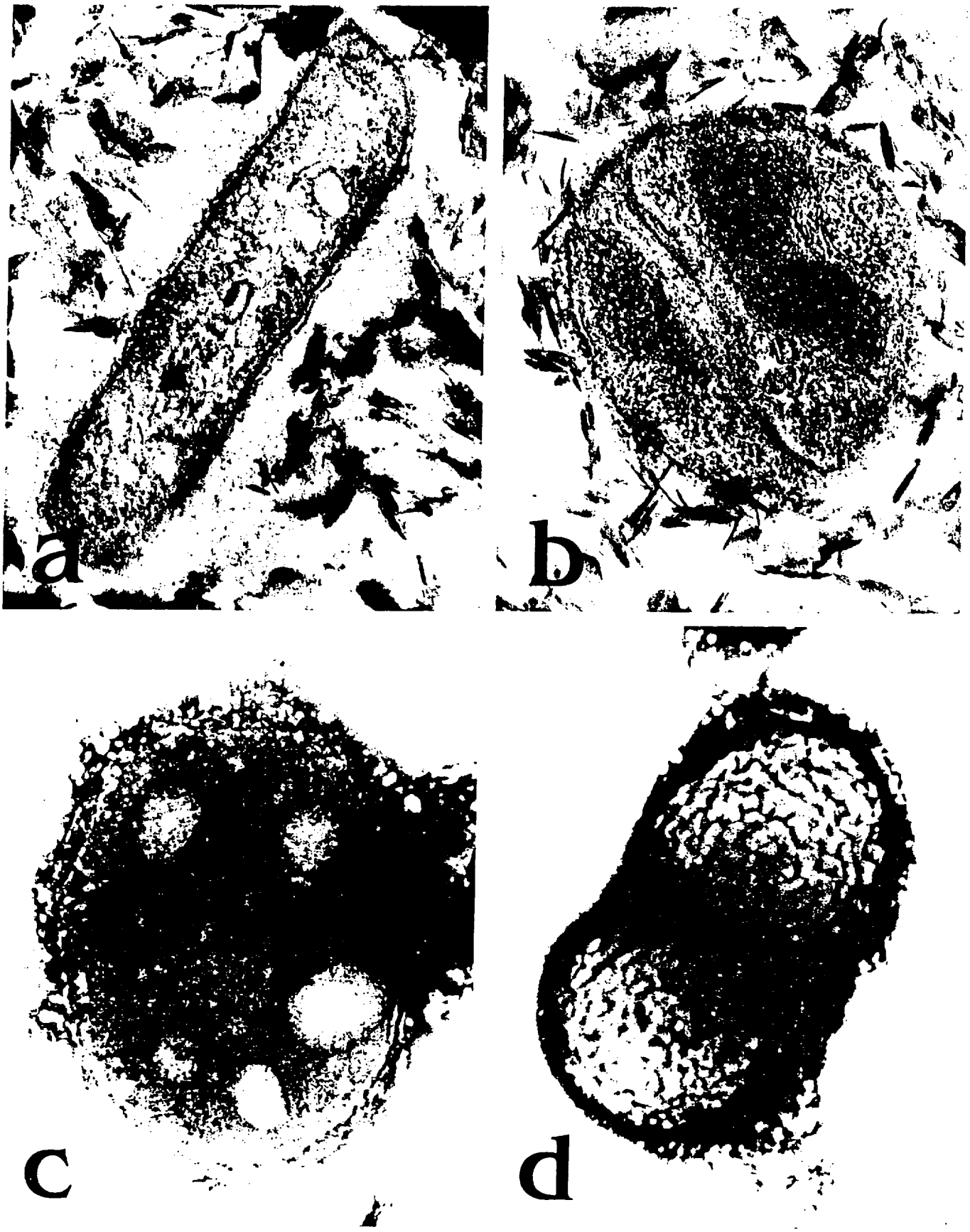

Biological Transformation of Organic Pollutants in Groundwater

John T. Wilson and James F. McNabb

R. S. Kerr Environmental Research Laboratory, U.S. Environmental Protection Agency, Ada, Oklahoma 74820

Recent investigations have discovered surprisingly high numbers of microorganisms in shallow water-table aquifers. Evidence is accumulating that these microorganisms may, under certain circumstances, transform many of the organic pollutants that enter the subsurface environment. These transformations can lead to total destruction of the pollutant or to the production of new organic pollutants.

Introduction

The phenomenal expansion of the chemical industry in this century, and particularly since World War II, has brought us many blessings and several new problems. Among these is widespread pollution of groundwater in industrial areas with organic contaminants and the growing pollution of groundwater in agricultural areas with pesticides and herbicides. The role played by microorganisms in the destruction of organic contaminants in surface water has long been appreciated. However, the importance of subsurface microorganisms in controlling the quality of groundwater has only recently become apparent.

Groundwater is Part of the Biosphere

In early studies of the numbers of microbes in soils, the microorganisms were counted by spreading dilutions of subsurface material on a culture medium and counting the colonies that developed. Because very few colonies developed from samples of soil taken below the root zone, early microbiologists concluded that this region of the earth was essentially devoid of life [*Waksman*, 1916]. As a result, an understanding of the true size and importance of the populations of organisms that occur naturally in groundwater was delayed. Recently, techniques have been developed that allow microbiologists to study all of the microbes in the subsurface and not just those that could grow on nutrient agar or on some similar growth medium.

Special staining procedures that distinguish cellular material from noncellular particles of the same size and shape have been adapted to subsurface material [*Ghiorse and Balkwill*, 1983]. After staining, the microbes can be counted directly in samples of subsurface material with a microscope. The technique has been applied to core material from several shallow water-table aquifers and associated material from the vadose zone. These cores were obtained by using special procedures developed to provide uncontaminated subsurface samples [*Wilson et al.*, 1983*b*]. The numbers of organisms were surprisingly high (Table 1). Numbers did not decline drastically with depth, and there was surprising uniformity of numbers at different seasons and in material from replicate bore holes at the same site.

The population density of organisms in the cores was comparable with the density of bacteria in nutrient-rich lakes [see *Pedros-Alio and Brock*, 1982]. In fact, the total biomass in regions below the root zone in North America is probably much higher than the bacterial biomass in the rivers and lakes of our continent. Shallow water-table aquifers and associated regions of the vadose zone, therefore, are an important microbial habitat, which until recently had been virtually ignored by microbiologists.

The groundwater microbes were studied by electron microscopy to learn something of their structure and taxonomy. When fine-grained subsurface material was examined, several morphological forms of bacteria were seen [*Ghiorse and Balkwill*, 1983; *Wilson et al.*, 1983*b*]. There was little evidence of yeasts or other fungi, protozoa, or higher animals. This makes the assemblage of bacteria in these environments unique, because organisms that are important scavengers and predators in other natural systems, such as protozoa, are missing. Sands and gravels in river valleys may contain a wide variety of higher organisms [*Danielpol*, 1976]. Coarse material in upland landscapes is yet to be examined.

To confirm the results of the microscopic examinations, the biomass of organisms in the core material was also estimated by extracting and quantifying certain biochemical compounds that are usually restricted to living organisms [*White et al.*, 1983]. The biochemical analyses for biomass, in general, showed good agreement with expected values based on cell numbers. Also in agreement with the direct count, the biochemical characterization failed to detect any of several biochemicals that are found in protozoa, fungi, or higher animals, but not in bacteria.

The biochemical characterization of subsurface material is potentially a very powerful tool. Certain physiological groups of bacteria, such as the sulfate reducers or the methane bacteria, can be detected by the presence of cellular constituents that are restricted to that group. On the other hand, the general nutritional state of the entire biological community can often be inferred from the ratio of the quantities of certain biochemicals found in most bacteria.

Biotransformations of Organic Pollutants

Organisms in the deeper subsurface environment can transform many important organic pollutants. The rate of transformation

Cover. Electron micrographs of microbial cells released from subsurface samples. (*a*) Thin section of cell released by the blending-centrifugation method. Note Gram-negative wall structure and presence of fibrous polysaccharide slime material around cell. (*b*) Thin section of cell released by the blending-centrifugation method. Note Gram-positive cell wall and presence of cross wall (division septum) within cell (CW). (*c*) Negative stain of cell released by the flotation method. Light areas within cell are probably PHB (poly-β-hydroxybutyrate) granules. (*d*) Negative stain of cell released by the flotation method. Note Gram-negative wall structure and that cell appears to be dividing. (Photo submitted by John T. Wilson and James F. McNabb; reprinted by permission of *Ground Water*. Copyright © 1983. All rights reserved.) (See p. 505 for article.)

TABLE 1. Numbers of Organisms in the Subsurface Environment

Site	Depth to Water Table, m	Subsoil§	Just Above Water Table§	Just Below Water Table§
Lula, Okla.*	3.6			
February 1981		6.8	3.4	6.8
June 1981		9.8	3.7	3.4
Fort Polk, La.†				
Borehole 6B	6.0	3.4	1.3	3.0
Borehole 7	5.0	7.0	1.3	9.8
Conroe, Texas‡	6.0	0.5	0.3	0.6
Long Island, N.Y.‡				
	6.0	—	—	36
	3.0	170	—	—
Pickett, Okla.†	5.0	—	—	5.2

*Wilson et al. [1983].
†Ghiorse and Balkwill [1982].
‡W. G. Ghiorse (personal communication, 1982).
§In millions per gram dry material.

is limited by the numbers and activity of the microorganisms, while the extent of transformation is most frequently limited by some requirement for metabolism such as oxygen, pH buffering capacity, or mineral nutrients.

As a result, the biological fate of a particular class of organic pollutant is controlled by the geochemical properties of the subsurface environment. For example, *Wilson et al.* [1983*a*] and *Wilson et al.* [1983*b*] found no evidence for biological degradation of chlorinated aliphatic hydrocarbons in three shallow aerobic aquifers. On the other hand, *Parsons* [1983] showed that many of these compounds could be transformed in anaerobic subsurface material. In muck soil from Florida, carbon tetrachloride was transformed to chloroform. Similarly, tetrachloroethylene was transformed to trichloroethylene, then to all three dichloroethylenes and perhaps to vinyl chloride. In a study of the fate of halogenated hydrocarbons in treated municipal wastewater after injection of wastewater into an aquifer, *Bouwer et al.* [1981] found that chloroform and several other halogenated methanes were transformed readily in the anaerobic water in the aquifer, and tri- and tetrachloroethylene disappeared at a somewhat slower rate.

The geochemical properties of the subsurface environment also limit the degradation of organic pollutants that are natural products, as opposed to synthetic industrial chemicals. *Ehrlich et al.* [1982] studied the fate of creosote waste in a contaminated aquifer and found that many phenolic compounds in the waste were being degraded to carbon dioxide and methane by an anaerobic consortium of bacteria in the aquifer. However, they found no evidence that polynuclear aromatic hydrocarbons such as naphthalene were being degraded under anaerobic conditions in the aquifer.

Predicting Degradation of Organic Pollutants

The relationship between the concentration of a pollutant and its fate is complex. At reasonably high concentrations (>100 μg/l) utilization of a pollutant can provide an ecological advantage, resulting in an increase in the numbers of microbes that metabolize the organic pollutant. At concentrations less than 10 μg/l, use of the pollutant usually does not provide enough of an advantage to lead to enrichment of active organisms. At concentrations greater than 1,000–10,000 μg/l, metabolism of the pollutant can entirely deplete oxygen or other metabolic requirements in the groundwater.

As a result, compounds that usually are considered degradable may not be transformed by the subsurface microorganisms if the compound is present at low concentrations. Similarly, compounds present at high concentration may be only partially degraded when oxygen is entirely depleted and can only be degraded further after dispersion or other physical processes mix the contaminated water with oxygenated water.

Table 2 presents the authors' opinions concerning the prospects for biotransformation of several important classes of organic pollutants in groundwater. These predictions are based on a cautious extrapolation from the behavior of these compounds in other natural systems and on our admittedly limited experience with their behavior in the subsurface environment. The research effort in this area is expanding rapidly. As our knowledge grows, microbiology should become a useful complement to the earth sciences in our search for a better understanding of the behavior of organic contaminants in the subsurface environment.

TABLE 2. Prospect of Biotransformation of Selected Organic Pollutants in Water-Table Aquifers

Class of Compounds	Aerobic Water, Concentration of Pollutant, μg/l		Anaerobic Water
	>100	<10	
Halogenated Aliphatic Hydrocarbons			
Trichloroethylene	none	none	possible*
Tetrachloroethylene	none	none	possible*
1,1,1-Trichloroethane	none	none	possible*
Carbon Tetrachloride	none	none	possible*
Chloroform	none	none	possible*
Methylene Chloride	possible	improbable	possible
1,2-Dichloroethane	possible	improbable	possible
Brominated methanes	improbable	improbable	probable
Chlorobenzenes			
Chlorobenzene	probable	possible	none
1,2-Dichlorobenzene	probable	possible	none
1,4-Dichlorobenzene	probable	possible	none
1,3-Dichlorobenzene	improbable	improbable	none
Alkylbenzenes			
Benzene	probable	possible	none
Toluene	probable	possible	none
Dimethylbenzenes	probable	possible	none
Styrene	probable	possible	none
Phenol and Alkyl Phenols	probable	probable	probable†
Chlorophenols	probable	possible	possible
Aliphatic Hydrocarbons	probable	possible	none
Polynuclear Aromatic Hydrocarbons			
Two and three rings	possible	possible	none
Four or more rings	improbable	improbable	none

*Possible, probably incomplete.
†Probable, at high concentration.

Acknowledgments

Although the research described in this article has been funded in part by the United States Environmental Protection Agency through Cooperative Agreement CR806931 to the National Center for Ground Water Research and through in-house research programs at the Robert S. Kerr Environmental Research Laboratory, it has not been subjected to Agency review and therefore does not necessarily reflect the views of the Agency and no official endorsement should be inferred.

References

Bouwer, E. J., B. E. Rittmann, and P. L. McCarty, Anaerobic degradation of halogenated 1- and 2-carbon organic compounds, *Environ. Sci. Tech. 15*, 596–599, 1981.

Danielpol, D. L., The distribution of the fauna in the interstital habitats of riverine sediments of the Danube and Priesting (Austria), *Int. J. Speleol. 8*, 23–51, 1976.

Ehrlich, G. G., D. F. Goerlitz, E. M. Godsy, and M. F. Hult, Degradation of phenolic contaminants in ground water by Anaerobic bacteria: St. Louis Park, Minnesota, *Ground Water, 20*, 703–710, 1982.

Ghiorse, W. C., and D. L. Balkwill, Enumeration and morphological characterization of bacteria indigenous to subsurface environments, *Dev. Ind. Microbiol., 24*, in press, 1983.

Parsons, F., Transformation of chlorinated organic solvents in ground water environments in South Florida, paper to be presented at the ACS Environmental Chemistry Symposium on Organic Contaminant Behavior in the Subsurface Environment, American Chemical Society, Washington, D.C., Aug. 28 to Sept. 2, 1983.

Pedros-Alio, C., and T. D. Brock, Assessing biomass and production of bacteria in eutrophic Lake Mendota, Wisconsin, *Appl. Environ. Microbiol., 14*, 203–218, 1982.

Waksman, S. A., Bacterial numbers in soil, at different depths, and in different seasons of the year, *Soil Sci., 1*, 363–380, 1916.

White, D. C., G. A. Smith, M. J. Gehron, J. H. Parker, R. H. Findlay, R. F. Martz, and H. L. Fredrickson, The ground water aquifer microbiota: Biomass, community structure, and nutritional status, *Dev. Ind. Microbiol., 24*, in press, 1983.

Wilson, J. T., J. F. McNabb, B. H. Wilson, and M. J. Noonan, Biotransformation of selected organic pollutants in ground water, *Dev. Ind. Microbiol., 24*, in press, 1983*a*.

Wilson, J. T., J. F. McNabb, D. L. Balkwill, and W. C. Ghiorse, Enumeration and characterization of bacteria indigenous to a shallow water-table aquifer, *Ground Water, 21*, 134–142, 1983*b*.

John T. Wilson is a soil microbiologist and microbial ecologist who has been actively involved in research dealing with biodegradation of organic contaminants in groundwater since receiving his Ph.D. from Cornell University in 1978. He is currently a microbiologist with the U.S. Environmental Protection Agency's Ground Water Research Branch at the Robert S. Kerr Environmental Research Laboratory in Ada, Oklahoma, where his research is concentrated on developing a kinetic description of the biotransformation of organic contaminants in the subsurface by indigenous organisms.

James F. McNabb has been a microbiologist with the Ground Water Research Branch of U.S. EPA's Robert S. Kerr Environmental Research Laboratory in Ada, Oklahoma, since the late 1960's. He has degrees from Texas Technological University and the University of Oklahoma and received in 1978 a Fulbright research grant to conduct groundwater research in New Zealand. His research interests involve many aspects of groundwater microbiology including the development of methods for the study of subsurface microbial activity.

Modeling of Trace Organics Biotransformation in the Subsurface

by Edward J. Bouwer[a] and Perry L. McCarty[b]

ABSTRACT

Biofilm processes are potentially important for transformations of organic micropollutants in ground water. Some theoretical hypotheses and empirical observations suggest that a concentration threshold exists for some compounds below which the concentration cannot be reduced by bacterial action. However, in the presence of one compound at a relatively high concentration, termed the primary substrate, another compound present at trace concentrations, termed the secondary substrate, can be biotransformed as well. These concepts were evaluated through laboratory column studies with several halogenated organic compounds of importance in ground water. A biofilm model can successfully describe utilization of trace substrates, and application to modeling the subsurface is discussed. A simplified batch model with first-order kinetics may be adequate for describing subsurface microbial processes when low active organism and pollutant concentrations exist over a large scale.

INTRODUCTION

The movement, transformations, and fate of trace and toxic organic compounds have become of increasing concern because of the potentially harmful effects such materials can have on humans and on the environment. Both inorganic and organic chemicals that enter the subsurface environment can be transformed by microbiological processes. Nonphotosynthetic microorganisms obtain energy for growth by oxidation of substrates in the presence of an electron acceptor, such as oxygen under aerobic conditions, and nitrate, sulfate, and carbon dioxide under anoxic conditions. The energy obtained from the oxidation/reduction reactions is used for cell growth and maintenance, which bring about direct transformations of inorganic and organic compounds. By consuming or producing oxidants, reductants, acids, and bases, microorganisms can also affect the chemical environment in the vicinity of growth, resulting in change in pH and the electrochemical potential of the system. Such environmental alterations can lead to abiotic degradation reactions such as hydrolysis and/or chemical oxidation or reduction of compounds. Microbial growth can also alter the permeability of aquifer material. Thus, many physical and chemical changes can be brought about in association with the decomposition or transformation of substrates by subsurface microorganisms.

The subsurface environment is generally characterized by low substrate and nutrient concentrations and high specific surface area which favor predominance of bacteria attached to solid surfaces in the form of biofilms (Zobell, 1937; Wuhrmann, 1972). Attached bacteria have an advantage over suspended bacteria as they can remain near the source of fresh substrate and nutrients contained in ground water that flows by them. A third microbiologically important characteristic of the subsurface environment is that because of the low concentrations, bacteria are usually required to utilize numerous different compounds to obtain sufficient energy to sustain themselves. Furthermore, a portion of the organic matter, particularly in aquifers containing recharged waste waters, leachates, or spilled chemicals, may consist of xenobiotic compounds.

An understanding of biofilm kinetics is useful, therefore, to adequately understand the kinetics of subsurface microbiological processes. This paper

[a]Environmental Engineering Program, Department of Civil Engineering, University of Houston–University Park, Houston, Texas 77004.

[b]Environmental Engineering and Science, Civil Engineering Department, Stanford, California 94305.

Received February 1984, accepted April 1984.

Discussion open until January 1, 1985.

conceptualizes the application of biofilm modeling to microbiological processes affecting transformations of organic micropollutants in the subsurface. Results of laboratory reactor experiments used to simulate an aquifer and to evaluate the ability of biofilms to transform several halogenated organic compounds present at trace concentrations are given to support the theoretical concepts.

BIOFILM KINETICS

The goal of modeling biofilm processes is to predict the flux of substrate into the film as a function of bulk concentration and quantifiable biofilm parameters. Rittmann and McCarty (1980a) developed a fixed-film model to simulate both the steady-state flux of a single rate-limiting substrate into a biofilm and biofilm mass (thickness) using independently determined rate parameters. Biofilm processes were simplified by considering an idealized biofilm composed of a homogeneous matrix of bacteria and the extracellular polymers that bind the bacteria together and to the surface. The model considers four basic processes which occur simultaneously to cause a flux of substrate from the bulk liquid into the biofilm: (1) mass transport of substrate from the bulk liquid across a fluid boundary layer and into the biofilm described by Fick's First Law, (2) utilization of the substrate and growth by bacteria, assumed to follow a Monod-type relationship, (3) diffusion of the substrate through the biofilm according to Fick's Law, and (4) growth and decay of the biofilm mass. Since details of the model development and solution have been published previously (Rittmann and McCarty, 1980a), no model formulations are presented here. This steady-state biofilm model successfully simulated the flux of substrate as a function of the biofilm parameters and the bulk substrate concentration in laboratory column studies (Rittmann and McCarty, 1980b) and engineered fixed-film processes, such as the submerged filter, rotating biological contactor, and trickling filter (Rittmann and McCarty, 1980c).

Microorganisms require energy to maintain themselves. Should the concentration of a substrate be very low, the organism may not get enough energy from oxidation of the substrate to supply maintenance requirements, and hence, organic compounds at trace concentrations may persist (Alexander, 1981). Boethling and Alexander (1979a; 1979b) showed that biodegradation of trace aqueous concentrations ($\mu g/l$) of glucose, diethanolamine, 2,4-dichlorophenoxyacetate (2,4-D), and 1-naphthyl-N-methylcarbamate (Sevin) was significantly retarded even though the compounds are normally biodegradable at millimolar concentrations. Even for resting or starved cells that appear to have essentially no maintenance energy requirements and that might constitute a significant portion of the indigenous bacteria in the subsurface (Wilson *et al.*, 1983), a concentration threshold can exist for substrates below which the concentration cannot be reduced by biochemical action. In this case, when the substrate is present below the concentration threshold, the energy requirements for active transport of metabolites and energy carriers within the cell and for enzyme induction and synthesis exceed the free energy available from substrate decomposition (Zehnder, 1983).

Rittmann and McCarty (1980a, 1980b) found both theoretically and experimentally that a single substrate cannot be reduced in concentration below some minimum level that is required for maintenance of the bacteria. This limiting value is determined by relating the rates of biofilm growth and loss as given by the relationship:

$$S_{min} = K_s \frac{b}{Yk - b}. \quad (1)$$

S_{min} is the minimum-substrate concentration for existence of a steady-state biofilm, K_s is the Monod half-maximum-rate concentration, b is the first-order decay coefficient, k is the maximum specific rate of substrate utilization by the bacteria, and Y is the cell growth yield. At concentrations below S_{min}, the entire biofilm would be in net decay and would eventually cease to exist. Hence, in order to sustain a biofilm reaction for the long term, the rate-limiting substrate must be present at a concentration greater than S_{min}. The value of S_{min} depends on substrate, electron acceptor, and the organism.

The concept of S_{min} suggests that when a biodegradable contaminant is introduced in the subsurface, the concentration would decrease to a finite level as the contaminant moved through the soil away from the source as a result of steady-state microbial utilization (Figure 1). Many organic micropollutants are present at concentrations below S_{min} and would apparently go unutilized. However, simultaneous utilization of several different substrates is possible; so cells can sometimes metabolize these trace compounds in the presence of another substrate, which provides the cells energy needs. This process is termed secondary utilization and is a mechanism which allows cells to

degrade compounds that could otherwise not provide enough energy to sustain the microbial cultures (McCarty *et al.*, 1981). The primary substrate, which can be one compound or the aggregate of many compounds, is present at a concentration greater than S_{min} and supports the long-term biofilm growth, while individual trace organic compounds, none of which could support biofilm growth alone, are called secondary substrates. Therefore, secondary utilization occurs when a secondary substrate is utilized by a biofilm that is supported by utilization of a primary substrate. A primary substrate provides the organism energy and carbon for cell synthesis, whereas secondary substrates may or may not contribute either to cell growth. A secondary substrate need not share enzymatic pathways with the primary substrate, although the bacteria must be capable of transforming both compounds.

Biofilm kinetic modeling of secondary utilization is derived from the relationship between the primary and secondary substrate. Since the primary substrate is the rate-limiting organic electron donor which contributes energy and carbon to the long-term growth and maintenance of the biofilm, the utilization of the primary substrate and growth of the biofilm can be described by a steady-state biofilm model that balances energy for growth with that used for biomass maintenance (Rittmann and McCarty, 1980a). This model cannot be used to describe secondary utilization since this contributes little to biofilm growth. An appropriate model for describing secondary-substrate flux into a biofilm is one based on the solutions developed by Atkins and Davies (1974) to which mass transport resistance was considered by Rittmann and McCarty (1981). This model simulates substrate flux into the biofilm for any substrate concentration if the biofilm mass and rate parameters are known. Steady-state utilization of secondary substrates can be described with this model by coupling the biofilm mass, which is controlled from degradation of the primary substrate, with concentration and individually determined rate parameters for each secondary substrate.

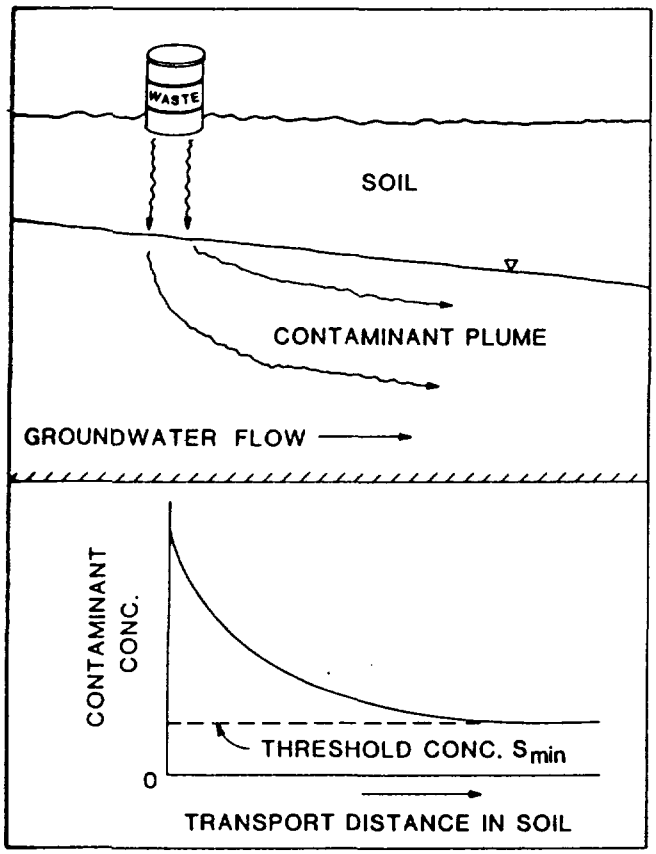

Fig. 1. Biotransformation of organic contaminant following introduction into the subsurface environment.

Substrate utilization within the biofilm was modeled with the Monod relationship,

$$\frac{d\,S_f}{dt} = -\frac{k\,X_f\,S_f}{K_s + S_f} \qquad (2)$$

in which S_f is the rate-limiting substrate concentration in the biofilm, t is time, and X_f is the active cell density. For secondary substrates, the concentration S_f is usually much less than K_s, and the above expression can be simplified and reduced to first order with respect to substrate concentration:

$$\frac{d\,S_f}{dt} = -\frac{k\,X_f}{K_s}\,S_f. \qquad (3)$$

Consequently, for trace substrates, there should be a linear relationship between substrate flux into the biofilm and substrate concentration. Once acclimation has occurred, the rate of degradation of secondary substrates also should be directly proportional to active organism concentration and the ratio of k to K_s.

LABORATORY EVALUATION OF SECONDARY UTILIZATION

Continuous-flow laboratory column studies under aerobic and methanogenic conditions were performed for periods longer than a year with mixed bacterial cultures to evaluate the concept of secondary utilization and to determine the transformability of several potentially hazardous halogenated organic compounds found in contami-

nated ground waters, often at relatively low concentrations (Bouwer and McCarty, 1981, 1982, 1983a). Glass beads were used as the support media for biofilms in order to simulate flow in the subsurface environment while minimizing sorptive effects. Acetate was used as the primary substrate to support bacterial growth. A group of priority pollutants was selected as secondary substrates at concentrations between 10 and 30 μg/l.

Secondary utilization was possible for several nonchlorinated aromatic compounds and chlorinated benzenes under aerobic conditions (Table 1) (Bouwer and McCarty, 1981). The nonchlorinated aromatic compounds were rapidly transformed to effluent concentrations near the detection limit with acclimation times of less than five days. Between ten days and five months were required for acclimation of the biofilm culture to the chlorinated benzenes. Experiments with carbon-14 radiolabeled substrates indicated that chlorobenzene, 1,3-dichlorobenzene, and 1,4-dichlorobenzene were oxidized to CO_2 without detectable intermediates in the presence of biofilm bacteria, confirming removal by biooxidation. The halogenated aliphatic compounds studied were not transformed by the aerobic biofilm or in aerobic batch biodegradation experiments. This is in agreement with their observed persistence in aerobic environments. Significant degradation of these compounds has not been observed during groundwater recharge (Roberts *et al.*, 1982), passage through GAC columns (McCarty *et al.*, 1979), riverbank filtration in Germany (Sontheimer, 1980), or waste-water percolation in soil columns (Bouwer *et al.*, 1981).

Evidence for secondary utilization of halogenated aliphatic compounds was also obtained under methanogenic conditions (Table 1) (Bouwer and McCarty, 1983a). Transformation of the brominated aliphatics to below the detection limit occurred with almost no acclimation period required, while significant removals of almost all

Table 1. Average Utilization of Substrates Fed Continuously to Aerobic and Methanogenic Biofilm Reactors After Acclimation

	*Aerobic biofilm column** (20 min. detention time)			*Methanogenic biofilm column** (2-day detention time)		
Substrate	*Influent conc., μg/l*	*Effluent conc., μg/l*	*% removal*	*Influent conc., μg/l*	*Effluent conc., μg/l*	*% removal*
Primary						
acetate	1.0 ± 0.05 mg/l	0.05 ± 0.0003 mg/l	95 ± 1	100 ± 5 mg/l	0.28 ± 0.1 mg/l	99 ± 1
Secondary						
Chlorinated benzenes:						
chlorobenzene	11.3 ± 2.6	1.05 ± 0.37	91 ± 4	22.1 ± 5	20.5 ± 5	7 ± 26
	1.57 ± 0.3	0.23 ± 0.09	85 ± 6	–	–	–
1,2-dichlorobenzene	9.6 ± 2.4	0.41 ± 0.2	96 ± 2	14.6 ± 3	14.0 ± 3	4 ± 27
1,3-dichlorobenzene	9.8 ± 1.8	7.6 ± 1.4	22 ± 20	10.4 ± 3	10.6 ± 3	−2 ± 29
1,4-dichlorobenzene	10.8 ± 1.8	0.20 ± 0.13	98 ± 1	9.8 ± 3	10.2 ± 3	−4 ± 29
1,2,4-trichlorobenzene	9.2 ± 1.6	0.92 ± 0.4	90 ± 5	11.4 ± 3	10.1 ± 3	11 ± 25
Nonchlorinated aromatics:						
ethylbenzene	9.1 ± 2	0.10 ± 0.1	99 ± 1	12.0 ± 4	11.2 ± 3	7 ± 26
styrene	7.6 ± 1.5	<0.05	>99	7.9 ± 2	7.3 ± 2	8 ± 26
naphthalene	13.8 ± 3.5	0.17 ± 0.12	99 ± 1	28.8 ± 7	29.5 ± 7	−2 ± 29
Halogenated aliphatics:						
chloroform	28.5 ± 4.2	29.1 ± 3.8	−2 ± 20	28 ± 7	0.35 ± 0.2	99 ± 1
carbon tetrachloride	†	–	–	17 ± 1	<0.1	>99
1,2-dichloroethane	†	–	–	22 ± 3	24 ± 3	−1 ± 20
1,1,1-trichloroethane	15.9 ± 3.3	15.5 ± 2.9	3 ± 27	18 ± 2	0.57 ± 0.5	97 ± 3
1,1,2,2-tetrachloroethane	†	–	–	27 ± 1	0.90 ± 0.7	97 ± 3
tetrachloroethylene	9.8 ± 3.7	9.9 ± 3.1	−1 ± 50	15 ± 4	3.7 ± 1.3	76 ± 10
bromodichloromethane	†	–	–	26 ± 3	<0.1	>99
dibromochloromethane	†	–	–	25 ± 2	<0.1	>99
bromoform	†	–	–	26 ± 2	<0.1	>99
1,2-dibromoethane	†	–	–	27 ± 2	<0.1	>99

* One standard deviation of the mean values is given.

† Compound not included in feed to aerobic column. These compounds were not degraded in aerobic batch cultures.

of the chlorinated aliphatics did not occur until after a ten-week lag period. Carbon-14 tracer experiments showed that some of the chlorinated aliphatics were nearly completely oxidized to CO_2 under methanogenic conditions, confirming removal by biooxidation. The aromatic compounds persisted under methanogenic conditions.

The column studies indicated that the type of electron acceptor present was an important factor affecting biotransformability of the priority pollutants studied. Additional experiments indicated a few of the halogenated aliphatic compounds (carbon tetrachloride and brominated trihalomethanes) could be transformed when incubated under anoxic conditions in the presence of denitrifying bacteria (Bouwer and McCarty, 1983b). None of the aromatic compounds showed significant utilization under denitrification conditions.

For the secondary substrates transformed under either aerobic or methanogenic conditions in the continuous-flow columns, the rates of decomposition were similar to those for acetate, the primary substrate, with 1,3-dichlorobenzene and tetrachloroethylene being exceptions. When the influent concentration of chlorobenzene was decreased from 11.3 to 1.57 μg/l, this resulted in a corresponding decrease in effluent concentration to 0.23 μg/l, resulting in 85 percent removal or about the same as that obtained previously (Table 1). Therefore, the first-order dependence between substrate flux into the biofilm and substrate concentration for the secondary substrates was confirmed.

Kinetic modeling of acetate (primary substrate), chlorobenzene, and 1,4-dichlorobenzene (secondary substrates) utilization in the aerobic biofilm reactor resulted in apparent ratios of k to K_s for the substrates of 3.8, 2.5, and 11 l/mg^{-1} day^{-1}, respectively (Bouwer and McCarty, 1984). Independent determination of k and K_s for secondary substrates is difficult because their utilization is not linked with biofilm growth. The measured ratio of k to K_s for acetate and chloroform biotransformation in the methanogenic biofilm reactor was 0.63 and 0.62 l/mg^{-1} day^{-1}, respectively. Although the utilization kinetics for each substrate appeared to be unique, the ratio of k to K_s for each secondary substrate was similar to the value for the primary substrate. Kinetic constants were within the general range expected for aerobic and methanogenic heterotrophic bacterial growth (Metcalf and Eddy, Inc., 1979). The active organism concentration in the aerobic and methanogenic columns was similar, so comparison of the k to K_s ratios indicates the overall decomposition rate under methanogenic conditions appeared to be five to ten times slower than under aerobic conditions.

MODEL SIMULATIONS OF LABORATORY RESULTS

Acetate utilization in the aerobic reactor was simulated with the steady-state biofilm model of Rittmann and McCarty (1980a) to yield substrate flux into the biofilm and biofilm mass. This biofilm mass was coupled with kinetic parameters determined for the secondary substrates in a second model developed for a biofilm of specified thickness (Rittmann and McCarty, 1981) to simulate utilization of the secondary substrates. This approach resulted in reasonable agreement between biofilm model simulations and the measured steady-state acetate, chlorobenzene, and 1,4-dichlorobenzene concentration profiles along the reactor length (Figure 2). The concentration profile data indicate that chlorobenzene and 1,4-dichlorobenzene utilization occurred in the same region of the columns as acetate utilization, verifying that primary and secondary substrate utilization occur simultaneously. Furthermore, these results show that if the biofilm mass for steady-state conditions is estimated from primary substrate utilization, then this mass together with rate parameters for the secondary substrates can be applied in a biofilm model to simulate removal of the trace substrates. The simulations appear adequate in terms of both the rate and the extent of secondary substrate removal.

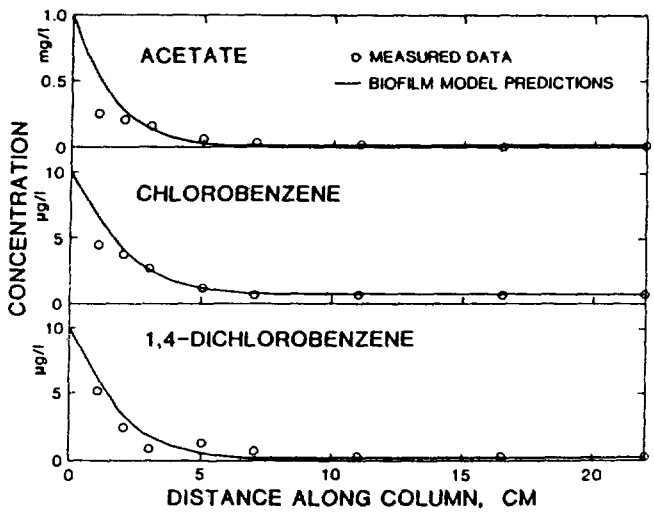

Fig. 2. Measured steady-state concentration profiles and model simulations in aerobic biofilm reactor.

DISCUSSION

The approach to modeling biotransformations of organic micropollutants described here should be applicable to subsurface contamination, such as landfill leachate plumes, infiltration of waste water from spreading basins, and waste-water injection for ground-water recharge, where sufficient primary substrate is available to support an active biofilm that is one to several cells thick. Rittmann *et al.* (1980) have described application of the steady-state biofilm model to an injection well system. Consideration of the kinetics of substrate utilization and growth of biofilm for these cases indicates that microbiological activity is likely to predominate within a small zone near the source of contamination. Here, secondary utilization of trace constituents can occur. However, a portion of trace substrates that have slow utilization rates relative to the primary substrate might pass through the biologically active zone and would remain undegraded and available to penetrate deep into the aquifer.

For large-scale subsurface contamination with low active organism concentrations and slow ground-water movement, biotransformation rates will be slow and limited by the reaction rate rather than mass transport. For this situation, which is representative of the subsurface some distance from a source of contamination, it may not be necessary to use a complex biofilm model to describe transformation rates. Here, a simple batch model using first-order decomposition kinetics may be adequate. Assuming batch conditions and substrate utilization according to equation (3), integration gives an expression for the half-life of the substrate, $t_{1/2}$:

$$t_{1/2} = \frac{\ln 2}{[(k\ X)/K_s]} \qquad (4)$$

Here, X is the average concentration of organisms capable of degrading the contaminant in the region of interest. Degradation half-lives under aerobic and methanogenic conditions resulting from typical subsurface organism concentrations (Wilson *et al.*, 1983) and rate parameters derived from the laboratory column studies are shown in Table 2. The $t_{1/2}$ for an organism concentration of 0.01 mg/l, or about 10^4 bacteria/ml, is about two weeks under aerobic conditions and 20 weeks under methanogenic conditions. Given a sandy aquifer with 25 percent porosity and average particle size of 1 mm, this corresponds to roughly one organism per sand grain. These calculations show that even at extremely low active organism concentrations, significant biotransformation rates of organic micropollutants can occur.

Table 2. Half-Lives of Biotransformation Modeled with First-Order Batch Kinetics as a Function of Active Organism Concentration

Organism concentration		*Degradation half-life, days*	
mg/l	*No./ml**	*Aerobic respiration†*	*Methanogenesis§*
10	10^7	0.014	0.14
1	10^6	0.14	1.39
0.1	10^5	1.39	13.9
0.01	10^4	13.9	139
0.001	10^3	139	1,390

* Organism dry weight taken as 10^{-12} g/cell.
† k/K_s = 5 l/mg cells-day.
§ k/K_s = 0.5 l/mg cells-day.

The laboratory findings and rate data compare favorably to some field evidence for biotransformation of organic micropollutants. Schneider *et al.* (1981) found evidence for 1,4-dichlorobenzene degradation during infiltration from the River Glatt under aerobic conditions with an apparent half-life of eight days. Tetrachloroethylene was found to be persistent in the aquifer. Evidence for biotransformation of trace organic compounds in the subsurface was obtained at the ground-water recharge project in the Palo Alto, California baylands where advanced treated municipal waste water was injected into a confined aquifer (Roberts *et al.*, 1982). After a three-month injection period, breakthrough of trihalomethanes, 1,1,1-trichloroethane, trichloroethylene, and tetrachloroethylene occurred at an observation well 10 m from the injection well. When injection was stopped, the aquifer slowly became anoxic, and the concentrations of trihalomethanes at the observation well were found to decrease indicating half-lives of 21 to 42 days. A much slower decline occurred in the concentrations of the chlorinated ethanes and ethenes, with apparent half-lives from 200 to 300 days.

Secondary utilization is a possible mechanism for transformation of trace substrates. This process requires an active organism population that is supported by other organic materials occurring in perhaps low concentrations, but still greater than S_{min} levels. Consequently, a possible approach to enhance biotransformation of organic micropollutants in a contaminated aquifer would be injection of biodegradable material as primary

substrate to increase the active microbial biomass. This approach to treatment was implemented with excellent success by the city waterworks of Karlsruhe, Germany (Nagel *et al.*, 1982). The aquifer for drinking-water supply had become contaminated with petrochemicals. Water from the most polluted well was treated with ozone and infiltrated again through the contaminated ground. Ozonation increased the biodegradable fraction of the dissolved organic carbon which led to a biological self-cleaning process in the underground. Water is now being pumped from the aquifer and distributed without any further treatment.

The laboratory studies clearly indicate that under proper conditions, many potentially hazardous organic compounds can be biotransformed, even when present at very low concentrations. The ability to successfully model and predict transformability of these compounds necessitates an ability to predict electron acceptor presence. In the subsurface environment following introduction of water containing biodegradable contaminants, oxygen, ammonia, nitrate, and sulfate, an ecological succession of microorganisms and biological processes might evolve with distance away from the source of contamination as depicted qualitatively in Figure 3. Different electron acceptors and redox conditions would prevail downstream from the initial point, and each particular environment would tend to favor the transformations of certain organic micropollutants such as those also listed in Figure 3. Future ground-water modeling research efforts need to consider competitive substrate utilization and kinetics of anoxic processes so that the electron acceptor availability downstream from a contamination source can be determined. For example, when oxygen is initially present, it can be used competitively for oxidation of organic compounds or for nitrification. Also, the kinetics of anoxic processes are not known well enough to be able to predict minimum substrate concentrations necessary for decomposition. Research on subsurface microbiology to characterize the indigenous microflora, to enumerate active organism concentrations, and to determine whether or not subsurface organisms are capable of transforming xenobiotic chemicals is needed to refine existing models for microbial processes.

CONCLUSIONS

Secondary utilization is a means by which bacteria can degrade very low concentrations of organic contaminants, even those which are below the S_{min} concentration required to sustain long-term biomass activity. The laboratory studies have shown that several potentially hazardous halogenated organic compounds frequently found as contaminants in drinking water and ground water can be transformed even when present at very low concentrations. A biofilm model can be used successfully to simulate utilization of trace substrates if the biofilm mass present is either known or predicted from steady-state utilization of a primary substrate, and if rate parameters are available for the secondary substrates. This modeling approach is best suited for subsurface contamination where relatively high primary substrate concentrations (mg/l) are present. For large-scale subsurface contamination with low active organism and contaminant concentrations, a simplified batch first-order model appears adequate. To successfully model and predict the transformations of several halogenated organic micropollutants necessitates an ability to predict electron acceptor presence. Once acclimation has

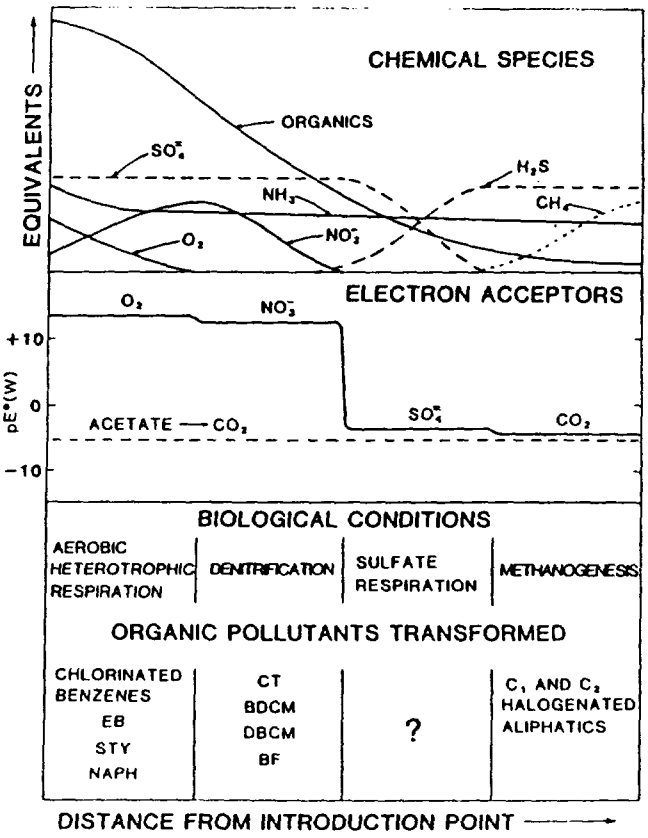

Fig. 3. Possible microbially-mediated changes in chemical species and redox conditions and regions favoring transformations of organic micropollutants as a function of travel distance in the subsurface environment (EB = ethylbenzene; STY = styrene; NAPH = naphthalene; CT = carbon tetrachloride; BDCM = bromodichloromethane; DBCM = dibromochloromethane; BF = bromoform).

occurred under favorable conditions, the degradation rate appears to be first order with respect to substrate concentration, and is also a function of active organism concentration and the ratio of k to K_s. Secondary utilization may be an important tool for cleaning up aquifers that have been contaminated with trace organic compounds.

ACKNOWLEDGMENTS

This research was supported in part by Grant No. EPA-R-808034010, Office of Research and Development, U.S. Environmental Protection Agency; Grant No. CME-7905707, National Science Foundation; and a National Science Foundation Graduate Fellowship.

REFERENCES

Alexander, M. 1981. Biodegradation of chemicals of environmental concern. Science. v. 211, pp. 132-138.

Atkinson, B. and I. J. Davies. 1974. The overall rate of substrate uptake (reaction) by microbial films. Part I. A biological rate equation. Transactions, Institution of Chemical Engineers. v. 52, p. 248.

Boethling, R. S. and M. Alexander. 1979a. Microbial degradation of organic compounds at trace levels. Environ. Sci. Technol. v. 13, no. 8, pp. 989-991.

Boethling, R. S. and M. Alexander. 1979b. Effect of concentration of organic chemicals on their biodegradation by natural microbial communities. Appl. Environ. Microbiol. v. 37, no. 6, pp. 1211-1216.

Bouwer, E. J. and P. L. McCarty. 1981. Biofilm degradation of trace chlorinated organics. Proceedings of the National Conference of Environmental Engineering, ASCE. Atlanta, Georgia, July 8-10. pp. 196-202.

Bouwer, E. J. and P. L. McCarty. 1982. Removal of trace chlorinated organic compounds by activated carbon and fixed-film bacteria. Environ. Sci. Technol. v. 16, no. 12, pp. 836-843.

Bouwer, E. J. and P. L. McCarty. 1983a. Transformations of 1- and 2-carbon halogenated aliphatic organic compounds under methanogenic conditions. Appl. Environ. Microbiol. v. 45, no. 4, pp. 1286-1294.

Bouwer, E. J. and P. L. McCarty. 1983b. Transformations of halogenated organic compounds under denitrification conditions. Appl. Environ. Microbiol. v. 45, no. 4, pp. 1295-1299.

Bouwer, E. J. and P. L. McCarty. 1984. Utilization rates of trace halogenated organic compounds in acetate-grown biofilms. Biotech. Bioeng. Submitted for publication.

McCarty, P. L., D. Argo, and M. Reinhard. 1979. Operational experiences with activated carbon adsorbers at Water Factory 21. J. Amer. Water Works Assoc. v. 71, no. 11, pp. 683-689.

McCarty, P. L., M. Reinhard, and B. E. Rittmann. 1981. Trace organics in groundwater. Environ. Sci. Technol. v. 15, no. 1, pp. 40-51.

Metcalf and Eddy, Inc. 1979. Wastewater Engineering: Treatment, Disposal, Reuse. McGraw-Hill Book Company, New York, NY.

Nagel, G., W. Kuehn, P. Werner, and H. Sontheimer. 1982. Sanitation of ground water by infiltration of ozone treated water. GWF-Wasser/Abwasser. v. 123, no. 8, pp. 399-407.

Rittmann, B. E. and P. L. McCarty. 1980a. Model of steady-state-biofilm kinetics. Biotech. Bioeng. v. 22, pp. 2343-2357.

Rittmann, B. E. and P. L. McCarty. 1980b. Evaluation of steady-state biofilm kinetics. Biotech. Bioeng. v. 22, pp. 2359-2373.

Rittmann, B. E. and P. L. McCarty. 1980c. Design of fixed-film processes with steady-state-biofilm model. Prog. Wat. Tech. v. 12, pp. 271-281.

Rittmann, B. E. and P. L. McCarty. 1981. Substrate flux into biofilms of any thickness. J. Environ. Eng. Div., ASCE. v. 107, no. EE4, pp. 831-849.

Rittmann, B. E., P. L. McCarty, and P. V. Roberts. 1980. Trace-organics biodegradation in aquifer recharge. Ground Water. v. 18, no. 3, pp. 236-243.

Roberts, P. V., J. Schreiner, and G. O. Hopkins. 1982. Field study of organic water quality changes during ground water recharge in the Palo Alto baylands. Water Res. v. 16, no. 6, pp. 1025-1035.

Schneider, J. K., R. P. Schwarzenbach, E. Hoehn, W. Giger, and H. R. Wasmer. 1981. The behavior of organic pollutants in a natural river-groundwater infiltration system. In Quality of Groundwater, Vol. 1: Studies in Environmental Science. W. van Duijvenbooden, P. Glasbergen, and H. van Lelyveld, eds. Elsevier Scientific Publishing Company, The Netherlands. pp. 565-568.

Sontheimer, H. 1980. Experience with riverbank filtration along the Rhine river. J. Amer. Water Works Assoc. v. 72, no. 7, pp. 386-390.

Wilson, J. T., J. F. McNabb, D. L. Balkwill, and W. C. Ghiorse. 1983. Enumeration and characterization of bacteria indigenous to a shallow water-table aquifer. Ground Water. v. 21, no. 2, pp. 134-142.

Wuhrmann, K. 1972. Stream purification. In Water Pollution Microbiology. R. Mitchell, ed. Wiley-Interscience, New York.

Zehnder, A.J.B. 1983. Personal communication. Department of Microbiology, University of Wageningen, The Netherlands.

Zobell, C. E. 1937. The influence of solid surface upon the physiological activities of bacteria in sea water. J. Bacteriology. v. 33, p. 86.

* * * * *

Edward J. Bouwer is Assistant Professor of Environmental Engineering at the University of Houston. He received Ph.D. and M.S. degrees from Stanford University, and his B.S. was obtained at Arizona State University. Dr. Bouwer's research interests include biological process design, biofilm kinetics, ground-water contamination, and degradation of trace halogenated organics.

Perry L. McCarty is the Silas H. Palmer Professor of Environmental Engineering at Stanford University. He received his Ph.D. degree from M.I.T., and his M.S. and B.S. degrees were obtained from Wayne State University. Dr. McCarty has published extensively and received numerous awards for his work on methane formation, biological process kinetics and stoichiometry, and the environmental fate of trace organic compounds.

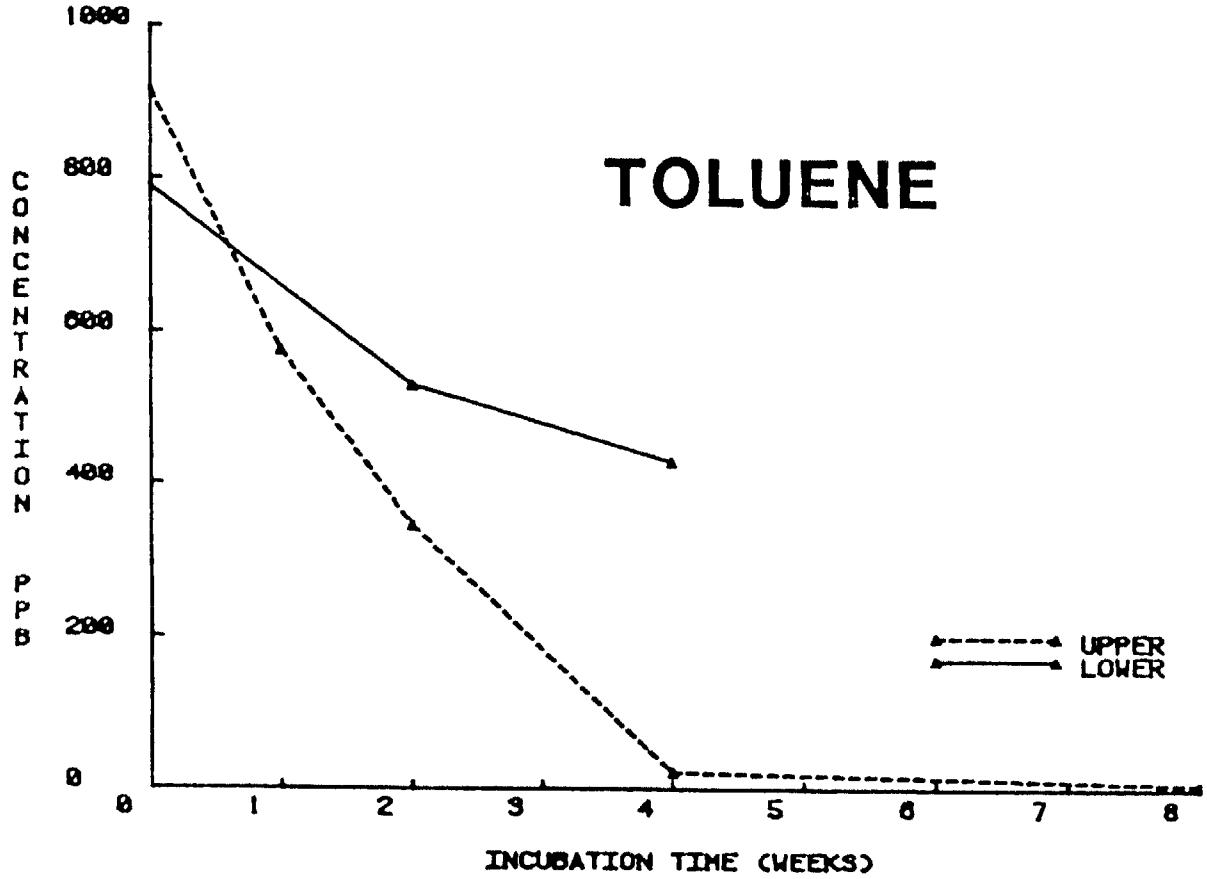

Toluene Degradation at Two Depths in
Uncontaminated Aquifer Material

AEROBIC PATHWAY UTILIZED BY BACTERIA FOR THE OXIDATION OF BENZENE

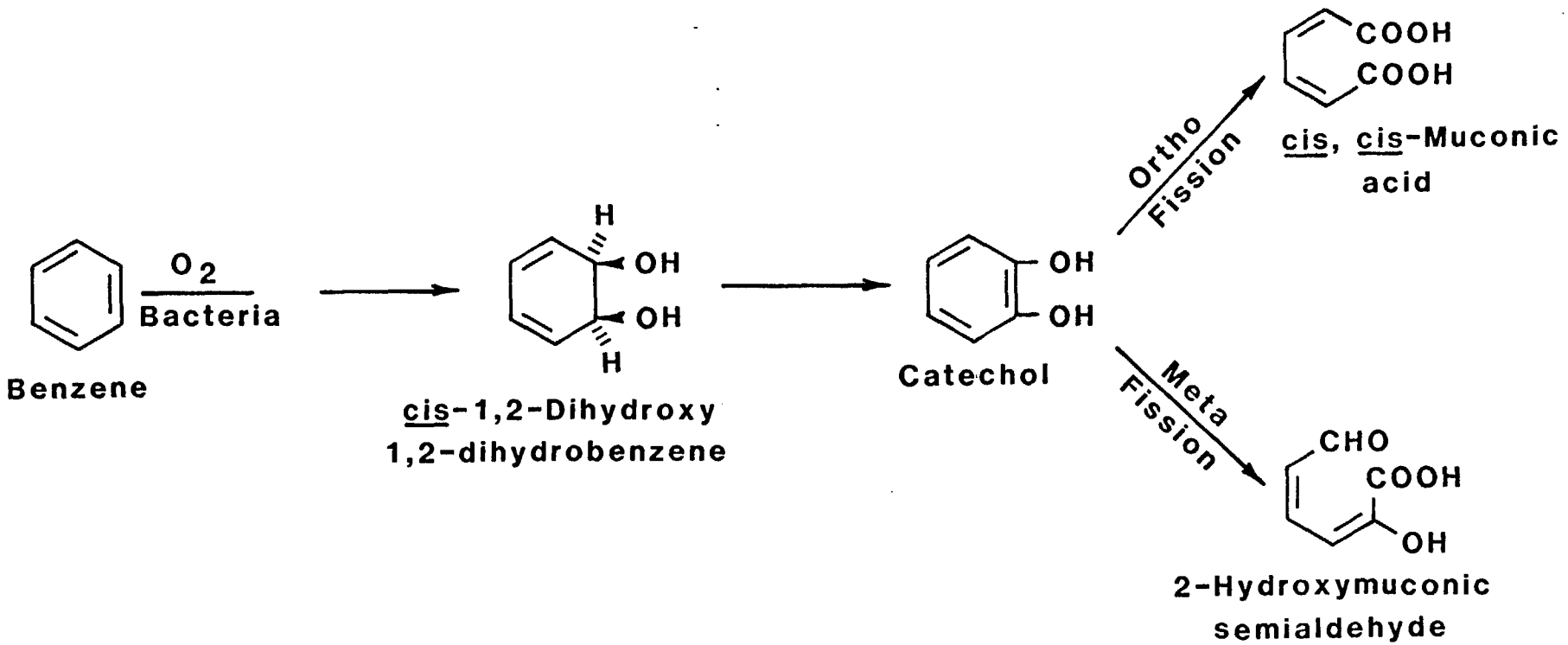

TWO AEROBIC PATHWAYS OF TOLUENE BIODEGRADATION

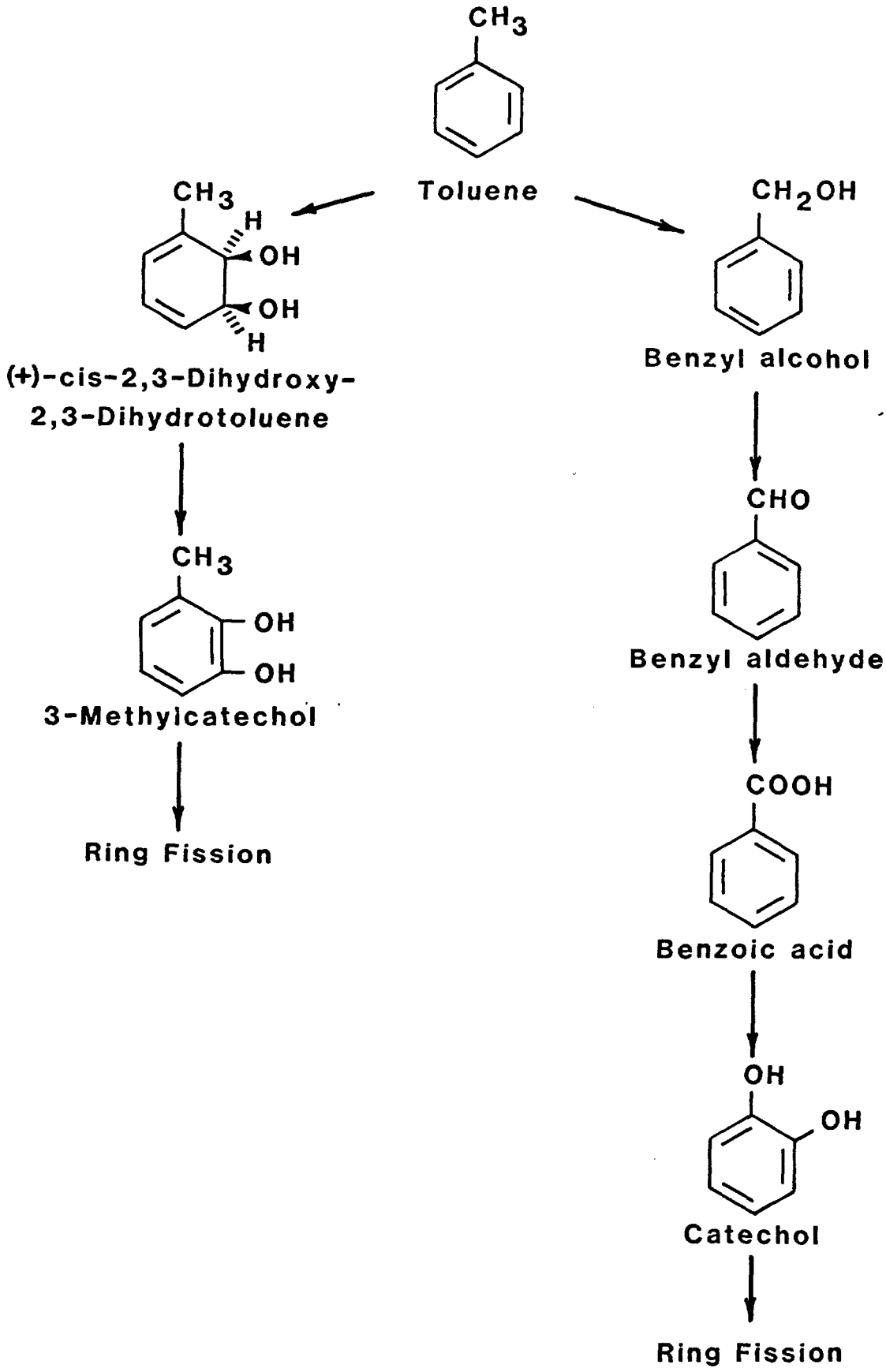

remaining, bound SO_4^- groups. Amide-modified 0.5-μm particles were ingested in the same proportion (100 percent efficiency) at which they were in suspension (treatment 4, Table 2), in contrast to the 0.5-μm unmodified polystyrene particles (treatment 1, Table 1). Addition of a surfactant caused a statistically significant reduction in capture efficiency of 0.5-μm unmodified particles (treatment 3, Table 1) to 44 percent and of amide-modified particles (treatment 5, Table 2) to 71 percent. These experiments indicate that capture efficiencies of the smallest particles can be affected by changing surface charge of the particles and by changing wettability. Neutral particles were captured more readily than particles with a net negative charge, and addition of a surfactant, which increases the wettability of both particles and animals, caused more particles to escape the filtering apparatus of the *Daphnia*.

Differential particle capture on the basis of charge and wettability has general significance for freshwater and marine filter feeding. Natural particles have a range of surface properties that affect their adsorption to surfaces and movement through fluids (*16*). Anomalous selective feeding by zooplankton may be explained on the basis of surface chemistry, in that the animals' filtering appendages may have had greater affinities for some particles than for others (*17*). Selective filter feeding by copepods (*18*) may in fact be due to surface chemistry interactions rather than size selection or taste selection. Surface charge is affected by *p*H (*16*), so we may expect that environments with extreme *p*H values will affect filter-feeding capabilities of small invertebrates. The elimination of certain zooplankton species from systems with elevated *p*H due to high rates of photosynthesis, or lowered *p*H due to dissolved humic substances or acid rain (*19*), may be due to a reduced ability of certain species to capture food as well as other effects mediated by *p*H. Finally, we may expect surface adaptations of filter-feeding animals and their prey to enhance or reduce particle capture. An example of this might be the nonwettability of the exoskeleton of cladocerans, which frequently imprison small individuals in the surface tension of the water, but may aid in particle capture. The interactions between surface chemistry and feeding may change some of our models in aquatic ecology.

JEROEN GERRITSEN
KAREN G. PORTER
Institute of Ecology and
Department of Zoology,
University of Georgia, Athens 30602

References and Notes

1. M. Anraku and M. Omori, *Limnol. Oceanogr.* **8**, 116 (1963); P. Nival and S. Nival, *ibid.* **21**, 24 (1976); C. Boyd, *ibid.*, p. 175.
2. M. A. R. Koehl and J. R. Strickler, *ibid.* **26**, 1062 (1981).
3. M. LaBarbera, *Science* **201**, 1147 (1978).
4. Films of *D. magna* feeding show that particles flow across the surface of the third filtering appendage and are intercepted in the distal region of the filtering comb near the body wall. Particles then begin to move with the filtering appendages. Examination by scanning electron microscopy showed no evidence of mucus or mucus pores on the appendages or in the region of the food groove.
5. E. M. Purcell, *Am. J. Phys.* **45**, 3 (1977); R. E. Zaret, in *Ecology and Evolution of Zooplankton Communities*, W. C. Kerfoot, Ed. (University Press of New England, Hanover, N.H., 1980), p. 3. $Re = \rho(ua/\mu)$, where ρ is fluid density, μ is viscosity, u is speed of flow, and a is the length of the object [G. K. Batchelor, *An Introduction to Fluid Dynamics* (Cambridge Univ. Press, Cambridge, 1970)].
6. Re's were calculated from appendage beat rates of 3 to 6 Hz (K. G. Porter, J. Gerritsen, J. D. Orcutt, Jr., *Limnol. Oceanogr.*, in press), appendage length 0.5 mm, width 0.25 mm, setal diameter 3.5 μm, and setular diameter 0.4 μm, with distance of appendage movement equal to an arc of 60°.
7. At low Re the magnitude of the boundary layer is $d/\sqrt{Re}$ (*8*), where d is the diameter of the setule.
8. C. P. Ellington, in *Swimming and Flying in Nature*, T. Y. T. Wu, C. J. Brokaw, C. Brennan, Eds. (Plenum, New York, 1975), p. 783.
9. The model was oscillated with dye on one side to observe the flow. Re of both model and *Daphnia* appendage were approximately the same, allowing comparison under the principle of dynamic similarity (*5*).
10. L. A. Spielman, *Annu. Rev. Fluid Mech.* **9**, 297 (1977); D. I. Rubenstein and M. A. R. Koehl, *Am. Nat.* **111**, 981 (1977). Sieving is a special case of direct interception, where particles impinge on two adjacent fibers. Inertial impaction of particles on the fibers can be ruled out for fine particle feeding because of the negligible inertia of small particles at low Re. Brownian (random) diffusion and gravitational deposition result in a longer path length of a particle through a filter, thus increasing the probability of encountering a fiber. To be effective, these mechanisms require a long transit time in the filter apparatus and are therefore probably negligible in zooplankton filter feeding.
11. Healthy adult animals (> 2 mm) were starved in particle-free water for 24 hours before the experiments. Particle suspensions were in equal concentrations by particle volume (Tables 1 and 2). Concentrations were verified by microscopical counts of stock suspensions followed by dilution to the required concentration. Animals ($N = 25$) were placed in 125 ml of feeding suspension on a revolving plankton wheel (1 rev/min) to prevent settling. Animals were sieved, washed in particle-free water, anesthetized in CO_2, and preserved in formaldehyde. Guts of eight to ten animals were dissected on slides and relative abundances of particles determined from at least ten nested subsamples, where 5.7-μm particles were counted at 160× magnification, and smaller particles were counted at 1000× with Nomarski interference contrast. Accuracy was verified with a focal-plane micrometer. Expected proportions of particles were calculated from the known concentrations in suspension and the known relative magnification.
12. Proportions of each size class present in the gut of each animal were transformed (arcsin–square root) to degrees for comparison to expected proportions. The probability levels for the multiple comparisons by *t*-tests, were controlled at the α level by use of α/k, where k is the number of comparisons. In Tables 1 and Table 2 $k = 3$. The 0.5-μm size class was then dropped from analysis, proportions of the larger particles were recalculated, retransformed, and analyzed with a *t*-test to determine if there was any difference in relative ingestion, independent of the smallest particles.
13. B. J. Peterson, J. E. Hobbie, J. F. Haney, *Limnol. Oceanogr.* **23**, 1039 (1978); S. S. Gellis and G. L. Clark, *Physiol. Zool.* **8**, 127 (1935).
14. H. J. van der Hul and J. W. Vanderhoff, *Br. Polym. J.* **2**, 121 (1970). All particles were from Dow Diagnostics.
15. Tween-20 (Fisher Chemical).
16. K. C. Marshall, *Interfaces in Microbial Ecology* (Harvard Univ. Press, Cambridge, Mass., 1976); R. R. P. Chase, *Limnol. Oceanogr.* **24**, 417 (1979).
17. *Daphnia* ingest more algae than equivalent-sized glass beads [A. M. Gliwicz, *Ekol. Pol. Ser. A* **17**, 663 (1969)]. Glass is wettable and may have less affinity for the filtering appendages. Bimodal feeding selectivity of *Daphnia* [M. S. Berman and S. Richman, *Limnol. Oceanogr.* **19**, 105 (1974)] is unlikely given our observations of *Daphnia* behavior [see (*6*)] but may be due to low affinity for intermediate-sized particles in the experiment.
18. S. A. Poulet and P. Marsot, *Science* **200**, 1403 (1978).
19. R. L. Kring and W. J. O'Brien, *Limnol. Oceanogr.* **21**, 313 (1976); W. G. Sprules, in *Ecology and Evolution of Zooplankton Communities*, W. C. Kerfoot, Ed. (University Press of New England, Hanover, N.H., 1980), p. 657.
20. We thank Y. Feig and A. Hooten for valuable assistance. J. Reeves and an anonymous referee provided statistical advice. Supported by NSF grants DEB 80-05582 and DEB 79-22633. Publication No. 9 of the Lake Oglethorpe Limnological Association.

24 December 1981; revised 30 March 1982

Deep Oxygenated Ground Water: Anomaly or Common Occurrence?

Abstract. *Contrary to the prevailing notion that oxygen-depleting reactions in the soil zone and in the aquifer rapidly reduce the dissolved oxygen content of recharge water to detection limits, 2 to 8 milligrams per liter of dissolved oxygen is present in water from a variety of deep (100 to 1000 meters) aquifers in Nevada, Arizona, and the hot springs of the folded Appalachians and Arkansas. Most of the waters sampled are several thousand to more than 10,000 years old, and some are 80 kilometers from their point of recharge.*

The geochemical and hydrogeologic literature provides a broad spectrum of notions regarding the occurrence of dissolved oxygen (DO) in ground water. The views range from the idea that DO is absent below the water table (*1*, *2*) to the idea that DO is purportedly generated by the radiolysis of water at depths of 2 to 3 km (*3*). The prevailing opinion (*1*, *4*, *5*) is that the bulk of DO in recharge water is consumed in the soil and unsaturated (or vadose) zones by microbial respiration and the decomposition of organic matter, or rapidly thereafter in the aquifer by various mineral-water and organic oxidative reactions. Despite the multitude of studies of ground-water geochemistry in the last decade, measurements of DO in

0036-8075/82/0611-1227$01.00/0

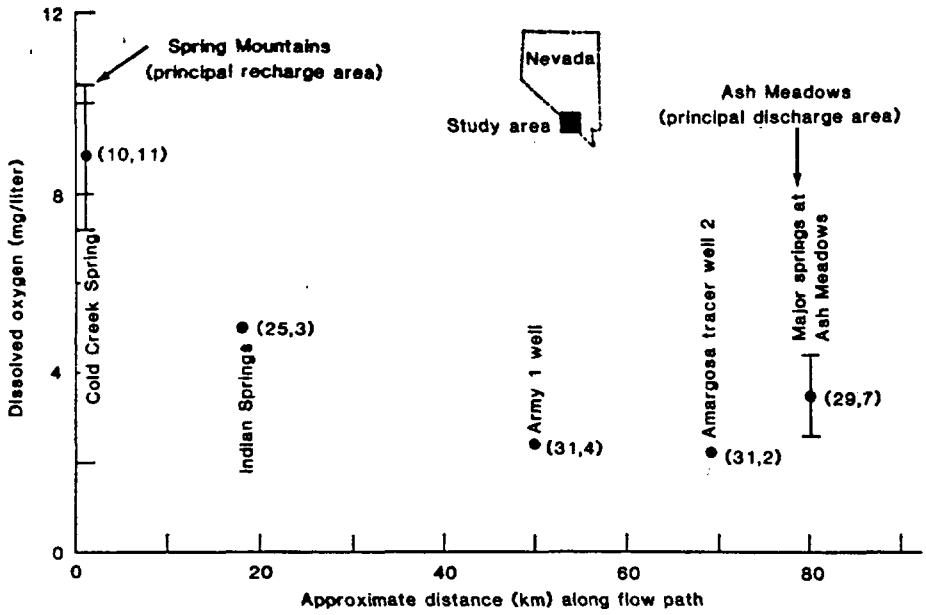

Fig. 1. Variation in the dissolved oxygen content of ground water along an approximately 80-km flow path in the Ash Meadows ground-water basin, south-central Nevada. The first number in parentheses is the temperature of the water (in degrees Celsius); the second is the number of measurements at the site, or at Ash Meadows the number of springs sampled. Error bars represent 1 standard deviation for Cold Creek Spring and seven Ash Meadows springs; the standard deviation is too small to show for the other three stations. Highly fractured Paleozoic carbonate rocks comprise the aquifer; hydrogeologic, hydrochemical, and isotopic studies of this ground-water flow system and location of the line of section and sampling sites are given in (*10*).

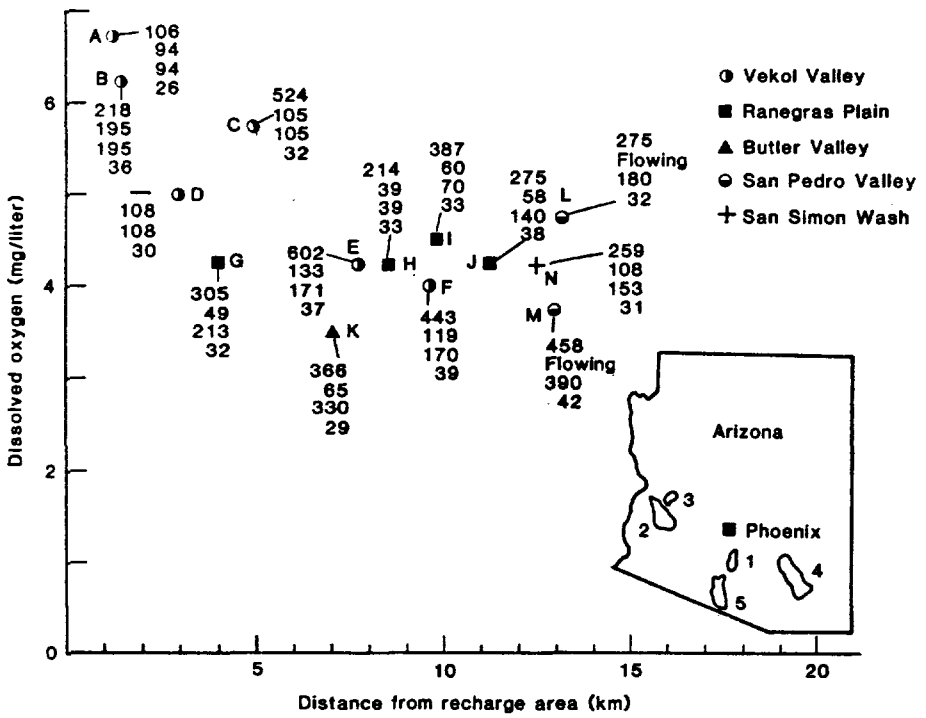

Fig. 2. Dissolved oxygen in deep ground waters versus the approximate distance from recharge areas in five intermontane basins of southern Arizona. Numbers on the index map identify the following locations: *1*, Vekol Valley; *2*, Ranegras Plain; *3*, Butler Valley; *4*, San Pedro Valley; and *5*, San Simon Wash. Numbers next to the well symbols are, from top to bottom: the well depth (in meters), the depth to water (in meters), the depth to the top aquifer (in meters), and the temperature (in degrees Celsius). Letters designate well locations, based on the U.S. Geological Survey and state of Arizona township, range, section, system: well *A*, (D-7-2)18ABA; *B*, (D-8-1)31CBC; *C*, (D-7-1)10CBC$_2$; *D*, (D-8-1)14BAA; *E*, (D-9-1)13BBD; *F*, (D-8-1)35ABD; *G*, (B-4-15)18BBB; *H*, (B-6-16)33AAA; *I*, (B-6-16)26AAD; *J*, (B-3-15)2DAB; *K*, (B-8-14)29CDD; *L*, (D-9-17)24DCC; *M*, (D-8-17)32DAA; and *N*, (C-16-1)10CCA.

water from shallow (< 100 m) aquifers (*6*) are not routine and such measurements have rarely been made for deeper ground water (*7*). It is our intent here to document the widespread presence of DO in significant (2 to 8 mg/liter) concentrations in water several thousand to more than 10,000 years old from deep aquifers of several lithologies in both arid and humid climates, and at distances as great as 80 km from recharge areas.

Because of the ease with which anoxic well waters can be oxygenated, special precautions were taken during sampling. The pumping water levels, in the high-capacity production wells chosen for sampling, were several meters to tens of meters above the pump intakes. In addition, many of these wells tap confined aquifers; in such wells, entrainment of air by pumping is unlikely because of the absence of unconfined flow. The sample bottles were purged and sealed within the full flowing discharge pipe. Sampling in the flowing artesian wells and springs was accomplished by filling and purging the sample bottles under water. We carried out replicate analyses in the field by using either a modified Winkler method or a dissolved oxygen meter (*8*). That our sampling techniques did not introduce O_2 is best shown by the absence of DO in water sampled in similar ways from deep aquifers (*9*) which contain organic detritus and in which DO should, intuitively at least, be absent.

Dissolved oxygen occurs at concentrations of 2 to 8 mg/liter in water from a variety of aquifers in the south-central Great Basin, Nevada. These aquifers—principally Paleozoic carbonate rocks, Tertiary welded tuffs, and Quaternary valley fill—occur at depths of 200 to 1000 m (*10*). Water table (more correctly potentiometric surface) depths in the region range from 200 to 660 m below the surface (*10*). The residence time of water from most of these aquifers is on the order of thousands to more than 10,000 years (*11*). Figure 1 shows the variation in DO along an 80-km flow path in the Paleozoic carbonate-rock aquifer of the Ash Meadows ground-water basin (*12*).

Dissolved oxygen has been observed in all shallow (< 100 m) and deep ground water from valley-fill aquifers in the southern Arizona portion of the Basin and Range Province. Unequivocal evidence of DO at depths of hundreds of meters was obtained from wells in several of the agriculturally less developed basins where well construction, thickness of aquifer tapped, location of recharge areas, and the absence of oxygenated irrigation return flow could be docu-

mented. The basins sampled and our results are shown in Fig. 2. In many of the areas sampled, the aquifers are overlain by a thick (> 100 m) clay stratum, which effectively precludes the possible mixing of deep water with shallow oxygenated ground water. Hydraulic and ^{14}C data (*13*) indicate water ages in excess of 10,000 years for most of the water sampled.

The DO content of thermal spring waters in the Valley and Ridge Province from western Georgia to eastern New York and the waters of Hot Springs National Park, Arkansas, ranges from 2 to 7 mg/liter (*14*). Water temperatures are between 30° and 60°C, and the minimum depths of water circulation are 250 to 2300 m. Hydrogeologic and isotopic evidence suggest relatively short flow paths (from recharge to discharge areas), on the order of a few kilometers to at most tens of kilometers (*14*). The flow to some springs is chiefly through carbonate rocks, whereas flow to other springs is entirely in siliceous reservoir rocks.

The ^{3}H data for some of these hot springs suggest that their DO content may represent a mixture of deeply circulating thermal water and relatively shallow, cooler, and younger ground water (*14*). However, several spring waters that have a DO content of 2 to 7 mg/liter have negligible ^{3}H ($< 1 \pm 1$ tritium unit). The low ^{3}H content is a clear indicator that these waters are, at the least, predominantly of pre–H-bomb (before 1952) age. The Arkansas waters have a ^{14}C age of about 4000 years (*14*).

The presence of DO in the deep carbonate-rock aquifers of the Great Basin and the folded Appalachians (*14*), like that in the shallower carbonate aquifers of Great Britain [Edmunds (*6*); Morgan-Jones and Eggboro (*6*)] did not completely surprise us, despite the great difference in the age of the shallow and deep waters. Commonly, recharge to such aquifers is oxygenated, after passage through soils, by flow through fissures and caverns in the unsaturated zone.

More importantly, flow through the dense carbonate-rock aquifers that we sampled is predominantly by way of solution-modified fractures rather than through intercrystalline pore space; relatively rapid flow through, and the low ratios of rock surface area to water volume in, such fractured aquifers would not favor removal of DO by chemical reactions. Moreover, in the middle and distal portions of regional flow systems comprised of carbonate-rock aquifers, oxidizable minerals, if originally present along fracture surfaces, are likely to be coated with calcite or dolomite precipitated from the ground water.

The presence of DO contents of 2 to 8 mg/liter in the deep valley fill and tuff aquifers of Nevada and Arizona, although unexpected, appears in hindsight to be qualitatively explainable. Valley-fill sediments of the Basin and Range Province were deposited under generally oxidizing conditions and probably remained exposed to oxidizing arid and semiarid climates for tens to hundreds of years prior to burial; after burial they commonly remained in oxidizing unsaturated zones for tens of thousands to perhaps hundreds of thousands of years, depending upon the rates of basin subsidence and the depth to the regional water table. Such depositional environments hardly favor the preservation of readily oxidizable organic or mineral matter. Moreover, recharge to such aquifers is commonly by way of the infiltration of oxygenated runoff along the bottoms of major arroyos; such recharge may have little contact with readily decomposable or relatively unoxidized soil organic matter.

More puzzling is the presence of DO in those Arkansan and Appalachian hot springs (*14*) whose water has passed principally through fractured siliceous rocks. Recharge to these humid-zone aquifers probably had to traverse an organic-rich soil zone; moreover, the reservoir temperature (30° to 60°C) should certainly have favored both the outgassing of the DO and mineral-water reactions. Perhaps all pertinent reactions (organic and inorganic) involving DO have gone to completion within the aquifer prior to the entry of the extant ground water, as hypothesized by Galloway (*7*) for the oxidative "tongues" found in sandstones containing roll-front uranium deposits.

We hope that this report will stimulate a systematic appraisal of DO in future geochemical studies of shallow and deep ground water. Such measurements, which can readily be made in the field, are essential for predictions of the movement of toxic transition metals (*15*) and actinide radionuclides in aquifer environments (*15*). The common assumption that reducing conditions prevail in deep aquifer environments must be tested on a case-by-case basis.

Note added in proof: Mineralogic evidence for deep oxidizing conditions in an 1800-m-thick Tertiary ash-flow and ash-fall tuff sequence in the Jackass Flats area of southern Nevada is given by Bish *et al.* (*16*). They found highly oxidized iron-titanium minerals in cores (test hole USW-G1, Yucca Mountain) from the upper 1600 m of this tuffaceous sequence. The water table is about 580 m deep at the site of the test hole. We measured DO (6 to 7 mg/liter) in ground water, from the upper 120 m of the saturated zone in this volcanic sequence, at nearby water-supply wells J-12 and J-13. We are not suggesting that the extant ground water caused the deep oxidation noted by Bish *et al.*, because such oxidation might well have occurred several million years ago. Rather we cite their work to suggest that oxidizing conditions were once, and may still be, present within this volcanic rock sequence at considerably greater depths than the water we sampled.

ISAAC J. WINOGRAD
U.S. Geological Survey,
Reston, Virginia 22092
FREDERICK N. ROBERTSON
U.S. Geological Survey,
Tucson, Arizona 85701

References and Notes

1. R. M. Garrels and C. L. Christ, *Solutions, Minerals, and Equilibria* (Harper & Row, New York, 1965), pp. 382–383.
2. M. Sato, *Econ. Geol.* **55** (1960), pp. 950 and 956.
3. L. K. Gutsalo, *Geochem. Int.* **8**, 897 (1971).
4. R. A. Freeze and J. A. Cherry, *Groundwater* (Prentice-Hall, Englewood Cliffs, N.J., 1980), pp. 117–118 and 245, figure 7.1 and table 3.10.
5. T. H. E. Heaton and J. C. Vogel, *Hydrol. Sci. Bull.* **25**, 4 (1980); D. R. Champ, J. Gulens, R. E. Jackson, *Can. J. Earth Sci.* **16**, 12 (1979).
6. Several recent studies have reported DO in young (after 1950) and shallow ground water, particularly water from carbonate rock and sand and gravel aquifers [S. G. Heidel, *J. Am. Water Works Assoc.* **57**, 239 (1965); W. Dyck, *J. Geochem. Explor.* **13**, 27 (1980); M. J. Baedecker and W. Back, *Ground Water* **17**, 429 (1979); W. M. Edmunds, in *Proceedings of a Symposium on Hydrogeochemistry and Biogeochemistry* (Clarke Company, Washington, D.C., 1973), vol. 1, pp. 500–526; M. Morgan-Jones and M. D. Eggboro, *Q. J. Eng. Geol.* **14**, 25 (1981)].
7. That DO might be found, or was once present, in deep ground water has been inferred by several authors. J. D. Hem [*U.S. Geol. Surv. Water Supply Pap. 1473* (1970), p. 221] and Freeze and Cherry (*4*) suggested that, in the absence of organic matter and in areas where little soil overlies fractured rock, DO might be retained in solution by ground water in detectable (> 0.1 mg/liter) concentrations for a long time. Economic geologists [H. C. Granger and C. G. Warren, *U.S. Geol. Surv. Open-file Rep. 79-1603* (1979); W. E. Galloway, in *Depositional and Ground Water Flow Systems in the Exploration for Uranium*, W. E. Galloway, C. W. Kreitler, J. H. McGowen, Eds. (Texas Bureau of Economic Geology, Austin, 1979), chap. 7, pp. 177–180; A. E. Saucier, *N.M. Bur. Mines Mineral Resour. Mem. 38* (1980), pp. 116–121] have inferred the former presence of oxygenated ground waters at distances of a few to perhaps 30 km from presumed paleorecharge areas in sandstones containing roll-front uranium deposits. Based on the distribution of oxidized ores, C. F. Park, Jr., and R. A. MacDiarmid [*Ore Deposits* (Freeman, San Francisco, ed. 3, 1975), pp. 85–91 and 468–469] inferred that locally, along highly permeable fracture zones, oxygenated ground water once descended to depths of 960 m at the Tsumeb mine in southwest Africa. However, they also subscribe to the notion that the depth of mineral oxidation is controlled by the water table, which, they point out, may occur at great depths in arid terrane. The only actual measurements and detection of DO in deep ground water that we are aware of are the following: A. I. Germanov, G. A. Volkov, A. K. Lisitsin, V. S. Serebrennikov, *Geochemistry (U.S.S.R.)* **3**, 322 (1959); I. J. Winograd and F.

(1976); J. C. Vogel, A. S. Talma, T. H. E. Heaton, *J. Hydrol.* **50**, 191 (1981); K. Wolfsberg, *Los Alamos Sci. Lab. Rep. LA-8739-PR* (1980), pp. 21–22; (*14*). Beneath uplands, such as those discussed by Germanov *et al.*, oxygenated young ground water is not unexpected at depths of hundreds of meters, because in recharge areas flow is dominantly downward. The deep waters sampled in the other studies cited were not exclusively from recharge areas. Unique evidence for the presence of deep oxygenated water comes from the distal portions of the Edwards aquifer system in the San Antonio, Texas, area. There, blind catfish (*Trogloglanis pattersoni*) live in caverns in this aquifer at depths of hundreds of meters in 27°C water containing DO at concentrations up to 4 to 5 mg/liter [G. Longley and H. Karnie, Jr., report prepared for the U.S. Fish and Wildlife Service, Albuquerque, N.M., under contract 14-16-0002-77-035 (1978)]. The ^3H content of water in this portion of the Edwards aquifer is as low as 1 tritium unit [F. J. Pearson, Jr., P. L. Rettman, T. A. Wyerman, *U.S. Geol. Surv. Open-file Rep. 74-362* (1975)], suggesting a water age, at the least, on the order of decades.

8. A Hach model OX-2P field kit (a modified Winkler method) and a YSI model 57 dissolved oxygen meter were used to measure the DO contents in our ground waters. The YSI meter is accurate to 0.1 mg/liter and the Hach field kit to 0.2 mg/liter. Measurements of DO (12 replicates) at a deep well in the Vekol Valley, Ariz., made with the Hach kit gave a mean of 4.3 mg/liter with a standard deviation of 0.2 mg/liter. This compared with a value of 4.1 ± 0.1 mg/liter, measured with the YSI meter on water from the same well. C. E. Boyd [*J. Environ. Qual.* **6**, 381 (1977)] compared the Hach field kit DO values with standard laboratory methods; in the range of interest to us (3 to 7 mg/liter), the Hach kit results were only 3 to 13 percent higher than those obtained by standard laboratory methods.
9. D. C. Thorstenson, D. W. Fisher, M. G. Croft, *Water Resour. Res.* **15**, 1479 (1979); I. J. Winograd and G. M. Farlekas, in *Isotope Techniques in Groundwater Hydrology 1974* (International Atomic Energy Agency, Vienna, 1974), vol. 2, pp. 69–93. Indirect geochemical evidence that neither our pumping nor our sampling procedures caused the oxygenation of naturally reduced ground waters consists in the virtual absence of iron in all our waters. The dissolved iron content of the southern Nevada ground waters, for example, varies from 15 to 40 μg/liter. If we had aerated moderately reduced [*Eh* (oxidation-reduction potential) −100 to +200 mV] waters, we would have expected iron contents—either dissolved or as precipitates on our filters—in the milligrams per liter range, in at least some of our waters, all of which have *p*H values in the range of 6.5 to 8.
10. See Winograd and Pearson (*7*); I. J. Winograd and W. Thordarson, *U.S. Geol. Surv. Prof. Pap. 712-C* (1975); W. W. Dudley, Jr., and J. D. Larson, *U.S. Geol. Surv., Prof. Pap. 927* (1976); I. J. Winograd and G. C. Doty, *U.S. Geol. Surv. Open-file Rep. 80-569* (1980); I. J. Winograd and I. Friedman, *Geol. Soc. Am. Bull.* **83**, 3691 (1972).
11. See Winograd and Pearson (*7*); H. C. Claassen, personal communication.
12. Several nonchemical factors are also likely to influence the DO content of water in this hydrogeologically complex aquifer. These include (i) probable reaeration of recharge water in the shallow subsurface during flow through caverns beneath the principal recharge area, the Spring Mountains; (ii) water temperature and pressure, both functions of the depth of burial of the aquifer; (iii) possible outgassing, or conversely absorption of O_2, in areas where the regional carbonate aquifer is unconfined, as beneath the ridges of the region (*10*); and (iv) mixing, in the central part of the Ash Meadows basin, of Spring Mountains water with deep oxygenated water from another source (*10*).
13. R. P. Wilson, *U.S. Geol. Surv. Open-file Rep. 79-1165* (1979); F. N. Robertson, in preparation.
14. W. A. Hobba, Jr., J. C. Chemerys, D. W. Fisher, F. J. Pearson, Jr., *U.S. Geol. Surv. Water Resour. Invest. 77-25* (1977); W. A. Hobba, D. W. Fisher, F. J. Pearson, Jr., J. C. Chemerys, *U.S. Geol. Surv. Prof. Pap. 1044-E* (1979); D. W. Fisher and J. C. Chemerys, personal communication; M. S. Bedinger, F. J. Pearson, Jr., J. E. Reed, R. T. Sniegocki, C. G. Stone, *U.S. Geol. Surv. Prof. Pap. 1044-C* (1979); F. J. Pearson, personal communication.
15. F. N. Robertson, *Ground Water* **13**, 516 (1975); R. G. Strickert, *Battelle Pacific Northwest Lab. Rep. PNL-3432* (1980); E. A. Bondietti and C. W. Francis, *Science* **203**, 1337 (1979).
16. D. L. Bish *et al.*, *Los Alamos Natl. Lab. Rep. LA-8840-MS* (1981), pp. 51–53.
17. We thank M. J. Baedecker, J. E. Biesecker, V. Carter, H. Claassen, M. Goldhaber, D. Fisher, B. F. Jones, R. Malcolm, and D. Thorstenson for their interest and helpful review comments. A. C. Riggs' field assistance in the Great Basin is gratefully acknowledged.

20 January 1982; revised 6 April 1982

Induction of Crisis Forms in Cultured *Plasmodium falciparum* with Human Immune Serum from Sudan

Abstract. *Serums from 90 individuals from three areas in Sudan were tested for inhibitory activity against cultures of* Plasmodium falciparum. *In addition to inhibitory activity against merozoite invasion, all of the serums demonstrated, in varying degrees, the ability to retard intraerythrocytic development, leading to crisis forms and parasite deterioration. These retardation factors could be removed by absorption of immune serum with parasite-infected erythrocytes and were demonstrable in purified immunoglobulin fractions. Serum from donors in hypoendemic Khartoum did not retard parasite development.*

Nearly four decades ago, Taliaferro and Taliaferro (*1*) reported that infections of *Plasmodium brasilianum* in *Cebus capucinus* monkeys progressed at a predictable rate and pattern until the host's immune response began to resolve the infection. The parasite's highly synchronous development then became severely retarded, and "crisis forms" of the parasite appeared (*1*). The crisis was characterized by significant changes in the synchrony of the parasite's developmental cycle, a reduced average number of merozoites per segmenter, and a retardation of the periodicity, resulting in many deteriorating schizonts within the infected erythrocytes. Since this early report, the term crisis form has become synonymous with obviously degenerating intraerythrocytic parasites seen in hemoprotozoan infections with *Babesia* and *Plasmodium* sp. (*2*). Experimental induction of crisis forms is not always consistent and, in rodent infections with *Babesia* and *Plasmodium* sp., nonspecific factors associated with *Corynebacterium parvum*, *Mycobacterium bovis* BCG, or endotoxin-stimulated macrophages appear to be important (*3*).

Studies of immunity to primate malaria—including malaria due to *P. falciparum* in man—have demonstrated that serums collected from experimentally infected animals, or from humans living in regions of malaria hyperendemicity, contain humoral factors that inhibit parasite development in vitro (*4*). Since the merozoite is the only extracellular stage of the blood infection, it is especially susceptible to immunologic attack, and numerous studies have confirmed that malaria-immune serum appears to act by blocking invasion of erythrocytes by the merozoites (*5*). Attempts to demonstrate inhibition of intracellular parasite development or to identify additional protective actions for malaria-immune serum have been, up to now, unsuccessful (*6*). One result of these studies has been to emphasize the merozoite as the source of protective antigen. We now report that serums collected from individuals living in malarious regions of the Sudan not only contain merozoite-blocking antibodies, but also cause intracellular parasite deterioration and classical crisis forms in cultures of *P. falciparum*.

We have collected more than 300 serum samples from three different regions in Sudan, and of these, 90 have been tested for parasite inhibition in continuous cultures of *P. falciparum*. Since in some areas, particularly Blue Nile Province, the villagers have access to chloroquine, all serums were dialyzed 1:1000 against RPMI 1640 medium. This procedure removes 98 percent of the chloroquine from serum (*7*). Because dialysis also removes hypoxanthine, a required nutrient not found in RPMI 1640, complete medium was supplemented with hypoxanthine to give a final concentration of $5 \times 10^{-5} M$ (*8*). All serums were heat-inactivated at 56°C for 30 minutes. Parasites of *P. falciparum*, strain FCR_3/Gambian, were synchronized with a modification of the sorbitol method (*9*); cultures were washed with 5 percent (weight to volume) aqueous sorbitol, cultured for 12 hours, washed again with sorbitol, returned to culture for 24 hours, then concentrated to 80 to 90 percent parasitemia by the gelatin–RPMI 1640 method (*10*). This procedure results in highly synchronous schizonts with a 6-hour age differential. The synchronized schizont-infected red cells were diluted to a 0.5 to 1.0 percent parasitemia with freshly washed O+ erythrocytes and dispersed into 96-well microculture plates so that each well received 3 μl of packed erythrocytes. The dialyzed serum was

0036-8075/82/0611-1230$01.00/0

ISSN 0067-2777

ASM

Abstracts of the Annual Meeting of the

American Society for Microbiology

1985

85th Annual Meeting

Las Vegas, Nevada

3–7 March, 1985

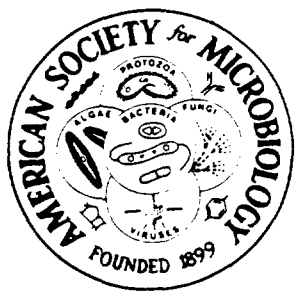

Environmental and General Applied Microbiology

Q 1 Alcohol Biodegradation in Groundwater Microcosms and Pure Culture Systems. R. BENOIT*, J. NOVAK, C. GOLDSMITH and J. CHADDUCK. Virginia Polytech. Inst. & State Univ., Blacksburg.

Soil was obtained from 3 U.S. sites from depths that ranged from surface to 100 feet by use of Shelby tubes in various types of samplers. Microbial biomass was determined by AO microscopy and various culture techniques. The deep soil had a viable count of 10^5 - 10^7 cfu/g soil at all sites. Yeasts were observed in some samples. Obligate oligotrophic bacteria were isolated, but facultative oligotrophic bacteria dominated the microflora. Obligate anaerobic bacteria and microaerophilic bacteria were isolated from deep soil, however, they were a small portion of the population. Many bacteria and yeasts were isolated which could catabolize methanol under aerobic or anaerobic conditions in culture media which contained methanol at low and high concentrations (greater than 1000 mg/l). Methanol was degraded in groundwater microcosms at low and high concentrations of substrate. Tertiary butyl alcohol (TBA) was more refractory, but it was biodegraded in microcosms at all sites. Several species of bacteria were isolated which degraded TBA under aerobic conditions. The hypothesis that methanol and TBA can be biodegraded by groundwater microorganisms is supported by these data.

Q 2 Mineralization of Xenobiotic Chemicals by Aquifer Sediments. MAUREEN A. DOOLEY*, ROBERT J. LARSON and ROY M. VENTULLO, Univ. of Dayton, Dayton, OH and The Procter and Gamble Company, Cincinnati, OH.

The ultimate degradation of xenobiotic chemicals by aquifer sediment microbial communities was measured. Trace levels (nM) of ^{14}C-labeled benzoates, chlorobenzene, phenol, cresol, or surfactants were added to replicate biometer flasks containing aseptically obtained sediments from Conroe, TX or Sault St.Marie (SSM), ONT. Kinetic data ($^{14}CO_2$ evolution with time) were analyzed by nonlinear regression models to generate first order rate constants and half lives. The rate and extent of biodegradation varied with both substrate and sediment type. Half lives of the chemicals tested ranged from 13 to 657 h. Generally, the chemicals degraded faster and to a greater extent in the SSM sediments. The number of degraders, determined by a ^{14}C-MPN technique, were also greater at SSM. Prior exposure of sediments to unlabeled chemicals led to a greater degradation of added ^{14}C-chemicals. The results demonstrate that aquifer sediment microorganisms can mineralize trace levels of organic chemicals and the rates can be affected by preexposure of the microbial community to a chemical.

Q 3 Microbial Numbers and Activity in the Subsurface at a Creosote Waste Site. J. M. THOMAS*, M. D. LEE, and C. H. WARD, Dept. of Environmental Science & Engineering, Rice University, Houston, Texas.

Microbial numbers and activity were determined in subsurface soil and ground water at a creosote waste site. Approximately 1 yr old core samples from a highly contaminated (15A11), slightly contaminated (16B7), and a pristine location (14B10) were plated on 2 kinds of solid media. Medium I was ground water agar and medium II was ground water agar amended with low concentrations of nutrients. Cell counts were highest when cores 15A11 and 16B7 were plated on medium II. Microbial growth from core 14B10 was never detected. To investigate the lack of growth from core 14B10, biological activity, measured as the ability to mineralize naphthalene, was compared between core 14B10 and fresh ground water collected from well 14. Mineralization was never detected when slurried core material amended with 31 ng naphthalene per ml was incubated for 6 wks; 36% of the naphthalene was mineralized by ground water after 1 wk. In an experiment using ground water amended with 46 ng naphthalene per ml, 5% was mineralized after 24 h and 30% was mineralized after 120 h of incubation. Direct counts of ground water and core material yielded 4.9×10^4 cells per ml and 6.2×10^5 cell per g of dry soil. The data suggest that media selection is important in enumeration of subsurface microorganisms and that prolonged storage of some cores may decrease biological activity.

Q 4 Isolation and Characterization of a Subsurface Amoeba. JAMES L. SINCLAIR* and WILLIAM C. GHIORSE, Cornell University, Ithaca, NY

Previous microscopic and chemical analyses of subsurface soil samples suggested that the number of eukaryotic microorganisms in groundwater-bearing sediments was extremely low. To determine if subsurface sediments are indeed devoid of eukaryotes, aseptically procured samples from at and below the groundwater interface from Conroe, Texas, Ft. Polk, Louisiana, and Lula, Oklahoma were examined for protozoa using a modified Singh glass ring enrichment technique. After 2 weeks of incubation with Enterobacter aerogenes as a food source, amoeba were found in 2 samples from the saturated zone interface at Lula, Oklahoma. Also found in the amoeba cultures was 1 species of fungus in samples from the interface and in the saturated zone of the same site. Repeated enrichments of 2 separate corings from this layer produce one species of a cyst-forming amoeba which was present at 111.1 g dry wt^{-1}. Measurements of the cysts and acridine orange-stained bacteria from the same site indicated that the encysted amoeba comprises 15% and the bacteria comprise 85% of the total biovolume of sediments in the interface zone. Morphologic and other characteristics of this amoeba have been studied. It is concluded that subsurface sediments can contain eukaryotic microorganisms. Because of their low population densities, subsurface eukaryotes are best studied with enrichment culture techniques.

Q 5 Biotransformation of Toluene in Methanogenic Subsurface Material. JOHN F. REES, BARBARA H. WILSON,* and JOHN T. WILSON, BioTechnica Ltd., Cardiff, Wales, U.K., Univer. of Oklahoma, Norman, OK, and R.S. Kerr Environmental Research Lab. (U.S. EPA), Ada, OK.

Toluene is an important constituent of leachate from many municipal landfills and hazardous waste disposal sites. Although toluene has been shown to degrade in several aerobic subsurface environments, there is little information on its behavior in anaerobic materials. The study material was methanogenic alluvium from the floodplain of the South Canadian River which receives leachate from the City of Norman landfill. This material was amended with toluene and benzene at 500 µg/liter of porewater and ethylbenzene and O-xylene at 200 µg/l pore water. Toluene degradation was apparent after 6 weeks; after 11 months the toluene concentration was reduced at least an order of magnitude. There was no significant degradation of the other aromatic hydrocarbons. Toluene was not lost from autoclaved material, implicating a biological process. When a fresh sample of methanogenic river alluvium was amended with ^{14}C-toluene, the toluene was transformed to water-soluble material that was much less volatile than toluene.

Occurrence and Distribution of Organic Chemicals in Two Landfill Leachate Plumes

Martin Reinhard* and Naomi L. Goodman

Department of Civil Engineering, Stanford University, Stanford, California 94305

James F. Barker

Earth Sciences Department, University of Waterloo, Waterloo, Ontario, N2L 3G1 Canada

■ The spatial distribution of trace organic compounds in leachate plumes of two sanitary landfills was established by using multilevel sampling devices. The majority of the compounds originated from decomposing plant material and included aliphatic and aromatic acids, phenols, and terpene compounds. Minor constituents, including chlorinated and non-chlorinated hydrocarbons, nitrogen-containing compounds, alkylphenol polyethoxylates, and alkyl phosphates, were of industrial and of commercial origin. Vertical concentration profiles indicated accumulation of chlorinated solvents beneath the leachate plume. Lateral distribution profiles indicated that the sorptive capacity of the sandy aquifer was apparently too low to prevent migration of aromatic hydrocarbons with a log $K_{octanol/water}$ of less than 3–4. The distribution of trace organics at the two sites was much more complex than that of inorganics commonly used to map leachate plumes. This indicates that extensive monitoring will be required to predict future impacts.

Introduction

Landfilling has long been the major disposal method for both domestic and industrial wastes. Unfortunately, many of the thousands of landfills, active or abandoned, have been operated with little regard for the dangers of groundwater contamination. In recent years, the number of sites in which landfill leachate is known to contaminate the underlying aquifer has been increasing, but only a few cases have been studied in detail with regard to geochemical processes (*1–6*). Likewise, few studies have addressed the occurrence of potentially hazardous organic chemicals in leachates of sanitary landfills (*7, 8*). To assess the impact on water quality at a given site, several questions must be asked: (i) What are the potentially harmful constituents in the leachate? (ii) What are the local hydrogeologic conditions? (iii) What is the significance of attenuating factors such as biological and/or chemical degradation, adsorption, ion exchange, precipitation, and hydrodynamic dispersion? These questions are difficult to answer, mainly because of the cost and complications involved in obtaining hydrogeological data and representative samples of groundwater, as well as a paucity of data on degradation and sorption constants.

The objective of this study was to characterize the organic constituents in landfill leachate plumes and to identify geochemical, physical, and biological processes that affect their distribution in the subsurface environment. The Groundwater Research Institute at the University of Waterloo has furnished several landfill sites with observation wells and piezometers and has established the extent of the leachate plumes (*3, 4, 9*). The sites studied here are located near North Bay and Waterloo, Ontario, Canada, on sandy, relatively permeable deposits. Their hydrogeological characteristics have been under investigation, and the principal features of the leachate plumes, i.e., the distribution of the major reactive and nonreactive leachate components, have been established (*3, 9*). Reactive components of leachates include sorbable and degradable organic compounds, and nonreactive components include conservatively behaving anions such as chloride (Cl^-). In this study the behavior of the reactive trace organics has been evaluated by using the Cl^- distribution as a reference. The findings discussed here should be useful for the design of more detailed studies on groundwater contamination by landfills and for selection of protocols for groundwater monitoring in similar hydrogeologic settings.

Summary of Site Descriptions

Woolwich. The Woolwich landfill is located in the northwestern part of the Regional Municipality of Waterloo, Ontario. It is situated on a deposit of glaciofluvial sand which is generally about 30 m thick and overlies a deposit of relatively impervious clayey till. The landfill occupies approximately 3.5 ha, 75% of which has been filled since operation began in the mid-1960s. The site has received rural and municipal as well as some industrial wastes. Rain and snow melts infiltrated the sand-covered refuse, and after migrating through the unsaturated zone, contaminated waters dispersed into the underlying groundwater located 10–15 m below the refuse.

The monitoring well network included 62 bundle piezometers (*10*), each having eight to nine individual piezometers screened over short intervals (<0.3 m) at varying depths between the water table and the bottom of the unconfined sand aquifer. The plume boundary shown in Figure 1 was delineated on the basis of chloride ion concentration. A background sample was obtained from piezometer W-D, located about 50 m east of the north end of the landfill.

As of 1982, it extended about 600 m to the south of the landfill and appeared to consist of two major segments. The high concentration zone originated in the eastern part of the landfill, which was in use from 1965–1975. The second plume segment was located in the southwest corner of the landfill and originated from more recent landfilling. Chloride concentration was greatest in the eastern segment with a maximum of about 500 mg/L. In contrast, the maximum concentration in the southwestern segment was about 100 mg/L. Chloride concentration decreased with distance, and 600 m downstream it was reduced by a factor of 10. Chloride concentration generally decreased with depth near the landfill, but profiles obtained at locations further downstream indicated that chloride was fairly evenly distributed throughout the aquifer.

North Bay. The North Bay site, operational since 1962, is located near the City of North Bay in north-central Ontario on the Precambrian Shield. The landfill lies on a complex deposit of bedded glaciofluvial sand (*9*). The aquifer overlies a discontinuous layer of silty–sandy glacial till deposited on biotite gneiss. The site has received domestic, commercial, and small quantities of industrial wastes. The area receives an average of 80 cm of precip-

0013-936X/84/0918-0953$01.50/0

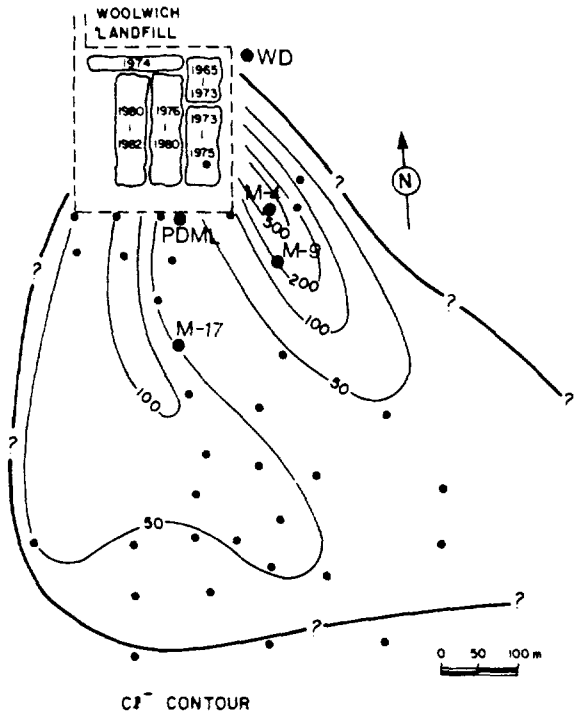

Figure 1. Woolwich, 1982. Landfill area, sampling locations, and extent of groundwater contamination. Leachate strength is indicated with contours of maximum Cl^- concentrations (mg/L).

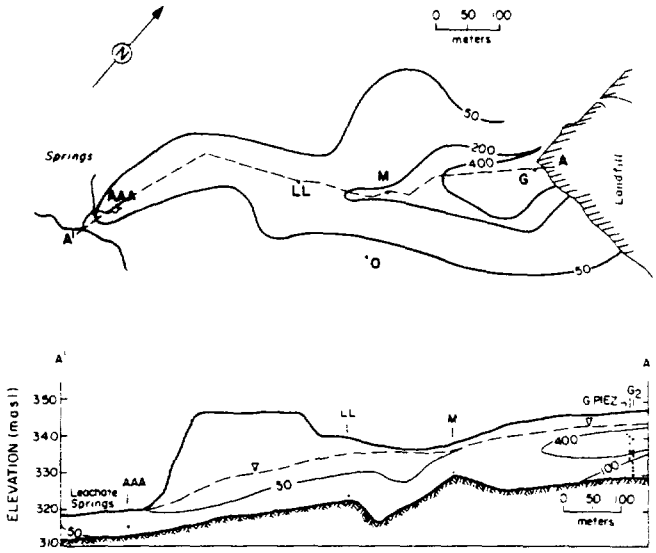

Figure 2. North Bay, 1982. (Top) Landfill area, sampling locations, and extent of groundwater contamination. Leachate strength is indicated with contours of maximum Cl^- concentrations (mg/L). (Bottom) Cross section of leachate plume and sampling locations along axis of plume (A to A').

itation per year, much of which penetrates the sandy cover and transports contaminants into the underlying groundwater through a very thin (0–5 m) unsaturated zone.

The plume stretched from beneath the landfill to the discharge area where the leachate-contaminated groundwater emerged as an area of springs (Figure 2). The most contaminated section of the plume appeared to fall relative to the groundwater table with increasing distance from the landfill. Beyond point G, the leachate strength was observed to be highest near the bottom of the sand aquifer and less contaminated water was found overlying the contaminated zone.

The plume appeared to be at a steady state with respect to all ions measured, except NH_4^+ and K^+. A background sample was obtained from multilevel observation well 0-4 located south of the leachate pond, about 50 m away from the boundary of the plume and well outside the bedrock depression that constrained the plume.

Sampling and Analysis

Sampling. At the North Bay site the water table was within 7–8 m of the surface, permitting the use of peristaltic suction sampling pumps. The sampling procedure was as follows: Teflon tubing was inserted to the bottom of the polyethylene piezometer tube and was connected to a 2-L suction flask. A peristaltic pump was connected after the flask so that the sample came in contact with only Teflon and glass after passing through the Nylon and polyethylene piezometer tip. Prior to sampling, 1–2 L of wellwater were removed and discarded. A 2-L sample was taken for analysis of organic acids, phenols, neutrals (including purgeables), and bases. In addition, 50-mL samples were taken for volatile organic analysis. The 50-mL vials were filled by inserting the Teflon tube into the piezometer and applying a slight suction to it before withdrawing, thereby using the tube as a bailer. The contents of the tube were drained into the vials, and several volumes of sample were displaced before capping the vial airtight. Chloride was determined in the 50-mL samples after the pentane extraction or in a subsample of the 2-L sample.

At Woolwich, where the water table was too deep for sampling by suction, samples were taken by using a triple-tube gas-drive sampler (*10*), constructed of Teflon and stainless steel except for a short length of Latex rubber packer. One well was equipped with a multilevel positive-displacement (PDML) sampler (*11*) which consisted of gas-operated polyethylene syringes and tubing placed at various depths. Two to four standing volumes were removed from each piezometer before sampling.

Samples from some wells tended to develop gas bubbles as they were brought to the surface, which may have caused some loss of volatile organics. Between samples, the equipment was rinsed with methanol and deionized water. Samples were packed in cooled containers, shipped by air freight to Stanford University, and stored under refrigeration until analyzed, which normally occurred within a week.

Analytical Procedures. Volatile halogenated organics with one and two carbons were analyzed by pentane extraction followed by electron-capture gas chromatography (GC) analysis (*12*). Purgeables were analyzed by using a closed-loop stripping (CLS) procedure (*13*). Base/neutrals and acid/phenols were analyzed by using a solvent extract analysis (SEA) method similar to EPA method 625 (*14*) but modified as follows: 2-L continuous extractors were used for the methylene chloride extraction (Continental Glass Blowing Corp., Richland, NY); base/neutrals (B/Ns) were extracted at pH 11; acid/phenols (A/Ps) were subsequently extracted at pH 2; the acid/phenol extracts were methylated with an excess of diazomethane, generated with a Diazald Kit (Aldrich Chemical Co., Milwaukee, WI); a fused silica (J & W Scientific, Rancho Cordova, CA) SE-52 capillary column (50 m, 0.3 mm i.d., 0.25 μm film thickness) was used for GC/MS analysis. Tracor and Carlo Erba (Model 2900) gas chromatographs and a Finnigan gas chromatography–mass spectrometer (GC/MS) (Model 4000 with INCOS data system) were used for VOA, CLS, and SEA analyses, respectively. Identifications were considered positive if both the gas chromatographic retention time and the mass spectrum agreed with those of a standard compound. Tentative identifications were based on computerized or manual matching of the un-

Table I. Woolwich: Vertical Profiles of Chlorides and Volatile Organics

Well M-4, 10/23/81

	depth below surface, m			
	19.6	21.0	22.5	25.6
chlorides, mg/L Cl^-	303	144	182	25.5
halogenated organics,[a] $\mu g/L$				
1,1,1-trichloroethane	5.4 ± 2.8	4.3 ± 0.08	9.1 ± 0.4	68.1 ± 4.6
trichloroethylene	2.9 ± 0.7	2.6 ± 0.3	2.9 ± 0.5	1.1 ± 0.3
tetrachloroethylene	1.7 ± 0.4	0.86 ± 0.39	1.5 ± 0.55	0.79 ± 0.09

Well PDML,[b] 11/11/81

	depth below surface, m					
	19.6	20.1	21.0	22.0	22.9	23.8
chlorides, mg/L	154	152	132	154	112	33.4
1,1,1-trichloroethane, $\mu g/L$	133	110	140	140	139	179
trichloroethylene, $\mu g/L$	0.6	0.6	1.1	1.0	1.0	1.2

[a] Average and standard deviation. [b] PDML, positive-displacement multilevel sampler (*11*).

known spectra against those of a reference library (*15*).

Volatiles and purgeables were quantified by using an internal standard method. A/P and B/N concentrations were estimated on the basis of the peak height relative to the peak height of a single characteristic ion fragment of the internal standards which were *p*-bromophenol and anthracene-d_{10}, respectively. The concentrations given were not corrected for differences in extraction efficiencies and differences in the detection sensitivities. Application of these corrections may change the given concentrations by more than an order of magnitude. Nevertheless, the values derived are adequate for comparison of concentrations at different locations. Chloride was analyzed titrimetrically by using the mercuric nitrate method (*16*). Total organic carbon (TOC) was measured with a Model DC-80 TOC analyzer (Envirotech-Dohrmann, Santa Clara, CA).

Results

Woolwich. (1) Vertical Distribution. Vertical concentration profiles for volatile compounds were measured at M-4 and PDML (Table I). Both wells were located near the boundary of the landfill, M-4 at the center of the eastern segment of the plume and PDML between the two leachate plume segments (Figure 1). The measured Cl^- concentrations were higher than 100 mg/L at all but the lowest well levels, where they were 26 and 33 mg/L, very close to the background concentration of 13 mg/L measured at WD.

The data for 1,1,1-trichloroethane (1,1,1-Cl_3EA), trichloroethylene (Cl_3EY), and tetrachloroethylene (Cl_4EY) did not conform to the Cl^- distribution. At M-4, a high 1,1,1-Cl_3EA concentration was observed at the bottom of the aquifer, while the upper levels showed an order of magnitude lower concentrations. In contrast, the 1,1,1-Cl_3EA profile at PDML was relatively even, with concentrations ranging from 110 to 179 $\mu g/L$. But as at M-4, the highest concentration was measured at the bottom where the Cl^- concentration was lowest. The profiles of both Cl_3EY and Cl_4EY at PDML were relatively constant to the bottom of the aquifer, again showing high values below the chloride-defined plume.

Table II. Woolwich: Chlorides, TOC, and Trace Organic Distribution[a]

	well (depth from surface, m)		
	WD[b] (25.1)	M-4-5 (19.6)	M-9-8 (24.6)
chlorides, mg/L Cl^-	13.1	300	215
TOC, mg/L	23.5	2040	472
Volatiles[c]			
1,1,1-trichloroethane	0.01 ± 0.005	5.4 ± 2.8	5.3 ± 3.2
trichloroethylene	<0.01	2.9 ± 0.5	5.3 ± 2.2
tetrachloroethylene	<0.01	1.7 ± 0.4	ND
Aromatic Hydrocarbons			
toluene	0.21	140	14
ethylbenzene	ND	98	0.08
p/m-xylene	ND	17	ND
o-xylene	ND	12	0.1
Phenols[d]			
phenol	ND	460	ND
methylphenol isomer	ND	610	63
ethylphenol isomer	ND	17	11
chlorocresol isomer	ND	13.6	ND
Alkyl Phosphates[d]			
tributyl phosphate	ND	1.2	0.4
triethyl phosphate	ND	15	10
Carboxylic Acids[d]			
benzoic acid	<0.1	$>10^3$	17
methylbenzoic isomer	ND	$>10^3$	30
dimethylbenzoic isomer	ND	$>10^3$	3.5
phenylacetic acid	ND	$>10^4$	$>10^2$
3-phenylpropanoic acid	ND	$>10^4$	1.9
4-phenylbutanoic acid	ND	9.7	0.8
palmitic acid	1.7	42	1.8
stearic acid	0.8	8.8	1.2
linoleic acid	ND	0.1	0.1
benzenedicarboxylic acid isomer	ND	6.1	1.1
nonanedioic acid	ND	68	NA
chlorinated unknown (M^+ 228?)	ND	5.4	0.4
dichlorohydroxybenzoic acid	ND	0.2	0.2
Nitrogen Containing[d]			
benzonitrile	ND	NA	2.5
methylbenzonitrile isomer	ND	0.8	8.8
aniline	ND	NA	9.9
tetramethylthiourea	ND	19	12
cyanobenzoic acid isomer	ND	ND	34

[a] All concentrations given in micrograms per liter, except chlorides and TOC which are in milligram per liter. ND, not detected; NA, not analyzed due to analytical interferences; <0.01, trace detected but not quantified. [b] Background well. [c] Average and standard deviation of three analyses. [d] Semiquantified; tentative identifications based on matching with references.

(2) Lateral Distribution. Samples from wells WD, M-4-5, M-9-8, and M-17-8 were taken to evaluate the lateral distribution of contaminants (Table II). The numbers following well identification indicate tube number. M-4-5 and M-9-8 were selected for sampling because of their closeness to the center streamline of the eastern plume segment. No significant contamination was found at M-17-8 (data not shown). The Cl^- concentration at M-4-5 was 300 mg/L, and the TOC concentration was 2040 mg/L. At M-9-8, approximately 70 m further downstream, the Cl^- concentration was lower by 30%, whereas the TOC concentration was lower by 77%. Whether this apparent retardation of TOC was due to biotransformation will be addressed in future studies.

Table III. Woolwich: Miscellaneous Compounds Tentatively Identified at M-4-5[a]

monocarboxylic acids	dicarboxylic acids
pentanoic acid	nonanedioic acid
2-methylpentanoic acid	decanedioc acid
hexanoic acid	undecanedioic acid
2-ethylpentanoic acid	unsaturated
heptanoic acid	$C_{17}H_{31}COOH$ (2 DB)[b]
2-ethylhexanoic acid	$C_{17}H_{33}COOH$ (1 DB)[b]
2-methylpentanoic acid	nitrogen-containing compounds
dodecanoic acid	cinnoline
cyclohexanoic acid	benzothiazole
2-methylcyclohexanoic acid	*N*-propylmethylbenzamide
miscellaneous	
cyclohexanone	

[a] Structural assignments based on matching of mass spectra with reference spectra (*15*). [b] DB, double bond.

The trace organic concentrations generally follow the trend indicated by TOC: high concentrations at M-4-5; significantly lower concentrations at M-9-8. The concentration decrease with distance was particularly significant for Cl_4EY, ethylbenzene, the xylene isomers, phenol, the chlorocresol isomers, the unchlorinated aromatic acids, and nonanedioic acid. Volatile halocarbon concentrations of tens to hundreds of micrograms per liter were found adjacent to the landfill (M-4, PDML; Table I), whereas concentrations at M-9 were much lower. More recent sampling has found volatile halocarbon concentrations below 1 μg/L at locations more than about 100 m from the landfill margin.

Generally, the carboxylic acids listed in Table II were present at M-4-5 in much higher concentrations than downstream at M-9-8. It is unclear whether this decrease in concentration, which exceeds 3–4 orders of magnitude in some instances, was due to sorption by the aquifer materials or biological or chemical transformation, or whether it was simply due to a retarded input relative to that of chloride. This attenuation is much more pronounced than that of TOC, and to infer that biotransformation is effectively removing these compounds appears reasonable. Two chlorinated organic acids were observed in the leachate plume. One was tenatively identified as a dichlorohydroxybenzoic acid; the other with an apparent molecular weight of 228 remains unknown. It is suspected that these compounds are mobile metabolites of unknown, immobile precursors.

The alkyl phosphates and the nitrogen-containing compounds were minor constituents. It is suspected that benzonitrile, methylbenzonitrile, aniline, tetramethylthiourea, cyanobenzoic acid, cinnoline, benzothiazole, and *N*-propylmethylbenzamide originated from wastes of a tire manufacturing plant, since several of these chemicals are used in tire manufacturing as intermediates or as vulcanization accelerators. Cyanobenzoic acid may be an oxidation product of methylbenzonitrile.

The acid/phenol fraction contained numerous other compounds including aliphatic and cyclic carboxylic acids, some of which were tentatively identified (Table III). Other compounds detected appear to be polycyclic carboxylic acids, but no reference spectra could be found, and their structure remains unknown.

North Bay. (1) Vertical Distribution. At location G, a piezometer and an upper (G-1) and a lower (G-2) multilevel device were installed. Eleven piezometer samples were analyzed for selected organics, TOC, and Cl^-. The Cl^- profile (Figure 3) indicates that the leachate plume was concentrated in the center and upper section of the aquifer as predicted from inorganic data obtained previ-

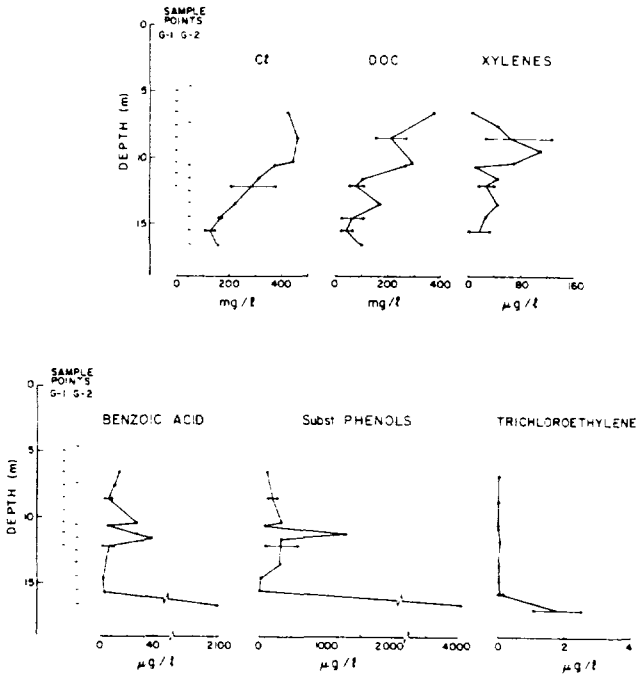

Figure 3. North Bay, July 11, 1982. Vertical profile of Cl^-, DOC, total xylenes, benzoic acid, total substituted phenols, and trichloroethylene at G.

ously (*3*). The DOC and some specific organic parameters such as total xylenes had similar concentration maxima. Benzoic acid and the sum of various phenols (phenol, methylphenol, 2,4-dimethylphenol, ethylmethylphenol) showed secondary concentration maxima at intermediate depths but had a much higher concentration in the lowermost sampling point. The volatile, chlorinated organic compounds showed a similar pattern with only traces being detected except at the deepest point (G-2-9), which contained low Cl^-. A previous sampling in 1981 also indicated a maximum Cl_3EY concentration of 14 μg/L at G-2-9, the lowest tube, significantly above that of the upper levels. Cl_4EY and 1,1,1-Cl_3EA followed the same trend in that their concentrations were above the detection limit only at the G-2-9 level.

(2) Lateral Distribution. To evaluate persistence and attenuation of selected components, samples were analyzed from wells along the centerline of the leachate plume indicated in Figure 2. In the samples taken downstream of G, the concentrations of volatiles were below the detection limit of 0.1 μg/L, and no plume of these volatiles could be discerned. The G-pz sample was taken as representative for the pollutant input of the 800-m plume stretching to AAA. The relative abundance of the aromatic hydrocarbons from G-pz, shown in Figure 4, was similar to that of the water-soluble fraction of diesel fuel (*17*, *18*), indicating that waste petroleum products, deposited at the landfill, were the major source of the aromatic hydrocarbons. The terpenoid compounds with the elemental composition $C_{10}H_xO_1$ (x = 20, 18, 16) are constituents of turpentine and other wood products and presumably were derived from buried plant material (*19*). The other compounds detected included *tert*-octylphenol, *tert*-octylphenolmonoethoxylate, tributyl phosphate, and dimethyl sulfoxide (Table IV).

Numerous compounds were persistent and apparently migrated from the landfill to the leachate spring located 800 m away. Attenuation appeared to be selective. For instance, camphor **22** and unknown **23**, *p*/*m*-xylene **6**, and *o*-xylene, which were major peaks in the G-pz sample, were close to or below the detection level at AAA-5. Conversely,

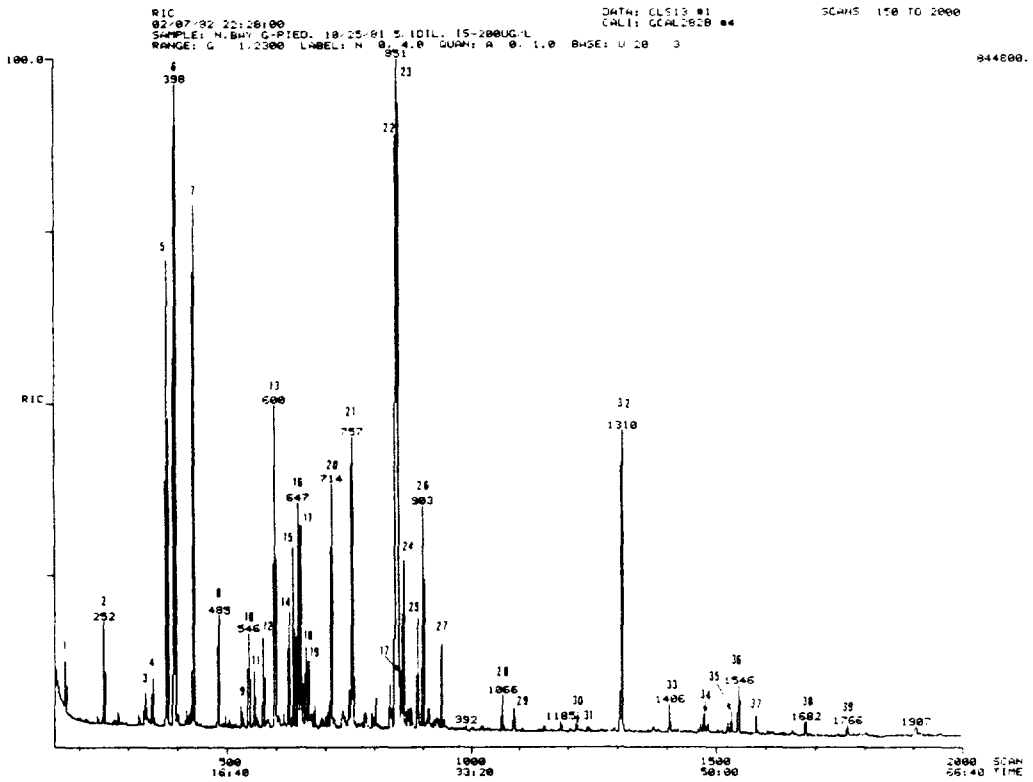

Figure 4. Reconstructed ion current chromatogram of CLS extract, North Bay, G-pz, 10/25/81. 50-m fused silica column, SE-52 (0.3 mm i.d., film thickness 0.25 μm); temperature programmed 40 (4 min) to 230 °C (3 °C/min). Peak numbers refer to Table IV. Internal standards (200 μg/L): peaks 20 (1-chloro-*n*-octane) and 32 (1-chloro-*n*-dodecane).

Table IV. List of Chemicals (Tentatively) Identified in Samples G-pz and AAA-5[a]

(Chlorinated) Aromatic Hydrocarbons

(1)[b] benzene
(2)[b] toluene
(4)[b] chlorobenzene
(5)[b] ethylbenzene
(6)[b] *p*/*m*-xylene
(7)[b] *o*-xylene
(8) isopropylbenzene
(9)[b] propylbenzene
(10) 1-ethyl-3-methylbenzene, 1-ethyl-4-methylbenzene
(11) 1,3,5-trimethylbenzene
(12) 1-ethyl-2-methylbenzene
(13) 1,2,4-trimethylbenzene
(14)[b] 1,4-dichlorobenzene
(16) 1,2,3-trimethylbenzene
(17) C_4-benzene[c]
(18)[b] 1,2-dichlorobenzene
(19) indan
(26)[b] naphthalene
(28)[b] 2-methylnaphthalene
(29)[b] 1-methylnaphthalene
tetrahydronaphthalene
C_1- and C_2-indans[c]
C_1-tetrahydronaphthalenes[c]

Miscellaneous

(3)[b] dimethyl sulfoxide
(30) phenyl ether
(34) octylphenol
(35) tributyl phosphate
(39) octylphenol monoethoxylate

Terpenes

(15) 1-methyl-4-(1-methylethyl)-7-oxabicyclo[2.2.1]heptane ($C_{10}H_{18}O$)
(18) 1,3,3-trimethyl-2-oxabicyclo[2.2.2]octane ($C_{10}H_{18}O$), cineole
(21) 1,3,3-trimethylbicyclo[2.2.1]heptan-2-one ($C_{10}H_{16}O$), *d*-fenchone
(22) 1,7,7-trimethylbicyclo[2.2.1]heptan-2-one ($C_{10}H_{16}O$), camphor
(23) unknown, spectrum similar to 8-methyl-1,8-nonanedial
(24) 1-isopropyl-4-methylcyclohexanol ($C_{10}H_{20}O$)
(25) 5-methyl-2-isopropylcyclohexanol ($C_{10}H_{20}O$), menthol

Most Abundant Ions of Unknowns (Intensity in Parentheses)

(33) *m*/*z* 145 (100), 41 (60), 57 (45), 20 (25), 127 (20)
(36) *m*/*z* 59 (100), 109 (48), 166 (39)
(37) *m*/*z* 145 (100), 215 (20), 127 (10)
(38) *m*/*z* M^+ 346 (10), 253 (100), 331 (25)

[a] Identified by matching against reference spectra (*15*); numbers refer to Figure 4. [b] Confirmed by comparison of GC retention times. [c] C_n, number of aliphatic carbons.

minor components at G-pz including chlorobenzene **4**, ethylbenzene **5**, and 1-methyl-4-(1-methylethyl)-7-oxabicyclo[2.2.1]heptane (**15**) (not quantified) were all major at AAA-5.

Selected pollutants were (semi)quantified in samples of G-pz, M-9, LL-9, and AAA-5 (Table V). Benzoic acid and C_2-benzoic and C_3-benzoic acid may be degradation products of alkylbenzenes leaching from the landfill, although other precursors may be possible. Degradation of the aromatic fraction of petroleum products is possible under aerobic conditions (*17*) and may occur at the surface of or in aerobic pockets within the landfill. The sum of

Table V. North Bay, 10/25/81: Chlorides, TOC, and Trace Organic Distribution[a]

	well				
	(background)	G-pz	M-9	LL-9	AAA-5
chlorides, mg/L	2.4	710 (1.0)	188 (1.0)	96.5 (1.0)	77.9 (1.0)
TOC, mg/L ((mg/L)/(mg/L))	3.3	600 (0.84)	205 (1.1)	109 (1.1)	79 (1.0)
		Aromatic Hydrocarbons			
benzene	0.3	47 (66)	4.5 (24)	2.1 (65)	2.1 (26)
toluene	0.2	59 (83)	0.8 (4)	0.6 (16)	3 (38)
ethylbenzene	0.1	480 (780)	30 (160)	26 (260)	14 (180)
m/*p*-xylene	<0.1	820 (1100)	60 (330)	13 (130)	0.5 (7)
o-xylene	ND	510 (720)	13 (71)	2 (21)	0.6 (8)
1,2,4-trimethylbenzene	<0.1	220 (310)	75 (410)	40 (410)	0.6 (8)
naphthalene	ND	110 (150)	21 (110)	10 (100)	3 (38)
2-methylnaphthalene	<0.1	20 (28)	5.6 (30)	2 (21)	1 (13)
1-methylnaphthalene	0.1	13 (18)	3.4 (18)	1.6 (16)	0.8 (10)
acenaphthene[b]	ND	0.9 (1.2)	1.2 (6.5)	0.1 (1.0)	0.2 (2.6)
fluorene[b]	ND	1.2 (1.7)	0.7 (3.8)	ND (-)	ND (-)
		Chlorinated Benzenes			
chlorobenzene	0.3	33 (46)	17 (92)	16 (165)	16 (205)
1,2-dichlorobenzene	0.2[c]	13 (18)	5.6 (30)	2.8 (29)	4.8 (61)
1,4-dichlorobenzene	<0.1	40 (56)	10 (54)	7 (72)	7 (90)
		Phenols[c]			
ethylphenol isomer	ND	6.3 (8)	1.8 (9)	ND (-)	ND (-)
		Carboxylic Acids[c]			
benzoic acid	NA	8.8 (12)	ND (-)	<0.1 (-)	1.0 (12)
C_2-benzoic[d] acid	NA	25 (35)	6.5 (35)	4.2 (4)	0.8 (10)
C_3-benzoic[d] acid	NA	7.3 (10)	2.3 (12)	1.9 (1.9)	0.1 (1.3)
methylbutanoic acid	NA	238 (330)	37 (210)	25 (260)	13 (170)
dehydroabietic acid	NA	15.5 (21)	1.9 (10)	0.6 (6)	0.6 (8)

[a] Concentrations in micrograms per liter, except where indicated; in parentheses concentrations relative to Cl^- (ng/L organic to mg/L Cl^-). NA, not analyzed; ND, not detected; <0.1, trace detected but not quantitated. [b] Semiquantified as 3,6-dimethylphenanthrene. [c] Semiquantified as anthracene-d_{10}; structural assignments based on matching of MS with reference spectra (*15*). [d] C_n, number of aliphatic carbons.

the individual aromatic hydrocarbons was in the range of 2 mg/L, close to the solubility limit for no. 2 fuel in water (*17*, *18*). This suggests that the groundwater becomes saturated with hydrocarbons when passing through the landfill area.

No significant contamination was detected at O-4, the background well. The concentrations measured at G clearly indicate the impact of the landfill. Generally concentrations decreased steadily with distance from the landfill, indicating the effectiveness of attenuating factors. To obtain a better picture of attenuation processes other than dispersion, the observed pollutant concentrations were corrected for dispersive dilution by using Cl^- as a conservative tracer (Table V). The relative TOC concentrations were remarkably constant and indicated that the bulk of the dissolved organics were refractory. The trace organics data were somewhat variable, but several trends appear to be significant. The relative concentrations of benzene, ethylbenzene, naphthalene, and the methylnaphthalenes were relatively constant at all four wells, suggesting that the adsorptive capacity of the aquifer for these compounds was exhausted and that hydrodynamic dispersion was the only attenuation mechanism. Apparently, these aromatic hydrocarbons were released at a constant rate over a period of several years, perhaps from a large pool of petroleum products. The apparent selective loss of the xylene isomers is of interest. Perhaps it indicates microbial transformation of these compounds, since physicochemical processes are not expected to affect selectively the fate of these chemicals to such a marked degree.

The relative concentrations of the chlorinated benzenes showed a tendency to increase from G-pz to AAA-5. This increase may have been due to a slow decrease in the leaching rate of these compounds. The behavior of the carboxylic acids was mixed. The concentrations of benzoic acid decreased between G-pz and M-9 but reappeared at AAA-5, whereas the relative concentrations of 2-methylbutanoic and dehydroabietic acid were fairly constant. Whether the two latter compounds are refractory or are intermediates that were formed and removed simultaneously remains to be investigated.

Discussion

Leachate Composition. Short-chain fatty acids, which have been reported to make up 49% of the dissolved organic carbon (DOC) of fresh leachate (*20*), are major contaminants adjacent to the Woolwich landfill but are less prevalent near the North Bay landfill. Qualitatively, the leachates examined resembled previously reported landfill leachate (*7*,*8*) and, interestingly, surface water from within the blast zone of the Mount St. Helens eruption, where decomposition of large amounts of plant material, destroyed by heat, wind, and pyroclastic flow, created biogeochemical conditions similar to those of a leachate plume, i.e., anoxic conditions, high DOC, iron and manganese concentrations, and enhanced bacterial activity (*21*–*23*).

As is indicated by the types of compounds detected at North Bay, methanogenesis appears to be the major removal process for DOC. Several of the compounds identified in leachates, including phenylpropanoic acid, phenylacetic acid, benzoic acid, cyclohexane carboxylic acid, cyclohexanone, and heptanoic acid, are intermediates in the anaerobic degradation of ferulic acid, a model lignin compound (*24*). The occurrence of these compounds is compatible with the methanogenic degradation of compounds similar to ferulic acid, although it cannot be con-

cluded that lignin degradation in fact occurs. The occurrence of methanogenesis is also supported by a previous study (25), which demonstrated the formation of methane from G to LL and its persistence from there to AAA. Oxygen was not detected at AAA.

At both sites, chlorinated hydrocarbons, such as mono- and dichlorobenzenes, Cl_3EY, Cl_4EY, and 1,1,1-Cl_3EA, were detected along with non-chlorinated aromatic hydrocarbons. At the North Bay site, Cl_4EY, Cl_3EY, and 1,1,1-Cl_3EA were detected only in groundwaters adjacent to the landfill, but not further downstream. Microbial dehalogenation under methanogenic conditions, which was shown to occur in laboratory experiments (26, 27), may have prevented groundwater contamination by these compounds. At the Woolwich site, where conditions appeared highly reducing but where methanogenesis has not yet been demonstrated, chlorinated aliphatic removal appears to have been less efficient. 1,1,1-Cl_3EA was detected in the range 110–179 $\mu g/L$ at PDML approximately 30 m south of the landfill and in the range 4.3–9.1 $\mu g/L$ at M-4, approximately 50 m to the southeast of the landfill (68.1 $\mu g/L$ were detected at 25.6-m depth). Although Cl^- had apparently migrated 600 m beyond the landfill, current sampling has indicated only sporadic traces of 1,1,1-Cl_3EA beyond M-9, suggesting that the chlorinated solvent plume has begun to emerge only recently or that attenuation by sorption or biodegradation was effective only further downstream.

Microbial transformations occurring within the site may lead to a removal of a compound, but it may also produce more soluble and, consequently, more mobile products. The occurrence of chlorinated aromatic acids at North Bay and of chlorinated phenol and cyanobenzoic acid at Woolwich may be examples of such an effect. Partial microbial degradation and subsequent mobilization should, therefore, be considered when wastes deemed to be water insoluble and immobile are deposited in landfills.

At well G-pz at the North Bay site, high total aromatic hydrocarbon concentrations were measured, but concentrations of individual components were far below their maximum solubility limit. The measured concentration of benzene was 47 $\mu g/L$, only a small fraction of its maximum solubility in water (1765 mg/L at 25 °C). This depressed benzene dissolution in water may be due to its low mole fraction in the hydrocarbon pool, which is presumed to be saturating the groundwater. The equilibrium concentration of an individual component of a multicomponent hydrocarbon mixture in aqueous phase can be estimated according to

$$C^i_{(H_2O)} = X^i_{(oil)} C^i_{s(H_2O)}$$

where $C^i_{(H_2O)}$ is the concentration in water, $C^i_{s(H_2O)}$ is the solubility limit, and $X^i_{(oil)}$ is the mole fraction of compound i in the multicomponent mixture (28). Hence, contamination by any compound, which preferentially partitions into the pool of petroleum, will be reduced to a fraction of its maximum solubility limit.

Vertical Distribution. At both sites, increased concentrations of chlorinated solvents including Cl_3EY, Cl_4EY, and 1,1,1-Cl_3EA were observed at the bottom of the water table aquifer near the landfill, underneath the plume defined by Cl^-. The best documented example is at location G at the North Bay site (Figure 3). At least three explanations of the vertical profiles can be suggested: (i) two-phase gravity flow of immiscible solvents with a density greater than one, (ii) differences in the spatial distribution of sources emanating solvents and Cl^- at the landfill, and (iii) unfavorable conditions for biotransformation underneath the plume, but active biotransformation within the plume.

The first explanation is that large amounts of these heavier-than-water solvents migrated downward by two-phase gravity flow, resulting in a pool of water-immiscible liquids at the bottom of the water table aquifer. Groundwaters flowing past this pool would incorporate some of the components and form a separate plume beneath the leachate plume defined by Cl^-.

Further analysis at site G in 1982 indicated high relative concentrations of other organics, including benzoic acid and phenols, which are less dense than water, at the deepest sampling point (Figure 3). It is conceivable that heavier-than-water liquids dissolved and transported components lighter than water to the bottom of the aquifer from where they leached into the groundwater. So far, there appears to be only laboratory investigations of two-phase flow (29). Although emulsions of trichloroethylene in an aquifer have been observed at the site of an accidental spill (30), detailed studies of two-phase flow of liquids heavier than water under field conditions have not been, to our knowledge, reported in the literature. Such flow may be significant, however, because deep aquifers, deemed to be unpolluted based on Cl^- measurements, may, in fact, be impacted.

The second explanation of this vertical distribution of concentrations is essentially hydrogeological. Points arranged vertically represent samples from different flow paths, probably emanating from further back in the landfill as depth at G increases. Thus, the observed concentration profiles may be the result of an uneven distribution of the wastes. However, it seems unlikely that such marked inhomogeneities would persist at this site.

The third explanation emphasizes variation in biotransformations that may occur during transport of contaminants through the landfill site to location G. On the basis of Cl^- data, there is much less leachate component present in the deepest sample, and biochemical conditions underneath the leachate plume may not be favorable for halogenated aliphatics degradation. However, methane concentrations (25) were similar within and below the chloride-defined plume, indicating that reducing conditions at G extended to the bottom of the aquifer. Whether the occurrence of chloro aliphatics in waters containing methane indicates inhibition of biotransformation is subject to further study.

Clearly, an inorganic contaminant such as Cl^- is not an adequate indicator of organic contaminant distribution, although it does provide qualitative identification of major zones of landfill-contaminated groundwater. Specific organic compounds may not be adequate indicators of contamination by other organics, because of the complexity of organic inputs and because biogeochemical attenuation processes tend to be selective for different compound classes. For example, chlorinated solvents may not persist in strongly reduced groundwaters at landfill sites where investigators may be tempted to use them as contamination-indicator parameters because of their perceived persistence, mobility, and relative ease of analysis.

Lateral Distribution. The principal attenuating processes for an organic compound, dispersive dilution, sorption, and biological degradation, cannot be evaluated individually in the absence of mass balance data, indicating both dissolved and sorbed concentration as a function of time. On the basis of water concentrations alone, data interpretation is ambiguous, although inferences with respect to pollutant behavior can be made on the basis of results from laboratory data and related field studies, and

on the basis of Cl^- data indicating advection and dispersion (*31–35*).

In a qualitative sense, all compounds that are detected in leachate-contaminated groundwaters may be regarded as mobile, as indicated by their presence in the mobile water phase. In this study, such compound groups included chlorinated hydrocarbons, aromatic hydrocarbons, phenols, alkyl phosphates, aliphatic and aromatic acids, various nitrogen-containing aromatics, terpenoid compounds, alkylphenol ethoxylates, and many other compounds still to be identified. Compounds such as the dichlorobenzenes with a log K_{ow} of 3.38 were detected 800 m away from the source, confirming the poor sorption characteristics of the sandy aquifer. It may be speculated that compounds with log K_{ow} greater than 3–4 were also deposited in the landfill but were effectively retained by sorption. If such compounds are present, then the long-term impact of their belated release to the groundwaters must be evaluated by additional studies.

Susceptibility to biodegradation under methanogenic conditions has been determined in the laboratory from a number of compounds detected, including 1,1,1-Cl_3EA, Cl_3EY, and Cl_4EY (*26, 27, 36*), phenol (*24, 37*), and benzoic and other aromatic acids (*24, 37–39*). In contrast, several aromatic compounds, including ethylbenzene, naphthalene, chlorobenzene, and 1,4- and 1,3-dichlorobenzene, were shown to persist under anaerobic conditions (*27*). On the basis of this laboratory evidence, the inferred biodegradation of 1,1,1-Cl_3EA, Cl_3EY, Cl_4EY, phenol, benzoic acid, and several substituted monoaromatic acids in the anoxic plume was expected, whereas chlorobenzene, 1,4- and 1,3-dichlorobenzenes, ethylbenzene, and naphthalene were expected to persist.

At the Woolwich site, where leachate evolution is at a relatively early stage, TOC and most trace organics were retarded relative to Cl^-. This observation could be explained by retarded production and release or adsorptive and/or biological attenuation of organics. The concentrations of fatty acids at M-4-5 were high, indicating that methanogenic removal may have been inefficient. The apparent persistence of 1,1,1-Cl_3EA and Cl_3EY during the approximately 2 years of residence time required for groundwaters to move from the landfill to M-9 indicates unfavorable biogeochemical conditions for complete biotransformation. Similarly, the occurrence of nitrogenous organics at M-9-8 indicates persistence and mobility for these compounds as well.

At the North Bay site, plume evolution has reached a steady state with respect to the major pollutants. Input of Cl^- and TOC appeared to have been relatively constant, and therefore, dispersion can be tentatively accounted for by using Cl^- as a conservative tracer (*25*). By sampling close to the center line of the plume defined by Cl^-, presumably samples of the same flow line were compared. TOC and several trace organic compounds including benzene, ethylbenzene, naphthalene, chlorobenzene, and 1,2- and 1,4-dichlorobenzene appeared to be attenuated by dispersion only. Their concentrations relative to that of Cl^- varied little, by less than a factor of 5, indicating saturation of the adsorptive capacity of the aquifer and persistence of these compounds (Table V). Of *m/p*- and *o*-xylene, however, the relative concentrations decreased about 2 orders of magnitude, and biotransformation of these compounds was suspected. Laboratory studies are needed to verify this supposition. The geochemistry of biogenic phenols and acids in leachate plumes should be given further attention, not just because these compounds may serve as indicators for the geochemical conditions but also because of their possible public health significance. Leaching of phenolic and other potentially hazardous compounds from domestic landfills may well be a threat to many drinking water supplies, a potential problem that should not be overlooked in view of the tens of thousands of domestic landfills in use.

Summary and Conclusions

The leachate plumes of two landfills were characterized with respect to specific trace organic compounds. The main fraction of the DOC appeared to be derived from decomposing plant material, as was indicated by the composition of the extracts. Aliphatic and aromatic acids, phenols, resin acids, and terpene compounds were the main components detected in the leachate plume. Compounds of commercial and industrial origin were detected in the leachate plume of both sites. The compounds included chlorinated benzenes, aromatic hydrocarbons, alkyl phosphates, alkylphenol ethoxylates, and nitrogen-containing compounds. The aromatic hydrocarbon composition suggested that the groundwater was in equilibrium with a pool of deposited petroleum products, leaching water-soluble, one- and two-ring aromatic hydrocarbons. The preliminary data indicate that most of these compounds were persistent and mobile in the methanogenic plume. The selective removal of the xylenes was hypothesized to be due to biotransformation. The persistence of chlorobenzene and 1,2- and 1,4-dichlorobenzene observed at a 800-m distance from the North Bay landfill site was in agreement with the reported stability of these compounds under methanogenic conditions (*27*). The apparent persistence of 1,1,1-Cl_3EA and Cl_3EY close to the Woolwich site but not at North Bay could reflect less methanogenic activity or unexplained inhibitory effects at the former site.

The nitrogenous aromatic compounds at the Woolwich site presumed to be leached from industrial rather than domestic wastes migrated to well M-9, indicating that these compounds were poorly sorbed and refractory under the conditions at this site. Their occurrence suggests that burying industrial wastes in municipal landfills may have been a widespread practice. Consequently, leaching of commercial and industrial toxicants from municipal landfills should be anticipated when the environmental impact of landfills is evaluated.

The data obtained for Cl_3EY and 1,1,1-Cl_3EA could suggest two-phase flow of an organic phase to the bottom of the aquifer. Further study of this process is needed because it has important implications for evaluation of groundwater contamination in the vicinity of landfills. Chloride or other conservative inorganics generally used for plume mapping may not be indicative of the actual distribution of specific organic contaminants. Deeper aquifers previously considered isolated from leachate may also be subject to contamination if dense organic phases exist in the landfill.

The study showed that results of laboratory studies simulating trace organic behavior in groundwater are essential to interpret field observations. Conversely, concepts and models must be evaluated by application to real situations, if they are to be used with confidence. Clearly, improved undestanding of transport and attenuating processes is required to design strategies for groundwater protection against contamination by landfilled industrial as well as domestics wastes.

Acknowledgments

Mark Gardner and Gary Hopkins provided organic and inorganic analytical data and Paul Johnson, Paul Plotz,

and Scott King provided the groundwater samples.

Registry No. 1,1,1-Cl_3EA, 71-55-6; Cl_3EY, 79-01-6; Cl_4EY, 127-18-4; toluene, 108-88-3; ethylbenzene, 100-41-4; *p*-xylene, 106-42-3; *m*-xylene, 108-38-3; *o*-xylene, 95-47-6; phenol, 108-95-2; methylphenol, 1319-77-3; ethylphenol, 25429-37-2; (chloromethyl)phenol, 30915-79-8; tributyl phosphate, 126-73-8; triethyl phosphate, 78-40-0; benzoic acid, 65-85-0; methylbenzoic acid, 25567-10-6; dimethylbenzoic acid, 30587-19-0; phenylacetic acid, 103-82-2; 3-phenylpropanoic acid, 501-52-0; 4-phenylbutanoic acid, 1827-21-1; palmitic acid, 57-10-3; stearic acid, 57-11-4; linoleic acid, 60-33-3; benzenedicarboxylic acid, 29010-86-4; nonanedioic acid, 123-99-9; (dichloromethoxy)benzoic acid, 92366-33-1; benzonitrile, 100-47-0; methylbenzonitrile, 25550-22-5; aniline, 62-53-3; tetramethylthiourea, 2782-91-4; cyanobenzoic acid, 31227-64-2; benzene, 71-43-2; 1,2,4-trimethylbenzene, 95-63-6; naphthalene, 91-20-3; 2-methylnaphthalene, 91-57-6; 1-methylnaphthalene, 90-12-0; acenaphthene, 83-32-9; fluorene, 86-73-7; chlorobenzene, 108-90-7; 1,2-dichlorobenzene, 95-50-1; 1,4-dichlorobenzene, 106-46-7; methylbutanoic acid, 35915-22-1; dehydroabietic acid, 1740-19-8.

Literature Cited

(1) Baedecker, M. J.; Back, W. *J. Hydrol. (Amsterdam)* **1979**, *43*, 393–414.
(2) Baedecker, M. J.; Back, W. *Ground Water* **1979**, *17*, 429–437.
(3) Cherry, J. A. In "Environment and Solid Wastes: Characterization, Treatment and Disposal"; Francis, C. W.; Auerbach, S. I., Eds.; Oak Ridge Life Sciences Symposium Series: Oak Ridge, TE, 1983; Chapter 13, pp 127–147.
(4) MacFarlane, D. S.; Cherry, J. A.; Gillham, R. W.; Sudicky, E. A. *Hydrol. (Amsterdam)* **1983**, *63*, 1–29.
(5) Nicholson, R. V.; Cherry, J. A.; Reardon, E. J. *J. Hydrol. (Amsterdam)* **1983**, *63*, 131–176.
(6) Champ, D. R.; Gulens, J.; Jackson, R. E. *Can. J. Earth Sci.* **1979**, *16*, 12–23.
(7) Dunlap, W. J.; Shew, D. C.; Scalf, M. R.; Cosby, R. L.; Robertson, J. M. In "Identification & Analysis of Organic Pollutants in Water"; Keith, L. H., Ed.; Ann Arbor Science: Ann Arbor, MI, 1976; Chapter 27, pp 453–477.
(8) DeWalle, F. B.; Chian, E. S. K. *J.—Am. Water Works Assoc.* **1981**, *73*, 206–211.
(9) Cherry, J. A.; Barker, J. F.; Buszka, P. M.; Hewetson, J. P.; Mayfield, C. I. In "Proceedings of the Fourth Annual Madison Conference of Applied Research and Practice on Municipal and Industrial Waste"; Department of Engineering and Applied Science, University of Wisconsin—Extension: Madison, WI, 1981; pp 393–411.
(10) Robin, M. J. L.; Dytynyshyn, D. J.; Sweeney, S. J. *Ground Water Monit. Rev.* **1982**, 63–65.
(11) Cherry, J. A.; Gillham, R. W.; Anderson, E. G.; Johnson, P. E. *J. Hydrol. (Amsterdam)* **1983**, *63*, 31–49.
(12) Henderson, J. E.; Peyton, G. R.; Glaze, W. In "Identification and Analysis of Organic Pollutants in Water"; Keith, L. H., Ed.; Ann Arbor Science: Ann Arbor, MI, 1976; Chapter 7, pp 105–111.
(13) Grob, K.; Zürcher, F. *J. Chromatogr.* **1976**, *117*, 285–294.
(14) *Fed. Regist.* **1976**, *44* (233), 69540–69552.
(15) Heller, S. R.; Milne, G. W. A. "EPA/NIH Mass Spectral Data Base"; U.S. Government Printing Office: Washington, DC, 1978.
(16) American Publich Health Association "Mercuric Nitrate Method"; American Publich Health Association: Washington, DC, 1976; pp 304–306.
(17) Kappeler, Th.; Wuhrmann, K. *Water Res.* **1978**, *12*, 327–342.
(18) Zürcher, F.; Thüer, M. *Environ. Sci. Technol.* **1978**, *12*, 838–843.
(19) Streibl, M.; Herout, V. In "Organic Geochemistry, Methods and Results"; Eglinton, G.; Murphy, M. T. J., Eds.; Springer-Verlag, New York, 1976; Chapter 16, pp 401–424.
(20) Chian, E. S. K.; DeWalle, F. B. *Environ. Sci. Technol.* **1977**, *11*, 158–163.
(21) McKnight, D. M.; Pereira, W. E.; Ceazan, M. L.; Wissmar, R. C. *Org. Geochem.* **1982**, *4*, 85–95.
(22) Wissmar, R. C.; Devol, A. H.; Staley, J. T.; Sedell, J. R. *Science (Washington, D.C)* **1982**, *216*, 178–181.
(23) Wissmar, R. C.; Devol, A. H.; Nevissi, A. E.; Sedell, J. R. *Science (Washington, D.C.)* **1982**, *216*, 175–178.
(24) Healy, J. B.; Young, L. Y.; Reinhard, M. *Appl. Environ. Microbiol.* **1980**, *39*, 436–444.
(25) King, K. S., unpublished M.Sc. Thesis, University of Waterloo, 1983.
(26) Bouwer, E. J.; McCarty, P. L. *Appl. Environ. Microbiol.* **1983**, *45*, 1286–1294.
(27) Bouwer, E. J. Ph.D. Thesis, Stanford University, 1982.
(28) Stumm, W.; Morgan, J. "Aquatic Chemistry", 2nd ed.; Wiley: New York, NY, 1981; Chapter 7, p 734.
(29) Schwille, F. In "Studies in Environmental Science"; van Diujvenbooden, W.; Glasberger, P.; H. van Lelyveld, H., Eds.; Elsevier: Amsterdam, The Netherlands, 1981, Vol. 17.
(30) Giger, W.; Molnar-Kubica, E. *Bull. Environ. Contam. Toxicol.* **1978**, *19*, 475–480.
(31) Cherry, J. A.; Freeze, R. A. "Groundwater"; Prentice-Hall: Englewood Cliffs, NJ, 1979; Chapter 9.
(32) McCarty, P. L.; Reinhard, M.; Rittmann, B. E.; *Environ. Sci. Technol.* **1981**, *15*, 40–51.
(33) Schweich, D.; Sardin, M. *J. Hydrol. (Amsterdam)* **1981**, *50*, 1–33.
(34) Roberts, P. V.; Schreiner, J.; Reinhard, M.; McCarty, P. L. *J. Water Pollut. Control Fed.* **1980**, *52*, 161–172.
(35) Schwarzenbach, R. P.; Westall, J. *Environ. Sci. Technol.* **1981**, *15*, 1360–1367.
(36) Bouwer, E. J.; Rittmann, B. E.; McCarty, P. L. *Environ. Sci. Technol.* **1981**, *15*, 596–599.
(37) Healy, J. B.; Young, L. *Appl. Environ. Microbiol.* **1978**, *35*, 216–218.
(38) Clark, F. M.; Fina, L. R. *Arch. Biochem.* **1952**, *36*, 26–32.
(39) Ferry, J. G.; Wolfe, R. S. *Arch. Microbiol.* **1976**, *107*, 33–40.

Received for review January 12, 1984. Revised manuscript received May 30, 1984. Accepted June 28, 1984. This study was supported by the Robert S. Kerr Environmental Research Laboratory of the U.S. Environmental Protection Agency and by the Lottery Trust Fund of Ontario, Canada. Although the information described in this article has been funded in part by the U.S. Environmental Protection Agency under Assistance Agreement R-808851 to the Civil Engineering Department, Stanford University, it has not been subjected to the Agency's required peer and administrative review and therefore does not necessarily reflect the views of the Agency, and no official endorsement should be inferred.

Summary of Calculations
Benzene and Toluene Vaporization

by

Alfred J. Wussler, P.E.

El Paso Natural Gas Company Company
February 25, 1985
El Paso, Texas

Summary of Calculations
Benzene and Toluene Vaporization
(Calculations Performed 2/25/85)

Question: What happens to benzene and toluene emitted to unlined ponds from San Juan Division wellhead separators?

Approach To The Problem: Determine the solubility of benzene and toluene in water. Assume any non-soluble organic floats on the water surface, and will evaporate.

Assumptions:

1. Benzene and toluene solubility do not vary appreciably with temperature and will be assumed constant.

2. The equilibrium surface temperature can be calculated in the same manner as for evaporation from a solid (Perry, P. 15-35).

3. Evaporation can be calculated based upon conduction and radiation effects using the average daily ambient temperature in the San Juan Basin.

4. Saturation humidity of benzene and toluene may be calculated from vapor pressure data and converted to pounds of hydrocarbon per pound of dry air.

$$H_s = P_{vapor}/P_{total}$$

References:

1. Perry's Chemical Engineer's Handbook, Fourth Edition, McGraw-Hill Book Company, 1963. PP 15-35 through 15-38 and PP 3-25, 3-41, 3-47, 3-58, 3-59 and 3-60.

2. International critical tables, Volume IV, P 177, #992 (Benzene/Toluene mixture freezing point) National Academy of Sciences, 1928.

3. Climates of the States, Gale Research Company, Detroit, Michigan, Volume 2, P. 684.

4. Engineering Data Book, Gas Processors Association, Tulsa, Oklahoma, Nineth Edition, PP 16-2 through 16-4.

Calculation Basis and Data

1. Water Solubilities, Reference #1, PP 3-25 & 3-41:

   Benzene = .07 Grams/100 Grams @ 22°C = 700 PPM
   Toluene = .05 Grams/100 Grams @ 16°C = 500 PPM

2. Effluent Discharge Rate:

   5 Bbl/Day = 28.07 Ft ^{3}/Day = 1752 #/Day (100% Water Basis)

3. Pond Surface Area:

   A square pond with approximately 7 ft.^{2} surface.

4. Benzene and toluene worst case discharge.

   Benzene = 580 PPM
   Toluene = 3950 PPM

5. Assumed wind velocity = 5 MPH = 2146 #/Hr. Ft.^{2}

Calculations:

Page 15-35 of reference 1 (attached) indicates that the rate of drying is controlled by the rate of heat transfer to the evaporating surface, and is equivalent to liquid evaporation.

The evaporation of liquid benzene and toluene will be calculated as a tray drying problem, with the evaporation taking place into the first one foot of air space above the pond.

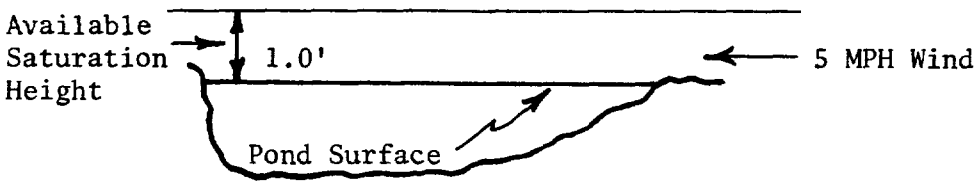

On P. 15-36, the following equation is derived:

$$\frac{dw}{d\theta} = \frac{\alpha G^{n} A}{\lambda D_{c}^{m}} (t - t_{s}')$$

A = Area for heat transfer and evaporation (Ft^{2})

λ = Liquid heat of vaporization at t_{s}' (BTU/#)

t = Gas temperature (°F)

t_{s}' = Evaporation surface temperature (°F)

G = Mass velocity of drying gas (#/Hr. Ft^{2})

D_{c} = Characteristic dimension of the system (Ft)

a, n, and m = Empirical constants.

$h_c = \frac{\alpha G^n}{D_c^m}$ = Heat transfer coefficient (BTU/Hr Ft^2) for convection.

D_c = $\frac{\text{4 Times Cross Sectional Area}}{\text{Perimeter of Flow Channel}}$

for a square pond = $\frac{4 \times \text{Length} \times 1}{4 \times \text{Length}} = 1$

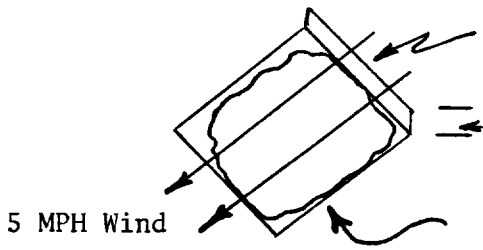

α = .01 (Equation 15-23, P. 15-36)
n = 0.8 " "
M = 0.2 " "

$$n_c = \frac{(0.01)\ (2146)^{0.8}}{(1.0)^{0.2}} = 4.63$$

Rate balance for evaporation heat transfer (equation 15-29a, P. 15-37).

$$\frac{\tau}{c_s}\ (Hs - H) = t - t_s' + \frac{hr}{h_c}\ E\ (t - t_s')$$

The following values are substituted:

τ = Heat of vaporization (Reference #4) Benzene = 169.10 BTU/# Toluene = 154.83 BTU/#

H_s = Saturation Humidity (Calculate from Reference #1 Vapor Pressure Data)

H = Humidity of the drying air (assumed 0 = no benzene or toluene present)

t = Average atmospheric temperature = 28°F (Reference #3)

h_r = Radiation heat transfer = 1.0 (from figure 10-10, Reference #1)

E = Emissivity = 0.9 (assumed)

These valves are substituted and the equations rearranged for trial and error solutions.

Benzene $H_S = \frac{.25}{169.10}\ (1 + \frac{.9}{4.63})\ (28 - t_s') = .0018\ (28 - t_s')$

Toluene $H_S = \frac{.25}{154.83}\ (1 + \frac{.9}{4.63})\ (28 - t_s') = .0019\ (28 - t_s')$

Vapor pressure data for benzene and toluene (PP. 3-47, 3-58, 3-59, and 3-60, Reference #1) are used to construct plots of H_s vs t for graphical trial and error solution (Figure A).

Equilibrium values obtained are:

Benzene H_s = .0336 t_s' = 9.3°F
Toluene H_s = .0167 t_s' = 19.2°F

Data from reference 2 is used to construct Figure B, a freezing point diagram for the floating benzene/toluene layer.

Benzene Solubility = 700 PPM
Benzene in Sample = 580 PPM ∴ All benzene is assumed dissolved in water.

Toluene Solubility = 500 PPM
Toluene in Sample = 3960 PPM

∴ 3460 PPM is liquid toluene on pond surface.

Figure B indicates 100% toluene is a liquid at 19.2°F (calculated t_s'), so toluene is not frozen and is free to evaporate.

(2146 #/Hr Ft^2 Dry Air) (7 Ft^2 Pond) = 15022 #/Hr. Dry Air

Calculated H_s toluene = .0167 #Toluene/# Dry Air

For a 5 MPH Wind
(.0167 # Toluene/# Dry Air) $\left(15022 \frac{\text{\# Dry Air}}{\text{HR}}\right)$ = 250.87 #/Hr Toluene evaporated

250.87 #/Hr is the balanced conduction and radiation evaporation rate for toluene.

Toluene discharged and not soluble = $\frac{3460}{1{,}000{,}000}$ (1752 #/D Water) = 6.06 #/Da

(6.06 # Toluene) $\left(\frac{\text{HR}}{250.87\#}\right)$ = .02 Hours

≃ 1.5 Minutes to Evaporate

Conclusion:

Excess (non-soluble) toluene will rapidly evaporate into the air with a 5 MPH wind velocity.

580 PPM Benzene
3960 PPM Toluene
4540 PPM Total

Evaporation = $\left(\frac{3460}{4540}\right)$ (100) = 76.21% of emitted benzene and toluene calculated to vaporize.

Therefore, premise that 50% of the compounds vaporize appears reasonable.

Table 10-1. Values of $(h_c + h_r)$
B.t.u./(hr.)(sq. ft.) (°F. from pipe to room)
For horizontal bare standard steel pipe of various sizes in a room at 80°F.

Nominal pipe diam., in.	Temperature difference, °F.														
	30	50	100	150	200	250	300	350	400	450	500	550	600	650	700
1	2.16	2.26	2.50	2.73	3.00	3.29	3.60	3.95	4.34	4.73	5.16	5.60	6.05	6.51	6.98
3	1.97	2.05	2.25	2.47	2.73	3.00	3.31	3.69	4.03	4.43	4.85	5.26	5.71	6.19	6.66
5		1.95	2.15	2.36	2.61	2.90	3.20	3.54	3.90						
10	1.80	1.87	2.07	2.29	2.54	2.82	3.12	3.47	3.84						

Bailey and Lovell [*Engineering*, 147, 60 (1939)] give values for $h_c + h_r$ up to Δt_c of 1000°F.

the loss of heat from surfaces to the surroundings because of the diathermanous nature of atmospheric gases (air). It is convenient to represent radiant-heat transfer, for this case, as a radiation film coefficient which is added to the film coefficient for convection giving the combined coefficient for convection and radiation $(h_c + h_r)$. In Fig. 10-10 values of the film coefficient for radiation h_r are plotted against the two surface temperatures for emissivity = 1.0.

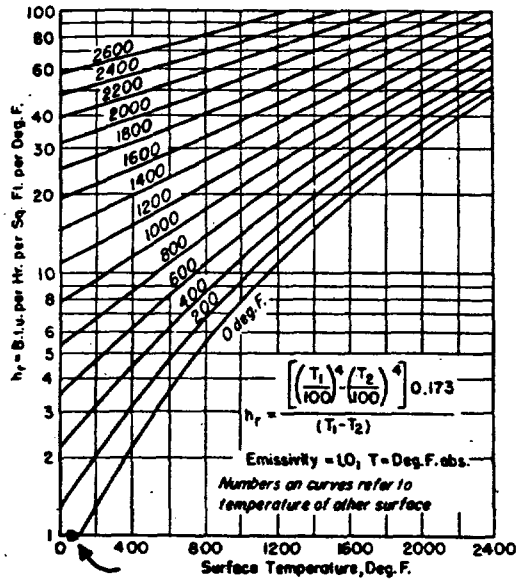

Fig. 10-10. Radiation coefficients of heat transfer h_r.

Table 10-1 based on data of Heilman and of McMillan shows values of $(h_c + h_r)$ from single horizontal oxidized pipe surfaces.

Forced Convection (No Change in Phase)

Viscous (Laminar) Flow (Reynolds Number < 2100). *For Heating or Cooling inside or outside Tubes Flow Parallel with Tubes.* In the laminar region fluid and heat flow are variable and somewhat unpredictable. Authorities agree that the most practical expression for prediction of heat transfer in this region is the correlation of Sieder and Tate [*Ind. Eng. Chem.*, **28**, 1429–1436 (1936)]. For reasonable values of tube diameter (less than 3 in.) and temperature difference (less than 100°F.) the Colburn-type equation is

$$\frac{h_{a.m.}}{cG}\left(\frac{c\mu}{k}\right)^{2/3}\left(\frac{L_u}{D}\right)^{1/3}\left(\frac{\mu_w}{\mu}\right)^{0.14} = \frac{1.86}{(DG/\mu)^{2/3}} = j \qquad (10\text{-}29)$$

The corresponding **Nusselt-type** equation is

$$\frac{h_{a.m.}D}{k}\left(\frac{\mu_w}{\mu}\right)^{0.14} = 1.86\left(\frac{DG}{\mu}\frac{c\mu}{k}\frac{D}{L_u}\right)^{1/3} \qquad (10\text{-}30)$$

In these equations, for flow outside tubes, substitute D_e for D. D_e = 4 × free cross-sectional area ÷ perimeter.

Either of these equations reduces to the **dimensional form** (flow inside tubes only)

$$h_{a.m.} = 24.2c^{1/3}k^{2/3}(\mu/\mu_w)^{0.14}\frac{w^{1/3}}{D_i^{1/3}L_u^{1/3}} \qquad (10\text{-}31)$$

Satisfactory results may be obtained from these equations if the significance of the variables is judiciously considered. The following suggestions are offered.

1. *The Length-to-diameter Ratio L_u/D.* The length term L_u is the length of path (in the direction of flow) in which the fluid is undisturbed. In both single and multipass exchangers it is thus the length of one pass. The ratio L_u/D may be substantially reduced (and the coefficient significantly increased) by installing turbulence promoters inside the tubes, but it is of questionable advisability to use values of L_u/D less than unity. The coefficient is not infinite at the entrance to the tube, a condition which might be deduced from Eq. (10-31) if the term L_u were not explicitly defined as undisturbed length.

2. *The Viscosity Ratio μ_w/μ.* When the bulk viscosity varies considerably over the range of heating or cooling, it is advisable to determine the coefficient for incremental lengths (each pass separately) because it would be difficult to select arbitrarily the correct average bulk viscosity.

3. *The Temperature Difference.* The subscripts (a.m.) on the symbol for heat-transfer coefficient indicate that with these equations the arithmetic-mean temperature difference is to be used. However, McAdams states ("Heat Transmission," 3d ed., p. 232, McGraw-Hill, New York, 1954) that there is only a small error, at values of wc/kL_u above 24, if logarithmic-mean temperature difference is used. Therefore, for most of the range of application, one may use the more convenient temperature difference.

4. *Limitations* (Flow inside Tubes Only). The theoretical basis for Eq. (10-29) dictates a limit of application. For values of wc/kL_u less than 10, the coefficient cannot exceed the value given by

$$h_{max} = \frac{2k}{\pi D}\frac{wc}{kL_u} \qquad (10\text{-}32)$$

equivalent to

$$h_{max} = \frac{DGc}{2L_u} = \frac{2}{\pi}\frac{wc}{DL_u} \qquad (10\text{-}32a)$$

The accuracy of Eq. (10-29) is reportedly low, possibly because of simultaneous natural convection effects. However, for design purposes, the equation should give conservative results. At high values of Δt, natural convection may be significant. The net heat-transfer coefficient may be approximated by adding the coefficients of natural convection (10-24) and laminar forced convection (10-29).

Transition Region (Reynolds Number 2100 to 10,000). *For Heating or Cooling inside or outside Tubes*

alfred d. wendler 4/1/1985

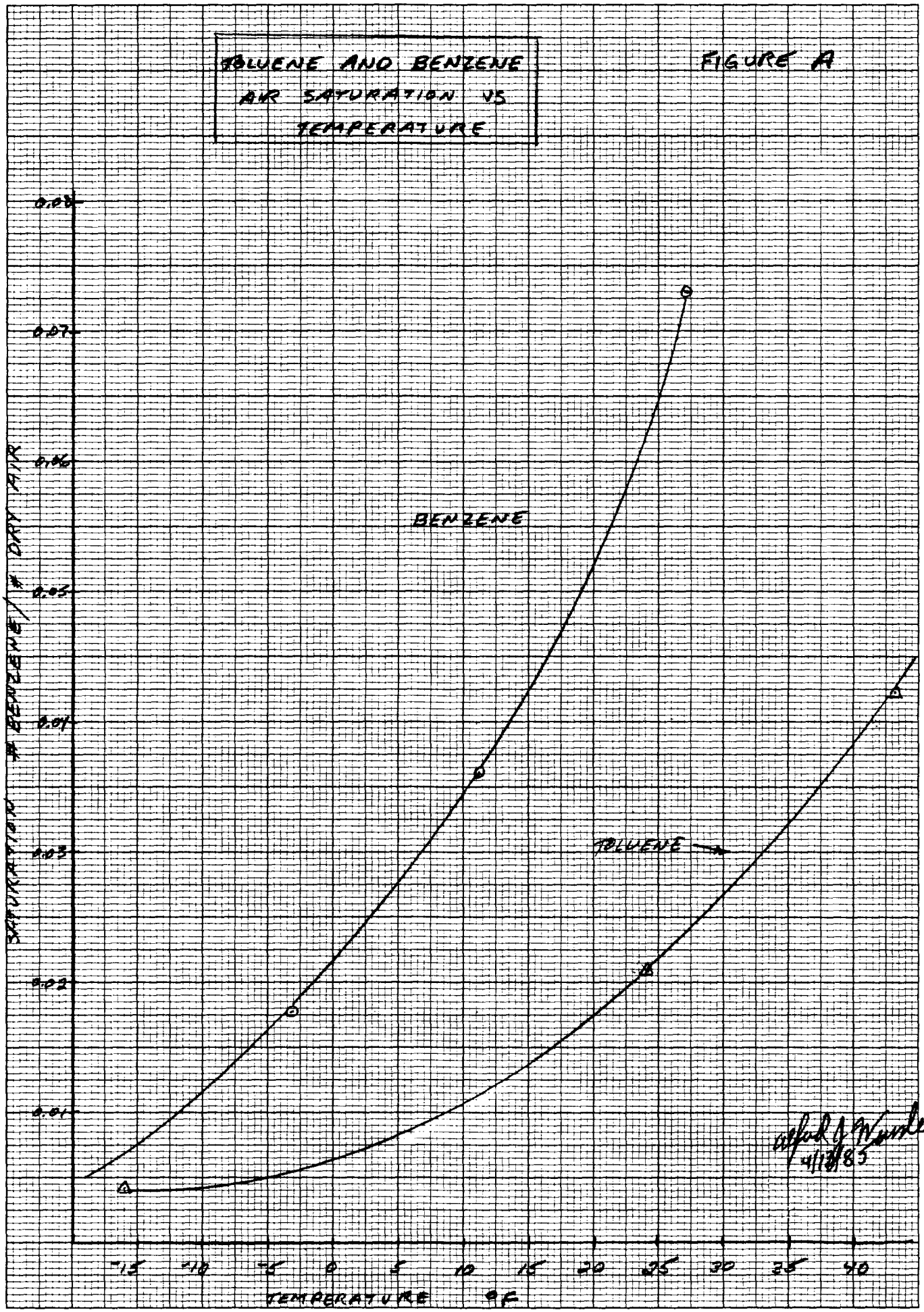

FREEZING POINT
VS
COMPOSITION
BENZENE/TOLUENE SYSTEM
ATMOSPHERIC PRESSURE

FIGURE B

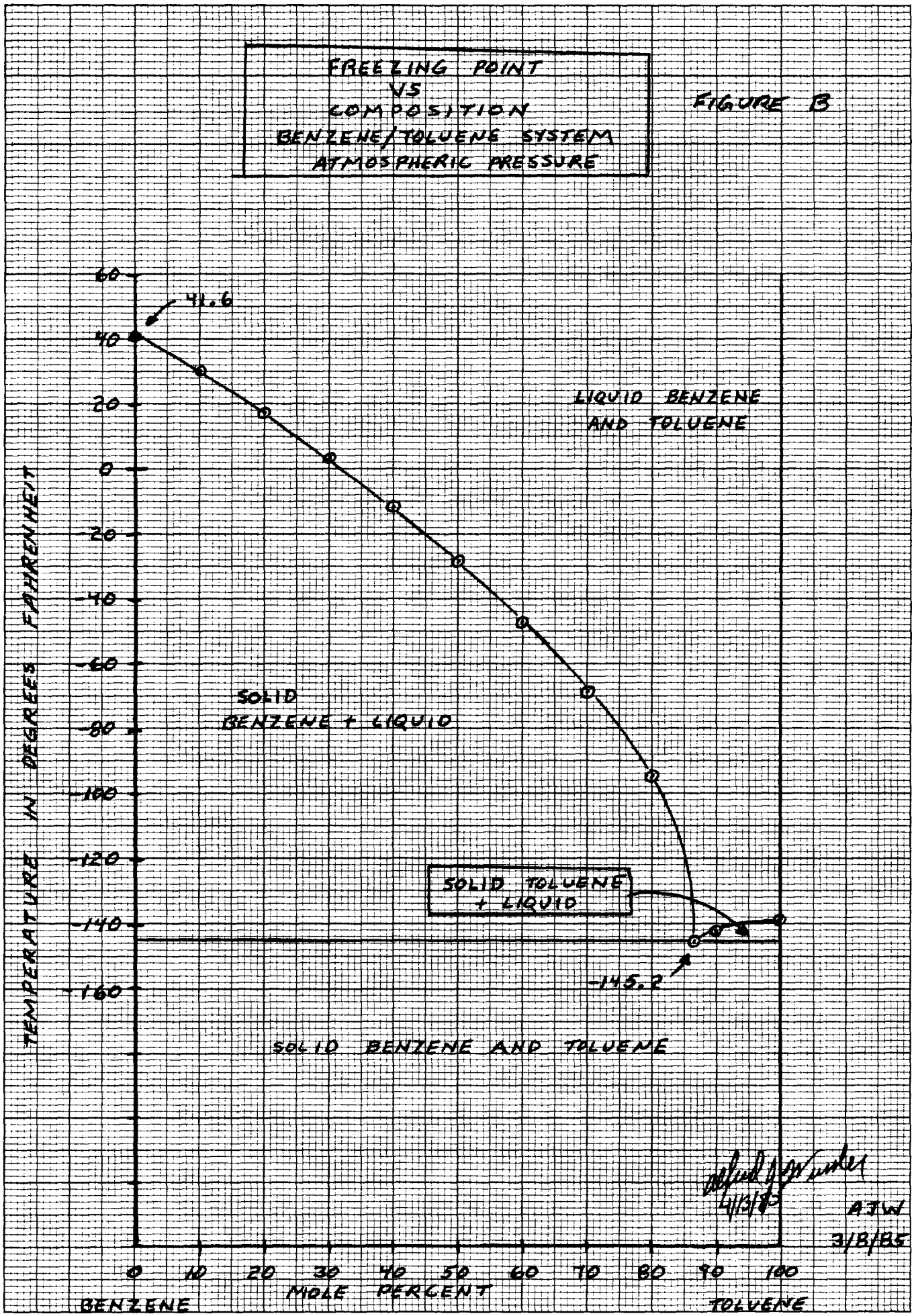

4/13/85

AJW
3/8/85

46 1320

K·E 10 X 10 TO ½ INCH 7 X 10 INCHES
KEUFFEL & ESSER CO. MADE IN U.S.A.

vs. W, as shown in Fig. 15-33*b*, or as $dW/d\theta$ vs. θ, as shown in Fig. 15-33*c*. These **rate curves** show that the drying process is not a smooth, continuous one in which a single mechanism controls throughout. Figure 15-33*c* has the advantage of showing how long each drying period lasts.

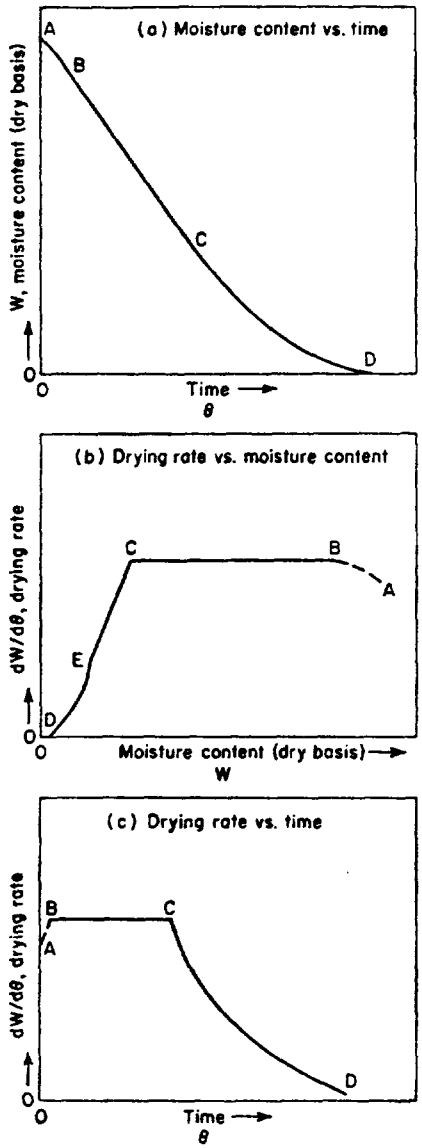

FIG. 15-33. The periods of drying.

Section BC on each curve represents the **constant-rate period**. In Fig. 15-33*a*, it is shown by a straight line of constant slope $dW/d\theta$, which becomes a horizontal line on the rate curves in Fig. 15-33*b* and *c*.

The curved portion CD of Fig. 15-33*a* is termed the **falling-rate period** and, as shown in Fig. 15-33*b* and *c*, is typified by a continuously changing rate throughout the remainder of the drying cycle. Point E (Fig. 15-33*b*) represents the point at which all the exposed surface becomes completely unsaturated and marks the start of that portion of the drying cycle during which the rate of internal moisture movement controls the drying rate. Point C, where the constant rate ends and the drying rate begins to fall, is termed the **critical moisture content**. The portion designated by AB represents a warming-up period, which may or may not be significant in the total process.

CONSTANT-RATE PERIOD

In the **constant-rate period**, drying proceeds by diffusion of vapor from the saturated surface of the material across a stagnant-air film into the environment. Moisture movement within the solid is rapid enough to maintain a saturated condition at the surface, and the rate of drying is controlled by the rate of heat transfer to the evaporating surface. The rate of mass transfer balances the rate of heat transfer, and the temperature of the saturated surface remains constant. The mechanism of moisture removal is equivalent to evaporation from a body of water* and is essentially independent of the nature of the solids.

Although temperature of the saturated surface remains constant, its level depends on the mode of heat transfer. If heat is transferred solely by **convection**, and in the absence of other heat effects, the surface temperature approaches the wet-bulb temperature. However, when heat is transferred by radiation, conduction, or a combination of these and convection, the temperature of the saturated surface is between the wet-bulb temperature and the boiling point of water. Under these conditions, the rate of heat transfer is increased and a higher drying rate results.

When heat is transferred to a wet solid by **conduction** through hot surfaces, and heat transfer by convection is negligible, the solids approach the boiling-point temperature rather than the wet-bulb temperature. In such cases, the drying rate will be appreciably higher than by convection drying with air at the same temperature as the heating surfaces. This method of heat transfer is utilized in indirect dryers (see Classification of Dryers, p. 15-45) in which the material is made to contact hot surfaces, frequently with vigorous agitation.

Radiation is also effective in increasing the constant rate by augmenting the convection heat transfer and raising the surface temperature above the wet-bulb temperature. In most drying operations, the effect of radiation is minor, although in some cases it is the primary mechanism, as in infrared drying.

When the heat for evaporation in the constant-rate period is supplied by a hot gas, a dynamic equilibrium is established between the rate of heat transfer to the material and the rate of vapor removal from the surface (see p. 15-2). This equilibrium between heat- and mass-transfer rates can be expressed as

$$\frac{dw}{d\theta} = \frac{h_t A\,\Delta t}{\lambda} = k_g A\,\Delta p \qquad (15\text{-}20)$$

where $dw/d\theta$ = drying rate, lb. water/hr.; h_t = total heat-transfer coefficient, B.t.u./(hr.)(sq. ft.)(°F.); A = area for heat transfer and evaporation, sq. ft.; λ = latent heat of evaporation at t_s', B.t.u./lb.; k_g = mass-transfer coefficient, lb./(hr.)(sq. ft.)(atm.); $\Delta t = t - t_s'$, where t = gas (dry-bulb) temperature, °F., and t_s' = temperature of surface of evaporation, °F.; $\Delta p = p_s - p$, where p_s = vapor pressure of water at surface temperature t_s', atm.; p = partial pressure of water vapor in the gas, atm.

When h_t is the coefficient of heat transfer by convec-

* The term water is used for convenience; the discussion applies equally well to other liquids.

tion only, then t_s' under equilibrium conditions is the wet-bulb temperature of the air, and p_s is the vapor pressure at this temperature. If heat is also supplied by radiation, then h_t is the sum $h_c + h_r$, where h_r is the radiation coefficient and h_c is the convection coefficient, and t_s' becomes higher than the wet-bulb temperature. A similar result, which is covered below, occurs when heat reaches the surface of evaporation by convection and conduction.

It is evident from Eq. (15-20) that the magnitude of the constant rate depends upon three factors: (1) the heat- or mass-transfer coefficient, (2) the area exposed to the drying medium, and (3) the difference in temperature or humidity between the gas stream and the wet surface of the solid. All these factors are the external variables, as noted above. The internal mechanism of liquid flow does not affect the constant rate.

Prediction of Heat- and Mass-transfer Coefficients

In convection phenomena, the heat-transfer coefficients depend on the geometry of the system, the gas velocity past the evaporating surface, and the physical properties of the drying gas. In estimating drying rates, the use of heat-transfer coefficients is preferred because they are usually more reliable than mass-transfer coefficients. In calculating mass-transfer coefficients from drying experiments, the partial pressure at the surface is usually inferred from the measured or calculated temperature of the evaporating surface. Small errors in temperature have negligible effect on the heat-transfer coefficient but introduce relatively large errors in the partial pressure and hence in the mass-transfer coefficient [for example, see Shepherd, Brewer, and Hadlock, *Ind. Eng. Chem.*, **20**, 388 (1938)].

For many cases in drying, the heat-transfer coefficient can be expressed as

$$h_c = \frac{\alpha G^n}{D_c^m} \tag{15-21}$$

where h_c = heat-transfer coefficient, B.t.u./(hr.)(sq. ft.)(°F.); G = mass velocity of drying gas, lb./(hr.)(sq. ft.); D_c = characteristic dimension of the system, ft.; α, n, and m are empirical constants. When radiation and conduction effects are negligible the constant rate of drying from a surface is thus given by the following heat-transfer expression derived from Eqs. (15-20) and (15-21):

$$\frac{dw}{d\theta} = \frac{\alpha G^n A}{\lambda D_c^m}(t - t_s') \tag{15-22}$$

When the liquid is water and the drying gas air, t_s' is the wet-bulb temperature.

In order to estimate drying rate from Eq. (15-22), values of the empirical constants are required for the particular geometry under consideration. For flow parallel to plane plates, exponent n has been reported to range from 0.35 to 0.8 [Chu, Lane, and Conklin, *Ind. Eng. Chem.*, **45**, 1586 (1953). Wenzel and White, *Ind. Eng. Chem.*, **43**, 1829 (1951). Chu *et al.*, *Ind. Eng. Chem.*, **51**, 275 (1958)]. The differences in exponent have been attributed to differences in flow pattern in the space above the evaporating surface. In the absence of applicable specific data, the heat-transfer coefficient for the parallel-flow case can be taken, for estimating purposes, as

$$h_c = \frac{0.01G^{0.8}}{D_c^{0.2}} \tag{15-23}$$

where the experimental data have been weighted in favor of an exponent of 0.8 in conformity with the usual Colburn j factor, and average values of the properties of air at 200°F. have been incorporated.

Experimental data for drying from flat surfaces have been correlated using the equivalent diameter of the flow channel or the length of the evaporating surface as the characteristic length dimension in the Reynolds number. However, the validity of one vs. the other has not been established. The proper equivalent diameter probably depends at least on the geometry of the system, the roughness of the surface, and the flow conditions upstream of the evaporating surface. For most tray-drying calculations, the equivalent diameter (four times the cross-sectional area divided by the perimeter of the flow channel) should be used.

For air flow impinging normal to the surface from slots, nozzles, or perforated plates, the heat-transfer coefficient can be obtained from the data of Friedman and Mueller ("Proceedings of the General Discussion on Heat Transfer," pp. 138–142, Institution of Mechanical Engineers, London, and American Society of Mechanical Engineers, New York, 1951). These investigators give

$$h_c = \alpha G^{0.78} \tag{15-24}$$

where gas mass velocity G is based on the heat-transfer area and α is given by Fig. 15-34. In Fig. 15-34, the plate spacing is defined as the distance between the slots, nozzles, or perforated plate and the evaporating surface, and the per cent free area is the percentage of the air-jet area to the evaporating surface area. Molstad, Farevaag, and Farrell [*Ind. Eng. Chem.*, **30**, 1131 (1938)] found that, when air from a duct is blown perpendicular to the drying surface, the heat-transfer coefficient is given by

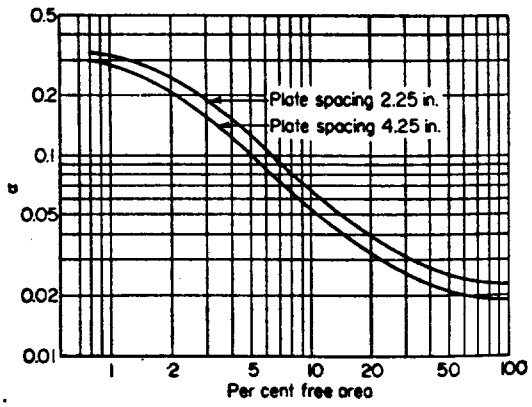

FIG. 15-34. Values of α for use with impinging-flow equation (15-24). (*Friedman and Mueller, "Proceedings of the General Discussion on Heat Transfer," Institution of Mechanical Engineers, London, and American Society of Mechanical Engineers, New York*, 1951.)

$$h_c = 0.37G^{0.37} \tag{15-25}$$

Equations (15-24) and (15-25) are strictly applicable only to the geometries studied, and care must be exercised if the geometry of interest differs greatly from those upon which the equations are based.

For through-circulation drying where the drying gases flow either upward or downward through a permeable bed of wet granular solids, the results obtained by Gamson, Thodos, and Hougen [*Trans. Am. Inst. Chem. Engrs.*, **39**, 1 (1943)] and Wilke and Hougen [*ibid.*, **41**, 441 (1945)] for the rates of adiabatic evaporation of water from

packed beds of porous solids are applicable. These are

$$\frac{h_c}{c_p G}\left(\frac{c_p \mu}{k}\right)^{2/3} = 1.064\left(\frac{D_p G}{\mu}\right)^{-0.41} \quad \text{for } \frac{D_p G}{\mu} > 350 \tag{15-26}$$

$$\frac{h_c}{c_p G}\left(\frac{c_p \mu}{k}\right)^{2/3} = 1.95\left(\frac{D_p G}{\mu}\right)^{-0.51} \quad \text{for } \frac{D_p G}{\mu} < 350 \tag{15-27}$$

where c_p = heat capacity of air, B.t.u./(lb.)(°F.); μ = gas viscosity, lb./(ft.)(hr.); k = gas thermal conductivity, B.t.u./(hr.)(sq. ft.)(°F./ft.); D_p = diameter of sphere having the same surface area as particle, ft.; other symbols have the same meanings as in Eq. (15-21). Substituting average additive properties of the drying gas leads to

$$h_c = 0.11\frac{G^{0.59}}{D_p^{0.41}} \quad \text{for } \frac{D_p G}{\mu} > 350 \tag{15-26a}$$

and

$$h_c = 0.15\frac{G^{0.49}}{D_p^{0.51}} \quad \text{for } \frac{D_p G}{\mu} < 350 \tag{15-27a}$$

Determination of Temperature of Evaporating Surface

When radiation and conduction are negligible the temperature of the evaporating surface approaches the wet-bulb temperature and is readily obtained from the humidity and dry-bulb temperature. Frequently, however, radiation and conduction cause the temperature of the evaporating surface to exceed the wet-bulb temperature. When this occurs the true surface temperature must be estimated in order to estimate the constant drying rate.

Under steady-state conditions the temperature of the evaporating surface increases until the rate of sensible heat transfer to the surface equals the rate of heat removed by evaporation from the surface. To calculate this temperature, it is convenient to modify Eq. (15-20) in terms of humidity rather than partial-pressure difference, as follows:

$$k_y(p_s - p) = k'(H_s - H) \tag{15-28}$$

where k' = mass-transfer coefficient, lb./(hr.)(sq. ft.)(unit humidity difference), and $k' = Pk_y(M_a/M_w)$ is a suitable approximation at low humidities; k_y = mass-transfer coefficient, lb./(hr.)(sq. ft.)(atm.); M_a = molecular weight of air; M_w = molecular weight of the diffusing vapor; p_s = vapor pressure of the liquid at the temperature of the evaporating surface, atm.; p = partial pressure of vapor in air, atm.; H_s = saturation humidity of the air at the temperature of the drying surface, lb./lb. dry air; H = humidity of the drying air, lb./lb. dry air; P = total pressure, atm. For air-water mixtures k' is approximately $1.6k_y$ at atmospheric pressure.

A rate balance between evaporation and heat transfer when radiation occurs may be written as follows:

$$\lambda k' A(H_s - H) = h_c A(t - t_s') + h_r A(t_r - t_s') \tag{15-29}$$

where λ = latent heat of evaporation, B.t.u./lb. at t_s'; A = area for both heat and mass transfer, sq. ft.; h_c = convection heat-transfer coefficient, B.t.u./(hr.)(sq. ft.)(°F.); h_r = radiation heat-transfer coefficient, B.t.u./(hr.)(sq. ft.)(°F.), as defined in Fig. 10-10; t = temperature of drying gases, °F.; t_s' = temperature of the wet surface, °F.; t_r = temperature of source radiating heat to the wet surface, °F.; ϵ = emissivity of surface receiving radiation.

Equation (15-29) may be modified by means of the psychrometric ratio for air–water vapor mixtures, $h_c/k' = c_s$, where c_s = heat capacity of humid air, B.t.u./(lb. dry air)(°F.), as defined on p. 15-2. Thus, Eq. (15-29) becomes

$$\frac{\lambda}{c_s}(H_s - H) = (t - t_s') + \frac{h_r \epsilon}{h_c}(t_r - t_s') \tag{15-29a}$$

Equation (15-29a) may be solved by trial and error or graphically as indicated in Example 23 to estimate the true values of H_s and t_s' and, hence, the actual drying rate. The values of λ and h_r depend on the value of t_s' but can generally be considered constant over the range of temperatures usually encountered in air drying.

Example 23. A wet material is drying in a tray, exposed to air at 300°F. and a humidity of 0.02 lb. water/lb. dry air. Air velocity is 450 ft./min., and the equivalent diameter of the flow channel is 1 ft. Determine the true surface temperature (1) when the effect of radiation is neglected and (2) when radiation is included.

Solution. If radiation is neglected, the wet-surface temperature is obtained from Fig. 15-4 as 114°F. with a corresponding value of $H_s = 0.0673$ lb. water/lb. air. If a metal tray directly above the wet material attains the air temperature of 300°F., t_r will be above 114°F. For this example, let $\epsilon = 0.9$ and from Eq. (15-23) $h_c = 3.3$. From Fig. 10-10, h_r is estimated to be 1.5. The heat of vaporization λ will be about 1020 and $c_s = 0.25$. Substituting in Eq. (15-29a),

$$\frac{1020}{0.25}(H_s - 0.02) = \left[1 + \frac{(0.9)(1.5)}{3.3}\right](300 - t_s')$$

$$H_s - 0.02 = 0.000345(300 - t_s')$$

The values of t_s and H_s may be obtained by solving the above by trial and error to give $H_s = 0.082$ and $t_s' = 120.4$°F. Alternatively, they may be obtained by drawing a line on a humidity chart through the point $H = 0.02$, $t = 300$ with slope = 0.000345 and reading at the intersection with the saturated-humidity curve (*cf.* Fig. 15-35) the values $H_s = 0.08$ and $t_s' = 120$°F., which check the trial-and-error solution. The effect of radiation is to increase the driving force for mass transfer by (0.082 − 0.02)/(0.0673 − 0.02), or 1.31, an increase of 31 per cent.

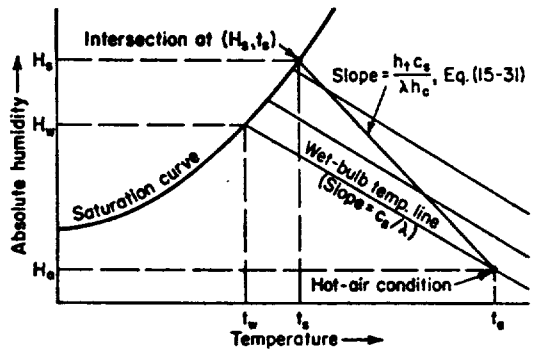

FIG. 15-35. Graphical estimation of surface temperature during constant-rate period.

Frequently, particularly in tray drying, heat arrives at the evaporating surface from the tray walls by conduction through the wet material. For this case where both radiation and conduction are significant, the total heat-transfer coefficient is given by Shepherd, Brewer, and Hadlock [*Ind. Eng. Chem.*, **30**, 388 (1938)] as

$$h_t = (h_c + h_r)\left[1 + \frac{A_u}{1 + d(h_c + h_r)/k}\right] \tag{15-30}$$

where h_t = total heat-transfer coefficient, B.t.u./(hr.)(sq. ft.)(°F.); A_u = ratio of outside unwetted surface to evaporating-surface area; d = depth of material in tray, ft.; k = thermal conductivity of the wet material,

B.t.u./(hr.)(sq. ft.)(°F./ft.). Note that h_r must be corrected for emissivity of the surface. For insulated trays, the arithmetic average of inside and outside unwetted area should be used.

Equation (15-30) assumes that all heat sources are at the same temperature and the convection coefficients to the evaporating surface and to the unwetted portions of the tray are equal. When radiation occurs from a source at a different temperature, the radiation coefficient can be corrected to the same basis by multiplying by the ratio $(t - t_s')/(t_r - t_s')$, where t, t_s', t_r are the drying gas, evaporating surface, and radiator temperatures, respectively.

A relationship for estimating the surface temperature t_s', based on the use of Eq. (15-30) to determine h_t, is as follows:

$$(H_s - H) = \frac{h_t c_s}{\lambda h_c}(t - t_s') \qquad (15\text{-}31)$$

Equation (15-31) can be solved numerically or graphically. Figure 15-35 indicates how H_s and t_s' may be determined graphically on a humidity chart by the point of intersection on the saturation-humidity curve of a straight line of slope $h_t c_s/\lambda h_c$ passing through point (H, t).

Estimation of Constant Rate

For drying calculations it is convenient to express Eq. (15-20) in terms of the decrease in moisture content rather than quantity of water evaporated. For evaporation from a tray of wet material, assuming no change in volume during drying, Eq. (15-20) becomes

$$\frac{dW}{d\theta} = \frac{h_t}{\rho_s d\lambda}(t - t_s') \qquad (15\text{-}32)$$

where $dW/d\theta$ = drying rate, lb. water/(hr.)(lb. dry solids); h_t = total heat-transfer coefficient, B.t.u./(hr.)(sq. ft.)(°F.); ρ_s = bulk density dry material, lb./cu. ft.; d = thickness of bed, ft.; λ = latent heat of vaporization, B.t.u./lb.; t = air temperature, °F.; t_s' = evaporating-surface temperature, °F. Note that $dW/d\theta$ is inherently negative.

A similar equation can be written for the through-circulation case:

$$\frac{dW}{d\theta} = \frac{h_t a}{\rho_s \lambda}(t - t_s') \qquad (15\text{-}33)$$

where a = sq. ft. of heat-transfer area/cu. ft. of bed, 1/ft.; other symbols are the same as for Eq. (15-32).

Values of ρ_s and/or a must be known in order to use Eqs. (15-32) and (15-33). The value of a is difficult to estimate without experimental data. When the void fraction is known, a can sometimes be estimated from the following relationships:

For spherical particles,

$$a = \frac{6(1 - F)}{(D_p)_m} \qquad (15\text{-}34)$$

For uniform cylindrical particles,

$$a = \frac{4(0.5D_c + Z)(1 - F)}{D_c Z} \qquad (15\text{-}35)$$

where F = void fraction; $(D_p)_m$ = harmonic mean diameter of spherical particles, ft.; D_c = diameter of cylinder, ft.; z = height of cylinder, ft. For cylindrical particles that are long relative to their diameter the term $0.5D_c$ in Eq. (15-35) can be neglected.

Application of the previous equations is illustrated below.

Example 24. An inorganic pigment having a bulk density of 40 lb./cu. ft. is being dried in a tray dryer which consists of two tiers of 44 stainless-steel trays, 1.25 in. deep and spaced 1.5 in. apart. The trays are 26 in. square and the equivalent diameter of the flow channel is 0.237 ft. Inlet air velocity is 300 ft./min. corresponding to a mass velocity of 1000 lb./(hr.)(sq. ft.). Inlet air temperature is 250°F. and its humidity is 0.072 lb./lb. corresponding to a wet-bulb temperature of 128°F. Calculate the initial and average drying rates in the constant-rate period.

Solution. The convection coefficient is calculated from Eq. (15-23) as

$$h_c = \frac{(0.01)(1000)^{0.8}}{(0.237)^{0.2}} = 3.3$$

This value must be corrected for radiation and conduction according to Eq. (15-30). For the trays of the dimensions specified, $A_c = 1.2$ and $d = 0.104$ ft.; h_r will be taken as 1.5 (once t_s' is calculated this value can be checked and the calculation repeated if necessary). The value of k is usually difficult to determine. For this example, let $k = 0.8$. Then

$$h_t = (3.3 + 1.5)\left[1 + \frac{1.2}{1 + (0.104)(3.3 + 1.5)/0.8}\right] = 8.4$$

Temperature of the evaporating surface is now calculated from Eq. (15-31):

$$(H_s - 0.072) = \frac{(8.4)(0.27)}{(1015)(3.3)}(250 - t_s')$$

By trial and error $t_s' = 138$°F. and $H_s = 0.147$ lb./lb. The initial drying rate is obtained from Eq. (15-32) as

$$\frac{dW}{d\theta} = \frac{8.4(250 - 138)}{(40)(0.104)(1015)} = 0.223 \frac{\text{lb.}}{(\text{hr.})(\text{lb. dry solids})}$$

In flowing across the trays the air temperature drops. If heat losses are negligible the air temperature leaving the tray is obtained by integrating the differential heat balance over the tray length to give

$$t_2 = t_s' + (t_1 - t_s') \exp. \frac{-h_t L_t}{G b c_s} \qquad (15\text{-}36)$$

where t_1, t_2, t_s' are inlet air, leaving air, and evaporating-surface temperatures, respectively, °F.; L_t = length of tray, ft.; b = tray spacing, ft. Then

$$t_2 = 138 + (250 - 138) \exp. \frac{-(8.4)(2.17)}{(1000)(0.125)(0.27)} = 203\text{°F.}$$

The logarithmic mean temperature difference is 86.8°F. and the average drying rate as calculated from Eq. (15-32) is 0.173 lb. water/(hr.)(lb. dry solids).

FALLING-RATE PERIOD

The drying process consists of a period in which the rate of evaporation is constant and one or more periods during which the rate is continuously decreasing (see p. 15-34). The latter periods are designated the **falling-rate periods** and begin when the constant-rate period ends, at the critical moisture content. If the final moisture content is above the critical moisture content (for the specified drying conditions), the whole drying process will occur under constant-rate conditions. If, on the other hand, the initial moisture content is below the critical moisture content, the entire drying process will occur in the falling-rate period. This period is usually divided into two zones: (1) the zone of **unsaturated surface drying** and (2) the zone where **internal moisture movement controls.**

In the first zone, the entire evaporating surface can no longer be maintained saturated by moisture movement within the solid. The drying rate decreases for the unsaturated portion, and hence the rate for the total surface decreases. In some cases the drying rate is a linear function of the water content of the solid as shown by line CE in Fig. 15-33*b*. Generally, however, the drying rate depends on factors affecting the diffusion of moisture away from the evaporating surface and those affecting the rate of internal moisture movement.

As drying proceeds, the point is reached where the evaporating surface is unsaturated. The plane of evaporation moves into the solid, and the drying process enters the second falling-rate period. The drying rate is now governed by the rate of internal moisture move-

Soil Analyses from Produced Water Pits and Immediate Surroundings in the San Juan, La Plata and Animas River Valleys

El Paso Natural Gas Company
March 7, 1985
El Paso, Texas

SOIL ANALYSES FROM PRODUCED WATER
PITS AND IMMEDIATE SURROUNDINGS IN THE
SAN JUAN, LA PLATA AND ANIMAS RIVER VALLEYS

Sample No.	Source	Sand Equivalent Value[1] (Average Empirical Value*)	% Passing No. 200 Seive[2]	% Moisture[3]	% Organic Matter[4]
0002	Mary Wheeler #1-E: 18" depth (30' Westerly Direction from Pit)	20	31.0	9.9	2.31
0004	McCoy No. C-1 (80' Southerly Direction from Pit): Top Soil	2	65.6	23.6	2.72
0005	McCoy No. C-1 (80' Southerly Direction from Pit): 18" Depth	31	33.0	7.8	1.08
0008	C&E Operators Pit: Sludge	2	45.0	24.9	-
0010	Utton No. 1 (30' Easterly Direction from Pit): 12"-14" Depth	9	54.3	13.0	2.36
0012	Sutton No. 1 (40' West Direction from Meter Run): 12"-14" Depth	18	27.1	13.2	2.01
0015	McWright No. 1 (80' Southerly Direction from Pit): 16"-18" Depth	17	32.3	10.2	1.67
0017	NYE No. 1 (60' Easterly Direction from Dehydration Pit): 16" Depth	23	31.8	8.7	1.51
0019	Larcher No. 3 (30' Southeast of Dehydration Pit): 14" Depth	18	38.1	12.6	1.83
0022	Animas River Bank (15' from actuar river)	69	7.8	4.7	1.46
0027	Alberding No. 1 (La Plata Riber Bank)	11	62.4	35.7	2.99
0028	Alberding No. 1 (80' Westerly from Pit): 16"-18" Depth	34	37.0	12.8	2.06
0031	Armenta Gas Com. A #1 (3' from Dip Pit to South): 12" Depth	0	95.2	20.6	3.58
0033	Lobato Gas Com. A1A & E1A (Soil 15' South of Dehy. Pit)	0	48.2	17.4	1.58
0034	Lobato Gas Com. A1A & E1A	0	85.9	29.9	2.31
0036	Jaquez Com. A #1: 8"-10" Depth	0	69.6	15.5	3.55

Analytical Method

1. ASTM D 2419
2. ASTM D 2487
3. ASTM D 2216
4. Furance @ 550°C

Note: Sand Equivalent Value - the higher the value, the more sand; the lower the value, the more clay it has.

*Avg. Empirical Value = $\frac{\text{Height of Sand}}{\text{Height of Clay}}$ x 100%

SUMMARY OF SAMPLING ACTIVITIES
SAN JUAN DIVISION
EL PASO NATURAL GAS COMPANY
FEBRUARY 26-28, 1985

Soil Analyses from Produced Water Pits and Immediate Surroundings in the San Juan, La Plata and Animas River Valleys

El Paso Natural Gas Company
March 7, 1985
El Paso, Texas

SOIL ANALYSES FROM PRODUCED WATER
PITS AND IMMEDIATE SURROUNDINGS IN THE
SAN JUAN, LA PLATA A NIMAS RIVER VALLEYS

Sample No.	Source	Sand Equivalent Value[1] (Average Empirical Value*)	% Passing No. 200 Seive[2]	% Moisture[3]	% Organic Matter[4]
0002	Mary Wheeler #1-E: 18" depth (30' Westerly Direction from Pit)	20	31.0	9.9	2.31
0004	McCoy No. C-1 (80' Southerly Direction from Pit): Top Soil	2	65.6	23.6	2.72
0005	McCoy No. C-1 (80' Southerly Direction from Pit): 18" Depth	31	33.0	7.8	1.08
0008	C&E Operators Pit: Sludge	2	45.0	24.9	-
0010	Utton No. 1 (30' Easterly Direction from Pit): 12"-14" Depth	9	54.3	13.0	2.36
0012	Sutton No. 1 (40' West Direction from Meter Run): 12"-14" Depth	18	27.1	13.2	2.01
0015	McWright No. 1 (80' Southerly Direction from Pit): 16"-18" Depth	17	32.3	10.2	1.67
0017	NYE No. 1 (60' Easterly Direction from Dehydration Pit): 16" Depth	23	31.8	8.7	1.51
0019	Larcher No. 3 (30' Southeast of Dehydration Pit): 14" Depth	18	38.1	12.6	1.83
0022	Animas River Bank (15' from actuar river)	69	7.8	4.7	1.46
0027	Alberding No. 1 (La Plata Riber Bank)	11	62.4	35.7	2.99
0028	Alberding No. 1 (80' Westerly from Pit): 16"-18" Depth	34	37.0	12.8	2.06
0031	Armenta Gas Com. A #1 (3' from Dip Pit to South): 12" Depth	0	95.2	20.6	3.58
0033	Lobato Gas Com. A1A & E1A (Soil 15' South of Dehy. Pit)	0	48.2	17.4	1.58
0034	Lobato Gas Com. A1A & E1A	0	85.9	29.9	2.31
0036	Jaquez Com. A #1: 8"-10" Depth	0	69.6	15.5	3.55

Analytical Method

1. ASTM D 2419
2. ASTM D 2487
3. ASTM D 2216
4. Furance @ 550°C

Note: Sand Equivalent Value - the higher the value, the more sand; the lower the value, the more clay it has.

*Avg. Empirical Value = $\frac{\text{Height of Sand}}{\text{Height of Clay}}$ x 100%

SUMMARY OF SAMPLING ACTIVITIES
SAN JUAN DIVISION
EL PASO NATURAL GAS COMPANY
February 26-28, 1985

The sampling procedure for soil samples is as follows: the top two to three inches of soil were scraped off. Using a shovel, a 14-inch-diameter circle was softened for the top sample to be taken. Where the water table was very shallow, the sample was taken between the top of the ground and the apparent surface of the water table. In areas high above the rivers, after the sample was taken, the hole was deepened approximately two to three feet to check for change of soil conditions. One-gallon freezer plastic zip-lock bags were used for sample containers. Early morning temperatures ranged between 30°-40°F. In some areas the ground was frozen. Afternoon temperatures ranged between 45°-50°F and it was breezy.

SAN JUAN VALLEY

Armenta Gas Com. A No. 1 - San Juan County, NM, Sec. D of Sec. 27, T-29-N, R-10-W.

Photo No. 1. Shown is the general area facing south towards the San Juan River which is approximately 150 yards from the drip pit.

Photo No. 2. The area within the drip pit is shown. The water table is almost at the ground surface. The water in the pit is seepage from groundwater.

Photo No. 3. The area where the soil sample was taken is shown which is 15 feet south of the dehydration/separator pit.

Photo No. 4. The area where the soil sample was taken at the edge of San Juan River downslope from the dehydration/separator pit is shown.

SAN JUAN VALLEY

Jaquez Com. A No. 1 - San Juan County, NM, Sec. M of Sec. 25, T-30-N, R-9-W.

Photo No. 1. - The general area facing southeast is shown. The San Juan River is located approximately 400 yards to the south of the meter drip pit.

Photo No. 2. - Shown is the area within the meter drip pit.

SAN JUAN VALLEY

Lobato Gas Com. A1A & E1A - San Juan County, NM, Sec. D of Sec. 3, T-39-N, R-9-W.

Photo No. 1. Shown is the general area facing south towards the San Juan River which is 100 feet from the dehydration/separator pit.

Photo No. 2. The area within the dehydration/separator pit, facing south, is shown.

Photo No. 3. Shown is the area where the soil sample was taken which is 3 feet south of the drip pit at a depth of 12 inches of a 14 inch-diameter-hole. Note the water table is very shallow. The picture was taken facing north.

LA PLATA VALLEY

Alberding No. 1 - San Juan County, NM, Sec. A, Sec. 3, T-31-N, R-13-W.

Photo No. 1 - The general area facing west towards La Plata River which is located 120 feet from the separator pit is shown.

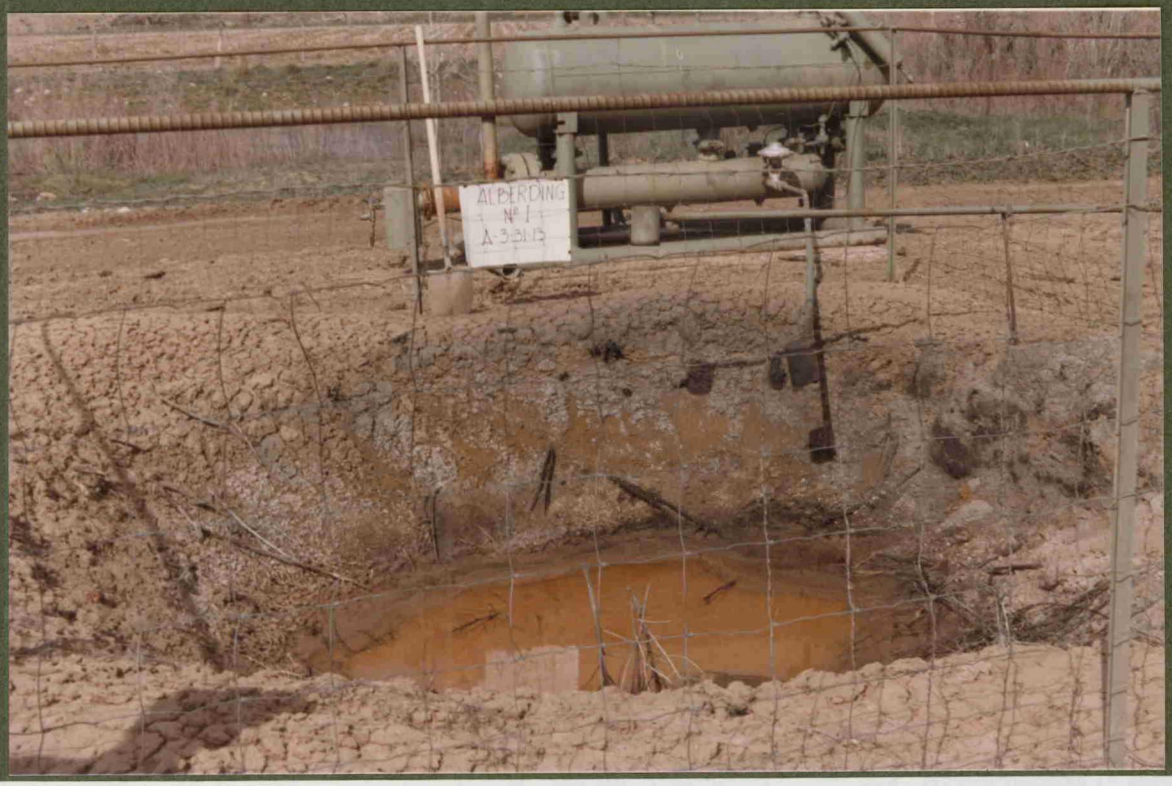

Photo No. 2. - The area shown is within the separator pit, facing west.

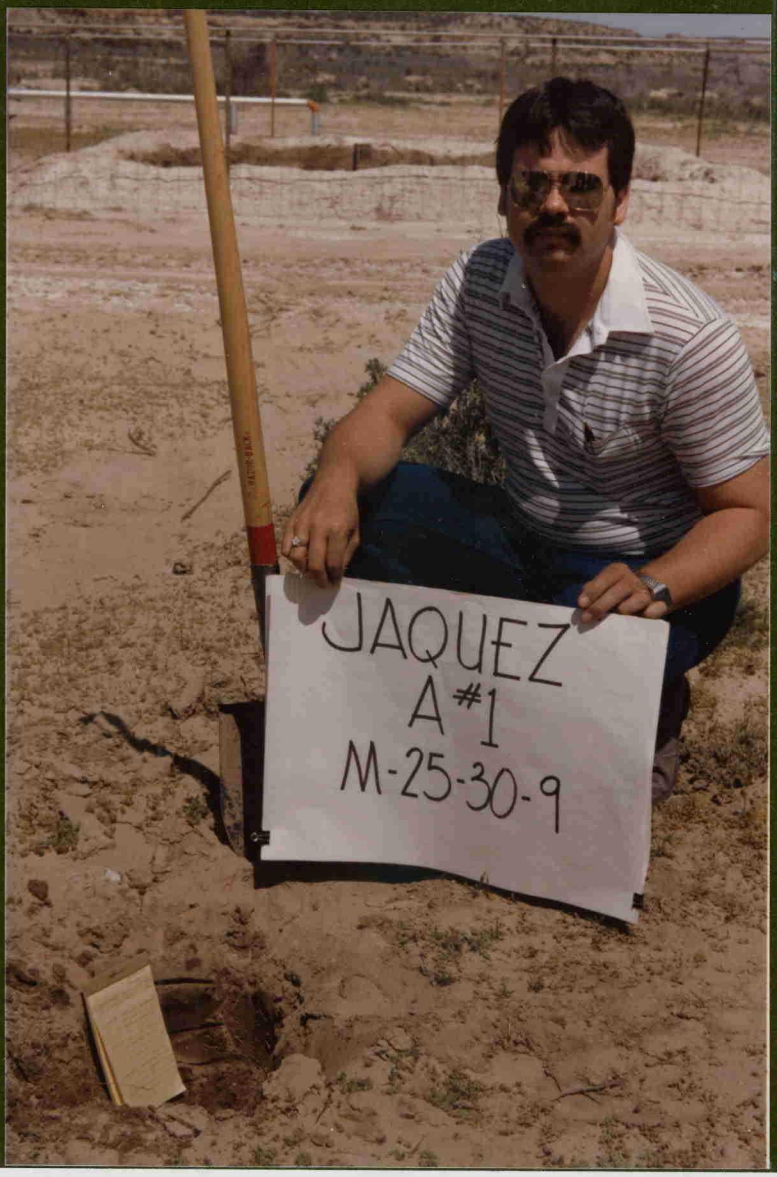

Photo No. 3. - Shown is the area where the soil sample was taken, which is 35 feet from the meter drip pit, facing northwest.

ANIMAS VALLEY

NYE No. 1 - San Juan County, NM, Sec. A of Sec. 23, T-31-N, R-11-W.

Photo No. 1. Shown is the general area, facing west. The Animas River is located to the east approximately one-half mile away.

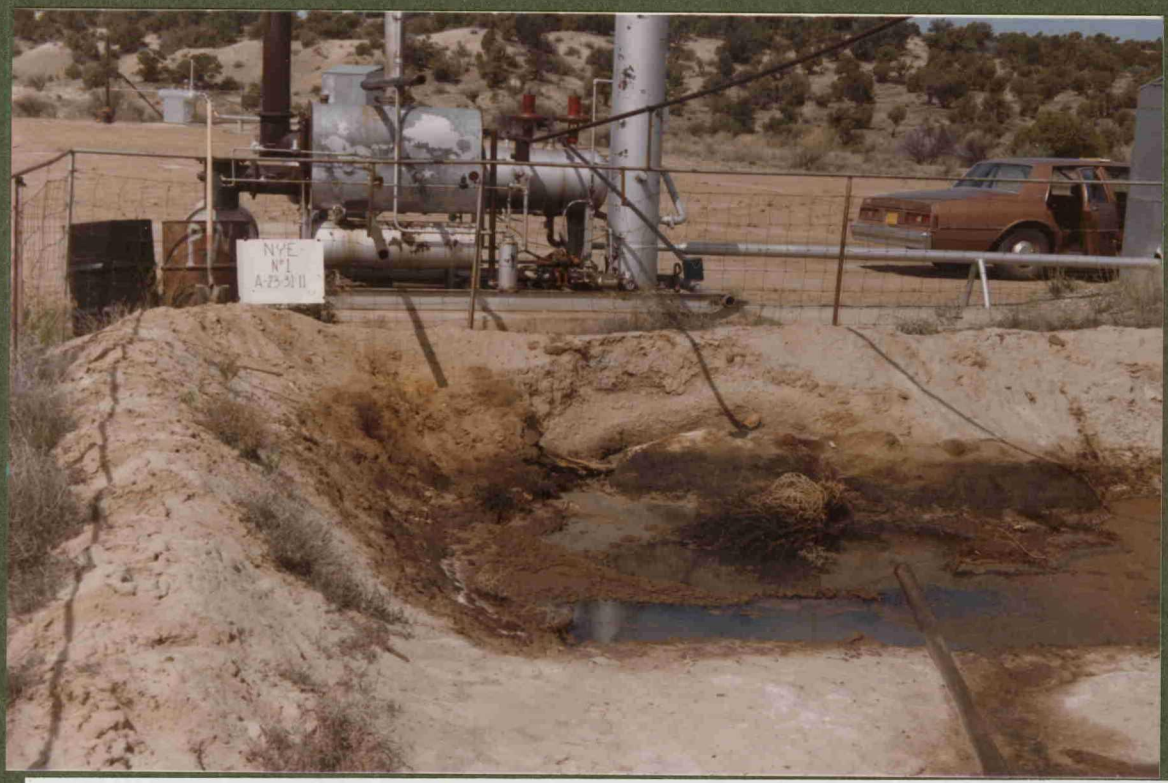

Photo No. 2. Shown is the area within the drip tank pit, facing west.

Photo No. 3. - The area shown is where the soil sample was taken which is downslope and 80 feet from the separator pit, facing west.

ANIMAS VALLEY

Utton No. 1 - San Juan County, NM, Sec. L of Sec. 7, T-30-N, R-11-W.

Photo No. 1. The general area, facing north, shows an apple orchard downslope of the meter drip pit.

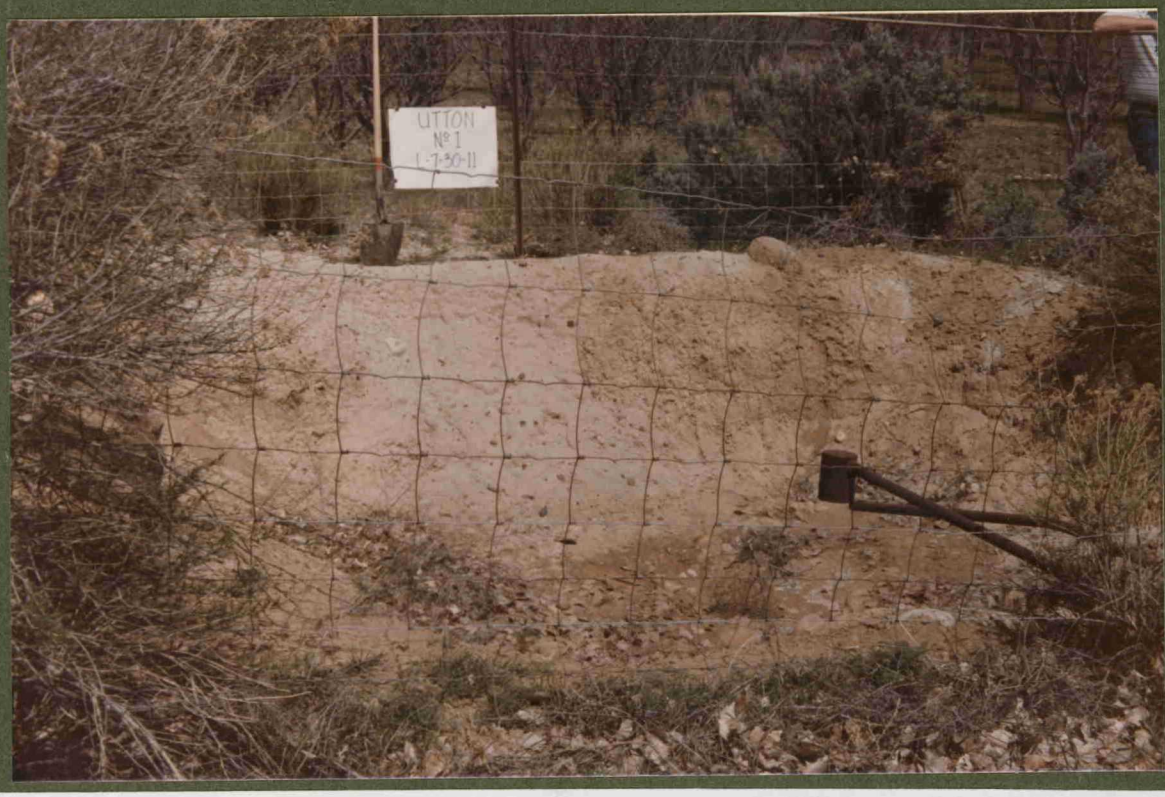

Photo No. 2. The area shown is within the meter drip pit, facing north.

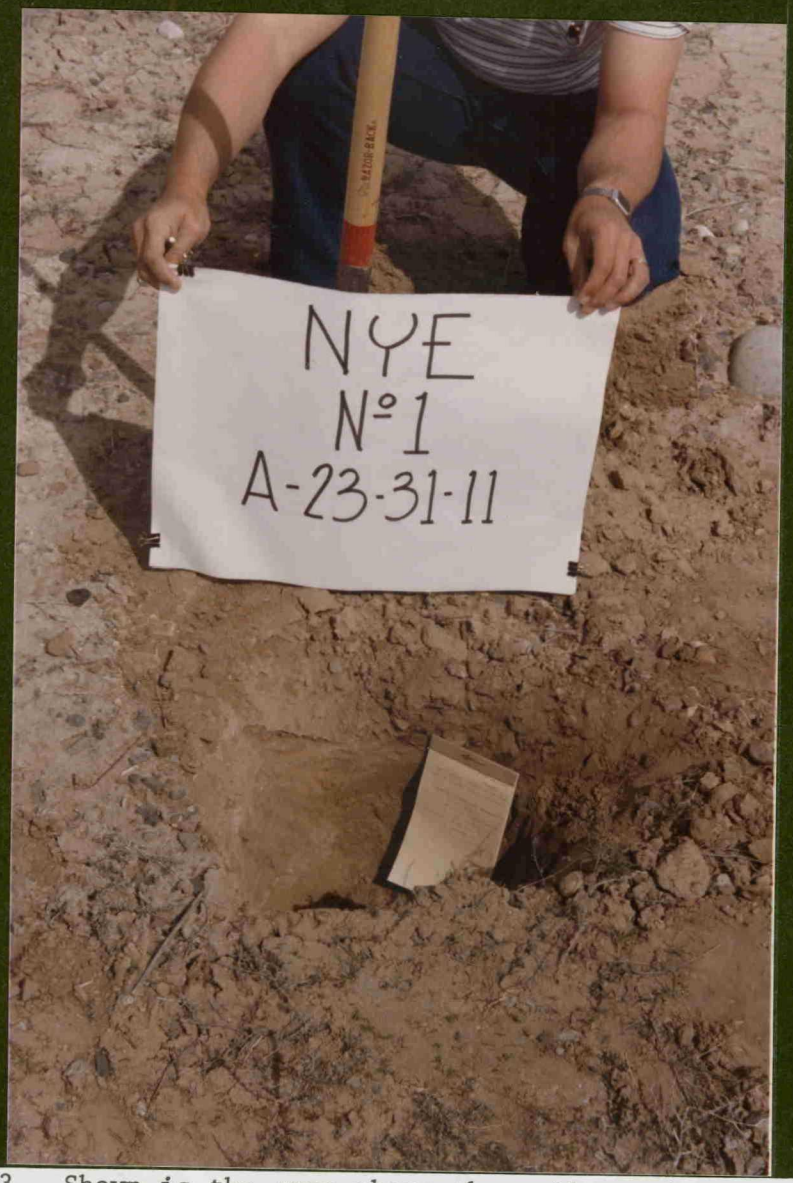

Photo No. 3. Shown is the area where the soil sample was taken, 60 feet downslope from the drip tank pit.

Photo No. 3. The area shown, facing towards the west, is where the soil sample was taken 30 feet east of the meter drip pit using a 14-inch-diameter hole with a depth of 18 inches. The water table is 30 inches.

ANIMAS VALLEY

Sutton No. 1 - San Juan County, NM, Sec. D. of Sec. 18, T-30-N, R-11-W.

Photo No. 1. Shown is the general area, facing south towards the Animas River.

Photo No. 2. The area shown is within the well blowdown pit, facing west. The area has a shallow groundwater table. Note seepage in the pit.

Photo No. 2. Facing west, the area shown is where the soil sample was taken, 40 feet east of the well blowdown pit. Used was a 14 inch diameter hole at a depth of 12 inches. The area has a shallow groundwater table.

ANIMAS VALLEY

McWright No. 1 - San Juan County, NM, Sec. 13 (northwest corner), T-30-N, R-12-W.

Photo No. 1. The general area shown is facing south towards the Animas River one-third mile downslope.

Photo No. 2. The area shown is within the dehydration/separator pit, facing south.

Photo No. 3. The area shown, facing north, is where the soil sample was taken, 80 feet south of the dehydration/separator pit. Used was a 14 inch-diameter-hole which was 18 inches deep. The water table was approximately 30 inches.

ANIMAS VALLEY

Animas River - San Juan County, NM at Randlemon No. 2 location, located in Sec. 26, T-31-N, R-11-W.

Photo No. 1. The general area shown is from the top of the hill, looking downslope, facing west.

Photo No. 2. The area shown is downslope and at the edge of the river bed where the soil sample was taken.

Photo No. 3. Shown is the area where the soil sample was taken.

ANIMAS VALLEY

McCoy No. C-1 - San Juan County, NM, Sec. 28, T-30-N, R-12-W.

Photo No. 1. The general area facing south towards the Animas River, which is approximately 300 yards from the dehydration pit, is shown.

Photo No. 2. The area shown is within the dehydration pit, facing south. Note the ground surface is covered with alkali and the water table is approximately at 24".

Photo No. 3. The area shown is where two soil samples taken, 80 feet south of the dehydration pit. The first sample was taken 3 inches below top soil. The second soil sample, from the same 14-inch diameter hole at 18 inches deep to saturated soil. The picture was taken facing north.

ANIMAS VALLEY

Larcher No. 3 - San Juan County, NM, Sec. 7, T-31-N, R-10-W, Unit N.

Photo No. 1. The general area, facing west towards Ruins Road, is shown.

Photo No. 2. The area within the dehydration pit, facing northwest, is shown.

Photo No. 3. Shown is the area of the soil sample, 29 feet from the dehydration pit, facing northwest.

ANIMAS VALLEY

Mary Wheeler No. 1-E - San Juan County, NM, SW4, SW4, Sec. 23, T-30-N, R-12-W.

Photo No. 1. The general area is shown, facing south towards the Animas River and 100 feet from the dehydration pit.

Photo No. 2. The area shown is within the dehydration pit, facing south.

Photo No. 3. Shown is the area, facing east, where the soil sample was taken, 30 feet west of the dehydration pit. Used was a 14-inch-diameter hole, 18 inches deep. The water table is approximately 24 inches deep.

Summary of Sampling Activities
San Juan Division
El Paso Natural Gas Company
February 26-28, 1985

SAN JUAN VALLEY

- Armenta Gas Com. A No. 1 - located in San Juan County, New Mexico, Section "D" of Section 27, Township 29 North, Range 10 West.

  A soil sample was taken 3 feet from the drip pit in a southerly direction at a depth of 12 inches of a 14-inch-diameter hole. The water table is almost at ground surface. The entire surrounding area was covered with alkali. The San Juan River is located to the south approximately 200 yards from the drip pit, which is on private land. A house, located to the east of the drip pit at a distance of approximately 60 feet, has a shallow drainage ditch which runs next to the pit and empties on ground surface.

- Lobato Gas Com. A1A & E1A - located in San Juan County, New Mexico, Section "D" of Section 3, Township 39 North, Range 9 West.

  Two soil samples were taken. The first sample was taken downslope 15 feet south of the dehydration/separator pit at a depth of 9 inches to the saturated soil of a 14-inch-diameter hole and an 9 inches deeper is the groundwater table. The San Juan River is located approximately 100 feet to the north of the pit. The second soil sample was taken at the edge of the river downslope from the pit.

- Jaquez Com. A No. 1 - located in San Juan County, New Mexico, in Section "M" of Section 25, Township 30 North, Range 9 West.

  A soil sample was taken 35 feet downslope to the south of the meter drip pit at a depth of 18 inches of a 14-inch-diameter hole. The San Juan River is located approximately 400 yards to the south of the pit.

LA PLATA VALLEY

- Alberding No. 1 - located in San Juan County, New Mexico, in Section "A" of Section 3, Township 31 North, Range 13 West.

  Two soil samples were taken. The first sample was taken downslope to the La Plata River, located approximately 80 feet to the west of the separator pit, at a depth of 16 inches of a 14-inch-diameter hole. The soil condition was very sandy. The second sample was taken approximately 118 feet west of the pit at the river's edge, at a depth of 6-8 inches of a 14-inch-diameter hole.

ANIMAS VALLEY

- NYE NO. 1 - located in San Juan County, New Mexico, in Section "A" of Section 23, Township 31 North, Range 11 West.

  A soil sample was taken 60 feet downslope, a 6 foot decline, in an easterly direction from the drip tank pit, at a depth of 16 inches of a 14 inch-diameter-hole. The soil condition was very sandy.

- McCOY NO. C-1 - located in San Juan County, New Mexico, in Section "A" of Section 28, Township 30 North, Range 12 West.

  Two soil samples were collected from the same hole downslope to the Animas River and 80 feet from the dehydration pit in a southerly direction. The top 2-3 inches were scraped off a 14-inch-diameter hole with the sample taken below the scraped area. An additional sample was taken 10 inches below the 14-inch-diameter hole. The water table is two feet deep, temperature 30-40°F. and the ground condition at the time of sampling was frozen.

- UTTON NO. 1 - located in San Juan County, New Mexico, in Section "L" of Section 7, Township 30 North, Range 11 West.

  A soil sample was taken 30 feet downslope from the drip pit in an easterly direction from a 14-inch-diameter hole at a depth of 18 inches. The water table in this area is approximately 30 inches.

- SUTTON NO. 1 - located in San Juan County, New Mexico, in Section "D" of Section 18, Township 30 North, Range 11 West.

  A soil sample was taken 40 feet from the blowdown pit in a westerly direction from a 14-inch-diameter hole at a depth of 12 inches deep. The area has a shallow water table.

- McWRIGHT NO. 1 - located in San Juan County, New Mexico, in Section 13 (northeast corner), Township 30 North, Range 12 West.

  A soil sample was taken 80 feet downslope from the dehydration pit in a southerly direction from a 14-inch-diameter hole at a depth of 18 inches. The water table in this area is approximately 30 inches.

- ANIMAS RIVER (at Randleman No. 1 Location) - located in San Juan County, New Mexico, in Section 26, Township 31 North, Range 11 West.

  A soil sample was taken 15 feet from the riverbed and approximately 50 yards from the Randleman No. 1 dehydration pit in a westerly location.

- LARCHER NO. 3 - located in San Juan County, New Mexico, in Section 7, Township 31 North, Range 10 West, Unit N.

  A soil sample was taken 29 feet from the dehydration pit downslope to the Animas River, located approximately 1/4 mile in a southeast direction, from a hole 14-inch-diameter at a depth of 14 inches.

- MARY WHEELER NO. 1-E - located in San Juan County, New Mexico, in the SW/4, SW/4 of Section 23, Township 30 North, Range 12 West.

  A soil sample was taken 30 feet west of the dehydration pit downslope towards the Animas River, which is approximately 100 feet away in a southwest direction, from a hole 14-inch-diameter at a depth of 18 inches with the water table at 24 inches deep.